Characterisation of the Co-chaperone Small Glutamine-rich Tetratricopeptide Repeat containing protein alpha as a Regulator of Androgen Receptor Activity in Prostate Cancer Cells

A thesis submitted to the University of Adelaide in total fulfilment of the requirements for the degree of Doctor of Philosophy

by

ANDREW PAUL TROTTA B.Sc. (Mol. Biol.), B.Sc. (Hons)

Department of Medicine

The University of Adelaide

Adelaide, South Australia

July 2011

This thesis is dedicated to my mum and dad. Thank you for all your love and support.

DECLARATION I

ACKNOWLEDGEMENTS II

ABBREVIATIONS V

ABSTRACT X

CHAPTER 1: INTRODUCTION 2

1.1 Overview 2

1.2 Development of the prostate 4

1.2.1 Androgen physiology 4

1.2.2 Development of the normal prostate 5

1.3 Prostate cancer and progression 9

1.3.1 Pathogenesis 9

1.4 Diagnosis 10

1.4.1 Clinically localized and advanced disease 11

1.5 Treatment 12

1.5.1 Localised Disease 12

1.5.2 Metastatic Disease 12

1.6 The androgen signalling axis 14

1.6.1 The androgen receptor 15

1.6.2 The androgen receptor gene 16

1.6.3 The androgen receptor protein and domains 19

1.7 Androgen receptor co-regulators 24

1.7.1 Co-activators 24

1.7.2 Co-repressors 25

1.7.3 Chaperones 26

1.8 The molecular chaperone complex and androgen receptor maturation 27

1.8.1 Chaperones involved in ligand binding and nuclear translocation 32

1.8.2 Chaperones and transcriptional activation 37

1.9 Chaperones in prostate cancer 37

1.10 Chaperones as therapeutic targets **39**
1.11 Tetratricopeptide repeat containing co-chaperones **40**
1.11.1 Structure of TPR domain 43
1.11.2 Hsp90 and Hsp70 TPR binding sites 43
1.11.3 Regulation of Hsp70 and Hsp90 ATPase activity by TPR co-chaperones 45
1.11.4 The role of TPR co-chaperones in steroid receptor signalling 46
1.11.5 Small glutamine-rich tetratricopeptide repeat containing protein alpha 54
1.12 Conclusions **59**
1.13 Objectives of this thesis **61**

CHAPTER 2: MATERIALS AND METHODS **63**
2.1 Materials **63**
2.2 Buffers and solutions **68**
2.3 General Methods **71**
2.3.1 Cloning procedures 71
2.3.2 Mammalian cell culture 76
2.3.3 General transfection methods 78
2.3.4 Mammalian two-hybrid interaction assays 80
2.3.5 Western blotting procedures 81
2.3.6 Real time PCR 83
2.3.7 Statistical analysis 84

CHAPTER 3: CHARACTERISATION OF THE SGTA HOMODIMERISATION INTERFACE **86**
3.1 Introduction **86**
3.2 Materials and Methods **90**
3.2.1 Plasmids 90
3.2.2 Creation of SGTA substitution and deletion variants 92
3.2.3 SGTA phylogeny tree 93

3.2.4 Secondary structure prediction, residue composition and logo creation 94
3.2.5 Co-Immunoprecipitation 94
3.2.6 *In vitro* luciferase assays 98
3.3 Results **99**
3.3.1 Characterisation of SGTA functional domains 99
3.3.2 Amino acid analysis of the SGTA homodimerisation domain 107
3.3.3 SGTA homodimerisation cannot be captured by co-immunoprecipitation. 111
3.3.4 Segmented deletions within the first 80 amino acids of the amino terminal domain ablate SGTA homodimersiation. 116
3.3.5 Inhibition of SGTA homodimerisation by expression of a peptide sequence encompassing SGTA amino acids 1-80 122
3.3.6 Deletion of SGTA intra-molecular domains does not alter the capacity for SGTA to form a homodimer. 125
3.3.7 Disruption of SGTA homodimerisation does not alter its ability to inhibit AR activity 128
3.4 Discussion **130**

CHAPTER 4: SGTA ACTS TO RESTRICT THE SENSITIVITY OF ANDROGEN RECEPTOR ACTIVITY 138
4.1 Introduction **138**
4.2 Materials and Methods **142**
4.2.1 Plasmids 142
4.2.2 Quantitative real time PCR and Immunoblot 142
4.2.3 Transient luciferase assay 143
4.2.4 Chromatin integrated reporter luciferase assay 143
4.2.5 Statistical analyses 144
4.3 Results **145**
4.3.1 Tetratricopeptide repeat containing co-chaperones are expressed in prostate cancer cell lines 145

4.3.2 Optimisation of AR and SGTA transactivation assays 149
4.3.3 SGTA decreases AR sensitivity to ligand 152
4.3.4 SGTA affects GR and PR transactivation activity 157
4.3.5 Deletions within the SGTA homodimerisation domain variably alter AR transactivation activity 160
4.3.6 The SGTA linker region is necessary for an effect on AR activity 160
4.4 Discussion **164**

CHAPTER 5: GLOBAL ANALYSIS OF SGTA BIOLOGICAL PATHWAYS IDENTIFIED PI3 KINASE AS A POTENTIAL TARGET IN PROSTATE CANCER CELLS **171**
5.1 Introduction **171**
5.2 Materials and Methods **173**
5.2.1 Small Interfering RNA (siRNA) transfections and Immunoblot 173
5.2.2 RNA Isolation and QRT-PCR 173
5.2.3 Microarray and Gene Ontology Analysis 173
5.2.4 Statistics 174
5.3 Results **176**
5.3.1 Knockdown of SGTA in C42B cells variably alters AR regulated genes 176
5.3.2 SGTA knockdown does not alter AR transcriptional activity at low ligand concentrations 182
5.3.3 SGTA knockdown alters the genome-wide expression profile of C42B cells. 187
5.3.4 Validation of SGTA knockdown microarray 191
5.3.5 SGTA knockdown affects cell proliferation gene ontology categories 196
5.3.6 SGTA down-regulates Class I phosphoinositide 3-kinase genes 200
5.3.7 SGTA knockdown modulates PI3 kinase-Akt activity 205
5.4 Discussion **207**

CHAPTER 6: THE EFFECT OF SGTA ON PROSTATE CANCER CELL PROLIFERATION 216

6.1 Introduction 216

6.2 Materials and Methods 219

6.2.1 Cell proliferation assays, siRNA knockdown and immunoblot 219

6.2.2 Cloning of SGTA into two independent stable integration mammalian expression vectors 220

6.2.3 Creation of stable transformants 221

6.2.4 Selection of stable transformants 221

6.2.5 Clinical cohort and creation of tissue microarrays 222

6.2.6 Immunohostochemistry 223

6.2.7 Statistics 224

6.3 Results 225

6.3.1 Knockdown of SGTA in C42B cells reduces cell proliferation 225

6.3.2 Stable SGTA over expression in LNCaP cells does not alter AR activity 231

6.3.3 Stably transfected LNCaP cells display reduced cell proliferation 231

6.3.4 Expression of AR and SGTA does not change in patient matched BPH and prostate cancer samples. 236

6.4 Discussion 240

CHAPTER 7: GENERAL DISCUSSION 247

7.1 Major Findings of this thesis 247

7.1.1 The characterisation of the SGTA homodimerisation domain and its effects on AR activity. 247

7.1.2 The linker region of SGTA is required for its inhibitory effects on AR activity 248

7.1.3 SGTA acts to restrain the sensitivity of AR activity in prostate cancer cells. 249

7.1.4 SGTA acts as a regulator of intracellular signalling pathways critical for prostate cancer cell proliferation 251

7.2 Future Directions 252

7.2.1 Indentifying the regions of SGTA that determine AR cytoplasmic retention 252
7.2.2 Identification of SGTA client proteins in prostate cancer 253
7.2.3 Further investigations into the effects of SGTA on PI3 kinase signalling in prostate cancer 254
7.3 Summary & Conclusions **255**

APPENDIX A: PRIMERS AND PCR CONDITIONS **257**
APPENDIX B: PLASMIDS **263**
APPENDIX C: MICROARRAY DATASET **273**
APPENDIX D: IPA CANONICAL PATHWAY ANALYSIS **302**
BIBLIOGRAPHY **307**

Declaration

This work contains no material which has been accepted for the award of any other degree or diploma in any University or other tertiary institution and, to the best of my knowledge and belief, contains no material previously published or written by another person, except where due reference is made in the text. I give consent to this copy of my thesis being made available in the University library, being made available for loan and photocopying, subject to the provisions of the Copyright Act 1968.

I also give permission for the digital version of my thesis to be made available on the web, via the University's digital research repository, the Library catalogue, the Australasian Digital Theses Program (ADTP) and also through web search engines, unless permission has been granted by the University to restrict access for a period of time.

Andrew P. Trotta

July 2011

Acknowledgements

I must start by thanking my amazing supervisors, Dr. Grant Buchanan, Professors Wayne Tilley, Villis Marshall and Gary Wittert. Grant your incredible enthusiasm for science, encouragement and belief in me was the driving force that made all this possible. Thank you for always supporting me during the tough times and making it possible for me to see this PhD through to the end. Wayne I would like to thank you for allowing me the opportunity to carry out my PhD in your laboratory. Your guidance and support has been invaluable throughout my studies, particularly when it was over a couple of glasses of wine.

To Gary and Villis, thank you for making it possible for me to do a PhD and for always taking an interest when I came to talk to you. I would like to thank the Freemasons Foundation Centre for Men's Health for financially supporting me throughout my PhD. To my unofficial supervisor, Elle Need thank you for your consistent mentorship and commitment, this thesis could not have been completed without your help. Also to the other members of the Molecular Ageing Laboratory, Erin Swinstead, Damien Leach, Tiffany Harris and Lauren Giorgio. Thank you for hearing all about my troubles in the lab over Friday afternoon drinks. Many thanks go to Melissa O'Loughlin for her assistance with western blots, real time PCR as well as for being such a great friend.

I would like to thank my fellow PhD students, Astrud Tuck, Miriam Butler, Sarah Carter, Ali Ochnick, and Karen Chiam. Sharing the PhD room with all of you has been an

amazing and crazy experience, thank you for being wonderful friends and making this such an enjoyable experience. All I can say is....Purple Monkey Dishwasher!!! I would like to particularly thank Astrud for being my strongest supporter and best friend during my Phd. After all the arguments, tears, laughs and antics we shared, you have always been an enormous source of encouragement and support. Thank you. I need to apologise to the honourary PhD students PC, Mr Boris Bubbles, Priscilla, Craig Spot and Alby. Sorry for killing you. I know you are in a happier place now.

I wish to acknowledge and thank my colleagues in the Dame Roma Mitchell Cancer Research Laboratories. Thank you to Drs Tina Bianco-Miotto, Lisa Butler and Theresa Hickey for all the moral support and providing a sympathetic ear when things were not looking that great. Thank you Lisa for reading this thesis and keeping a close eye on me towards the end. I would also like to thank Joanna Gillis for being such an amazing teacher when I first started as well as providing many laughs with her cranky lab notes. To the other research assistants, Natalie Ryan, Ean Phing Lee, Sook Ching Lee, Adrienne Hanson and Scott Townley, thank you for providing technical assistance, many laughs and drinks over the last 3 years. I must also thank the post-docs in the lab, Drs Maggie Centenera and Luke Selth for reading this thesis and for encouraging me to continue till the end. Also Drs. Vanessa Thompson, Nicole Moore, and Tanya Day were a constant source of inspiration and support throughout my studies. Thank you to Dr. Jeffery Barrett for all your hard work in establishing the stable SGTA cell lines. Personal thanks must go to Dr. Tanja Karasoulos for convincing me that this process is worthwhile and to live without regrets. Those early morning Mount Lofty walks were a great way to clear my head.

To all my family and friends who supported me every moment of this journey I cannot thank you enough. I am forever grateful to my parents for their love and support and guidance when I needed it. I love you. I thank my two amazing brothers David and Chris for always showing an interest my career no matter how strange it must have sounded to them. Many thanks must go to Paul and Nins for all the fun time we shared throughout my studies and in particular our journeys throughout the USA. Special thanks go to my O&G peeps Kathryn, Emily, Laura, Kate for all the many special moments we shared and to Rachael (BB) Nowak for your friendship and love over the years.

Finally, I must thank my partner Joey. Thank you for being such an important part of my life over the last year. You have been my rock when times were tough and patient with me when I didn't know the way forward. I am forever grateful. I love you.

Abbreviations

3C	chromatin conformation capture
17-AAG	17-allylamino-demethoxygeldanamycin
Aβ	intracellular beta amyloid
ADT	androgen depriation therapy
AF	activation function
AF-1	activation function 1 (amino acids 38-360)
AF-2	activation function 2
AF-5	activation function 5 (amino acids 360-535)
ATCC	American Type Culture Collection
AR	androgen receptor
ARE	androgen response element
ADP	adenosine diphosphate
ATP	adenosine triphosphate
APS	ammonium persulphate
bp	base pair
BPH	benign prostatic hyperplasia
BSA	bovine serum albumin
$CaCl_2$	calcium chloride
cAMP	cyclic adenosine monophosphate
cDNA	complementary DNA
ChIP	chromatin immunopreicpitation
ChIP-chip	chromatin immunopreicpitation microarray
ChIP-seq	chromatin immunoprecipitation sequencing
cm	centimetre
CoIP	co-immunoprecipitation
CREB	cAMP-response-element-binding protein
CsA	cyclosporine A
CSP	cysteine string receptor
Cyp40	cyclophilin 40
DAB	3’3’-diaminobenzidine tetrahydrochloride
DBD	DNA binding domain
DCC	dextran coated charcoal
dH_2O	distilled water
Dex	dexamethasone
DHEA	dehydroepiandrosterone

DHT	5α-dihydrotestosterone
DMSO	dimethyl sulphoxide
DNA	deoxyribonucleic acid
dNTPs	deoxyribonucleotide triphosphates
DRE	digital rectal examination
dsDNA	double stranded DNA
DTT	dithiothrietol
E2	17β-estradiol
EC_{50}	half maximal effective concentration
ECL	enhanced chemiluminescence
EDTA	ethylenediamine tetra-acetic acid
ER	estrogen receptor
EtOH	ethanol
FBS	foetal bovine serum
FKBP	fk506 binding protein
g	gram
g	relative centrifugal force
GAPDH	glyceraldehyde-3-phosphate dehydrogenase
GFP	green fluorescent protein
GTPase	small gunosine triphosphatase
GR	glucocorticoid receptor
hr	hour
H	hinge region
HAT	histone acetyltransferase
HCl	hydrochloric acid
HD	homodimerisation domain
HDAC	histone deacetylase
HEPES	4-(2-hydroxyethyl)-1-piperazineethanesulfonic acid
hGHR	human growth hormone receptor
HGPIN	high-grade prostatic intraepithelial neoplasia
HIV	human immunodeficiency virus
HRE	hormone response element
HRP	horse radish peroxidise
Hsc	constitutively expressed heat shock protein
Hsp	heat shock protein
Hip	heat shock interacting protein
Hop	heat shock organising protein
IgG	immunoglobulin class G
IHC	immunohistochemistry

IMVS	Institute of medical and veterinary sciences
IPTG	isopropyl-thio-b-D-galactoside
Jak	Janus kinase
kB	kilo base
KCl	potassium chloride
kd	dissociation constant
kDa	kilo Dalton
kg	kilogram
l	litre
LB	Luria Broth
LBD	ligand binding domain
LGPIN	low grade prostatic intraepithelial neoplasia
LHRH	luteinizing hormone releasing hormone
LiCl	lithium chloride
LNCaP	lymph node carcinoma of the prostate
LR	linker region
M	molar
mA	milliampere
MAPK	mitogen activated protein kinase
MCS	multiple cloning site
mg	milligram
min	minute
$MgCl_2$	magnesium chloride
$MgSO_4$	magnesium sulphate
mL	millilitre
mM	millimolar
mm	millimetre
MOPS	morpholinopropane sulphonic acid
MR	mineralocorticoid receptor
mRNA	messenger RNA
msec	millisecond
NaCl	sodium chloride
Na_2Mo_4	sodium molybdate
N/C	amino terminal/carboxyl terminal
NCOR	nuclear co-repressor
ng	nanogram
$(NH_4)SO_4$	ammonium sulphate
NLS	nuclear localisation sequence
nm	nanometer

nM	nanomolar
NS	non specific siRNA
NTD	amino-terminal transactivation domain
p300/CBP	CREB-binding protein
PAGE	polyacrylamide gel electrophoresis
PB	probasin
PBS	phosphate buffered saline
PC3	prostate carcinoma 3
PCR	polymerase chain reaction
PDGFRα	platelet derived growth factor receptor alpha
PIN	prostatic intraepithelial neoplasia
PI3K	phosphatidylinsoitiol-3-kinase
pM	picomolar
PP5	serine/theronine protein phosphatase 5
PPIase	peptidylprolyl isomerase
PR	progesterone receptor
Prog	progesterone
PSA	prostate specific antigen
QRD	glutamine-rich domain
QRT-PCR	quantitative real-time PCR
RFLP	restriction fragment length polymorphism
RGH	Repatriation General Hospital
RNA	ribonucleic acid
RNase	ribonuclease
rpm	revolutions per minute
RT	reverse transcriptase
SA	South Australia
SD	standard deviation
SDS	sodium dodecyl sulphate
sec	second
SEM	standard error of the mean
SGTA	small glutamine rich TPR containing protein alpha
siRNA	small interfering RNA
SM	sodium molybdite lysis buffer
SMRT	silencing mediator of retinoic and thyroid hormone receptors
SRC-1	steroid receptor coactivator 1
STAT	signal transducer and activator of transcription
T	testosterone
TBE	tris borate EDTA

TBP	TATA binding protein
TBS	tris buffered saline
TBST	tris buffered saline-tween 20
TE	tris EDTA
TEMED	N,N,N',N'-tetramethylethylenediamine
Tm	melting temperature
TPR	tetratricopeptide repeat
tRNA	transfer RNA
TSS	transcription start site
TURP	transurethral resection of the prostate
USA	United States of America
UTR	untranslated region
UV	ultraviolet
V	volt
v	volume
W	watt

Other:

^{0}C	degrees Celsius
Δ	deletion
μg	microgram
μL	microlitre
μm	micron
μM	micromolar

Abstract

Prostate cancer remains one of the leading causes of cancer related morbidity and mortality in Australian men. The androgen receptor (AR) is an intracellular transcription factor that mediates the biological actions of circulating androgens to drive the growth and survival of prostate cancer cells. However, current treatment options for non-localised, advanced stage prostate cancer invariably fail, which is a consequence of continued AR signalling during all stages of disease progression. Therefore, understanding the regulatory mechanisms of AR action is essential for the development of more effective therapies.

Molecular regulation of the AR can occur during the process of protein maturation. This includes the incorporation of tetratricopeptide repeat (TPR) containing co-chaperones into the heat shock protein 90 (Hsp90) molecular chaperone complex, which collectively acts to generate AR proteins capable of high affinity ligand binding, nuclear translocation and gene regulation. The co-chaperone small glutamine-rich TPR containing protein alpha (SGTA) acts to restrict AR nuclear translocation and thereby regulate AR transcriptional activity. The clinical implications of SGTA are evident by a decline in protein levels with prostate cancer progression. The loss of SGTA may therefore disrupt the regulatory process of AR cytoplasmic retention, and thus contribute to continued AR activity. However the precise regions of SGTA that mediate these effects or how SGTA may contribute to prostate cancer proliferation have yet to be elucidated. The aims of this thesis were to further characterise the mechanisms of SGTA action on AR signalling, to further

define the biological actions of SGTA in prostate cancer cells and to determine the functional consequences these actions have on prostate cancer growth.

SGTA is unique amongst the steroid receptor associated TPR co-chaperones through its ability to form homodimers. Therefore, the requirement of the SGTA homodimerisation domain may be essential in deciphering how SGTA affects AR activity. Deletion mapping combined with structural prediction analysis revealed that the first 80 amino acids of the amino terminus are required to form SGTA homodimers, as well as maintain SGTA protein steady state levels. Further studies also confirmed that SGTA homodimerisation occurs independently of the Hsp90 interacting TPR domain or glutamine-rich carboxyl terminus, implying that interactions between SGTA and the Hsp90 molecular chaperone complex do not contribute to the formation of SGTA homodimers. Moreover, inhibition of SGTA homodimerisation did not alter the ability of SGTA to inhibit AR activity. These studies demonstrate that while the SGTA homodimerisation is characterised by conserved structural elements within the first 80 amino acids, SGTA can sufficiently act as a monomer to inhibit AR activity.

Further investigations into the mechanisms of how SGTA affects AR transactivation activity demonstrated that SGTA restricts the ligand sensitivity of AR activity across multiple androgen responsive luciferase reporters in a low hormone environment. These studies also revealed that the strongest inhibitory effect by SGTA was observed on those loci that exhibited the greatest fold change to androgen treatment. Additionally, the effects of SGTA on AR are not mediated through the homodimerisation, TPR or glutamine-rich domains. These results suggest that SGTA has the ability to constrain the sensitivity of AR

activation to ligand in a castrate environment and therefore SGTA may act as a buffer against aberrant AR responses.

To determine the functional consequences of modulating SGTA levels in prostate cancer cells, both SGTA over expression and knockdown models were developed. Modulation of SGTA levels in prostate cancer cell lines decreased proliferation. This effect was not a result of altered AR activity, as determined by expression of the androgen regulated gene prostate specific antigen (PSA). Collectively, these results suggest that the impact of SGTA on prostate cancer cell proliferation is independent of AR signalling. Microarray analysis was used to determine the effects of SGTA knockdown on the prostate genome, which demonstrated that cells depleted of SGTA differentially regulated the expression of genes involved in cell cycle regulation. Specifically, genes with decreased expression included several within the Class I phophoinositide-3 kinase (PI3 kinase) pathway, a critical pro-proliferation signalling pathway in prostate cancer. Consequently, knockdown of SGTA resulted in decreased Akt phosphorylation at the threonine 308 (T308) and serine 473 (S473) residues, which are key indicators of active PI3 kinase signalling. Collectively, these studies demonstrated that SGTA is able to modulate the expression and/or activity of multiple signalling pathways within prostate cancer cells to influence cell proliferation.

The findings from this thesis provide novel insights into the structural and functional complexity of SGTA action on AR activity in prostate cancer cells. Importantly, this highlights the potential mechanistic consequences that SGTA may have for AR and other signalling pathways that occur during prostate cancer pathogenesis and provides the basis for further investigations evaluating SGTA as a novel therapeutic target in prostate cancer.

CHAPTER 1

Introduction

Chapter 1: Introduction

1.1 Overview

Prostate cancer is the most commonly diagnosed non skin cancer in Australian men. Each year, approximately 17,000 new prostate cancer cases are diagnosed equating to 30% of all male cancer patients (Bech Ganner, Negrello et al. 2010). Moreover, prostate cancer is the second leading cause of cancer related death, with approximately 3000 cases annually (Bech Ganner, Negrello et al. 2010). While the aetiology of prostate cancer remains unclear, age has been established as the most significant risk factor for disease development. Nonetheless, many exogenous risk factors have also been identified that can contribute to prostate cancer, such as smoking, diet and geographical location (Giovannucci, Liu et al. 2007; Allen, Key et al. 2008; Gudmundsson, Sulem et al. 2008; Yaspan, McReynolds et al. 2008).

Prostate cancer therapeutic options vary depending on the stage of disease at the time of diagnosis. For the majority of men who present with clinically localized or organ confined tumours, surgical removal of the prostate (radical prostatectomy) and/or radiotherapy are potentially curative treatments (Catalona and Smith 1994; Pound, Partin et al. 1999; Zietman, Chung et al. 2004). For men diagnosed with metastatic disease, hormonal manipulation (androgen deprivation therapy (ADT)) and/or targeting the mediator of androgenic action, the androgen receptor (AR), are primary treatment options. While patients on ADT initially experience a decrease in symptoms and tumour burden, the

majority relapse within 6-12 months and the cancer progresses to a "castrate resistant" state, at which time treatment options are limited (Scher, Buchanan et al. 2004). While previously it was assumed that the AR had no role in castrate resistant disease, it is now recognized that the AR remains the key mediator for cellular survival throughout all stages of prostate cancer progression (Feldman and Feldman 2001; Scher and Sawyers 2005). The underlying mechanisms proposed for AR action in disease initiation and progression following treatment failure are diverse (Buchanan, Irvine et al. 2001; Feldman and Feldman 2001; Scher and Sawyers 2005), but in individual cases remains elusive.

The heat shock protein 90 (Hsp90) molecular chaperone complex has been implicated in the production of a mature AR protein capable of binding ligand, nuclear translocation and gene transactivation (Pratt and Toft 1997). Many of these steroid receptor properties can be modulated by the incorporation of tetratricopeptide repeat (TPR) containing co-chaperones into the Hsp90-receptor complex. Due to its important role in the generation of competent AR proteins, Hsp90 has been selected as a novel therapeutic target for the treatment of prostate cancer. However, despite a number of Hsp90 inhibitors having produced promising *in vitro* data, they have invariably failed in clinical trials (Trepel, Mollapour et al. 2010). Therefore, it is necessary to understand the greater complexities surrounding the actions of the chaperone system as well as the contribution provided by the TPR co-chaperones in the regulation of steroid receptor activity. This knowledge will not only be essential in improving the efficacy of Hsp90 inhibitors, but may also lead to the identification of new therapeutic targets for the treatment of prostate cancer. To this end, our laboratory has identified the TPR co-chaperone small glutamine-rich TPR containing

protein alpha (SGTA) as a binding partner of the AR that acts to exclude the receptor from the nucleus until a ligand concentration threshold has been reached (Buchanan, Ricciardelli et al. 2007). Although the underlying mechanisms of SGTA action in prostate cancer remain elusive, the effects on AR activity may represent a novel means of controlling aberrant AR actions in prostate cancer.

This chapter outlines the essential role androgens and the AR play in the normal prostate and cancer. In particular, highlighting the important regulatory components of the molecular chaperone system, the impact chaperones have on AR activity and how these complexes can be therapeutically targeted.

1.2 Development of the prostate

1.2.1 Androgen physiology

Androgens are a class of steroid hormone that include testosterone (T), 5α-dihydrotestosterone (DHT), dehydroepiandrosterone (DHEA) and its sulphated form DHEA-S; which are required for the development of a male phenotype, production of external genitalia and maintenance of secondary sexual characteristics (Kaufman and Vermeulen 2005). Testosterone production begins during weeks 6-7 of gestation when the fetal mesonephric cells of the testis differentiate into functional Leydig cells. At approximately 12 weeks gestation the genital tubercle mesenchyme up regulates the steroidal metabolism enzyme 5α-reductase, which catalyses the conversion of T to the more biologically potent androgen DHT. This conversion acts to enhance the relatively weak androgenic potency of T as DHT has an approximately 10 fold higher dissociation

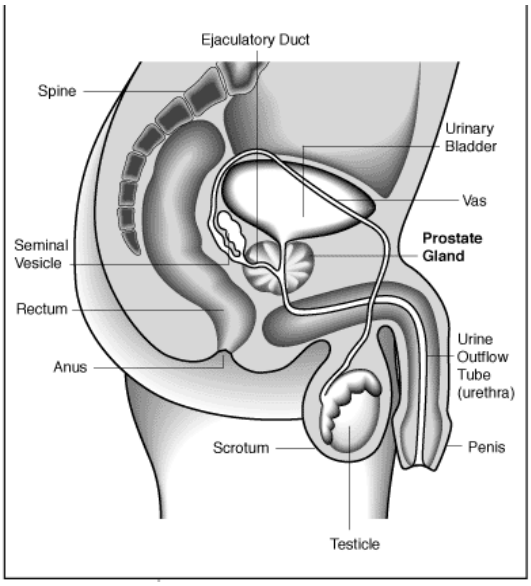
constant (Kd) for the androgen receptor (AR) (Wilson and French 1976; Deslypere, Young et al. 1992). The presence of DHT facilitates a series of morphological changes, including the differentiation of the Wolffian ducts into the epididymis, vas deferens and the seminal vesicles as well as the formation of the prostate and external male genitalia (reviewed in (Wilhelm and Koopman 2006).

1.2.2 Development of the normal prostate

The prostate is a walnut sized gland that encapsulates the urethra at the base of the bladder (Figure 1.1A). The growth and development of the prostate begins at approximately 10 weeks gestation and is a slow process that is heavily reliant on the presence of androgens. The production and secretion of androgens from the foetal testes results in the outgrowth of buds from the epithelial layer of the urogenital sinus into the urogenital sinus mesenchyme (Cunha, Donjacour et al. 1987; Marker, Donjacour et al. 2003). During puberty, a surge in circulating androgen levels as well as the up-regulation of 5α-reductase type II, results in the final stages of epithelial cell differentiation and the formation of a mature prostate (Cunha, Ricke et al. 2004). The final glandular structure is organised into three distinct zones: the peripheral zone (70%), the central zone (20-25%) and the transitional zone (5-10%), which all maintain a well defined gladular structure of epithelial tubuloalveolar ducts embedded in a matrix of stromal tissue (reviewed in (Cunha, Donjacour et al. 1987). These uniformly branched ducts consist of three major cell types, luminal secretory epithelial cells, encased in a thin layer of morphologically indistinguishable basal and neuroendocrine cells (Figure 1.1B). The basal cells surround the epithelial cells and physically separate them from the stroma, which is mainly

comprised of smooth muscle, but also contains fibroblastic, neuronal, lymphatic and vascular cell types. Although little is known about the function of the basal cells, it has been recently proposed that this layer harbours a subpopulation of multipotent stem cells that may play a role in tumourogenesis (Lawson, Zong et al. 2010). The epithelial cell layer functions by secreting serine proteases, such as prostate specific antigen (PSA), from their apical surface into the lumen of the duct.

A



B

NOTE:
These figures are included on page 7 of the print copy of the thesis held in the University of Adelaide Library.

C

Figure 1.1 Prostate biology and the pathobiology of prostate cancer progression. **A:** Anatomical location of the prostate and other male urogenital organs. The prostate is a small organ that surrounds the urethra and the neck of the bladder. **B:** Schematic depiction of glandular architecture of epithelial tubuloaveolar ducts of the adult prostate. A well defined basement membrane encases a continuous layer of morphologically indistinguishable basal and neuroendocrine cells and a lining of luminal epithelial cells that produces secretions into the ductal lumen (Abate-Shen and Shen 2000). **C:** Representation for a proposed mechanism of the histological changes observed during the progression of prostate cancer (Abate-Shen and Shen 2000).

1.3 Prostate cancer and progression

Prostate cancer remains a major cause of cancer related mortality and morbidity in men, which is due to a high degree of morphological and genetic heterogeneity (Schroder, van der Maas et al. 1998; Arora, Koch et al. 2004). Prostate cancers can range from slow growing latent tumours that remain indolent for up to 15 years without treatment (Johansson, Andren et al. 2004), to aggressive tumours with metastatic potential. The difficulty over the years for pathologists and researchers has been to differentiate between these patho-physiological states and to treat those cancers that will develop into clinically relevant disease.

1.3.1 Pathogenesis

The zonal architecture of the prostate displays a discrepancy in association with prostatic disorders such as benign prostatic hyperplasia (BPH) and prostate cancer. BPH is a common non-malignant enlargement of the prostate that develops in the transitional zone of the prostate and arises by the extensive proliferation of basal and stromal cells (Montironi, Bostwick et al. 1996; Cheng, Shan et al. 1998). Although not life threatening, symptoms of BPH include urinary obstruction, bladder infections and sexual dysfunction. Conversely, prostate cancers develop primarily within epithelial cells in the peripheral zone, however there is increasing evidence that signals from the basal cells may induce cancer initiating events leading to the development of prostate cancer (Goldstein, Huang et al. 2010; Lawson, Zong et al. 2010). While prostatic intraepithelial neoplasia (PIN) is considered a precursor to the development of prostate cancer, the relationship between the

two has yet to be fully defined. Diagnosis of PIN is classified at the histological level by hyperplasia of the luminal epithelial cells, reduction in the number of basal cells, enlargement of the nuclei and altered nuclear/cytoplasmic ratio (Bostwick 1992). Currently, PIN can be pathologically classified as low-grade PIN (LGPIN) or high-grade PIN (HGPIN), whereby the progression from LGPIN to HGPIN is marked by increased epithelial proliferation, invasion of the epithelia into the stroma and chromosomal abnormalities (Montironi, Bostwick et al. 1996; Bostwick, Shan et al. 1998) (Figure 1.1C). Studies have shown that the prevalence of PIN increases with age (Sakr, Haas et al. 1993), whereas HGPIN is now considered to be a strong predictor of prostate cancer as it is concurrently found with malignant disease (Bostwick, Pacelli et al. 1996; Bostwick, Shan et al. 1998).

1.4 Diagnosis

Currently, detection of prostate cancer occurs by the measurement of serum PSA combined with a digital rectal examination (DRE). However, confirmation of a diagnosis requires further examination by transrectal digital or ultrasound guided biopsy followed by examination of the histological architecture of the specimen. The Gleason grading system is used for pathological prognosis and is based on the glandular architecture of the tumour. Gleason scores (2-10) represent the differentiated characteristics and aggressiveness of the cancer, with higher numbers representing more aggressive tumours (Gleason and Mellinger 1974). Though PSA is expressed in the prostate, it is not a disease-specific marker as patients with BPH are also diagnosed with increased PSA levels above the normal range of 0 – 4.0 ng/mL (Stamey, Yang et al. 1987; Smith, von Eschenbach et al.

2001). Moreover, PSA is able to form complexes with other serum proteins, and thus additional measurements of free and total PSA are required to improve the positive predictive value of PSA testing. The implementation of PSA assays combined with DRE in community wide screening programs has been instrumental not only in the detection of early stage disease, but also for the prediction of post-operative relapse. Additionally, PSA velocity analysis, which is a measure of changing PSA levels over time, has allowed clinicians to predict the severity of the disease prior to surgery (D'Amico, Chen et al. 2004). However, PSA alone remains a poor predictor of patient survival as the mortality rate for prostate cancer has remained relatively unchanged for the last 20 years (Etzioni, Ankerst et al. 2007; Vickers, Savage et al. 2009; Bech Ganner, Negrello et al. 2010).

1.4.1 Clinically localized and advanced disease

Locally invasive prostate cancer is characterised by extensive epithelial proliferation, disruption of the basal membrane structure and invasion into the stroma. The use of basal cell specific markers, such as 34β-E12, cytokeratin 5/6 and p63 has been useful for pathologists to differentiate between *in-situ* carcinoma and invasive cancer (Hameed and Humphrey 2006). Advanced staged prostate cancer is characterised by an invasion of cells into the prostatic capsule and surrounding tissue, whereas metastatic disease has a propensity to travel to distal sites such as the bone, liver, lungs and lymph nodes (Bubendorf, Schopfer et al. 2000).

1.5 Treatment

1.5.1 Localised Disease

Men who are diagnosed with clinically localised prostate cancer are generally treated by surgical removal of the prostate (radical prostatectomy) and/or radiotherapy comprising of external-beam radiotherapy or brachytherapy. Although radiotherapy is less invasive than surgery, it has been shown that radical prostatectomy is a more effective treatment option for patients with a life expectancy greater than 10 years (Byrne 1996). For the majority of men, this type of treatment is potentially curative, but approximately 30% will relapse within 5 years of surgery and/or radiotherapy as determined by a biochemical recurrence of rising serum PSA (Catalona and Smith 1994). The presence of undetectable micro-metastatic disease at the time of diagnosis and treatment has been proposed as a mechanism for this patient relapse (Deguchi, Yang et al. 1997).

1.5.2 Metastatic Disease

During the 1940's Huggins and colleagues observed that prostate cancer growth relied on a continuous supply of androgens, and thus established that surgical removal of the testes (castration or orchidectomy) provided a procedural means depriving the tumour cells of this essential growth stimulant, delaying tumour progression and providing relief for patients (Huggins and Hodges 1972). This technique has formed the basis of contemporary endocrine blockade therapy for metastatic prostate cancer by inhibiting the production and/or action of androgens. Methods for achieving medical castration exist in a number of forms including i) targeting the hypothalamic-pituitary-gonodal axis, which drives

testicular androgen production, through luteinizing hormone-releasing hormone (LHRH) agonists or antagonists (i.e. goserelin, leuproelin) or estrogens (diethylstilbestrol and estramustine phosphate) and ii) AR antagonists (i.e. cyproterone acetate, hydroxyflutamide and bicalutamide) that act to competitively block the intracellular actions of androgens mediated by the AR. Whilst the treatment of metastatic disease is initially successful in approximately 80-90% of patients as determined by a reduction in tumour volume and serum PSA levels, ADT will invariably fail ultimately leading to castrate resistance. This is partially due to the intracellular conversion of adrenal androgens and/or the over expression of steroid enzymes, such as Cyp17 that allow *de novo* androgen synthesis (Montgomery, Mostaghel et al. 2008; Knudsen and Penning 2010). The development of androgen biosynthesis inhibitors, such as abiraterone acetate, have been effective at reducing intracellular androgen levels in several recent clinical trials as a treatment for prostate cancer patients (Attard, Reid et al. 2008; Danila, Morris et al. 2010; Attard, Richards et al. 2011).

Typically, tumour recurrence is observed within 5 years of ADT with an estimated survival rate of 16 months (Smaletz and Scher 2002). While there is currently no cure for patients with this stage of the disease, two published randomized trials reported that the implementation of taxane based chemotherapy agents such as paclitaxel and docetaxel as single agents or in combination with estramustine in patients with advanced stage disease improved survival rates from a few months to over 1 year (Petrylak, Tangen et al. 2004; Sonpavde and Palapattu 2010). These findings have led to the implementation of taxane-based therapy as a treatment option for castrate resistant prostate cancer patients. Beyond

chemotherapy, other treatments for late stage prostate cancer are at best palliative, for example, the combination of mitoxantrone with prednisone for the palliation of bone pain in castrate resistant patients (Tannock, Osoba et al. 1996).

In order to improve the efficacy of current treatment options as well as the growing need to develop new ways of specifically targeting prostate cancer cells, it is essential to understand the molecular biology and mechanisms of androgen action during the events of prostate cancer initiation and its progression to castrate resistance.

1.6 The androgen signalling axis

The androgen receptor (AR) is not only a critical component of androgen signalling, it is expressed in virtually all stages of prostate cancer, including ADT-resistant tumours (Brolin, Lowhagen et al. 1992; Bentel and Tilley 1996; Hobisch, Culig et al. 1996). It is now known that the survival of prostate cancer cells in an androgen deprived environment, is not due to a loss in androgen sensitivity, but rather continued AR activity (Feldman and Feldman 2001; Scher and Sawyers 2005). Indeed, the relevance of AR in prostate cancer cell survival is evident by knockdown of AR expression or immuno blockade of AR activity by an anti-AR antibody, which inhibits cellular proliferation of castrate resistant cell lines (Zegarra-Moro, Schmidt et al. 2002; Yang, Fung et al. 2005; Cheng, Snoek et al. 2006).

Aberrant AR activity in castrate resistant prostate cancer may arise through a variety of mechanisms, including *AR* gene amplification, the presence of somatic AR mutations that confer a gain-of-function, which have been documented in up to 50% of prostate cancers

(Buchanan, Greenberg et al. 2001), intracellular *de novo* synthesis and accumulation of androgens, increased expression of AR co-activators that promote AR transcriptional activity and/or cross talk between AR and other signalling pathways, such as MAPK, JAK/STAT and PI3K/Akt (Buchanan, Irvine et al. 2001; Dehm and Tindall 2005; Scher and Sawyers 2005; Zhu and Kyprianou 2008). Collectively these studies highlight the importance of AR signalling to continue prostate cancer growth, and that the AR still remains a viable therapeutic target. Therefore, further understanding the molecular mechanisms of AR signalling may provide a novel means of developing more effective therapies for prostate cancer patients

1.6.1 The androgen receptor

The AR is a transcription factor that mediates the cellular actions of androgens, such as T and its more potent metabolite DHT. The AR is a member of the class III nuclear receptor family, which comprises all of the steroid receptors including the progesterone receptor (PR), glucocorticoid receptor (GR), estrogen receptors α and β (ERα and ERβ) and the mineralocorticoid receptor (MR). The actions of these receptors are mediated through a series of orchestrated events that includes protein maturation via associations with chaperone complexes, ligand binding, translocation into the nuclear compartment, association with co-regulator proteins, integration onto DNA elements and interaction with the transcriptional machinery resulting in the subsequent regulation of target genes involved in cellular processes such as cell cycle progression, proliferation and response to intracellular lipid production and metabolism (Wang, Li et al. 2009).

1.6.2 The androgen receptor gene

The monoallelic *AR* gene is localized on the long arm of the X chromosome (Xq11.2-12) is greater than 90 kilo bases (Kb) in length and is organized into 8 exons that encode 919 amino acids (Figure 1.2A). The proximal promoter region for the *AR* spans the positions -74 to +87 around two separate transcriptional state sites (TSS) (positions +1/2/3 and +12/13 respectively) and is utilised for the expression of AR mRNA in multiple cell and tissue types (Tilley, Marcelli et al. 1990; Faber, van Rooij et al. 1993). While the *AR* promoter region lacks a classical TATA or CCAAT box required for interactions with the TATA binding protein (TBP) and Sp1 binding respectively, there is a long, species conserved homopurine stretch upstream of a CG box which facilitates Sp1 binding (Tilley, Marcelli et al. 1990; Faber, van Rooij et al. 1993; Takane and McPhaul 1996).

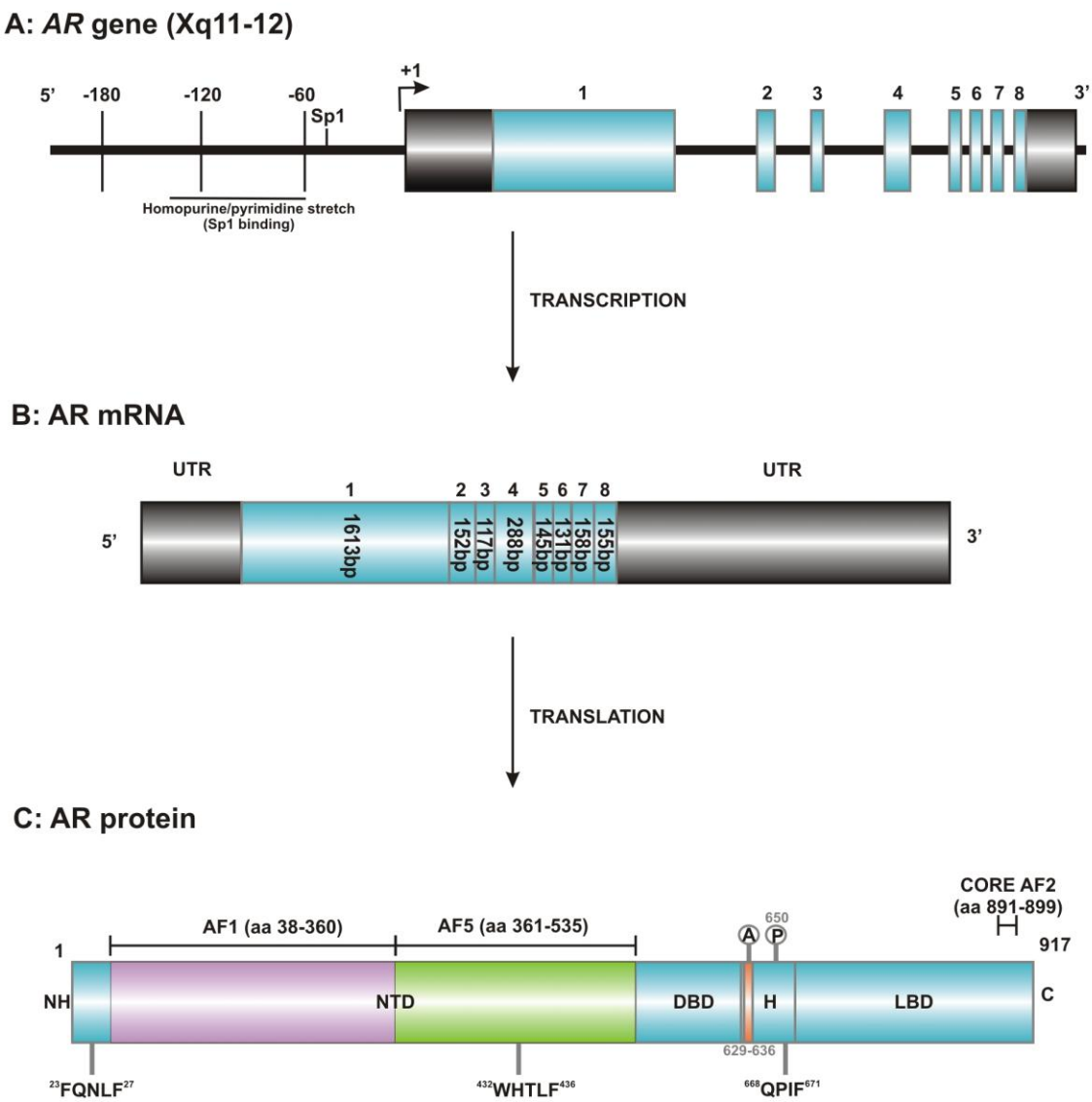

A: AR gene (Xq11-12)
5'
-180
-120
-60
Sp1
+1
1
2
3
4
5 6 7 8
3'
Homopurine/pyrimidine stretch
(Sp1 binding)
TRANSCRIPTION
B: AR mRNA
UTR
1
2 3 4 5 6 7 8
UTR
5'
1613bp
152bp
117bp
288bp
145bp
131bp
158bp
155bp
3'
TRANSLATION
C: AR protein
CORE AF2
(aa 891-899)
AF1 (aa 38-360)
AF5 (aa 361-535)
650
A
P
1
917
NH
NTD
DBD
H
LBD
C
629-636
23FQNLF27
432WHTLF436
668QPIF671

Figure 1.2 The *AR* gene, mRNA and protein structure. **A:** The *AR* gene consists of 8 exons, transcribed from a promoter containing no TATA or CAAT box. Instead, the promoter contains a long homopurine or pyrimidine stretch along with several Sp1 binding sites. **B:** The mature AR mRNA is 3569 bp long and contains a short 5' untranscribed region (UTR) and a long 3' UTR. **C:** The AR protein is 917 amino acids long and contains a long amino terminal domain (NTD), DNA binding domain (DBD), hinge region (H) and a ligand binding domain (LBD). The AR NTD contains two activation functions, 1 and 5 (AF1 and AF5). P; serine phosphorylation site at residue 650, A; acetylation site and the ^{23}FQNLF^{27}, ^{432}WHTLF^{436} and ^{668}QPIF^{671} motifs are shown in their respective locations. The AR-LDB contains amino acids that form the activation function 2 (AF2).

1.6.3 The androgen receptor protein and domains

The AR protein contains 919 amino acids encompassing 4 domains with discrete functions that are conserved to differing degrees amongst the steroid receptors: an amino terminal transactivation domain (NTD) that is divergent amongst the steroid receptors and responsible for the majority of the transactivation activity of the receptor, a highly conserved domain responsible for DNA binding (DBD), a relatively well conserved domain responsible for binding ligands (LBD) and a short non-conserved hinge region that separates the DBD from the LBD and was originally described as a linker region (Figure 1.2C). Each of these domains is explained in more detail below.

1.6.3.1 The amino terminal transactivation domain

The human AR-NTD consists of 555 amino acids, which is encoded by the first exon of the *AR* gene (Tilley, Marcelli et al. 1989; Jenster, van der Korput et al. 1992), and contains two broadly defined transactivation function regions AF1 (residues 38-360) and AF5 (residues 361-535). While both the AF1 and AF5 regions are responsible for the majority of the transactivational activity exhibited by the AR through interactions with co-regulators and the general transcriptional machinery, it has been shown that AF1 is required for AR transactivation activity, whereas AF5 is responsible for the transactivation activity of constitutively active LBD truncated AR variants (Jenster, van der Korput et al. 1995; Chamberlain, Whitacre et al. 1996; Shang, Myers et al. 2002; Need, Scher et al. 2009). The activation function-2 unit (AF2) present in the AR-LBD is involved in a ligand-dependent inter-domain interaction with two LXXLL-like motifs (^{23}FQNLF^{27} and ^{432}WNTLF^{436};

where X denotes any amino acid), in a conformational process known as the amino terminal/carboxyl terminal (N/C) interaction. The N/C interaction has been associated with an increase in AR steady state levels, decreased rate of ligand dissociation, decrease in receptor degradation and increased AR transactivation activity (Langley, Zhou et al. 1995; Zhou, Lane et al. 1995; He and Wilson 2002; Buchanan, Yang et al. 2004; Need, Scher et al. 2009). Investigations into the spatial and temporal ligand-dependent movements of the AR have found that the N/C interaction occurs rapidly in cytoplasm, but is lost upon receptor immobilization within the nucleus, possibly when AR binds to chromatin as a homodimer (van Royen, Cunha et al. 2007).

1.6.3.2 The DNA binding domain

The AR-DBD is encoded by exons 2 and 3 of the *AR* gene and is structurally conserved in relation to the other steroid receptors. The DBD consists of two cysteine rich zinc fingers that form the structure that binds the major groove of DNA at specific sites known as response elements. The first zinc finger contains a P-box, which consists of a stretch of five amino acids that recognise the ARE nucleotide sequence, whereas the second zinc finger contains a five amino acid region called the D-box, which contributes to DNA dependent AR homodimerisation and stabilisation as well as specificity and affinity of DNA binding (Schoenmakers, Alen et al. 1999; Shaffer, Jivan et al. 2004; Centenera, Harris et al. 2008).

Historically from candidate studies it was observed that the AR homodimer is able to bind to two different types of response elements i) a more general response element termed

hormone response elements (HRE) and ii) the more specific androgen response elements (ARE). Both types of response elements consist of two hexameric half-sites of a consensus sequence 5'-TGTTCT-3' arranged as either direct or inverted repeats separated by three nucleotides (Centenera, Harris et al. 2008). However, more recent whole genome studies using array and/or sequencing technology, such as chromatin immunoprecipitation chip array (ChIP-chip) or ChIP sequencing (ChIP-seq) have revealed in an unbiased manner that the majority of AR binding sites contain either a non-canonical or no discernable ARE sequence at all (Wang, Li et al. 2007; Massie and Mills 2008). These findings suggest that the AR contains intrinsic flexibility to interact with multiple DNA elements, potentially on regions of chromatin that have been previously demarcated to remain open/active and/or have bound additional transcription factors (Massie, Adryan et al. 2007; Wang, Li et al. 2007; Jia, Berman et al. 2008; Wang, Li et al. 2009). Although it was initially thought that AR binding sites would be predominately located within proximal promoter regions, these non-biased whole genome approaches have uncovered that the majority of AR DNA occupancy occurs at non-promoter regulatory elements located greater than 10 kilobases away from the TSS of the nearest androgen regulated gene (Massie, Adryan et al. 2007; Wang, Li et al. 2007; Jia, Berman et al. 2008; Wang, Li et al. 2009). Whether these distal AR sites are directly involved in long-range control of gene transcription is unknown, however it has been proposed through the use of chromatin conformation capture (3C) experiments, that genes are configured into looped structures that juxtapose AR bound enhancer sites and allow focal regulation of genes at transcriptional hubs (Kadauke and Blobel 2009).

1.6.3.3 Ligand binding domain

The LBD consists of the carboxyl 250 amino acids and is encoded by exons 4 through to 8. The crystal structure of the AR-LBD displays a similar three dimensional structure to the other steroid receptors. This domain consists of 12 alpha helices and 4 beta strands arranged in a 3 layer alpha helical structure when bound to ligand (Matias, Donner et al. 2000). High affinity androgenic ligands, such as T and DHT, make direct contact with alpha helices 3, 4, 5, 7 and 11 as well as one of the beta sheets, which results in significant intra-molecular conformational changes, and consequently results in the N/C interaction as described above. Whilst the AF2 pocket is a major site for the co-regulator binding, the actions of the N/C interaction with the ^{23}FQNLF^{27} motif in the AR-NTD prevents co-regulator interactions until the N/C interaction is lost upon DNA binding (van Royen, Cunha et al. 2007).

1.6.3.4 Hinge region

Several studies have now shown that the 41 amino acid hinge region is involved in multiple stages of the AR signalling axis, including AR cytoplasmic-nuclear shuttling, DNA binding and transactivation (Zhou, Sar et al. 1994; Moilanen, Rouleau et al. 1997; Wang, Lu et al. 2001). Somatic AR gene mutations in advanced prostate cancer samples co-localise to the amino acid sequence ^{668}QPIF^{671} peptide located at the boundary of the hinge region and the LBD. These mutations result in a 2-4 fold increase in AR transactivation activity, potentially through altered co-regulator interactions at this site (Buchanan, Yang et al. 2001). The hinge region is also subject to post-translational

modifications, such as phosphorylation and acetylation. Serine phosphorylation within the hinge region is conserved amongst the steroid receptors, and in the case of AR occurs at a serine residue at position 650 (S650) (Denner, Schrader et al. 1990). In addition, S650 forms part of the PEST sequence, comprising of amino acids 646-651, and acts as a signal for ubiqutin-dependent AR degradation by the 26S proteasome (Sheflin, Keegan et al. 2000). In support of this finding, the E3 ubiquitin ligase CHIP protein has been shown to interact with phosphorylated S650 (Rees, Lee et al. 2006).

In addition to phosphorylation, the AR hinge region is also susceptible to acetylation by the histone acetyltransferases p300/cAMP response element binding protein at a species conserved ^{629}RKKXKK^{633} motif (Fu, Wang et al. 2000). This region forms part of a larger AR nuclear localization sequence (NLS) (^{617}RKCYEAGMTLGARKLKK^{633}). The NLS is activated in a ligand-dependent manner, resulting in the translocation of the AR from the cytoplasm to the nucleus (Thomas, Dadgar et al. 2004; Haelens, Tanner et al. 2007; Cutress, Whitaker et al. 2008). The rate of AR nuclear translocation is regulated by proteins that can bind to the AR hinge region, for example, the co-chaperone SGTA is able to retain the non-ligand bound AR in the cytoplasm (for more details refer to section 1.11.5), whereas upon hormone activation, SGTA dissociates from the hinge region allowing the recruitment of SNURF and filamin proteins to actively traffic the AR into the nucleus (Ozanne, Brady et al. 2000; Poukka, Karvonen et al. 2000; Buchanan, Ricciardelli et al. 2007).

1.7 Androgen receptor co-regulators

The ability of the AR to activate gene transcription or repression involves not only the general transcriptional machinery, but also hundreds of other factors termed co-regulators, which fall into two broad classes, those that enhance (co-activators) or inhibit (co-repressors) gene transcription. Co-regulators can be further subdivided into two different categories depending on their functional characteristics. Type I or classical co-regulators have the ability to alter AR activity while the receptor is bound to DNA through the means of chromatin remodelling or the recruitment of the basic transcriptional machinery, whereas type II or non-classical co-regulators act by modulating AR protein stability, ligand binding, intra and intermolecular conformational changes, receptor sub-cellular localization and/or disrupting the interaction with other co-regulators (Heinlein and Chang 2002).

1.7.1 Co-activators

The best characterized AR co-activators are members of the p160 steroid receptor co-activator (SRC) family (SRC/p160). Proteins in this family contain intrinsic histone acetyltransferase (HAT) activity that facilitates the remodelling of chromatin, allowing the maintenance of transcriptionally opened sites of chromatin (McKenna, Lanz et al. 1999). Moreover, SRC/p160 members directly interact with the AR at multiple points within the AR-NTD and the AR-LBD AF2 through an LXXLL motif (Alen, Claessens et al. 1999; McKenna, Lanz et al. 1999). This function allows SRC/p160 proteins to act as a platform for secondary co-activators, such as CREB-binding protein (CBP)/p300, to be recruited to

the AR-chromatin complex, which then acts to further remodel the DNA as well as forming a bridge between AR and the basal transcriptional machinery (Dallas, Yaciuk et al. 1997; Fu, Wang et al. 2000).

1.7.2 Co-repressors

Whilst the role and activity of AR co-activators has been the centre of much research over the past decade, the mechanism of action by which co-repressors suppress AR transcriptional activity is less well understood. As many co-activators have histone acetylase activity to open transcriptional DNA hubs, co-repressors are able to recruit histone deacetylases (HDACs). Two of the best characterized co-repressors that mediate AR transcriptional repression via the recruitment of HDACs are silencing mediator for retinoid and thyroid hormone receptors co-repressor (SMRT) and the nuclear receptor co-repressor (NcoR). Both SMRT and NcoR are recruited to the AR bound chromatin in response to either antagonist (i.e. hydroxyflutamide) or agonist (i.e. DHT) treatment (Hodgson, Astapova et al. 2005; Yoon and Wong 2006). As previously mentioned in section 1.6.3.1 the AR N/C interaction plays an important role in AR protein stabilization, receptor dimerisation and ligand mediated transcriptional activity. The interaction of NcoR with both the NTD-AF1 and LBD-AF2 regions blocks the N/C interaction, an effect that can be reversed by the over expression of the co-activators SRC-1 and CBP (Wu, Kawate et al. 2006). The opposing roles of co-activators and co-repressors combined with their relative expression may therefore be critical for the regulation of AR transcriptional activity.

1.7.3 Chaperones

Chaperones are a collection of evolutionary conserved proteins that coordinate in multiple complexes to assist in the procedures of correct folding and maturation of client substrates. As such, many of these chaperone proteins are constitutively expressed in order to maintain the homeostatic balance of the intracellular proteome (reviewed in (Taipale, Jarosz et al. 2010). The family of heat shock proteins (Hsp) specifically function together to protect the proteome from misfolding and/or aggregation during times of exogenous stress, such as heat, hypoxia and acidosis in order to maintain cell survival (Zou, Cao et al. 2008).

One of the most important and highly conserved components of the chaperone system is Hsp90. The central role of Hsp90 is highlighted by its ability to interact with approximately 200 different client proteins, many of which are involved in essential signalling transduction pathways, such as the steroid receptors (Pratt and Toft 1997; Zhao, Davey et al. 2005). The Hsp90 amino terminal domain contains an ATP binding site that is utilised for the hydrolysis of ATP to ADP, whereas the carboxyl terminus allows the formation of Hsp90 homodimers (Prodromou, Roe et al. 1997; Ali, Roe et al. 2006). However, Hsp90 ATPase activity ultimately requires the presence of approximately 20 accessory proteins termed co-chaperones (Taipale, Jarosz et al. 2010). Located within the Hsp90 carboxyl terminus is a 5 amino acid motif (MEEVD) that formulates a highly conserved tetratricopeptide repeat (TPR) binding site (Scheufler, Brinker et al. 2000). The association of TPR co-chaperones at the MEEVD motif can regulate both Hsp90 ATP hydrolysis and interaction with client proteins (Scheufler, Brinker et al. 2000). Other

chaperones that are essential for protein maturation include Hsp70 or its constitutively expressed form Hsc70, which are both functionally similar to Hsp90, as they also possess an amino terminal domain capable of ATPase activity and a carboxyl terminal EEVD TPR binding motif (Nicolet and Craig 1991; Scheufler, Brinker et al. 2000). The coordination between Hsc/Hsp70, Hsp90 and the TPR containing co-chaperones provide a stable framework in which the intracellular proteome is maintained during cellular stress responses. However, it has been shown that cancer cells are able to utilise the molecular chaperone system in order to maintain homeostasis and promote cell survival and proliferation (Trepel, Mollapour et al. 2010). This is generally achieved via the Hsp90 complex protecting and stabilising many intracellular cellular proteins, including over expressed oncoproteins, such as the AR in prostate cancer.

1.8 The molecular chaperone complex and androgen receptor maturation

Historically, the role and importance of the molecular chaperone system in steroid receptor biology has focused primarily on GR, PR and ERα/β (reviewed in (Pratt and Toft 1997). Given the structural and functional homology that exists between all of the steroid receptors it is likely that a similar mechanism of chaperone action exists for AR protein maturation and function.

Molecular chaperones were initially discovered by their ability to recognise and shield exposed hydrophobic regions of unfolded or partially folded proteins, preventing unproductive interactions, such as irreversible aggregation (Zou, Cao et al. 2008; Taipale,

Jarosz et al. 2010). Under normal physiological conditions the interactions between molecular chaperones and steroid receptors facilitate a structured sequence of receptor folding leading to the generation of a high affinity ligand binding pocket (Figure 1.3). In general terms, during the processes of translation and release from the ribosomal complex, the nascent receptor undergoes a series of binding and release cycles by Hsc70. After the initial interaction with Hsc70, the recruitment of heat shock protein (Hsp) 40/Ydj1 and the Hsp70 co-chaperone heat shock interacting protein (Hip/p48) stabilizes the intermediary chaperone complex on the nascent peptide allowing time for local folding to occur (Cyr 1995; Bukau and Horwich 1998). Heat shock organizing protein (Hop/p60) then binds to the complex, allowing for the recruitment of a homodimer of Hsp90 (Freeman, Felts et al. 2000). The inclusion of Hop within the chaperone complex not only acts as a bridge between the Hsp90 and Hsp70 proteins, it contributes to the efficacy of protein folding, by inducing conformational changes within both Hsp client proteins (Pratt, Galigniana et al. 2004).

During the final stages of maturation the receptor acquires a high affinity ligand binding conformation. This is achieved through the interaction between the co-chaperone p23 and Hsp90, which stabilises the Hsp90-receptor interaction (Freeman, Felts et al. 2000; Davies, Ning et al. 2002; Georget, Terouanne et al. 2002). The addition of p23 into the complex also results in the displacement of Hip, Hop and Hsp70 allowing the recruitment of one of a number of TPR containing co-chaperones such as the immunophilins FK506 binding protein (FKBP) 51 and 52, cyclophilin 40 (Cyp40), the serine/theronine protein phosphatase 5 (PP5) or SGTA to either restrain the receptor in a relatively steady mature

complex for ligand binding or actively process the receptor for transportation into the nucleus once ligand is bound (Smith 2004). Details of the biological and molecular actions of TPR proteins in AR signalling will be discussed further in section 1.11.

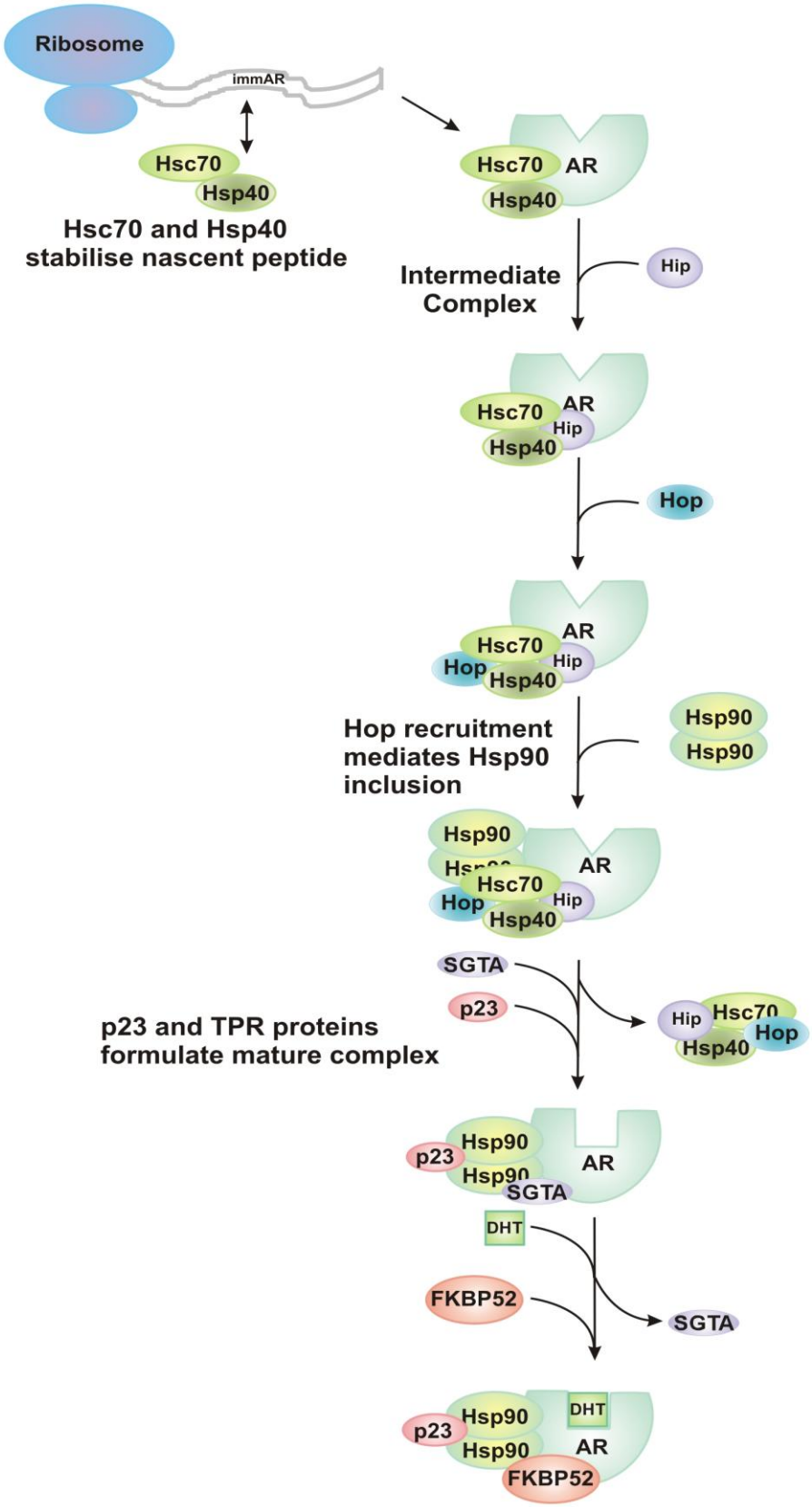

Ribosome
immAR
Hsc70
Hsp40
Hsc70 and Hsp40
stabilise nascent peptide
Hsc70
AR
Hsp40
Intermediate
Complex
Hip
Hsc70
AR
Hip
Hsp40
Hop
Hsc70
AR
Hop
Hip
Hsp40
Hop recruitment
mediates Hsp90
inclusion
Hsp90
Hsp90
Hsp90
Hsc70
AR
Hop
Hip
Hsp40
SGTA
p23
p23 and TPR proteins
formulate mature complex
Hip
Hsc70
Hop
Hsp40
Hsp90
p23
Hsp90
AR
SGTA
DHT
FKBP52
SGTA
Hsp90
DHT
p23
Hsp90
AR
FKBP52

Figure 1.3: Androgen receptor maturation. The maturation of the nascent AR protein involves repetitive binding of heat shock protein (Hsp) 40 and Hsp70. The recruitment of Hsp interacting protein (Hip) forms an intermediary complex allowing Hsp organising protein (Hop) to recruit an Hsp90 dimer and p23. The dissociation of the Hsp70/40 complex and the recruitment of a tetratricopeptide repeat (TPR) containing co-chaperone (e.g. SGTA) allows the receptor to be stabilised for ligand (DHT) binding. Dissociation of TPR proteins allows the immunophilin FKBP52 to bind producing an AR capable of translocating from the cytoplasm into the nucleus. FKBP52; FK506 binding protein, 52 kDa; SGTA: small glutamine-rich tetratricopeptide repeat containing protein alpha; AR: androgen receptor; Hsp90: Heat shock protein 90; Hsc70: Constitutively expressed variant of heat shock protein 70; Hsp40: Heat shock protein 40.

1.8.1 Chaperones involved in ligand binding and nuclear translocation

The steroid receptor LBD is the primary binding site for chaperones, which may be due to either the loosely organized structure of the LBD in a hormone-free environment and/or the requirement for steroid receptors to generate a precisely ordered structure that is capable of binding ligands. The events of ligand binding to the LBD results in a conformational change that is similar amongst all steroid receptors. The biological difference between agonist and antagonist binding is a result of small, but functionally important differences in the induced structural conformation of the LBD. Agonist ligands will interact with alpha helices within the LBD, which results in the most carboxyl helix (helix 12) forming a lid over the ligand binding pocket. This action leads to the formation of the AF2 pocket, providing a surface permissible for the N/C interaction, whereas upon antagonist binding, helix 12 is displaced (Moras and Gronemeyer 1998). Even though molecular chaperones interact with the LBD to facilitate ligand binding, the role of chaperones in the process of helix 12 positioning is currently unknown. This may be due to either the transient nature of the Hsp70/Hsp90-AR interaction or the uncertainty of specific chaperone binding sites in the AR-LBD. Nonetheless it remains clear that receptors undergo a dynamic and constant folding/refolding cycle driven by conformational changes within Hsp90, until the steroid receptor LBD is in a state that is capable of binding ligand (Georget, Terouanne et al. 2002; Pratt, Galigniana et al. 2004).

Although the AR-LBD maybe a major site for chaperone interactions, it has been shown that the E3 ubiqutin ligase CHIP will interact with the similarly disorganised AR-NTD, resulting in AR ubiquitination and degradation (He, Bai et al. 2004). However, a later

report demonstrated that CHIP mediated AR degradation occurs via interactions between CHIP and the AR hinge region (Rees, Lee et al. 2006). Nevertheless, it appears that the outcome from the vast majority of interactions between chaperones and steroid receptors is to not only to maintain a competent structure, but also to regulate specific steroid receptor actions.

While partial disassembly of the chaperone complex from the steroid receptor is generally considered the first step that permits cytoplasmic-nuclear shuttling, it is not completely driven by ligand binding. Hsp90 mediated hydrolysis of ATP is considered to be the initiating event that leads to both the disassociation and recruitment of different TPR-containing co-chaperones within the complex (Smith, Schowalter et al. 1990; Smith, Stensgard et al. 1992). The conformational changes within the receptor that take place upon ligand binding formulate the secondary stages of TPR co-chaperone exchange, such as the displacement of FKBP51 and/or SGTA for either FKBP52, Cyp40, or PP5, which are all capable of recruiting the cytoskeleton transport protein dyenin (Davies, Ning et al. 2002; Davies, Ning et al. 2005; Buchanan, Ricciardelli et al. 2007), leading to the microtubule directed transport of the receptor into the nucleus via the nuclear pore (Figure 1.4).

The nuclear pore is a cylindrical channel embedded within the nuclear envelope. While small molecules are able to passively diffuse into the nucleus, proteins with a molecular weight greater than 40 kDa require active transportation by adaptor proteins called importins (Kaku, Matsuda et al. 2008). Both importin α and β are recruited as a heterodimer to the AR NLS located within the hinge region. After which, a small

guanosine triphosphatase (GTPase) directs the importins and their cargo into the nucleus (Kaku, Matsuda et al. 2008). Although the exact mechanism for the cytoplasmic-nuclear shuttling of AR still remains unclear, the importance of the TPR co-chaperones in regulating both AR cytoplasmic localization and transcriptional competence is exemplified by the discovery of SGTA within the Hsp90-AR complex and its ability to retain the receptor in the cytoplasm prior to ligand binding (Buchanan, Ricciardelli et al. 2007).

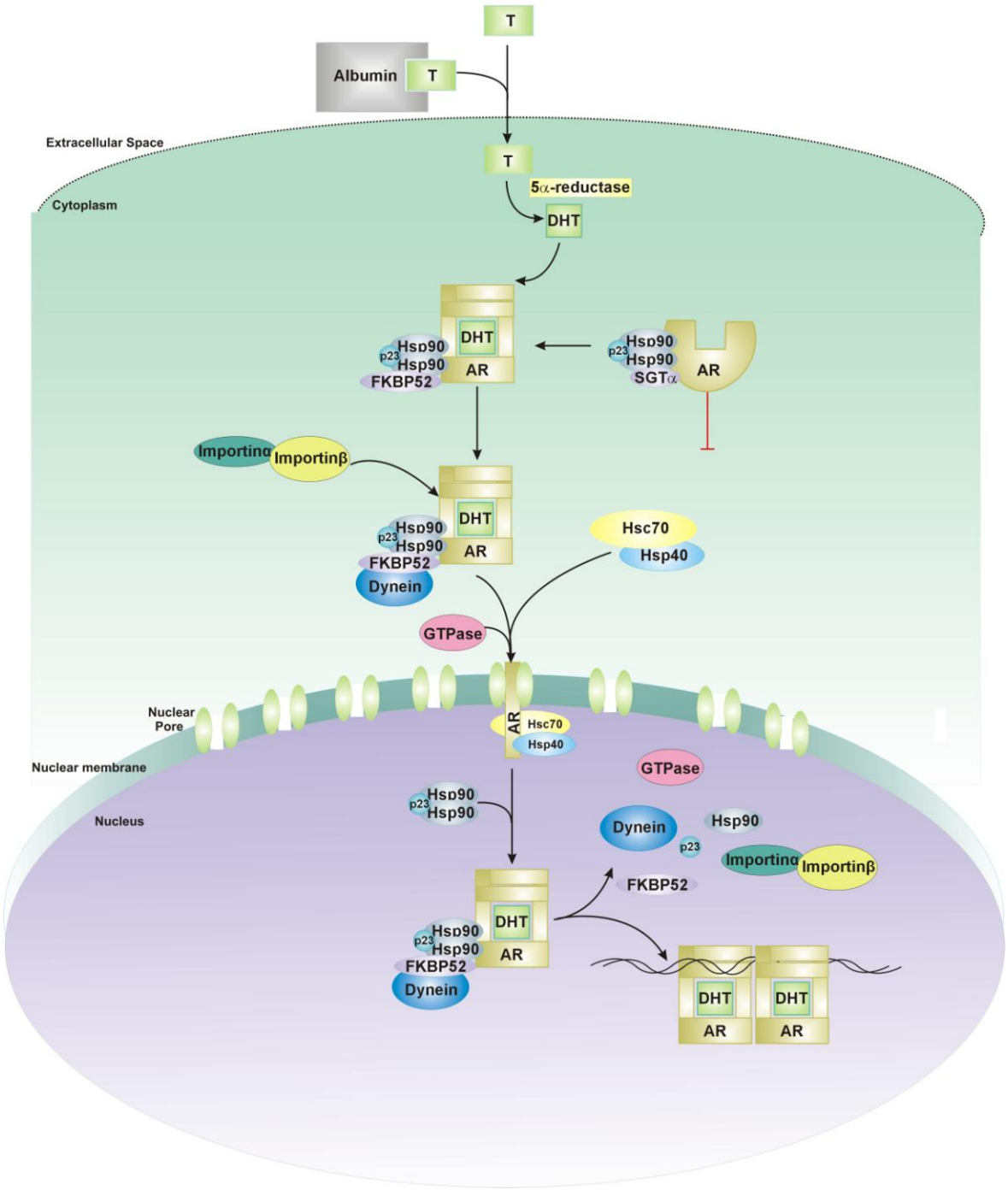

T
Albumin
T
Extracellular Space
T
5α-reductase
Cytoplasm
DHT
DHT
Hsp90
p23
Hsp90
FKBP52
AR
Hsp90
p23
Hsp90
SGTα
AR
Importinα
Importinβ
DHT
Hsp90
p23
Hsp90
FKBP52
AR
Dynein
Hsc70
Hsp40
GTPase
Nuclear
Pore
AR
Hsc70
Hsp40
Nuclear membrane
GTPase
Hsp90
p23
Hsp90
Nucleus
Dynein
Hsp90
p23
Importinα
Importinβ
FKBP52
DHT
Hsp90
p23
Hsp90
AR
FKBP52
Dynein
DHT
AR
DHT
AR

Figure 1.4: Cytoplasmic-nuclear AR shuttling. The ligand bound AR is stabilised through interactions with the Hsp90 molecular chaperone complex, which includes a Hsp90 dimer, p23 and the tetratricopeptide repeat (TPR) containing co-chaperone SGTA. Upon ligand (DHT) binding one of the TPR containing immunophilins FKBP52, Cyp40 or PP5, FKBP52 is shown here for clarity, is recruited. The immunophilins provide the capacity for the receptor to associate with the microtubule transport protein dynein, which carries the receptor into the nucleus. Hsc70, Hsp40, importin α and β are required for the transport of the receptor through the nuclear pores. A small GTPase protein is also necessary to direct this process. The presence of Hsc70 and Hsp40 indicates that localised unfolding and refolding of the receptor maybe required for the receptor to pass through the nuclear membrane. Components of the transport machinery dissociate from the AR in the nucleus, which allows the receptor to associate with DNA. FKBP52; FK506 binding protein, 52 kDa; SGTA: small glutamine-rich tetratricopeptide repeat containing protein alpha; AR: androgen receptor; Hsp90: Heat shock protein 90; Hsc70: Constitutively expressed variant of heat shock protein 70; Hsp40: Heat shock protein 40.

1.8.2 Chaperones and transcriptional activation

Aside from modulating AR protein maturation and ligand binding activities in the cytoplasm, there is direct evidence that molecular chaperones play a role in the regulation of AR-mediated gene activation and repression. For example, Bag-1L, an Hsp70-associated co-chaperone, interacts with the ligand bound AR-NTD at AF1. The AR-Bag-1L complex is recruited to the AREs located at the PSA promoter and enhancer regions, whereby Bag-1L acts to enhance AR transactivation activity (Froesch, Takayama et al. 1998; Shatkina, Mink et al. 2003). However, Bag-1L can also bind at these ARE sites in the absence of AR, perhaps as a means of priming the site for recruitment of AR, other co-activators and/or the general transcriptional machinery (Shatkina, Mink et al. 2003). Conversely, over-expression of the co-chaperone p23 acts to decrease AR transcriptional activity (Freeman, Felts et al. 2000). Mechanistically, this effect is thought to occur via p23, and to a lesser extent Hsp90, mediating the disassembly of chromatin-bound steroid receptor complexes, and thereby reducing gene transactivation (Freeman and Yamamoto 2002).

1.9 Chaperones in prostate cancer

One of the hallmarks of cancer is the enhanced utilization of the Hsp90 machinery to buffer the cell against multiple cytotoxic stresses within the microenvironment, but to also protect the proteome from misfolding and aggregation (Trepel, Mollapour et al. 2010; Hanahan and Weinberg 2011). It has been recognized that increases in chaperone activity facilitates “oncogene addition” allowing tumour cells to favour pro-survival, proliferative

and malignant phenotypes (reviewed in (Whitesell and Lindquist 2005; Trepel, Mollapour et al. 2010). Increased Hsp90 expression has been detected in both PIN and prostate cancer samples compared to adjacent non-malignant specimens (Cardillo and Ippoliti 2006). Indeed, in prostate cancer, altered expression of a number of chaperone proteins has been consistently documented. For example, in clinical samples of BPH, Bag-1L is exclusively expressed in basal cells. However, in prostate cancer expression is observed in the luminal epithelial cells, while absent in the basal cells. The expression patterns of Hsp70 match that of Bag-1L, highlighting a potential synergistic mechanism to enhance epithelial specific AR activity (Shatkina, Mink et al. 2003). Increased expression of the small molecular weight chaperone Hsp27 has also been reported to be associated with prostate cancer progression, high Gleason grade and castrate resistant disease (So, Hadaschik et al. 2007). Additionally, it has been demonstrated that expression of the Hsp90 associated co-chaperone Cdc37 interacts with the AR-LBD to increase hormone-dependent AR activity (Rao, Lee et al. 2001). Moreover, Cdc37 over-expressing transgenic mice display epithelial cell hyperplasia, while increased expression of Cdc37 has been observed in human prostate cancer specimens compared to normal tissue and that higher levels of Cdc37 leads to a pro-proliferative and anti-apoptotic phenotype (Stepanova, Yang et al. 2000; Schwarze, Fu et al. 2003).

It has also been reported that expression of several TPR containing co-chaperones is altered in prostate cancer progression, such that the levels of FKBP51 and Cyp40 are increased in metastatic disease, whereas the expression of SGTA in decreased (Buchanan, Ricciardelli et al. 2007; Periyasamy, Hinds et al. 2010). Given that these co-chaperones

have been found to influence AR protein maturation, subcellular localisation and transcriptional activity, these alterations in protein levels may act as contributing factors for enhanced AR activity with prostate cancer progression (Buchanan, Ricciardelli et al. 2007; Periyasamy, Hinds et al. 2010).

1.10 Chaperones as therapeutic targets

Over the past decade, our knowledge of the roles that chaperones play in cancer initiation and maintenance has dramatically increased and therefore the development of pharmacological modifiers of chaperone action has been an attractive option for potential anticancer agents. The Hsp90 inhibitor, 17-Allylamino-17-demethoxygeldanamycin (17-AAG), was the first agent to enter clinical trials in 1999, and currently there are now 13 Hsp90 inhibitors in either phase II or III clinical trials (Trepel, Mollapour et al. 2010). The majority of these inhibitors competitively block the Hsp90 ATPase binding pocket resulting in the degradation of client proteins (Solit and Rosen 2006; Chen, Sawyers et al. 2008). However, initial *in vitro* and *in vivo* studies highlighted several complications with these compounds, such as high levels of toxicity or partial AR agonist activity. These complications have halted the progress of Hsp90 inhibitors being clinically approved for the treatment of prostate cancer (Trepel, Mollapour et al. 2010). From these initial studies researchers have been expanding the spectrum of potential chaperone targets. Hsp27 has been investigated as a potential prognostic marker and drug target as its expression correlates with poor patient outcome (Foster, Dodson et al. 2009), and depletion of Hsp27 via oligodeoxynucleotides and short interference RNA results in a suppression of cell growth and increase in apoptosis (Liu, Rocchi et al. 2009).

It has been shown that each of the TPR co-chaperones displays a unique biological function and that their relative abundance affects the Hsp90-directed ligand binding, localisation and transcriptional activity of steroid receptors (Barent, Nair et al. 1998; Cheung-Flynn, Prapapanich et al. 2005; Yong, Yang et al. 2007; Schulke, Wochnik et al. 2010). Currently, the TPR co-chaperones are being actively investigated as an alternative means of targeting either Hsp90 activity and/or client proteins (Horibe, Kohno et al. 2011). Therefore, understanding the capacity for each of these factors to influence AR function within the prostate is essential.

1.11 Tetratricopeptide repeat containing co-chaperones

As discussed above, the family of co-chaperone proteins form a core component within the overall molecular chaperone machinery. An important sub-group within co-chaperones are a group of proteins that contain an evolutionary conserved protein-protein interaction domain known as the tetratricopeptide repeat (TPR) (D'Andrea and Regan 2003). These TPR containing co-chaperones serve as adapter molecules that can influence steroid receptor protein folding, maturation, transcriptional activity and degradation (Smith 2004). Listed in Table 1.1 are the known steroid receptor associated TPR co-chaperones, and a brief summary of the effect of their interactions with heat shock proteins and steroid receptors.

Table 1.1: Summary of known TPR containing co-chaperones, interactions with heat shock proteins, steroid receptors and consequences of those interactions.

TPR Co-chaperone	Heat Shock protein Interaction	Steroid Receptor Interaction	Effect of Interaction	References
Hop	Hsp70, Hsp90	PR, GR	• Promotes assembly of Hsp90-steroid receptor complexes	(Dittmar, Hutchison et al. 1996; Chen and Smith 1998)
Hip	Hsp70, Hsp90	PR, GR	• Assists Hop in chaperone-steroid receptor complex assembly	(Pratt and Toft 1997)
FKBP51	Hsp90	MR, PR, GR and AR	• MR cytoplasmic retention • Decreases GR ligand binding affinity • Decreases steroid receptor transcriptional activity	(Denny, Valentine et al. 2000; Scammell, Denny et al. 2001; Gallo, Ghini et al. 2007; Schulke, Wochnik et al. 2010)
FKBP52	Hsp90	MR, PR, GR, and AR	• Increases Hsp90 ATPase activity • Transports steroid receptors to the nucleus • Enhances steroid receptor transcriptional activity	(Davies, Ning et al. 2002; McLaughlin, Smith et al. 2002; Schulke, Wochnik et al. 2010)
PP5	Hsp70, Hsp90	MR, PR, GR, ERα and AR	• Protein phosphatase activity • Inhibits steroid receptor transcriptional activity	(Chen, McPartlin et al. 1994; Chinkers 1994; Schulke, Wochnik et al. 2010)

TPR Co-chaperone	Heat Shock protein Interaction	Steroid Receptor Interaction	Effect of Interaction	References
Cyp40	Hsc70, Hsp90	GR, MR, ERα, AR	• Promotes protein folding • Inhibits AR activity	(Ratajczak and Carrello 1996; Periyasamy, Hinds et al. 2010)
CHIP	Hsp70, Hsp90	PR, GR, ERα and AR	• Inhibits Hsp70 ATPase activity • Ubiquitin ligase activity results in protein degradation	(Connell, Ballinger et al. 2001; Kampinga, Kanon et al. 2003; He, Bai et al. 2004; Fan, Park et al. 2005)
Tpr2	Hsp70, Hsp90	PR, GR, MR and AR	• Enhances Hsp70 and Hsp90 ATPase activity • Inhibits steroid receptor transcriptional activity	(Brychzy, Rein et al. 2003; Schulke, Wochnik et al. 2010)
XAP2	Hsp90	?	• Inhibits GR, PR and AR activity	(Schulke, Wochnik et al. 2010)
SGTA	Hsc70, Hsp70, Hsp90	AR	• Inhibits Hsc/Hsp70 ATPase activity • Inhibits AR nuclear translocation and transcriptional activity	(Liu, Wu et al. 1999; Angeletti, Walker et al. 2002; Buchanan, Ricciardelli et al. 2007)

1.11.1 Structure of TPR domain

The TPR motif is a structural region characterized by a variable number of tandem repeats made up of 34 amino acids (Lamb, Tugendreich et al. 1995). Each of these tandem repeats forms a helix-turn-helix motif that are packed together to create a series of anti-parallel alpha-helical hairpins when taken together create an amphipathic groove that serves as a protein-protein interaction surface (Scheufler, Brinker et al. 2000). X-ray crystallography experiments have determined the structures of multiple TPR domains as well as revealing a number of side chains that project into this groove that are involved in determining the specificity of interaction for each TPR protein (Smith 2004). This is supported by phylogenetic evidence that suggests while the TPR domain of these chaperones is structurally conserved, each of the TPR co-chaperones has evolved different functional characteristics that may offer specificity for steroid receptor signalling. Indeed, as cellular systems became more complex, the synthesis of "fine-tuning" or "regulatory" TPR proteins such as SGTA, Cyp40, FKBP51 and FKBP52 allowed for a greater control over steroid receptor activity and the overall cellular response to hormone signals (Schlegel, Mirus et al. 2007).

1.11.2 Hsp90 and Hsp70 TPR binding sites

The TPR containing co-chaperones are able to integrate into the Hsp70/Hsp90 chaperone complex via interactions between the co-chaperone TPR domain and the conserved EEVD motif in the carboxyl terminus of Hsp70 and Hsp90 (Ratajczak and Carrello 1996; Chen, Sullivan et al. 1998; Carrello, Ingley et al. 1999; Russell, Whitt et al. 1999). The TPR co-

chaperones FKBP51, FKBP52, Cyp40 and PP5 contain several highly conserved basic residues that form a structure known as a two-carboxylate clamp, which protrudes into the TPR binding groove to create the electrostatic interactions required to anchor the TPR domain to the EEVD motif (Russell, Whitt et al. 1999; Scheufler, Brinker et al. 2000; Ward, Allan et al. 2002; Sinars, Cheung-Flynn et al. 2003; Wu, Li et al. 2004). Data generated from competition assays between different TPR co-chaperones and Hsp90 has revealed that the Hsp90 MEEVD motif displays binding specificity for one TPR protein over another (Owens-Grillo, Czar et al. 1996; Chen, Sullivan et al. 1998; Young, Obermann et al. 1998).

Although residues in the TPR domain and EEVD motif may be essential for the association of TPR proteins with Hsp70/90, additional investigations using deletion mapping and protein crystallography have demonstrated regions adjacent to the TPR domain also contribute to the stability of the TPR-Hsp70/90 interaction. Meanwhile, hydrophobic residues upstream of the EEVD motif, such as the Hsp90 homodimerisation domain can dictate the specificity of TPR binding (Ratajczak and Carrello 1996; Barent, Nair et al. 1998; Chen, Sullivan et al. 1998; Scheufler, Brinker et al. 2000; Ward, Allan et al. 2002). Indeed, it appears the sequence similarity between TPR domains of different co-chaperones offers a finite contribution to the Hsp70/90 interaction, as shown by the ability of FKBP52 and Cyp40 to interact with Hsp90 deletion variants in a similar manner despite sharing less than 30% TPR sequence identify. Conversely, FKBP51, which shares approximately 60% sequence identify with FKBP52, displays a markedly different interaction with the same Hsp90 variants (Chen, Sullivan et al. 1998). Taken together,

these studies imply a high degree of specificity and selectivity for the incorporation of TPR containing co-chaperones into Hsp70/90-steroid receptor complexes, and importantly allows the potential for the development of TPR specific drugs to target the different effects TPR containing co-chaperones have of steroid receptor activity.

1.11.3 Regulation of Hsp70 and Hsp90 ATPase activity by TPR co-chaperones

The ability of both Hsp70 and Hsp90 to bind and modulate the folding of client proteins is ATP-dependent. Therefore, the presence of ATPase modulating co-chaperones offers a level of regulation of client activity. Although the Hsp90 ATPase domain resides within the amino terminus, this region alone is insufficient to hydrolyse ATP to ADP; rather Hsp90 requires the presence of regulatory elements within the carboxyl terminus to perform this activity (Prodromou, Siligardi et al. 1999). The mechanism of ATP hydrolysis is a dynamic process that involves a series of conformational changes within the Hsp90 structure. Firstly, Hsp90 utilise its carboxyl terminus to form a homodimer, which creates an "open" conformation, which allows ATP binding at the amino terminus. Upon nucleotide binding the two amino termini are drawn together in a series of conformational changes that forms the second dimerisation interface, which is called the "closed" conformation. Hsp90 in the closed conformation mediates ATP hydrolysis to ADP, after which the amino terminal domains are released from one another returning Hsp90 to the open state (Zuehlke and Johnson 2010). Several studies have determined that these specific Hsp90 conformations can dictate which co-chaperones it can interact with. For instance, p23 and Hop will only bind the closed conformation and arrest further ATP conversion,

whereas AhaI is an activator of ATP hydrolysis and interacts with the opened Hsp90 conformation (Johnson, Schumacher et al. 1998; McLaughlin, Sobott et al. 2006; Hessling, Richter et al. 2009; Zuehlke and Johnson 2010). Additionally, the binding of specific TPR co-chaperones can modulate the ATPase activity of Hsp70 and Hsp90, for example, the E3 ubiquitin ligase CHIP can attenuate Hsp70 ATPase activity during the GR degradation process (Connell, Ballinger et al. 2001; Kampinga, Kanon et al. 2003), and Tpr2 is able to increase the ATPase activity of Hsp70, which leads to the dissociation of Hsp90 from an Hsp70/90 complex (Brychzy, Rein et al. 2003; Kampinga, Kanon et al. 2003). Hop and p23 have also been shown to decrease Hsp90 ATPase activity, whereas SGTA decreases Hsc70 activity (Prodromou, Siligardi et al. 1999; Angeletti, Walker et al. 2002). In contrast, FKBP52 increases ATP hydrolysis when interacting with the GR heterocomplex, presumably during the energy-dependent steps of transporting the receptor into the nucleus (McLaughlin, Smith et al. 2002). Together, these results position the TPR containing co-chaperones as important regulations of the actions of Hsp70/90 on client protein activity.

1.11.4 The role of TPR co-chaperones in steroid receptor signalling

From more than 100 different TPR containing proteins currently known to be expressed in humans, only 8 have been found to exist in complexes with steroid receptors (Buchanan, Ricciardelli et al. 2007; Schulke, Wochnik et al. 2010) (Figure 1.5). Although direct interactions between TPR co-chaperones and steroid receptors have been reported (Schulke, Wochnik et al. 2010), the majority of interactions occur in conjunction with the Hsp70 and/or 90 molecular chaperone complex (Pratt, Galigniana et al. 2004). However, it has been proposed that the ability of each Hsp90 dimer to only interact with one TPR

protein per steroid receptor complex provides a means of generating functional specificity across the steroid receptors, as the TPR co-chaperones exhibit preferential binding to particular chaperone-receptor complexes. For example, PP5 is bound to GR in high concentrations, whereas FKBP51 will bind to GR, PR and MR complexes in preference of FKBP52. Cyp40, on the other hand, has been discovered in ERα complexes (Ratajczak, Carrello et al. 1993; Barent, Nair et al. 1998; Pratt, Galigniana et al. 2004). The partnership between TPR co-chaperones and steroid receptors offers a unique opportunity to investigate specific mechanisms of steroid receptor activity, as well as the important physiological roles that TPR co-chaperones play in coordinating the cells response to hormone signals from the extracellular environment. Described in the following sections are the effects of some of the TPR co-chaperones that are known to affect the latter stages of steroid receptor maturation and overall activity.

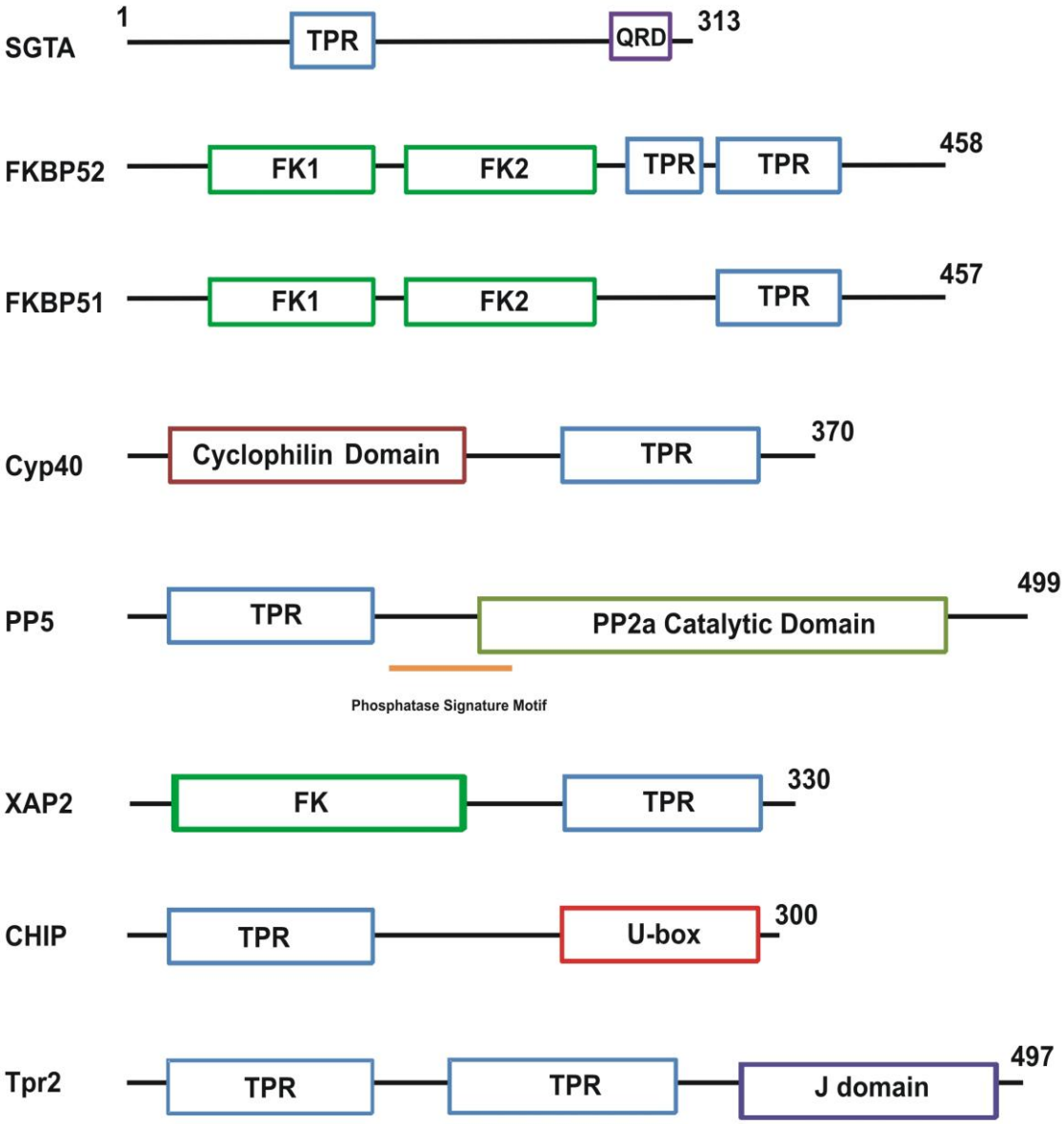

SGTA
1
TPR
QRD
313
FKBP52
FK1
FK2
TPR
TPR
458
FKBP51
FK1
FK2
TPR
457
Cyp40
Cyclophilin Domain
TPR
370
PP5
TPR
PP2a Catalytic Domain
499
Phosphatase Signature Motif
XAP2
FK
TPR
330
CHIP
TPR
U-box
300
Tpr2
TPR
TPR
J domain
497

Figure 1.5: Schematic representations of the 10 known steroid receptor associated tetratricopeptide repeat (TPR) co-chaperones. Structures delineate known location of TPR and other functional domains. SGTA: Blue box: TPR domain, Purple box: glutamine-rich domain (QRD); FKBP51/52: Green box: peptidylprolyl isomerase (PPIase) and FK506 binding domain, Blue box TPR domain; Cyp40: Red box: PPIase and cyclosporin A binding domain; PP5: Blue box: TPR domain, Green box: phosphatase domain; XAP2: Green box: PPIase and FK506 binding domain; Blue box: TPR domain; CHIP: Blue box TPR domain, Red box: E3 ubiqutin ligase (U-box) domain; Tpr2: Blue box: TPR domain, Purple box: Hsp70 interacting J-domain.

1.11.4.1 FK506 binding proteins (FKBP) 51 and 52

The immunophilin co-chaperones FKBP51 and FKBP52 were discovered through their ability to bind the immunosuppressive drug FK506 (Peattie, Harding et al. 1992). Both proteins share a similar domain organisation with approximately 75% amino acid sequence similarity. The amino terminus contains two PPIase domains (FK1 and FK2) that catalyse the *cis-trans* conversion of proline residues in nascent polypeptides. The PPIase domain is also the binding site for the immunosuppressant compounds FK506 and rapamycin (Peattie, Harding et al. 1992; Baughman, Wiederrecht et al. 1995), whereas the carboxyl terminus contains TPR domains that interact with Hsp90 (Sinars, Cheung-Flynn et al. 2003). A linker region that separates FK1 and FK2 provides both structural and functional diversity between the FKBPs, as shown by the exclusivity of FKBP52 phosphorylation at amino acids residue threonine 143, enables the transportation of GR into the nucleus (Cox, Riggs et al. 2007).

The physiological importance of the immunophilins is evident in the generation of homologous deletion knockout mice for *FKBP4*, the gene that encodes FKBP52 (Cheung-Flynn, Prapapanich et al. 2005; Yong, Yang et al. 2007). Female knockout mice were infertile due to a loss of uterine PR-A expression, whereas their male counterparts displayed penile hypospadias and prostate dysgenesis, but testicular formation and spermatogenesis remained normal, despite a 50% decrease in testicular AR protein levels. However, the Yong *et al* study failed to find these differences in AR protein levels, implying that the above phenotype may not be directly attributed to AR activity, although further analysis is required (Cheung-Flynn, Prapapanich et al. 2005; Yang, Wolf et al.

2006; Yong, Yang et al. 2007). Given that FKBP52 acts to increase the hormone binding capacity and mediates the nuclear translocation of AR, PR and GR complexes, the physiological effects observed in the FKBP52 knockout mice may be due to a loss in steroid receptor ligand sensitivity, nuclear transportation and/or transcriptional activity (Riggs, Roberts et al. 2003; Davies, Ning et al. 2005; Riggs, Cox et al. 2007).

As FKBP51 and FKBP52 share a high degree of sequence identity it could be assumed that their effects on steroid receptors may be similar. In contrast to the FKBP52 knockout mouse, FKBP51 null mice have normal male reproductive organs and are fertile (Yong, Yang et al. 2007). However, FKBP51 over expression is associated with glucocorticoid resistance in New World primates, which has been attributed to a decrease in GR hormone binding affinity (Denny, Valentine et al. 2000; Scammell, Denny et al. 2001), whereas up regulation of FKBP51 in castrate resistant prostate cancer promotes the assembly of the Hsp90-AR complex leading to enhanced AR activity (Ni, Yang et al. 2010). Collectively, these findings imply that the function of FKBP52 appears to be important in prostate organogenesis, whereas FKBP51 may play a greater role during the stages of disease initiation and progression (Periyasamy, Hinds et al. 2010).

1.11.4.2 Cyclophilin 40

The cyclosporin A binding immunophilin Cyp40 was one of the first TPR co-chaperones identified to interact with a steroid receptor (Ratajczak, Carrello et al. 1993). Structurally similar to FKBP51/52, Cyp40 contains a multifunctional cyclophilin domain at the carboxyl terminus with PPIase catalytic activity that is required for protein interactions and

binding cylcosporin A, while the amino terminus contains a TPR domain that links Hsp90 to client proteins (Ratajczak, Carrello et al. 1993; Ratajczak and Carrello 1996). The presence of an 8 amino acid insert loop that projects from the amino terminal of the cyclophilin domain allows Cyp40 to be sub-classified amongst 5 of the known 22 human cyclophilin proteins (Ratajczak, Ward et al. 2009). Site directed mutagenesis experiments have revealed that this divergent loop is important for cyclosporin A binding and interaction with different protein targets, but not for PPIase enzymatic activity (Liu, Chen et al. 1991; Dornan, Taylor et al. 2003). Moreover, an acidic linker region that separates the amino and carboxyl domains has been demonstrated to contain chaperone/protein folding activity, while also contributing to the interaction with Hsp90 (Ratajczak and Carrello 1996). Cyp40, like the other TPR co-chaperones, recognises the Hsp90 and Hsc70 EEVD TPR binding motif, although Cyp40 preferentially binds to Hsp90 over Hsc70 due to a number of hydrophobic residues within the TPR two carboxylate clamp (Carrello, Allan et al. 2004). Despite this preference, FKBP52 will act to exclusively displace the Hsp90-Cyp40 interaction (Owens-Grillo, Czar et al. 1996; Ratajczak and Carrello 1996; Carrello, Allan et al. 2004). This divergence in client protein recognition suggests that the TPR proteins may be able to dictate their actions to specific stages of the protein maturation cycle through competitive inhibition.

Recently it has been demonstrated that the levels of both FKBP51 and Cyp40 increase in clinical samples of prostate cancer progression from an androgen dependent state to castrate resistant disease (Periyasamy, Hinds et al. 2010). Moreover, the increase in FKBP51 and Cyp40 levels enhances AR transcriptional activity in a low hormone

environment, which leads to a pro-proliferative phenotype in prostate cancer cells (Periyasamy, Hinds et al. 2010).

1.11.4.3 Protein Phosphatase 5

Protein phosphatase 5 (PP5) is a member of the serine/threonine protein phosphatase family. Unlike the other protein phosphatases that exist in oligomeric complexes, PP5 remains in a monomeric form that is structurally comprised of an amino terminal TPR domain, a central PPIase-like domain that facilitates dynein binding and a carboxyl terminal phosphatase catalytic domain (Chen, McPartlin et al. 1994; Chinkers 1994; Hinds and Sanchez 2008). PP5 was the first of the co-chaperones to have its TPR domain crystal structure determined (Das, Cohen et al. 1998). Ten years later, the entire protein structure was crystallised, which further supported the fact that the presence of the TPR domain made PP5 structurally and functionally different from the other protein phosphatases (Yang, Roe et al. 2005). Whereas other protein phosphatases, such as PP1 and PP2A maintain a high basal activity, PP5 remains quiescent, due to the intramolecular positioning of the TPR domain that blocks access to the phosphatase catalytic site and thereby leaves PP5 in an auto-inhibited state until interaction with Hsp90 (Yang, Roe et al. 2005). Like many of the other steroid associated TPR co-chaperones, PP5 actively forms a complex with Hsp90 and Hsp70 (Hinds and Sanchez 2008). The high affinity interaction between Hsp90 and PP5 requires the displacement of the TPR domain from the PP5 carboxyl terminus, subsequently leading to the exposure of the catalytic site and stimulating phosphatase activity (Yang, Roe et al. 2005). The PP5 TPR domain is also

displaced and PP5 phosphatase activity generated in response to arachidonic acid and acyl-CoA (Chen and Cohen 1997; Zeke, Morrice et al. 2005).

As a regulator of protein phosphorylation, PP5 has been shown to participate in the modulation of cellular signalling pathways involved in growth arrest, apoptosis and DNA damage response (Zuo, Dean et al. 1998; Morita, Saitoh et al. 2001; Ali, Zhang et al. 2004). Additionally, PP5 over expression inhibits the transcriptional activity of ERα, PR, GR, and AR (Ikeda, Ogawa et al. 2004; Schulke, Wochnik et al. 2010). Increased levels of PP5 have been shown to increase breast cancer cell proliferation and are related to disease progression (Golden, Aragon et al. 2004; Golden, Aragon et al. 2008).

1.11.5 Small glutamine-rich tetratricopeptide repeat containing protein alpha

Contrary to the other steroid receptor TPR associated co-chaperones, SGTA does not possess any enzymatic activity for either protein folding (e.g. PPIase) or post-translational modifications (e.g. phosphatase). Rather, SGTA consists of three recognized domains, a centralized TPR, which is involved in interactions with Hsp90, Hsp70, growth hormone receptor and myostatin; a glutamine-rich carboxyl terminus that interacts with cysteine string protein, and an amino terminus region implicated in SGTA homodimerisation (Cziepluch, Kordes et al. 1998; Angeletti, Walker et al. 2002; Schantl, Roza et al. 2003; Tobaben, Varoqueaux et al. 2003; Wang, Zhang et al. 2003; Liou and Wang 2005) (Figure 1.6). Interestingly, the capacity of SGTA to form homodimers is unique amongst the steroid receptor associated TPR co-chaperones; however the requirement for SGTA

homodimerisation as a means of transmitting its effects onto client protein activity remains unknown.

The human SGTA gene is located on chromosome 19p13.3, which produces a protein that consists of 313 amino acids. SGTA was initially identified as a viral protein that interacts with the capsule proteins Gag and Vpu of the human immunodeficiency virus type 1 (HIV-1) and the non-structural protein, NS1, of the parvovirus (Callahan, Handley et al. 1998; Cziepluch, Kordes et al. 1998). The expression of SGTA in HIV-1 acts to inhibits the release of viral particles from infected cells, suggesting that SGTA may act to control the subcellular localisation of client proteins (Dutta and Tan 2008). Although the biological mechanism of SGTA action in viral protein synthesis and release remains obscure, it is evolutionary conserved and highly expressed in a wide variety of mammalian tissues (brain, liver, spleen, thymus, prostate, testis, ovary, colon, small intestine), indicating that SGTA may play an as yet undiscovered role that is integral to a common physiological process within these tissues (Cziepluch, Kordes et al. 1998; Kordes, Savelyeva et al. 1998; Winnefeld, Grewenig et al. 2006; Buchanan, Ricciardelli et al. 2007).

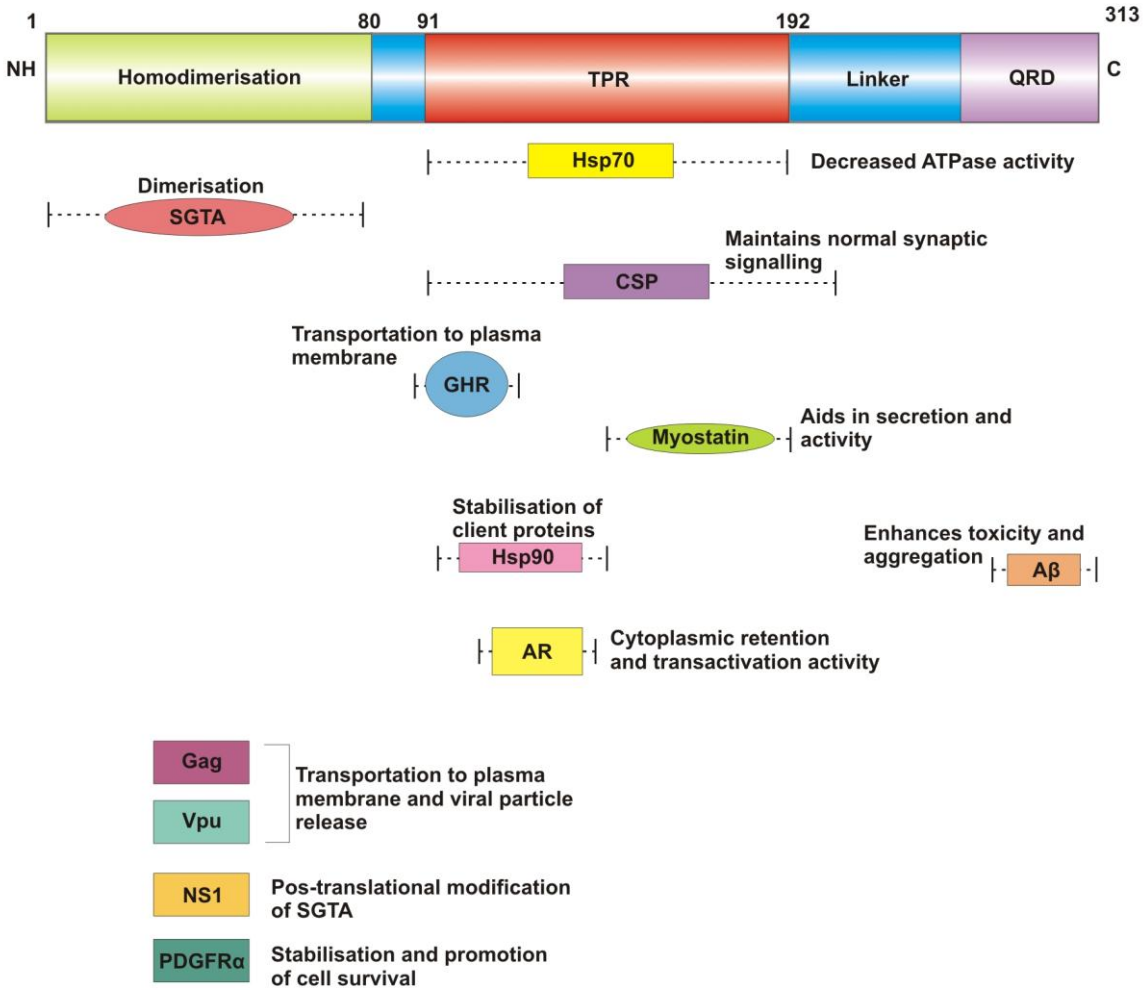


Figure 1.6 Schematic diagram of SGTA domains. Homodimerisation (amino acids 1-80); tetratricopeptide repeat (TPR; amino acids 91-192) linker region (amino acids 200-263) and glutamine-rich domain (QRD; amino acids 270-313). The interaction sites (if known) of its client proteins, with a brief description of known effects derived from the SGTA interaction have been delineated.

The SGTA TPR domain consists of three tandem TPR motifs that remain structurally conserved to other known TPR domains, despite a low degree sequence similarity. The crystal structure of the SGTA TPR domain revealed that it shares the highest level of similarity with the CHIP TPR domain, which includes several hydrophobic side chain residues that allow both TPR co-chaperones to interact with Hsp70 and Hsp90 respectively (Fonte, Kapulkin et al. 2002; Dutta and Tan 2008). Supportive evidence from other studies has demonstrated that SGTA interacts with the constitutively expressed Hsc70 and heat shock induced Hsp70, and inhibits the ATPase activity of both proteins (Liu, Wu et al. 1999; Angeletti, Walker et al. 2002). Although Hsp70 and Hsp90 share a similar TPR binding motif, the evidence for SGTA interacting with Hsp90 is not conclusive, whereby some studies have reported an interaction, while others have described either a weak or nonexistent interaction (Angeletti, Walker et al. 2002; Winnefeld, Grewenig et al. 2006). Taken together, these reports suggest that SGTA interacts strongly with the chaperone complex during the early stages of nascent protein refolding, while weakly interacting with Hsp90 during the latter stages. In support of a potential role in early protein maturation, knockdown of SGTA in an *Caenorhabditis elegans* model of Alzheimer's disease results in a decrease in animal paralysis by partially reducing the toxicity of intracellular beta amyloid (Aβ) protein accumulation (Fonte, Kapulkin et al. 2002). Further research into the biological function of SGTA by Winnefeld and colleagues has discovered a potential role in cell cycle and apoptosis (Winnefeld, Rommelaere et al. 2004; Winnefeld, Grewenig et al. 2006), which can be supported by the observation of an interaction between SGTA and critical tyrosine kinase cell surface receptors involved in cell proliferation and survival signalling pathways, such as the human growth hormone receptor (hGHR) and platelet

derived growth factor receptor alpha (PDGFRα) (Schantl, Roza et al. 2003; Moritz, Li et al. 2010).

Our laboratory was the first to identify SGTA as an AR interacting partner during a yeast two hybrid screen designed to investigate proteins that interact with the AR hinge region (Buchanan, Ricciardelli et al. 2007). Although SGTA is structurally dissimilar to the other steroid receptor associated TPR co-chaperones, it acts to inhibit AR nuclear transportation and transcriptional activity (Buchanan, Ricciardelli et al. 2007). The proposed positioning of SGTA interaction site in the AR hinge (^{638}KLQEEGEA^{645}) lies adjacent to the AR NLS, which may the influence the capacity for AR to translocate into the nucleus. A similar motif present in GR hinge region has been shown to interact with FKBP52 as a means of trafficking the receptor into the nucleus upon dexamethasone treatment (Owens-Grillo, Czar et al. 1996). It is therefore possible that SGTA may act to competitively block the FKBP52-AR interaction, and thus prevent AR cytoplasmic-nuclear transportation. Additionally, as SGTA is known to loosely co-localize with microtubules, the Hsp90-SGTA complex may tether AR to the cytoskeleton or associated microtubule proteins prior to hormone stimulation (Handley, Paddock et al. 2001; Winnefeld, Rommelaere et al. 2004). Moreover, SGTA levels are significantly lower in clinical samples of metastatic prostate cancer compared to primary and non-malignant disease, which was concomitant with an observed increase in AR levels and nuclear localisation (Buchanan, Ricciardelli et al. 2007). This suggests that the loss of SGTA in conjunction with a gain of AR levels may provide a permissive environment for enhanced AR activity. However, the biological consequences of lower SGTA levels in prostate cancer have yet to be revealed.

Nevertheless, as a relatively new member of the steroid receptor associated TPR co-chaperone family, deciphering the mechanisms of SGTA action on androgen signalling may offer a unique and specific way of disrupting AR activity in prostate cancer.

1.12 Conclusions

In conclusion, the physiological actions of androgens are mediated through the AR during all stages of normal prostate development as well as prostate cancer initiation and progression. Although both the production of androgens and the AR have been direct therapeutic targets in the treatment of prostate cancer, they invariably fail over time; allowing the cancer to progress to a castrate resistant state. The maintenance of prostate cancer growth in a castrate environment is not due to a loss of sensitivity to hormone, but rather the persistence of an active AR signalling axis. Hence, understanding the mechanistic actions of the initiating stages of the AR signalling pathway has already led to novel ways of inhibiting AR activity. In particular, the molecular chaperone complex, which plays a vital role in the cellular processes of steroid receptor folding, ligand binding, nuclear translocation, transcriptional activity and degradation, has been selected as a novel therapeutic target for the treatment of prostate cancer. During the late stages of AR maturation, several TPR-containing co-chaperones, such as SGTA associate with the Hsp90-receptor complex. SGTA acts prior to ligand binding to retain AR in the cytoplasm thus altering its absolute transactivation activity. However, the capacity for SGTA to affect AR activity across multiple responsive loci in the prostate genome has yet to be assessed, while the specific structural regions of SGTA that mediate these effects remain unknown. In particular, understanding the requirement of the SGTA homodimerisation domain may

help define how SGTA mediates its inhibitory effects on AR activity, and offer a means of specifically targeting the AR in prostate cancer. Finally, given that SGTA levels decrease with prostate cancer progression, the characterisation of the broad biological function of SGTA in prostate cancer cells will help delineate the potential consequences an alteration in SGTA levels may have on AR activity and the growth of prostate cancer cells.

1.13 Objectives of this thesis

The overall objective of this thesis is to define the actions of the co-chaperone protein SGTA in the AR signalling axis, as well as assess the functional effects of altering SGTA levels in prostate cancer cells.

Therefore the aims of this thesis are to:

1. To decipher the nature of the SGTA homodimerisation domain and determine the contribution that SGTA homodimers make to AR activity

2. To determine the requirement of discrete SGTA domains for the biological control of AR function

3. To investigate the functional consequences a loss of SGTA has on the transcription profile of prostate cancer cells

4. To assess if SGTA plays a role in the proliferation of prostate cancer cells *in vitro*

CHAPTER 2

Materials and Methods

Chapter 2: Materials and Methods

2.1 Materials

Reagents	Reagent Supplier
5α-dihydrotestosterone (DHT)	Sigma-Aldrich (St Louis, MO, USA)
Acrylamide/Bis solution	BioRad Laboratories (Hercules, CA, USA)
Agarose, analytical grade	Promega Corporation (Madison, WI, USA)
Agarose gel running apparatus	BioRad Laboratories (Hercules, CA, USA)
Ampicillin	Sigma-Aldrich (St Louis, MO, USA)
Anti-AR (N-20) Rabbit Polyclonal Antibody	Santa Cruz Biotechnology (Santa Cruz, CA, USA)
Anti-AR (C-19) Rabbit Polyclonal Antibody	Santa Cruz Biotechnology (Santa Cruz, CA, USA)
Anti-calnexin Mouse Polyclonal Antibody	Affinity Bioreagent (Golden, CO, USA)
Anti-ERα (HC-20) Rabbit Polyclonal Antibody	Santa Cruz Biotechnology (Santa Cruz, CA, USA)
Anti-Flag M2 Mouse Polyclonal Antibody	Sigma-Aldrich (St Louis, MO, USA)
Anti-FKBP51 (H-100) Rabbit Polyclonal Antibody	Santa Cruz Biotechnology (Santa Cruz, CA, USA)
Anti-FKBP52 Rabbit Polyclonal Antibody	Santa Cruz Biotechnology (Santa Cruz, CA, USA)
Anti-GAL4-DBD Rabbit Polyclonal Antibody	Santa Cruz Biotechnology (Santa Cruz, CA, USA)
Anti-HA Rabbit Polyclonal Antibody	Santa Cruz Biotechnology (Santa Cruz, CA, USA)
Anti-Hsp90 Rabbit Polyclonal Antibody	Santa Cruz Biotechnology (Santa Cruz, CA, USA)
Anti-Lamin A/C Rabbit Polyclonal Antibody	Cell Signaling Technology Inc (Dranvers, MA, USA)
Anti-Mek-1 Rabbit Polyclonal Antibody	Thermo Scientific (Fremont, CA, USA)
Anti-mouse IgG/HRP-conjugated	DakoCytomation (Glostrup, Denmark)

Anti-PR (C-19) Rabbit Polyclonal Antibody	Santa Cruz Biotechnology (Santa Cruz, CA, USA)
Anti-rabbit IgG/HRP-congugated	DakoCytomation (Glostrup, Denmark)
Anti-Alpha Tublin Mouse Monoclonal Antibody	Upstate (Temecula, CA, USA)
Anti-SGTA Mouse Polyclonal Antibody	Abnova (Neihu District, Taiwan)
Anti-SGTA Mouse Polyclonal Antibody	ProteinTech (Chicago, IL, USA)
BigDye™ Terminator	Applied Biosystems (Boston, MA, USA)
Bovine Serum Albumin (BSA)	New England Biolabs (Beverly, MA, USA)
Bradford Protein Dye Reagent	BioRad Laboratories (Hercules, CA, USA)
Bromophenol Blue	Sigma-Aldrich (St Louis, MO, USA)
Calcium Chloride	Ajax Finechem (Seven Hills, NSW, Australia)
Cells (COS-1, PC-3, LNCaP)	American Type Culture Collection (ATCC; Rockville, MD, USA)
CFX PCR cycler	BioRad Laboratories (Hercules, CA, USA)
Charcoal	Asia Pacific Specialty Chemicals (Seven Hills, NSW, Australia)
Complete Protease Inhibitor Cocktail Tablets	Roche Applied Science (Penzberg, Germany)
Deoxynucleotide Triphosphates (dNTPs) (10 mM) each	Promega Corporation (Madison, WI, USA)
Developer and Rapid Fixer	AGFA (Mortsel, Belgium)
Dexamethasone	Sigma-Aldrich (St Louis, MO, USA)
Dextran	Amersham Biosciences (Buckinghamshire, England)
DL-Dithiothreitol (DTT)	Sigma-Aldrich (St Louis, MO, USA)
DMSO	BDH Laboratory (Kilsyth, Vic, Australia)
DNA engine tetrad thermal cycler	BioRad Laboratories (Hercules, CA, USA)
ECL™ Hyperfilm™	Promega Corporation (Madison, WI, USA)
ECL™ Western Blotting Detection Reagents	Amersham Biosciences (Buckinghamshire, England)
Estradiol	Sigma-Aldrich (St Louis, MO, USA)

Ethylene-diamene tetra-acetic acid (EDTA)	Sigma-Aldrich (St Louis, MO, USA)
Ethanol (Molecular Biology Grade)	Ajax Finechem (Seven Hills, NSW, Australia)
Ethidium Bromide	Pharmacia Biotech (Seven Hills, NSW, Australia)
Foetal Calf Serum (FCS)	Sigma-Aldrich (St Louis, MO, USA)
Glycerol	Sigma-Aldrich (St Louis, MO, USA)
Glycine	Sigma-Aldrich (St Louis, MO, USA)
Glycogen	Roche Applied Science (Penzberg, Germany)
GraphPad Prism Statistical Software version 5	GraphPad Software Inc (La Jolla, CA, USA)
Hybond ^{TM}-C Extra Nitrocellulose Transfer Membrane	Amersham Biosciences (Buckinghamshire, England)
Hydrochloric Acid	Ajax Finechem (Seven Hills, NSW, Australia)
2 X iQ SYBR Green Supermix	BioRad Laboratories (Hercules, CA, USA)
iQ real time PCR cycler	BioRad Laboratories (Hercules, CA, USA)
Isopropanol (Molecular Biology Grade)	Ajax Finechem (Seven Hills, NSW, Australia)
Kanamycin	Sigma-Aldrich (St Louis, MO, USA)
L-Glutamine (100X)	Sigma-Aldrich (St Louis, MO, USA)
Luria Broth components	Becton Dickinson (Sparks, MD, USA)
Lipofectamine^{TM} 2000 Transfection Reagent	Invitrogen (San Diego, CA, USA)
Luciferase Assay System	Promega Corporation (Madison, WI, USA)
LumiStar Galaxy luminometer	BMG LABTECH (Morington, Vic, Australia)
Magnesium Chloride	Ajax Finechem (Seven Hills, NSW, Australia)
Methanol	Ajax Finechem (Seven Hills, NSW, Australia)
Microscope, inverted	Olympus America Inc (Center Valley, PA, USA)
My iQ software	BioRad Laboratories (Hercules, CA, USA)
Nanodrop spectrophotometer	Nanodrop Technologies (Wilmington, DE, USA)

Neuro Probe Chemotaxis system with 12 µm filter	Neuro Probe Inc (Gaithersburg, MD, USA)
Passive Lysis 5X Buffer	Promega Corporation (Madison, WI, USA)
PfU DNA Polymerase, including 10X buffer	Promega Corporation (Madison, WI, USA)
Phenol Red Free RPMI 1640 Liquid Medium (1X solution)	Sigma-Aldrich (St Louis, MO, USA)
Phosphate Buffered Saline (PBS)	Sigma-Aldrich (St Louis, MO, USA)
Progesterone	Sigma-Aldrich (St Louis, MO, USA)
QIAquick Gel Extraction Kit	QIAGEN (Hilden, Germany)
QIAquick PCR Purification Kit	QIAGEN (Hilden, Germany)
QIAGEN Plasmid Maxi Kit	QIAGEN (Hilden, Germany)
QIAprep Spin Miniprep Kit	QIAGEN (Hilden, Germany)
Restriction Digest Enzymes, including 10X Buffer and 100X BSA	New England Biolabs (Beverly, MA, USA)
RNeasy Spin Kit	QIAGEN (Hilden, Germany)
RPMI 1640 Liquid Medium (1X solution containing 2.05 nM L-Glutamine)	Sigma-Aldrich (St Louis, MO, USA)
SeeBlue Plus2 Pre-stained Protein Standard	Invitrogen (San Diego, CA, USA)
Shrimp Alkaline Phosphatase	Roche Applied Science (Penzberg, Germany)
Skim milk powder	Diploma (Melbourne, Vic, Australia)
Sodium Chloride	Ajax Chemicals (Auburn, NSW, Australia)
Sodium dodecyl sulphate (SDS)	Sigma-Aldrich (St Louis, MO, USA)
Sodium hydroxide	Sigma-Aldrich (St Louis, MO, USA)
Sodium molybdate	Sigma-Aldrich (St Louis, MO, USA)
iScript™ cDNA synthesis kit	BioRad Laboratories (Hercules, CA, USA)
Syringe with 25G needle	Becton Dickinson (Franklin Lakes, NJ USA)
Syringe filters, 0.2 µm	Nalgene (Rochester, NY, USA)
T4 DNA ligase including 10X buffer	Roche Applied Science (Penzberg, Germany)
Taq DNA polymerase	New England Biolabs (Beverly, MA, USA)
TEMED	Sigma-Aldrich (St Louis, MO, USA)

Tris	Sigma-Aldrich (St Louis, MO, USA)
Triton-X 100	Sigma-Aldrich (St Louis, MO, USA)
Trypsin (10X solution)	Sigma-Aldrich (St Louis, MO, USA)
Trypan blue	Sigma-Aldrich (St Louis, MO, USA)
Tween®20	Sigma-Aldrich (St Louis, MO, USA)
Vector NTi computer suite	Invitrogen (San Diego, CA, USA)
Whatman Filter	Whatman International Ltd (Maidstone, England)
Water	1. Sterilised reverse osmosis (RO) water 2. Baxter water (Baxter Healthcare, NSW, Australia) 3. Nuclease free water (Applied Biosystems, CA, USA)

2.2 Buffers and solutions

All solutions were stored at room temperature and made utilising RO water unless otherwise stated

10% APS
1 g APS in 10 mL water
Stored at -20°C

Dextran coated charcoal (DCC) in Tris/EDTA buffer

0.5% Charcoal	5 g
55 mM Dextran	0.5 g
20% Glycerol	100 mL

Made up to 1L in Tris/EDTA buffer and stirred overnight at 4°C

6X protein loading dye

4X Tris-Cl/SDS	7 mL
Glycerol	3 mL
SDS	1 g
DTT	0.93 g
Bromophenol Blue	1.2 mg

RIPA lysis buffer
10 mM Tris (pH 7.4)
150 mM NaCl
1 mM EDTA
1% Triton X-100
Made up to 100 mL with water
2X protease and phosphatase inhibitor tablets added, allowed to dissolve and 1 mL aliquots stored at -20°C

10X SDS-PAGE Glycine running buffer

Tris base	75.75 g
Glycine	360 g
SDS	25 g
Water	to 2.5 L

7.5% SDS-PAGE Separating gel

1 M Tris (pH 8.8)	3.75 mL
Acrylamide/Bis	1.9 mL
20% SDS	50 µL
10% APS	50 µL
TEMED	10 µL
Water	4.3 mL

SDS-PAGE Stacking gel

1 M Tris (pH 6.8)	625 µL
Acrylamide/Bis	500 µL
20% SDS	25 µL
10% APS	25 µL
TEMED	5 µL
Water	3.7 mL

10X SDS-PAGE Transfer buffer

25 mM Tris base	75.75 g
Glycine	360 g
Water	to 2.5 L

1X SDS-PAGE transfer buffer

Methanol	800 mL
10X transfer buffer	400 mL
Water	to 2.8 L

Stored at 4°C

50X Tris-acetate buffer

Tris base	242 g
Glacial acetic acid	57.1 mL
0.5 M EDTA (pH 8.0)	100 mL

Make to 1 L with water

10X TBS

0.5 M Tris	121.1 g
1.5 M NaCl	58.4 g
Water	to 2.5 L

pH to 7.4

TBS + Tween®20 (TBST)

Tween®20	5 mL
TBS	to 2.5 L

4X Tris-Cl/SDS

Tris-Cl	3.025 g
SDS	0.2 g

Made up Tris-Cl and pH to 6.8 prior to addition of SDS followed by the addition of water to a final volume of 50 mL

Tris/EDTA buffer

0.01 M Tris base	1.211 g
1.5 mM EDTA	0.588 g
0.01 Na_2Mo_4	2.42 g
10% Glycerol	100 Ml
Water	to 1 L

pH to 7.4

Trypan blue

0.01% trypan blue in sterile PBS

6X Type III load dye (Maniatis)

0.25%	bromophenol blue
0.25%	xylene cyanol FF
30%	glycerol in water

2.3 General Methods

Experimental procedures included in two or more chapters are reported in this section while more specific experimental detail is provided within each chapter.

2.3.1 Cloning procedures

2.3.1.1 Transformation of chemically competent cells

Bacterial cells were thawed on ice for 10 min and transferred to ice cold 15 ml centrifuge tubes. Approximately 10 ng of plasmid DNA was added to the cells, incubated on ice for 10 to 30 min, heat shocked at exactly 42°C for 45-50 sec and immediately incubated on ice for 2 min. Thereafter 900 µL of LB medium was added to the cells, which were then incubated at 37°C for 1 hr with shaking at 225 rpm. 300 µL of culture was spread onto LB-agar plates containing either 100 µg/mL ampicillin or 50 µg/mL kanamycin and incubated overnight at 37°C.

2.3.1.2 Isolation of plasmid DNA from bacterial cultures for sequencing

Liquid bacterial cultures were prepared by inoculation of 5 mL LB containing 50 µg/mL ampicillin or 50 µg/mL kanamycin with a single colony streaked from a glycerol stock or transformed according to the method described in section 2.3.1.1 and grown overnight at 37°C with shaking at 225 rpm. Plasmid DNA was prepared utilising the QIAprep spin Miniprep kit according to manufacturer's specifications. DNA was eluted in 40 µL TE buffer (pH 8.0). The plasmid DNA from both methods was quantified by UV spectrophotometry and diluted to appropriate concentration for transfection into

mammalian cells. Concentration of DNA was additionally verified by gel agarose electrophoresis.

2.3.1.3 Isolation of plasmid DNA from bacterial cultures for transfection

Depending on the quantity of DNA required for transfection, small 10 mL LB cultures or starter 5 mL LB cultures containing 50 μg/mL of the required selection antibiotic were prepared from a single colony on an LB-agar selection plate and shaken at 225 rmp at 37°C overnight or for 8 hr respectively. Plasmid DNA was isolated from the small culture using the QIAGEN plasmid mini kit according to the manufacturer's instructions and DNA was dissolved in 40 μL TE (pH 8.0). The 5 mL starter culture was utilised to inoculate 100 mL LB with required selection antibiotic at a dilution of 1:1000. This culture was grown overnight at 37°C with shaking at 225 rpm. The QIAGEN plasmid maxi kit was utilised to isolate plasmid DNA from the culture according to the manufacturer's instructions and plasmid DNA was dissolved in 200 μL TE (pH 8.0). The plasmid DNA from both methods was quantified by UV spectrophotometry and diluted to the appropriate concentration for transfection into mammalian cells. Concentration of DNA was additionally verified by gel electrophoresis.

2.3.1.4 Agarose gel electrophoresis

To make TAE-agarose gels, 100 mL TAE was added to the appropriate amount of analytical grade agarose (0.8 g for 0.8% gels and 1 g for 1% gels) and microwaved on high Watts for approximately 1 min until the particles were dissolved. The TAE-agarose was allowed to cool to approximately 60°C when 0.5 μg/mL of ethidium bromide was added and the gel was poured into a gel casting apparatus. Gels were allowed to cool for at least

30 min whereupon they were placed into a gel running apparatus and submerged in TAE. DNA was loaded into the wells with 1X load dye. The appropriate size DNA ladder (1 kB or 100 bp) was run in each gel. Typically running parameters were 100 volts for 40 min followed by visualisation under UV light.

2.3.1.5 PCR product purification

Products resulting from PCR were diagnosed by agarose gel electrophoresis, described in section 2.3.1.4. If the resulting product consisted of a single product without smearing, products were cleaned of PCR reagents and primers utilising the QIAquick PCR purification kit, according to the manufacturer's instructions. Products were eluted from the column with 30 µL TE (pH 8.0) or water, depending upon the downstream application.

2.3.1.6 Gel purification of PCR products and restriction fragments

Gel purification of PCR products was necessary for PCR products with smearing or with multiple products, and for the purification of all restriction fragments. The digested or PCR product was run on an agarose gel according to section 2.3.1.4. The required fragments or products were excised from the gel under long wave UV light, with time of exposure kept to a minimum. Bands in the gel were purified utilising the QIAquick gel extraction kit according to manufacturer's instructions and eluted in 30 µL of TE (pH 8.0) or water depending on downstream application.

2.3.1.7 Sequencing of plasmid DNA

Plasmids were sequenced utilising AmpliTaq^{TM} DNA polymerase FS dye terminator cycle sequencing chemistry with the ABI PRISM^{TM} BigDye^{TM} Terminator Cycle Sequencing

Ready Reaction Kit. Each sequencing reaction contained 100 ng plasmid DNA and 5 pM primer along with the required kit components. Reaction parameters were 96°C for 3 min, followed by the addition of the BigDye enzyme mix, then 25 cycles of 95°C for 10 sec, 55°C for 15 sec and 60°C for 4 min. Sequencing products were cleaned and precipitated by isopropanol precipitation.

2.3.1.8 Isopropanol precipitation of sequencing reactions

Sequencing reactions were precipitated and cleaned with the addition of 80 µL 100% isopropanol to the 20 µL sequencing reaction containing 1 µL glycogen as a DNA carrier. Reactions were incubated for 20 min at room temperature and then centrifuged at maximum speed in a microcentrifuge for 20 min. The supernatant was aspirated and the DNA was washed with 250 µL 100% isopropanol. The reactions were centrifuged for a further 5 min at maximum speed in a microcentrifuge, the supernatant was aspirated and pellets air-dried for 10 min. The IMVS molecular pathology service dissolved and ran the reactions on an ABI 377 automated sequencer, an in-house service offered to IMVS and University of Adelaide research students and staff.

2.3.1.9 Creation of point mutations and deletions in expression vectors

Point mutations or deletions in the SGTA cDNA within the expression vectors pcFH and pM-GAL4-DBD were created utilising either the one-step site directed or the two sided splicing by overlap extension PCR method (Horton, Hunt et al. 1989; Zheng, Baumann et al. 2004). For the creation of point mutations sense and antisense primers each containing the mutation was designed over the region to be mutated. These primers were used together in 50 µL PCR reactions utilising a proofreading polymerase, *Pfu* DNA

polymerase, with wildtype SGTA as the template. PCR reactions contained 1.5 mM $MgCl_2$, 10 mM dNTPs each, 20 mM Tris-HCl (pH 8.8), 10 mM KCl, 10 mM $(NH_4)_2SO_4$, 2 mM $MgSO_4$, 0.1% Triton® X-100, 0.1 mg/ml BSA, 100 ng each primer and 20 ng of pM-SGTA as template. These reactions were denatured for 5 min at 94°C before addition of 1 unit of *Pfu* DNA polymerase. Reactions cycled through the following conditions 16 times, 94°C for 1min; 52°C for 1min; 78°C for 12 min. Reactions then underwent a final extension at 68°C for 1 hr and then maintained at 4°C. For overlap extension PCR, sense and antisense primers were used separately in individual PCR reactions with either wildtype SGTA upstream or downstream sense and antisense primers utilising the PCR conditions described above. Reactions were cycled 40 times with the conditions listed in Appendix A1 for each specific primer pair. Both PCR products were gel purified according to section 2.3.1.6 and utilised as the template in a third PCR reaction containing the above reagents but using only the wildtype sense and antisense primers with the cycling conditions outlined in Appendix A1. This PCR reaction was either PCR or gel purified as described in sections 2.3.1.5 and 2.3.1.6 respectively and digested overnight with the appropriate restriction enzymes. The required length products were purified via gel purification and the fragment was ligated into the expression vector overnight at 16°C utilising T4 DNA ligase. The resulting plasmid mixture was transformed into DH5α bacterial cells and plasmid DNA was prepared utilising the procedures outlined in sections 2.3.1.2 and 2.3.1.3 respectively. All plasmids were restriction verified followed by sequence verification on both strands over the entire length of the PCR product and insertion sites. Sequence verified plasmids were then maxi- or mini-prepped for transfection according to the method outlined in section 2.3.1.3. Point mutations made in expression vectors are notated with the wildtype amino acid, amino acid number

and the variant amino acid, for example S31P – serine, amino acid number 31 mutated to proline.

2.3.2 Mammalian cell culture

2.3.2.1 Cell culture maintenance

Cell lines were maintained in growth medium which contained RPMI-1640 medium supplemented with 5-10% foetal bovine serum (FBS) at 37°C in 5% CO_2. All procedures were performed utilising aseptic conditions in a laminar flow cabinet. COS-1 and LNCaP cells were obtained from the American Type Culture Collection (Rockville, MD, USA). The $PC3^{AR+}$ subline used in this thesis was derived from long term culture of PC3 cells, which have been previously been described to contain AR mRNA, but non-functional AR protein (Buchanan, Craft et al. 2004). The PC3 cell line with a stably integrated luciferase reporter has also been previously described (Need, Scher et al. 2009). The C42B cell line used in this study was derived from subcutaneous LNCaP xenografts in castrated nude mice as described in (Wu, Hsieh et al. 1994).

2.3.2.2 Cell passaging

When cells reached 90% confluency, medium was aspirated from tissue culture flasks cells were washed with 5 mL room temperature sterile 1X PBS, replaced with 5 mL 1X trypsin and incubated at 37°C for 5 min. Once cells were detached from the flask, 20 mL growth medium was added and the cell suspension was centrifuged at 1500 rpm for 5 min. The supernatant was aspirated and cells were resuspended in 10 mL growth medium. An aliquot of cells was taken for cell counting utilising a haemocytometer with Trypan blue

exclusion, and 1 mL of cell suspension was placed into a new flask with 20 mL or 35 mL of growth medium for a T-75 or a T-150 flask respectively.

2.3.2.3 Freezing of cell lines

Cell were trypsinised as described above and resuspended in 4 mL medium containing 45% FBS, growth medium with 10% DMSO. Cell suspension was frozen in a Nalgene freezing apparatus at -1°C per minute down to -80°C. For long term storage, cells were placed in liquid nitrogen.

2.3.2.4 Thawing of cell lines

Stored frozen vials of cells were quickly thawed in a waterbath at 37°C and placed in 10 mL growth medium containing double the concentration of FBS (10%). The cell suspension was centrifuged for 5 min at 1500 rpm. Supernatant was aspirated and cells resuspended in growth medium containing 10% FBS before being placed into a T-25 tissue culture flask.

2.3.2.5 Charcoal stripping of foetal bovine serum (DCC-FBS)

Dextran coated charcoal (DCC) was centrifuged at 4000 rpm for 30 min at 4°C. Supernatant was discarded and 50 mL foetal bovine serum was added to the charcoal pellets and rotated for 2 hr at room temperature. The serum-charcoal was centrifuged at 4000 rpm for 30 min and serum transferred to new tubes containing fresh dextran-coated charcoal pellets, followed by 2 hr rotation at room temperature. The serum-charcoal was centrifuged at 4000 rpm for 30 min at 4°C and FBS was filtered sterilised and stored in 25 mL aliquots at -20°C.

2.3.3 General transfection methods

2.3.3.1 General transfection protocol and analysis of luciferase activity

AR negative human prostate cancer cells, PC3, human AR positive prostate cancer cells C42B and the transformed monkey kidney cells COS-1 were seeded in 96-well plates in RPMI-1640 medium containing 5% FBS at a density of 10,000, 20,000 or 25,000 cell/well and incubated for 24 hr. Immediately prior to transfection, cells were washed with serum free, phenol red free RPMI-1640 media. Transfection was performed for 4 hr in the same medium with the appropriate vectors (see sections below) mixed with LipofectAMINE^{TM} (0.4 μL for each 96 well) according to the manufacturer's protocol. Four hours after transfection, the reaction mix was carefully removed, and cells overlaid with stripped growth medium (phenol red free RPMI-1640 medium supplemented with 5% DCC-FBS) and 0.01-100 nM of the appropriate steroid (stock solution was dissolved in ethanol and added to the medium at no greater than 1 μL/mL) or ethanol carrier alone. Cells were incubated for 24 hr and then harvested directly from plates by adding 30 μL 1X passive lysis buffer per well and freezing overnight at -80°C. To assay for luciferase activity, plates were thawed on ice and 10 μL from each well was transferred to an optical plate and assayed immediately for reporter activity with the Luciferase^{TM} Assay System using a plate reading luminometer. The remaining sample for each experimental variable was pooled and cleared via centrifugation for 10 min at 10,000 rpm at 4°C. Lysate was transferred to fresh ice cold tubes and stored at -80°C until immunoblotting.

2.3.3.2 AR transactivation assays

For assays of AR transactivation in the presence of SGTA, the plasmid mix included 5 ng

of wtAR (pCMV-AR3.1) with 0-40 ng of full length SGTA or SGTA variant expression vectors (pcFH-SGTA) and 50 ng of the appropriate responsive reporter construct. For transfection of deletion variants, molar concentration of vector was kept constant via the addition of empty expression vector to account for equal numbers of promoters per well and total DNA was kept constant by the addition of the prokaryotic plasmid pBS(sk-) to the transfection mixes. Cells were treated with 0.01-100 nM DHT or vehicle (ethanol) for 24 hr and assayed for luciferase activity as described in section 2.3.3.1.

2.3.3.3 *In vivo* luciferase assay

For the *in vivo* luciferase assay, the PC3 luciferase stable cell lines were plated at a density of 15,000 cell/well in 96 well plates and allowed to adhere for 24 hr. Cells were transfected with 50 ng of pCMV-AR3.1 and 100 ng of pcFH-SGTA or an equivalent molar amount of the SGTA deletion expression plasmids while controlling for the total DNA transfected with the prokaryotic plasmid pBS(sk-). Cells were treated with 0.01-100 nM DHT or vehicle (ethanol) for 24 hr and assayed for luciferase activity as described in section 2.3.3.1.

2.3.3.4 Transfection of small interfering RNAs (siRNAs)

C42B cells were plated in 6 well plates at a density of 200,000 cell/well in 6 well plates and incubated for 24 hr. Immediately prior to transfection, cells were washed with serum free, phenol red free RPMI-1640 media. Transfection was performed for 4 hr in the same medium with the appropriate siRNAs mixed at a final concentration of 5 nM per siRNA with Oligofectamine^{TM} (15 μL for each well) according to the manufacturer's protocol. Four hours after transfection, cells were overlaid with stripped growth medium for a final

concentration of 5% and incubated for 24-72 hr. Cells were overlaid with 0.01-100 nM of the appropriate steroid (stock solution was dissolved in ethanol and added to the medium at no greater than 1 μL/mL) or ethanol carrier alone for 16-24 hr. Cells were either lysed for protein or RNA according to the method described in sections 2.3.5.3 and 2.3.6.1 respectively.

2.3.4 Mammalian two-hybrid interaction assays

2.3.4.1 SGTA homodimerisation assay

SGTA homodimerisation assays were performed in cultured COS-1 cells plated at a density of 20,000 cells/well in 96-well plates and allowed to adhere for 24 hr. Cells were transfected with 10 ng of pM-SGTA and pVP16-SGTA or equivalent molar amounts of the nominated SGTA variants and 25 ng of pGK-1 utilising 0.4 μL per well of LipofectAMINE^{TM} 2000 reagent. Each of the SGTA expression vectors were co-transfected with expression vectors containing a protein not known to interact with SGTA (e.g. pM-SGTA was co-transfected into cells with pVP16-T antigen) as a control for intrinsic activity, or inappropriate interaction due to over expression. DNA and molar concentration of expression vector was kept constant throughout all of the mammalian two-hybrid interaction assays. Cells were transfected for 4 hr, after which the transfection medium was replaced with DCC-FBS medium. Cells were left for 24 hr to allow luciferase expression and lysed in 30 μL passive lysis buffer per well and immediately placed at -80°C overnight. Plates were thawed on ice and 10 μL per well was measured for luciferase activity according to the method outlined in section 2.3.3.1.

2.3.5 Western blotting procedures

2.3.5.1 Western blotting utilising luciferase assay lysates

Luciferase assay lysate was prepared according to the method outlined in section 2.3.3.1 and an equal volume of this lysate (25 µL per well) was loaded onto a 7.5-15% SDS-PAGE gel. A protein standard was loaded into the left most lane on all western gels. These gels were run for 30 min at 15 mA, followed by approximately 1 hr at 25 mA, until the dye front left the bottom of the gel. Gels were then transferred to nitrocellulose membrane for 90 min at 250 mA. Membranes were then blocked for at least 1 hr in 5% skim milk powder in 1X TBST (Blotto). The primary antibody was diluted in 1% Blotto and placed on the membrane overnight at 4°C. Three 10 min washes of the membrane in TBST were performed before horse radish peroxidise (HRP)-conjugated immunoglobulins diluted 1:2000 in 1% Blotto were placed on the membrane for 30 min at room temperature. The membrane was washed three times for 10 min each in 1X TBST and bands were detected via ECL™ western blotting detection reagents and exposure to film according to the manufacturer's recommendations.

2.3.5.2 Transfection of cells to over express protein for western blotting

To prepare lysate of soluble proteins for western blotting, cells were transfected in 6 well plates (200,000 cells/well) according to the general method outlined in section 2.3.3.1, but scaled up to involve the transfection of at least 33 ng DNA per well and LipofectAMINE™ 2000 reagent at 10 µL per well. Cells for western blotting were treated with 0.01-10 nM DHT or the equivalent amount of vehicle (ethanol) and cells were left to over express the protein for at least 24 hr. Cells were then lysed according to the method

outlined in section 2.3.5.3.

2.3.5.3 Preparation of lysates in RIPA buffer

Cells for lysis were placed onto ice and growth medium was aspirated and replaced with 1 mL cold 1X PBS to wash the cells. The wash was aspirated fully and replaced with 150 µL cold RIPA buffer with phosphatase and protease inhibitors added. Cells were scraped from the surface of the dish utilising a sterile cell scraper and collected utilising a 25 gauge needle and syringe. Lysate was syringed 8 to 10 times and placed into cold 1.5 mL microcentrifuge tubes. Lysates were cleared via centrifugation for 10 min at 10,000 rpm at 4°C. The supernatant was collected and placed into fresh cold sterile microcentrifuge tubes. Protein concentration was determined utilising the method of Braford, outlined in section 2.3.5.4.

2.3.5.4 Bradford method to quantify protein concentration

Protein concentration in lysates was estimated according to the method of Bradford. This method involves the addition of a dye which binds primarily to basic and aromatic amino acids residues. Upon binding of proteins causes a colour shift in the dye. In a 96-well plate, 40 µL of Protein Assay dye reagent concentrate was added to 160 µL RO water for the blank standard and also to duplicates of 249, 248, 247, 246, 245 and 244 µL water for each of the standards to be created. Standards were then created by the addition of 1, 2, 3, 4, 5 and 6 µL of BSA at 0.1 mg/mL to each of these samples respectively. Lysates were prepared by the addition of 1 µL to 40 µL of Protein Assay dye concentrate with 159 µL RO water. Samples were mixed on a plate shaker for 10 sec and then allowed to sit at room temperature for 5 min before reading on an ultra microplate spectrophotometer at an

absorbance of 595 nm. A standard curve was generated utilising the readings from the BSA standards and lystate protein concentration calculated from this curve. An equal concentration of protein was loaded onto 7.5% SDS-PAGE gels and immunoblotted according to the method outlined in Section 1.3.5.1.

2.3.6 Real time PCR

2.3.6.1 Isolation of RNA from transfected cells

After transfection of cells according to the method outlined in 2.3.3.3, cells were placed onto ice and treatment medium was aspirated and replaced with 1 mL cold 1X PBS to wash the cells. The wash was aspirated and cells were lysed and RNA isolated utilising the RNeasy RNA isolation kit from QIAGEN according to the manufacturer's instructions. RNA was eluted from the column with 40 µL of nuclease-free water and 1 µL was utilised for spectrophotometry and run on an agarose gel to determine RNA integrity.

2.3.6.2 First strand cDNA synthesis

For all cDNA synthesis reactions, the iScript^{TM} cDNA synthesis kit was utilised and reactions were performed on 1 µg RNA according to manufacturer's instructions. All cDNA samples were diluted 1:20 and stored in -80°C. Control samples lacking RNA and one lacking reverse transcriptase were included in the synthesis reactions.

2.3.6.3 Real time PCR reactions

For real time PCR, 5 µL from all cDNA undiluted cDNA samples were pooled to create a standard curve which was run on each PCR plate. This sample was diluted serially, 1:5, 1:25, 1:125, 1:625 and 1:3125 in nuclease-free water. One µL of each RNA was

used per well on either the 96-well or 384-well reaction plate. RT-PCR was performed utilising the iQ SYBR green master mix and 5 pmol of sense and antisense primers listed in Appendix A3. The housekeeper gene *GAPDH* was used as a normalisation control. All reactions were performed in triplicate on the same plate with the following cycling parameters: 95°C for 3 min followed by 40 cycles of 95°C for 15 sec, 55°C for 15 sec and 72°C for 30 sec, and a melt curve performed from 55°C to 95°C at 0.5°C per 10 sec. Data were analysed using either iQ5 or CFX Manager software.

2.3.7 Statistical analysis

Statistical analysis was performed where indicated in the figure legends or specific methods sections utilising either Graphpad prism or R software.

CHAPTER 3

Characterisation of the SGTA

Homodimerisation Interface

Chapter 3: Characterisation of the SGTA homodimerisation interface

3.1 Introduction

The molecular co-chaperone family contains a specific class of tetratricopeptide (TPR) containing proteins that can integrate into the Hsp70 and/or Hsp90 chaperone complex during the processes of steroid receptor protein folding and maturation. Although it is known that the inclusion of TPR co-chaperones is not necessary for steroid receptor maturation, they act to fine tune different stages of the steroid receptor folding cycle, as well as modulate properties of steroid receptor function such as ligand binding, nuclear transportation and transcriptional activity (Pratt and Toft 1997; Prescott and Coetzee 2006).

The TPR domain is structurally conserved from prokaryotes to mammals and constitutes one of the most common repeat domain structures found in the proteome (Blatch and Lassle 1999). In general, the TPR domain acts as the mediator for interactions with client proteins, while the diversity of biological activities exhibited by these co-chaperones is generated through variable sequences flanking the TPR domain. For example, FKBP51 and FKBP52 contain peptidyl prolyl isomerase (PPIase) activity, which catalyses the *cis-trans* isomerisation of proline bonds and is considered to be a rate limiting step in protein folding (reviewed in (Galat 2003). Cyp40 also contains a structurally and functionally similar PPIase domain to the immunophilin co-chaperones (Ratajczak, Ward et al. 2009), whereas the serine/threonine phosphatase PP5, contains both PPIase-like and

phosphatase activity, which is actively involved in the dephosphorylation of GR upon oestrogen treatment (Zhang, Leung et al. 2009). CHIP, on the other hand, contains a U-box E3 ubiquitin ligase domain that allows direct ubiquitination of steroid receptors destined for proteasomal degradation (He, Bai et al. 2004; Wang and DeFranco 2005). The importance of these TPR proteins in steroid receptor signalling is exemplified by the generation of the FKBP52 knockout mouse, which displays an aberrant morphology in a number of hormone sensitive tissues. These physiological effects can be explained by the actions of the FKBP52 PPIase domain, which increases the hormone sensitivity of AR, GR and PR. Interestingly, the similarly structured FKBP51 does not display any of these physiological effects, suggesting that the TPR flanking regions provide a precise control mechanism over the biological function of specific TPR proteins (Riggs, Roberts et al. 2003; Cheung-Flynn, Prapapanich et al. 2005; Riggs, Cox et al. 2007; Yong, Yang et al. 2007).

SGTA is unique amongst the steroid receptor associated TPR containing co-chaperone family for two reasons. SGTA does not contain any intrinsic enzymatic activity and it is the only steroid receptor associated co-chaperone that is able to form a homodimer (Liou and Wang 2005). Despite the lack of enzymatic activity, our laboratory has demonstrated that SGTA is able to shift the sensitivity of AR ligand dependent activity and exclude the receptor from the nucleus (Buchanan, Ricciardelli et al. 2007). Structurally, SGTA contains three recognised domains; the centralised TPR involved in interactions with Hsp90, Hsp70, growth hormone receptor (GHR) and myostatin; a glutamine rich carboxyl terminus (QRD) that interacts with cysteine string receptor (CSP) and thereby alters synaptic transmission, and the homodimerisation domain (Cziepluch, Kordes et al. 1998;

Angeletti, Walker et al. 2002; Schantl, Roza et al. 2003; Tobaben, Varoqueaux et al. 2003; Wang, Zhang et al. 2003; Liou and Wang 2005).

While the biological necessity of SGTA homodimerisation in the interaction of SGTA with client proteins remains elusive, the formation of protein dimers is a common event during the activation of signal transduction pathways (Klemm, Schreiber et al. 1998). For instance, Hsp90 homodimerisation is required for ATPase hydrolysis, interaction with TPR co-chaperones, and the stabilisation of steroid receptors, all of which culminate in the events of ligand binding and transcriptional activity (Radanyi, Renoir et al. 1989; Smith, Whitesell et al. 1995; Czar, Galigniana et al. 1997; Grenert, Johnson et al. 1999).

Tobaben and colleagues were the first to identify that SGTA self associates during the validation of their yeast two hybrid screen for CSP interacting partners, however they did not determine the regions necessary (Tobaben, Varoqueaux et al. 2003). Broad deletion mapping experiments performed by Liou *et al* demonstrated that the SGTA amino terminus is necessary for the formation of SGTA homodimers (Liou and Wang 2005). Finally, initial investigations conducted in our laboratory demonstrated the requirement of the amino terminus for SGTA homodimerisation resided in the first 80 amino acids (Buchanan, Ricciardelli et al. 2007). Although, one study has demonstrated that deletion of the homodimerisation domain resulted in a 3 fold increase in the interaction between SGTA and the hGHR (Schantl, Roza et al. 2003), a comprehensive investigation of amino acid residues necessary for SGTA homodimerisation and its consequences for co-chaperone activity has yet to be conducted.

The requirement of homodimerisation for SGTA action on AR is also unknown. However,

given that Hsp90 generates one TPR binding site per steroid receptor complex, the maintenance of SGTA homodimers within the chaperone complex may be of particular importance for the regulation of AR activity. The aims of this chapter were to i) characterise the contribution of individual regions of the amino terminus to SGTA homodimerisation, ii) determine if the first 80 amino acids of SGTA are sufficient for homodimerisation, and iii) determine the effect of SGTA homodimerisation on AR transactivation activity.

3.2 Materials and Methods

3.2.1 Plasmids

Plasmids for mammalian two-hybrid and transactivation assays are listed in Appendix B1 and B2 respectively (Figure 3.1). Constructs specifically created for this thesis are described in detail below and listed in Appendix B. All constructs were sequenced verified on both strands by automated sequencing as described in chapter 2.3.1.7 before being prepared according to chapter 2.3.1.3 for use in transfections. SGTA expression vectors TAG: (SGTA, SGTA 1-270, SGTA 1-199, SGTA 80-313, SGTA 80-270, SGTA 80-200, SGTA Δ1-199, SGTA Δ200-263, SGTA 80-313 Δ200-263, SGTA 1-270 Δ91-192; where TAG indicates either the vP16 activation domain or the Gal4-D binding domain), AR expression vector pCMV-AR, pBS(sk-), androgen responsive ARR3-tk-Luc and the mammalian two-hybrid pGK-1 reporters have been previously described (Tilley, Marcelli et al. 1989; Buchanan, Craft et al. 2004; Buchanan, Ricciardelli et al. 2007). The pcFH-SGTA plasmid was generated in our laboratory.

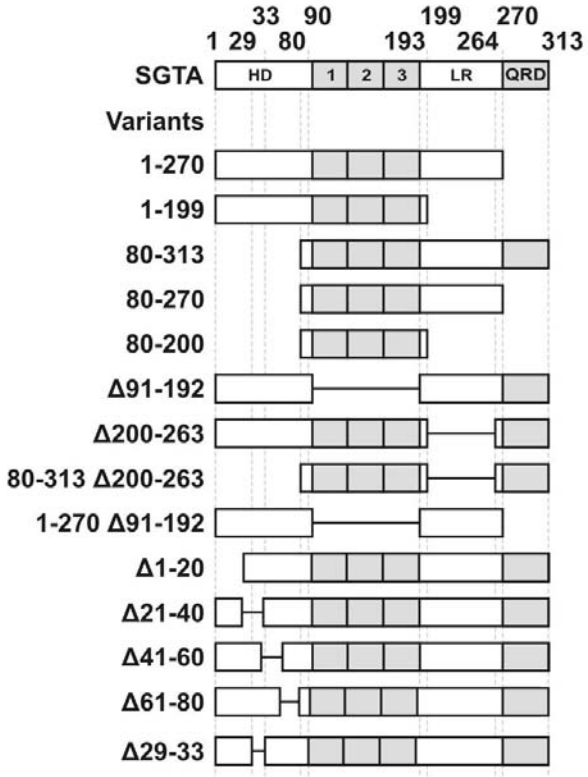


Figure 3.1: SGTA variants investigated in this study. Deletions of the SGTA coding sequence were created by two sided splicing with an overlap extension PCR method. Diagram represents SGTA homodimerisation domain (HD), TPR domains (1,2,3), linker region (LR) and glutamine-rich domain (QRD).

3.2.2 Creation of SGTA substitution and deletion variants

Deletion of regions containing amino acids 1-20, 21-40, 41-60, 61-80 and 29-33 in Gal4-DBD-SGTA was performed by overlap extension as described in chapter 2.1.3.9 utilising primers and PCR conditions listed in Appendix A1. Sequence verified deletion variants were subcloned into the vP16 expression vector utilising the restriction enzyme pair *EcoRI* and *XbaI*. The SGTA 1-80 sequence was amplified using the adapter primer method. Primers were designed with *XbaI* and *BamHI* restriction sequence at the 5' end of the sense and antisense primers respectively. The Gal4-DBD-SGTA expression vector was used as a template in PCR reactions utilising cycling conditions listed in Appendix A1. PCR products were purified according to chapter 2.3.1.5 and digested with *XbaI/BamHI* at 37°C overnight. Digested products were excised and purified by gel extraction according to chapter 2.3.1.6 and subcloned into the similarly digested and purified empty Gal4-DBD or vP16 vectors. The incorporation of the sequence was verified by restriction enzymatic digestion and automated DNA sequencing.

SGTA point mutations were created using the one step site directed mutagenesis method. Briefly, these substitutions were introduced into the pcFH-SGTA expression vector, which drives SGTA expression via the cytomegalovirus promoter (pCMV). Designated mutagenesis primers are listed in Appendix A1. PCR reactions were set up according to the method described in chapter 2.3.1.9. Presence of the desired base change was confirmed by automated DNA sequencing of both strands according to method in chapter 2.3.1.7 and 2.3.1.8 respectively. Primer sequences used in sequencing reactions are listed in Appendix A1.

Deletion of either the Flag or HA tags from the pcFH-SGTA expression vector were made using the long oligonucleotide cloning method. Briefly, overlapping primers were designed to amplify the Flag/HA region. The sequence of either Flag or HA was removed from the primer sequence depending on which tag was to be deleted. As in the adapter primer method described above, *EcoRI* and *XbaI* restriction endonucelase recognition sequences were designed at the 5' of sense and antisense primers respectively for deletion of the Flag tag, whereas *EcoRI* and *BamHI* were incorporated into the primer set designed to delete the HA tag. Digested products were excised and purified as described in chapter 2.3.1.6. Primers were reconstituted to a concentration of 100 pmol/µL in nuclease-free water. Ten µL of both sense and antisense primers were combined and heated at 95°C in a heating block for 5 min then allowed to slowly reach room temperature, allowing the primers to anneal. Annealed oligonucelotides were ligated into the appropriately digested pcFH vector as previously described above. Full length SGTA was subsequently subcloned into Flag tagged (pcF) or HA tagged (pcH) vectors utilising the *XbaI* and *BamHI* restriction sites. Correct orientation of the fragment was determined by restriction digest analysis and ligation sites verified by automated DNA sequencing utilising primers listed in Appendix A1.

3.2.3 SGTA phylogeny tree

Twenty species distinct SGTA protein sequences were downloaded into the Vector NTI computer suite. All accession numbers for protein sequences are indicated in the figure legend. The phylogenetic tree was generated utilising the AlignX program and was built using the Neighbor Joining method as described by Saitou and Nei (Saitou and Nei 1987).

The phylogeny tree was rooted using the androgen receptor *Homo sapiens* amino acid sequence.

3.2.4 Secondary structure prediction, residue composition and logo creation

The nnpredict online server (www.cmpharm.ucsf.edu/~nomi/nnpredict.html) (Katzman, Barrett et al. 2008) was used to define potential alpha helical and beta sheet structural elements in human SGTA. Amino acid composition analysis was performed using Composition Predictor (www.cprofiler.org/) with the number of bootstrap iterations set at 10,000 and p value < 0.05 (Vacic, Uversky et al. 2007). Serine, threonine and tyrosine amino acid phosphorylation prediction was performed using the NetPhos 2.0 online server (http://www.cbs.dtu.dk/services/NetPhos/) (Blom, Gammeltoft et al. 1999). Sequence logos were created using Weblogo (http://weblogo.berkeley.edu/).

3.2.5 Co-Immunoprecipitation

For co-immunoprecipitation of SGTA homodimers, COS-1 cells (2,000,000 cells/ 10 cm dish) were seeded in RPMI-1640 growth medium containing 5% FBS. Cells were co-transfected with pcH-SGTA and pcF-SGTA (5 µg each) or empty vector control utilising LipofectAMINE™ 2000 transfection reagent according to the manufacturer's protocol. Cells were incubated for 24 hours prior to the utilisation of one of the protocols described below.

Protocol 1: *CoIP lysis buffer*. After 24 hours incubation the transfection mix was aspirated and cells were washed twice with 5 mL ice cold 1X PBS, 500 µL of ice cold Co-IP lysis buffer (100 mM NaCl, 20 mM Tris (pH 7.5), 10% glycerol, 1% NP40, 10 mM $MgCl_2$, 2 mM EDTA, 1 mM DTT and 1X protease inhibitor) was added. Cells were scraped

and homogenised 6 times through a 26 gauge needle. Lysates were cleared by centrifugation (maximum speed for 10 min at 4°C) and supernatant was transferred into an ice cold 1.5 mL tube, while 10% of the supernatant was transferred into a separate tube. For protein immunoprecipitation, either 5 µg of anti-Flag antibody or normal anti-rabbit IgG isotype antibody control was added to the supernatant and incubated at 4°C overnight with rotation. Recombinant Protein G covalently attached to superparamagnetic Dynal® beads (Dynal® Protein G) were utilised to immunoprecipitate either anti-Flag or control antibodies. Prior to immunoprecipitation Dynal® Protein G beads (10,000,000 beads/sample) were washed by addition to 1 mL ice cold lysis buffer, inverted twice and then placed on a magnetic rack for 1 min, the lysis buffer was removed and replaced by fresh, ice cold lysis buffer and beads were resuspended by slow rotation for 5 min at room temperature. The wash process was repeated 3 times and beads resuspended in a final volume of 80 µL lysis buffer. Lysates containing anti-Flag or control antibodies were cleared of any precipitates by centrifugation at maximum speed for 10 min at 4°C, supernatant were collected into a fresh ice cold 1.5 mL tube and 15 µL of pre-washed Dynal® Protein G beads were added to each sample, incubated at 4°C with rotation for 60 min. Samples were removed from rotation and Dynal® Protein G-antibody-protein complexes were magnetically extracted and washed in 1 mL ice cold lysis buffer with slow rotation for 5 min at room temperature. Samples were washed 5 more times in lysis buffer and then a final wash in ice cold 1X PBS. The wash was removed and beads resuspended in 40 µL 1X PBS and 20 µL loading dye. Protein complexes were eluted from the beads by the addition of denaturing SDS-PAGE loading dye to the samples followed by incubation at 100°C for 5 min. Beads were removed from the samples by centrifugation at

maximum speed for 1 min. For immunoprecipitation validation, 25 µL of lysate was analysised utilising an anti-Flag antibody for immunoblot analysis according to the method described in chapter 2.3.5, while analysis for SGTA interaction utilised anti-HA antibody.

For the following protocols, Immunoprecipitation of pcFH-SGTA and detection by immunoblot was completed as described in Protocol 1, unless otherwise indicated.

Protocol 2: *Igepal Lysis buffer.* Cells were lysed in Igepal lysis buffer (100 mM NaCl, 50 mM Tris (pH 8.0), 20 mM HEPES (pH 7.5), 1% Igepal CA-360, 0.5% sodium deoxycholate, 1 mM DTT and 1X protease inhibitor).

Protocol 3: *Chromatin immunoprecipitation (ChIP) lysis buffer.* Cells were harvested in 500 µL of 1X PBS with protease inhibitors and lysates collected into an ice cold 1.5 mL tube. The cells were pelleted by room temperature centrifugation at maximum speed, PBS wash was aspirated and 350 µL SDS lysis buffer (1% SDS (w/v), 10 mM EDTA (pH 8.1), 50 mM Tris-HCl (pH 8.1) and 2X protease inhibitor) was added to cell pellet and incubated on ice for 10 min. Cells were homogenised 6 times utilising a 26 gauge needle attached to a 1 mL syringe. Lysates were cleared by centrifugation and supernatant was transferred into an ice cold 1.5 mL tube, 10% of supernatant was transferred into a separate tube as input control. One hundred µL of lysate was transferred into an ice cold 1.5 mL tube and combined with 900 µL ice cold dilution buffer (0.01% SDS (w/v), 1.1% TritonX 100, 1.2 mM EDTA (ph 8.1), 16.7 mM NaCl and protease inhibitor) and pre-cleared for 60 min at 4°C with 45 µL of 50:50 protein G sepharose slurry in 1X TE buffer (pH 8.1) and 200 µg yeast transfer RNA (tRNA). Samples were centrifuged at 4°C and the supernatant

was transferred to fresh, ice cold tubes and protein immunoprecipitations were performed as described in Protocol 1. Immunprecipitation complexes were bound to 45 µL of 50:50 protein G sepharose slurry in the presence of 200 µg tRNA for 60 min at 4°C with rotation. The beads were pelleted by gentle centrifugation (5000g) at 4° C for 1 min and the supernatant aspirated. Beads were washed for 5 min with each of the following ice cold solutions: once with low salt immune complex wash buffer (0.1% SDS (w/v), 1% TritonX 100, 2 mM EDTA (pH 8.1), 20 mM Tris-HCl (pH 8.1), 150 mM NaCl), solution were transferred into a fresh, ice cold 1.5 mL tube and washed once with high salt immune complex wash buffer (0.1% SDS (w/v), 1% TritonX 100, 2 mM EDTA (pH8.1), 20 mM Tris-HCl (pH 8.1) and 500 mM NaCl), once with lithium chloride (LiCl) wash immune complex wash buffer (0.25 M LiCl, 1% Igepal CA-360, 1% sodium deoxycholate, 1 mM EDTA (pH 8.1) and 10 mM Tris-HCl (pH 8.1) and twice with 1X TE buffer (pH 8.1). Protein complexes were eluted from the beads for immunoblot analysis as described in Protocol 1.

Protocol 4: *Formaldehyde fixation.* Cells were harvested as described in Protocol 3 with the following modifications. Prior to cell scraping in 1X PBS with protease inhibitors, cells were fixed for 10 min with 1% formaldehyde and washed twice in 1X ice cold PBS. Detection of immunoprecipitated protein complexes followed the ChIP method as described in Protocol 3. Reversal of formaldehyde cross-linking occurred by boiling samples in loading dye at 100°C. Samples were analysed by immunoblot as described in Protocol 1.

Protocol 5: *Sodium Molybdate (SM) lysis buffer.* Cells were lysed in SM lysis buffer (20 mM Tris (pH 7.4), 25 mM NaCl, 2 mM DTT, 20 mM Na_2Mo_4, 0.1% NP40 and 1X protease inhibitor).

Protocol 6: *NETN lysis buffer*. Cells were lysed in NETN lysis buffer (20 mM Tris (pH 7.5), 100 mM NaCl, 1 mM EDTA (pH 8.1), 0.5% NP40, 1 mM DTT, and 1X protease inhibitor).

3.2.6 *In vitro* luciferase assays

In vitro AR transactivation assays were performed in cultured PC3 cells (10,000 cells/well in 96 well plate) transfected with 2.5 ng pCMV-AR3.1 and the equivalent molar ratio of pcFH-SGTA and/or pcFH-SGTA 1-80 and 50 ng of ARR3-tk-Luc reporter according to the method outlined in chapter 2.3.3.2.

3.2.7 Statistical analysis

Statistics were performed using Graphpad Prism Version 5 software for Windows (Graphpad Software, California, USA). Non-parametric Mann-Whitney U or One-way ANOVA tests were used to determine differences between groups as indicated in figure legends. A p-value < 0.05 was considered statistically significant.

3.3 Results

3.3.1 Characterisation of SGTA functional domains

The family of TPR containing co-chaperones, including SGTA, are expressed in a wide variety of species ranging from yeast to humans, implying either structural and/or biological conservation (D'Andrea and Regan 2003). In order to determine the evolutionary conservation of SGTA domain structures, a phylogenetic relationship between SGTA amino acid sequences from 20 different species was analysed (Figure 3.2). The SGTA phylogeny tree demonstrates segregation of SGTA sequences as expected based on currently known species relations (Ragan 2009). The inter-relationships between species on the SGTA phylogeny is consistent with phylogenetic trees for Hsp90 and ten distinct co-chaperone proteins, including FKBP52, Cyp40, PP5 and Hop (Johnson and Brown 2009). This display of structural conservation amongst SGTA and other TPR containing co-chaperones implies that they play important biological roles in the maintenance of the Hsp90 chaperone system.

To further analyse the evolutionary conservation of SGTA domains, we aligned the SGTA protein sequence from several species presented in the phylogeny tree described in Figure 3.2. The amino acid sequence within the functional domains: homodimerisation (amino acids 1-80), TPR (amino acids 91-192), the QRD (amino acids 270-313) and the linker region (amino acids 200-263) demonstrates conservation within the functional domains (Figure 3.3), further supporting the maintenance of SGTA biological function throughout evolution (Johnson and Brown 2009). The sequence alignment shows a large degree of

variation across species between amino acids 67-89, which encompasses part of the homodimerisation domain (Figure 3.3). It is possible therefore, that SGTA homodimerisation has been maintained throughout evolution.

Secondary structure prediction analysis across the entire human SGTA amino acid sequence revealed a high content of alpha helices within the homodimerisation, TPR and QRD regions (Figure 3.4). The hydrophobicity of the alpha helix backbone is able to embed the secondary structure into favourable environments such as the internal surface of globular proteins or within plasma membranes (Kumar and Bansal 1998). However, alpha helices also provide a structural rigidity that allows for favourable protein-protein interactions such as those seen between tandem TPR domains and client proteins. It is therefore likely that the alpha helical content within the homodimerisation domain allows for the interaction between two SGTA molecules.

Protein phosphorylation is an important post translational regulatory mechanism that can control the biological activity of many proteins, including TPR co-chaperones (Cox, Riggs et al. 2007). As SGTA has been previously described as a phospho-protein (Moritz, Li et al. 2010), we next used the NetPhos 2.0 online phosphorylation prediction program to examine potential phosphorylated residues (Figure 3.4). The NetPhos 2.0 program utilises experimentally validated serine, threonine and tyrosine sites as a background screen to predict potential phosphorylation sites (Blom, Gammeltoft et al. 1999; Blom, Sicheritz-Ponten et al. 2004). This analysis demonstrated phosphorylation sites could potentially exist at serine residues 25, 31, 76, 83, 87, 210, 252, 294, 301, 305, 307 and 306; threonine residues 66, 80, 95, 264, and 266 and on tyrosine residues 157, 161, and 194. In

agreement with this *in silico* phosphorylation screen, serine residue 305 has recently been experimentally confirmed as a *bone fide* phosphorylation site (Moritz, Li et al. 2010). In addition to the regulation of biological processes, it has also been demonstrated that phosphorylation acts as an important regulatory mechanism for the formation of protein homodimers (Khokhlatchev, Canagarajah et al. 1998). The analysis of SGTA phosphorylation within this chapter therefore implicates serine residues 25, 31 and 76 and threonine residues 66 and 80 as potentially important amino acid residues for the formation of SGTA homodimers.


Androgen receptor (Homo sapiens)
SGTA (Monodelphis domestica)
SGTA (Danio rerio)
SGTA (Tetraodon nigroviridis)
SGTA (Xenopus Laevis)
SGTA (Xenopus tropicalis)
SGTA (Gallus gallus)
SGTA (Ornithorhynchus anatinus)
SGTA (Mus musculus)
SGTA (Rattus norvegicus)
SGTA (Callithrix jacchus)
SGTA (Bos taurus)
SGTA (Sus scrofa)
SGTA (Canis familiaris)
SGTA (Equine Caballus)
SGTA (Cercopithecus aethiops)
SGTA (Macaca fascicularis)
SGTA (Macaca mulatta)
SGTA (Homo sapiens)
SGTA (Pan troglodytes)
SGTA (Pongo abelii)

Figure 3.2 Sequence analyses of SGTA amino acids from multiple species. The reference sequence for each species was downloaded into the Vector NTi computer suite (Accession numbers: Tree root – **Androgen receptor Human:** *Homo sapiens* (AAA51772.1); **Tropical fish:** *Danio rerio* (BC067176.1); **Puffer fish:** *Tetraodon nigroviridis* (CAF90177.1); **Possum:** *Monodelphis domestica* (NW_001581861); **Frog:** *Xenopus laevis* (LOC414520); **Frog:** *Xenopus tropicalis* (gi:77627448); **Pheasant:** *Gallus gallus* (AJ721018.1); **Platypus:** *Ornithorhynchus anatinus* (NW_001794137); **Mouse:** *Mus musculus* (BC003836.1); **Rat:** *Rattus norvegicus* (NP_073194); **Marmoset monkey:** *Callithrix jacchus* (XP_002761612); **Cow:** *Bos taurus* (NP_001033119); **Pig:** *Sus scrofa* (XP_003123075); **Dog:** *Canis familiaris* (gi:57102202); **Horse:** *Equine caballus* (gi:194238503); **Vervet Monkey:** *Cercopithecus aethiops* (AAW30383); **Macaque monkey:** *Macaca fascicularis* (BAE01321); **Rhesus monkey:** *Macaca mulatta* (NP_001181661); **SGTA Human:** *Homo sapiens* (gi:49457556); **Chimpanzee:** *Pan troglodytes* (NP_003012); and **Orangutan:** *Pongo abelii* (XP_002828469). Phylogeny tree was rooted using the AR *Homo sapiens* sequence. The tree was developed utilising the AlignX program and was built using the Neighbor Joining method developed by Saitou and Nei (Saitou and Nei 1987). The distance between species relates to the degree of divergence between SGTA sequences.

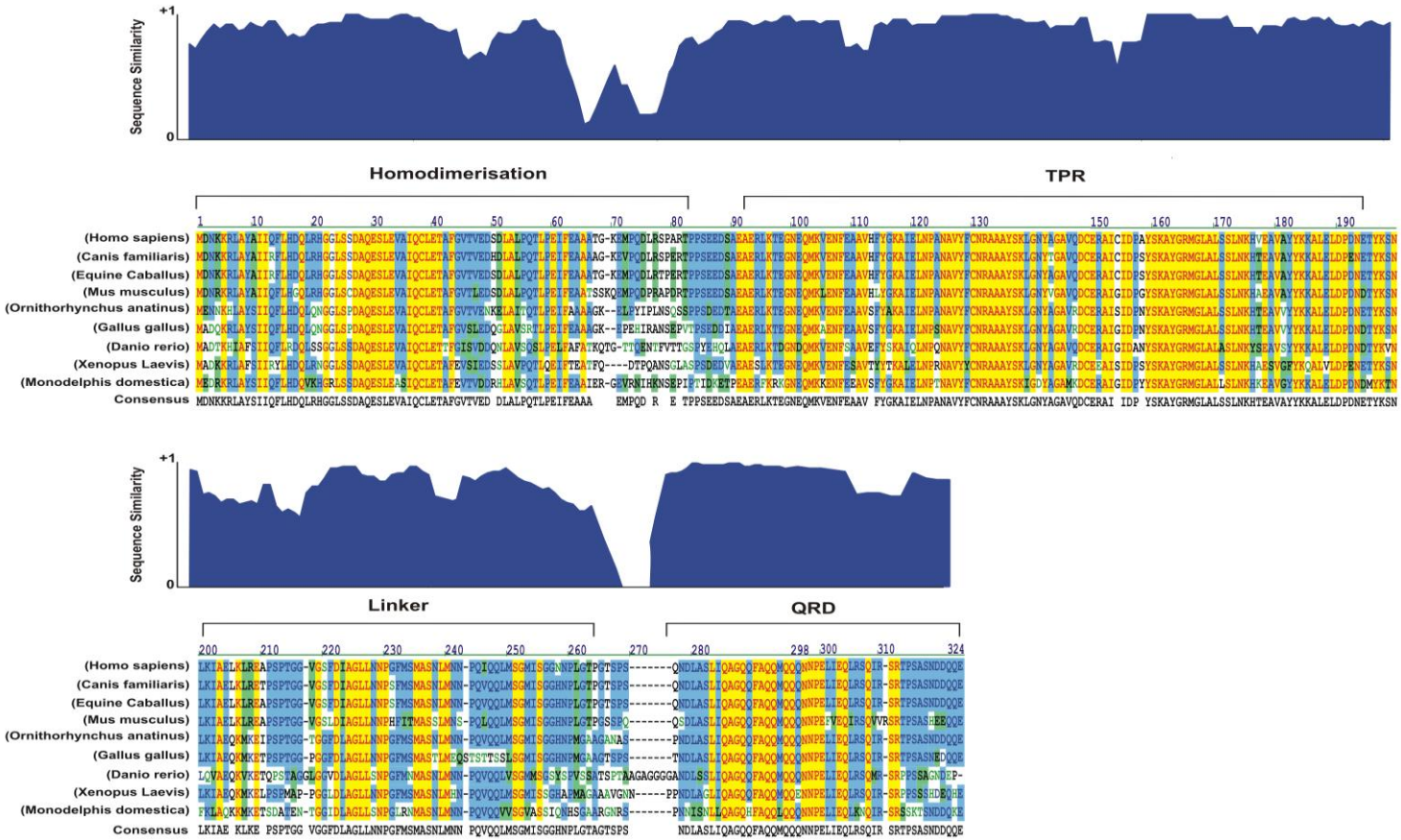

Sequence Similarity
+1
0
Homodimerisation
TPR
(Homo sapiens)
(Canis familiaris)
(Equine Caballus)
(Mus musculus)
(Ornithorhynchus anatinus)
(Gallus gallus)
(Danio rerio)
(Xenopus Laevis)
(Monodelphis domestica)
Consensus
Linker
QRD

Figure 3.3: High degree of amino acid sequence similarity within SGTA domain structures across species. SGTA sequences were aligned utilising the AlignX program which operates on the ClustalW algorithm. Residues with a *yellow* background indicate complete identity between species; a *green* background indicates similarity in amino acids and a *blue* background indicates residues containing a conservative amino acid difference between species. Those amino acids in *green* on a *white* background indicate weakly similar residues, while non similar amino acids are depictured with a *black* on a *white* background. *Blue* plot above sequences represents the alignment similarity across species. The y-axis represents an arbitrary value given to each residue depending if it is identical, similar or weakly similar compared to the corresponding residue of the consensus sequence (value = 1, 0.5 or 0.2 respectively). The value for each residue is normalised by the sum of values for each residue divided by the total number of sequences in the alignment.

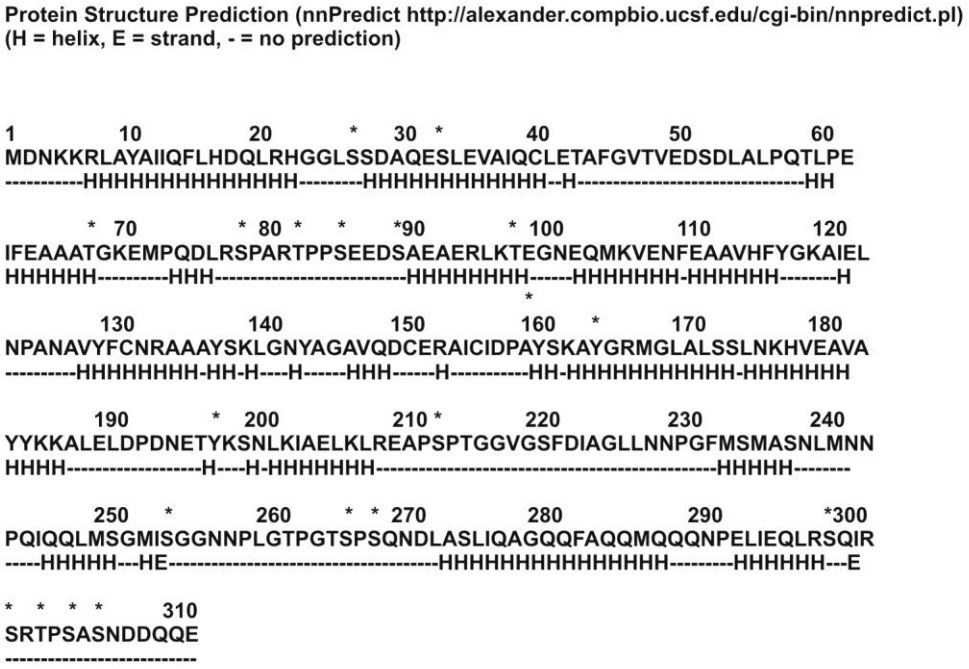


Figure 3.4: SGTA homodimerisation, TPR and QRD domains contain alpha helices and putative phosphorylation sites. Secondary amino acid structure analysis was conducted on the human SGTA sequence utilising the SGTA protein secondary structure. Human SGTA amino acid sequence was used as input in the nnpredict secondary structure prediction program (www.cmpharm.ucsf.edu/~nomi/nnpredict.html). H represents alpha helix, E represents beta sheet, - represents no prediction and * represents predicted phosphorylation sites.

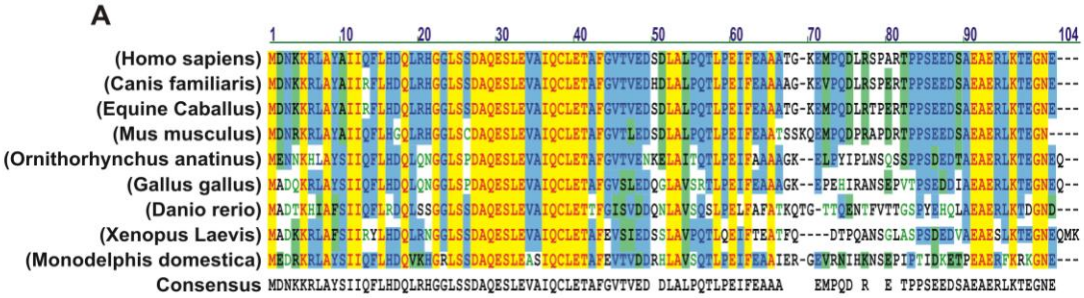
3.3.2 Amino acid analysis of the SGTA homodimerisation domain

To determine the residues necessary for SGTA homodimerisation, sequence alignment of only the SGTA homodimerisation domain (amino acids 1-80) demonstrated a high degree of sequence similarity across 9 different species (Figure 3.5A). The sequence alignment from Figure 3.5A was compressed into an amino acid logo, which displays the frequency at which residues occur in all of the sequences (Figure 3.5B). The longest stretch of residues that are most similar across species occurred from amino acids 27 to 41, suggesting that this evolutionary conserved region may form an essential part of the homodimerisation surface. Interestingly, the SGTA ^{29}QESLE^{33} sequence is very similar to AR ^{642}QEEGE^{662} residues previously implicated by our laboratory as mediating the SGTA-AR interaction (Buchanan, Ricciardelli et al. 2007). Moreover, the serine residue at position 31 (S31) may be a phosphorylation site (Figure 3.4), and thus may be an important mediator in SGTA homodimerisation.

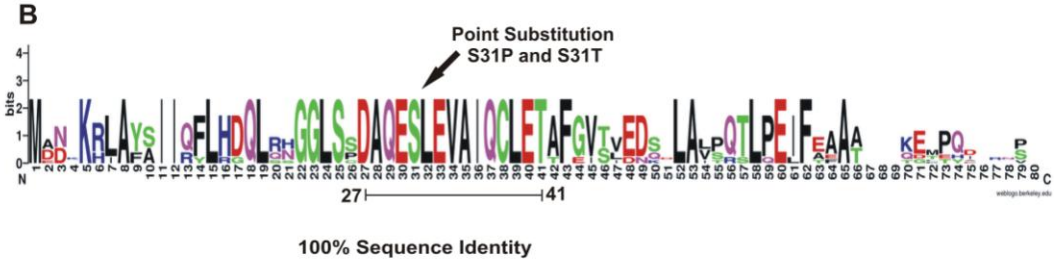
Amino acid composition analysis highlights that the 1-80 sequence is significantly enriched in hydrophobic residues, such as alanine and leucine, and depleted in positively charged amino acids ($p<0.05$; Figure 3.5C). In agreement with the secondary structural prediction (Figure 3.4), the SGTA homodimerisation domain contains an abundance of alpha helices. Furthermore, the amino acids within the homodimerisation domain are depleted in flexible characteristics, whereas bulky amino acids are prevalent. Collectively, this composition analysis provides further evidence to suggest that the SGTA homodimerisation domain consists of a structurally rigid surface that enforces stable protein-protein interactions as previously reported for other homodimers (Larsen,

Olson et al. 1998). However, the limitations from these computational analyses is that they cannot conclusively determine the amino acids required for SGTA homodimerisation, and therefore further experimentation is needed in order to identify those residues and determine if the homodimerisation domain is necessary for SGTA biological function.

A



B



100% Sequence Identity

C

Component	Enriched/Depleted	p-Value (equal to)
Alanine residues	Enriched	0.02
Leucine residues	Enriched	0.004
Positively charged	Depleted	0.03
Hydrophobic	Enriched	0.02
Exposed	Depleted	0.0006
Flexible	Depleted	0.002
High solvation potential	Depleted	0.02
Frequent in alpha helices	Enriched	0.02
Frequent in beta structure	Enriched	0.02
Frequent in coils	Depleted	0.004
Bulky	Enriched	0.02

Figure 3.5: SGTA homodimerisation amino acid sequence remains relatively similar across species. A: Amino acid alignment of SGTA homodimerisation domain as described in Figure 3.3. **B:** Logo of SGTA amino acid sequences derived from **A**. Each residue in the logo indicates the amino acid similarity within species, while the overall height of the symbols represents the relative frequency. Arrow indicates the position of serine 31. **C:** Analysis of amino acid residue composition and secondary structure on the first 80 amino acids of human SGTA was performed utilising the Composition Predictor program (www.cprofiler.org/). The background distribution was set at surface residues determined by the Molecular Surface Package, the number of bootstrap iterations used for non-parametric estimation of the confidence intervals for the reported amino acid composition was set at 10,000 and significance was determined at p value < 0.05. The exposed amino acid component is a measure that relates to the availability of polar residues usually found on protein surfaces. The solvation potential is a measure for the preference of amino acids to be buried or exposed to solvent, a low potential relates to the enrichment of "buried" proteins (Jones and Thornton 1997). Bulky amino acids, such as leucine, isoleucine, tyrosine and valine all contain hydrophobic side chains, which contribute to the steric hindrance of secondary and tertiary protein structures (Zimmerman, Eliezer et al. 1968).

3.3.3 SGTA homodimerisation cannot be captured by co-immunoprecipitation.

Previous investigations into SGTA homodimerisation have mainly used traditional protein interaction screening techniques, such as the yeast and/or mammalian two-hybrid assays (Tobaben, Varoqueaux et al. 2003; Buchanan, Ricciardelli et al. 2007). In this thesis we use the co-immunoprecipitation (CoIP) method, which is one of the gold standards of investigating protein-protein interactions. In order to use CoIP with investigating amino acid residues involved in SGTA homodimerisation, two independent SGTA expression vectors were engineered to express either Flag or HA at the amino terminus, which allowed the use of a Flag antibody to immunoprecipitate Flag-SGTA, while a HA antibody was utilised to detect HA-SGTA as an interacting partner.

Despite the availability of an array of published CoIP lysis buffers, the first buffer used was one previously optimised in our laboratory by Dr. Luke Selth. Immunoblot analysis of 10% input samples from CoIP experiments demonstrated successful expression of Flag and HA tagged SGTA (Figure 3.6A-F; *left* and *right* panels: 10% input). Although immunoprecipitation of Flag-SGTA was successful (Figure 3.6A; *left* panel), the proportion of precipitated protein compared to 10% input was low. Immunoblot analysis with HA antibody did not capture an interaction (Figure 3.6A; *right* panel). Next, the CoIP lysis buffer was changed to an Igepal lysis buffer which had been previously optimised in our laboratory by Ms Melissa O'Loughlin and used to detect the interaction between SGTA and AR (Buchanan, Ricciardelli et al. 2007). Despite good expression of Flag-

SGTA, no immunoprecipitation was detected (Figure 3.6B; *left* panel), and HA-SGTA could not be captured (Figure 3.6B; *right* panel).

Chromatin immuoprecipitation (ChIP) is a protocol commonly used to capture proteins in complex with DNA. We next used a modified ChIP lysis buffer optimised in the laboratory by Dr. Eleanor Need for detection of SGTA homodimerisation interactions. Immunoblot analysis demonstrated good protein levels and immunoprecipation of Flag-SGTA (Figure 3.6C; *left* panel), however no interaction was captured due to poor steady state HA-SGTA protein levels (Figure 3.6C; *right* panel). Despite the variability in the relative levels of the respective proteins, it is possible that the SGTA homodimerisation interaction may be transient. In order to capture this interaction formaldehyde was utilised in the ChIP lysis buffer to cross link interacting proteins. As observed in Figure 3.10C the steady state levels of both Flag and HA tagged proteins remained low, and no interaction could be captured (Figure 3.6D; *left* and *right* panels).

We next examined the possibility of stabilising chaperone complexes by adding molybdate into the lysis buffer (Pratt and Toft 1997; Davies, Ning et al. 2002). The sodium molybdate (SM) lysis buffer was optimised in the laboratory by Ms Joanna Gillis. Although Flag-SGTA protein levels were high, both Flag immunoprecipitation (Figure 3.6D; *lef*t panel) and HA-SGTA protein levels remained low (Figure 3.6D; *right* panel). Finally, we used the NETN buffer, which is commonly used for CoIP experiments including one previously reported for SGTA (Winnefeld, Grewenig et al. 2006). Consistent with several of the other buffer conditions used, expression and immunoprecipitation of Flag-SGTA was successful (Figure 3.6E; left panel), but due to low HA-SGTA protein levels an interaction

could not be captured (Figure 3.6E; right panel). Collectively, SGTA homodimerisation interaction could not be captured by CoIP despite several optimisation attempts. It appears that the failure to capture the interaction was due to a number of technical limitations, which may include the relative steady state levels of tagged SGTA proteins, the stability and/or transient nature of protein interactions within various lysis buffers. Although both magnetic and sepharose beads were used in this study, it is possible that a low binding affinity between Flag antibodies and beads reduces the amount of SGTA protein precipitated out of solution. Consequently, the mammalian two-hybrid system previously used by our laboratory to capture SGTA homodimerisation (Buchanan, Ricciardelli et al. 2007) will be utilised here to investigate the amino acid regions required for SGTA homodimerisation.

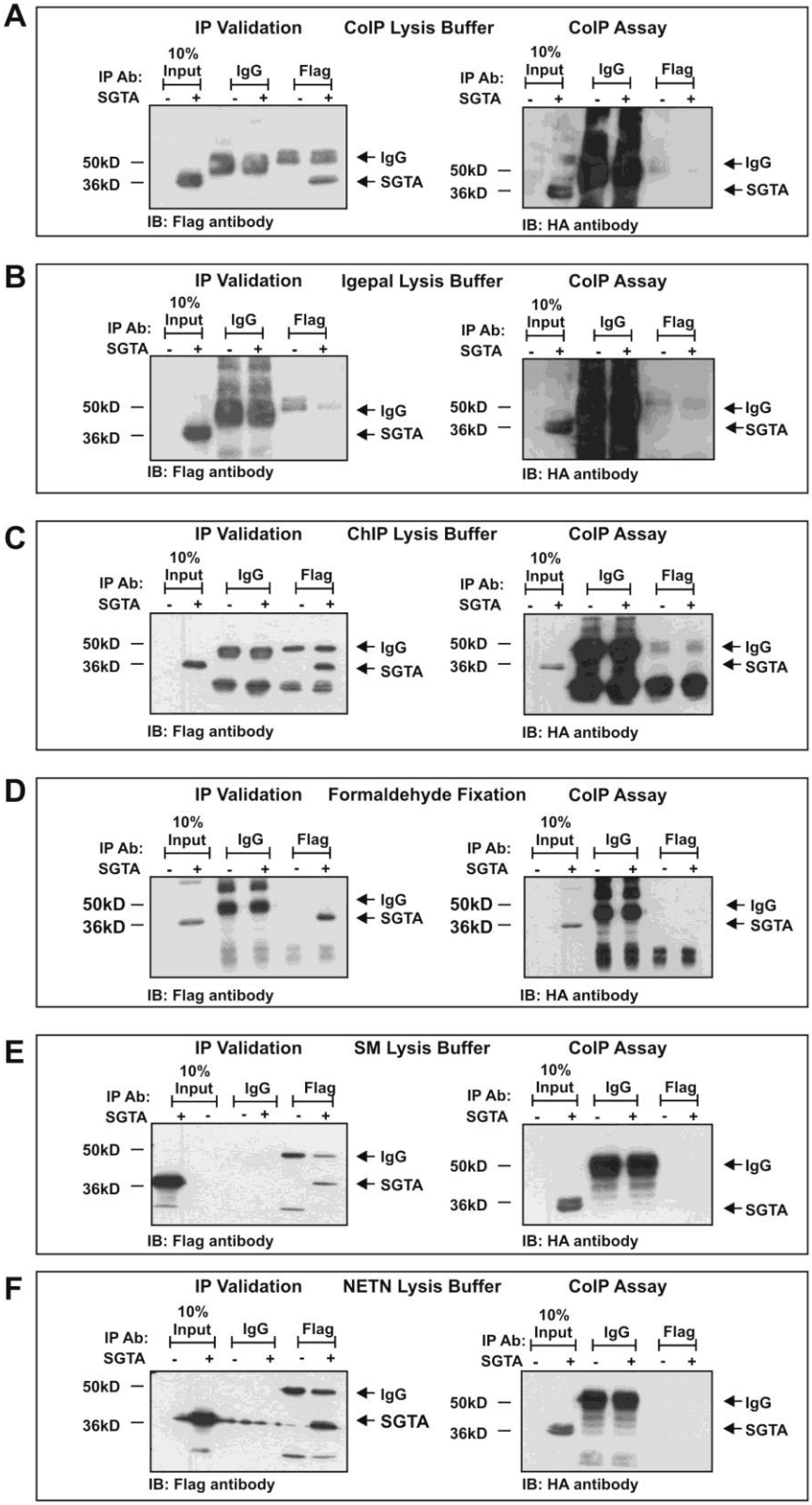

A
IP Validation
CoIP Lysis Buffer
CoIP Assay
10% Input
IgG
Flag
IP Ab:
SGTA
50kD
36kD
IgG
SGTA
IB: Flag antibody
IB: HA antibody
B
IP Validation
Igepal Lysis Buffer
CoIP Assay
C
IP Validation
ChIP Lysis Buffer
CoIP Assay
D
IP Validation
Formaldehyde Fixation
CoIP Assay
E
IP Validation
SM Lysis Buffer
CoIP Assay
F
IP Validation
NETN Lysis Buffer
CoIP Assay

Figure 3.6: Co-immunoprecipitation experiments does not confirm SGTA homodimerisation. A-F: COS-1 cells (2 x 10^6 cells/10 cm dish) were transfected with 5 ug pcH-SGTA and pcF-SGTA or empty vehicle control. Cells were lysed with different lysis buffers as described in section 3.3.4. Ten percent of total cell lysate was collected as input control prior to the immunoprecipitation of Flag-SGTA (pcF-SGTA). Equal volumes of input or precipitated lysate were run on SDS-PAGE gels and blotted for Flag-SGTA for validation of IP (*left panels*). Thereafter, anti-HA antibody was utilised to assess the interaction between Flag-SGTA and HA-SGTA (*right panels*).

3.3.4 Segmented deletions within the first 80 amino acids of the amino terminal domain ablate SGTA homodimersiation.

In order to determine the necessary amino acids required for SGTA homodimerisation, SGTA variants were created with 20 amino acid segments deleted along the homodimerisation domain (Figure 3.1). In agreement with a previous study from our laboratory, deletion of the first 80 amino acids resulted in a significant loss of SGTA homodimerisation ($p<0.01$; Figure 3.7A) (Buchanan, Ricciardelli et al. 2007). Additionally, deletion of any 20 amino acid segment within the first 80 amino acids of the amino terminal domain also abolished SGTA homodimerisation ($p<0.01$; Figure 3.7A). Despite deletion of residues 61-80 resulting in a greater decrease of SGTA protein levels compared with the other deletion variants (Figure 3.7B), denaturing immunoblot analysis demonstrated that the loss of SGTA self association could not be explained by a complete loss of SGTA steady state protein levels (Figure 3.7B). As previously described in section 3.3.2, the ^{29}QESLE^{33} motif in the SGTA homodimerisation domain is potentially important to the stabilisation and/or formation of SGTA homodimers. Deletion of these amino acids (SGTA variant: Δ29-33) does not alter protein steady state levels compared to full length SGTA (Figure 3.7B).

Non-denaturing PAGE gels were used next to analyse the native protein states of the SGTA variants. Two SGTA complexes were observed at 64 kDa and 36 kDa, which may represent SGTA homodimeric and monomeric forms respectively (Figure 3.7C). Although the formation of complexes containing SGTA and other proteins cannot be discounted

using this method, segmented deletions within the homodimerisation domain (Δ1-20, Δ21-40, Δ41-60, Δ61-80, and Δ29-33) resulted in a disruption of the observed banding pattern. The results from both of the denaturing and non-denaturing PAGE gels suggest that deletions within the homodimerisation domain lead to a disordered secondary structure and a potential loss in the ability for SGTA to form a homodimer. In agreement, a dose dependent increase in transfected DNA expression vector demonstrated that none of the variants were able to rescue SGTA homodimerisation, despite an increase in protein levels. Although the steady state levels of SGTA Δ41-60 never reached full-length SGTA levels (Figure 3.8A and B).

As the SGTA amino acid sequence ^{29}QESLE^{33} is required for SGTA homodimerisation, we next investigated the importance of the S31 residue as a potential phosphorylation site and mediator of homodimerisation. Amino acid substitution was performed by replacing the serine residue with either the non-phosphorylated proline or the phosphor-mimic threonine residue, which are denoted as S31P and S31T respectively. Although deletion of ^{29}QESLE^{33} abolished SGTA homodimerisation, point mutation at the central serine residues varied; S31P had no effect while S31T halved the interaction ($p<0.01$; Figure 3.8C). These results were not due to changes in protein steady state levels. Collectively, these results suggest that SGTA homodimerisation is reliant on the structural stability of the entire domain, rather than a specific motif within the domain.

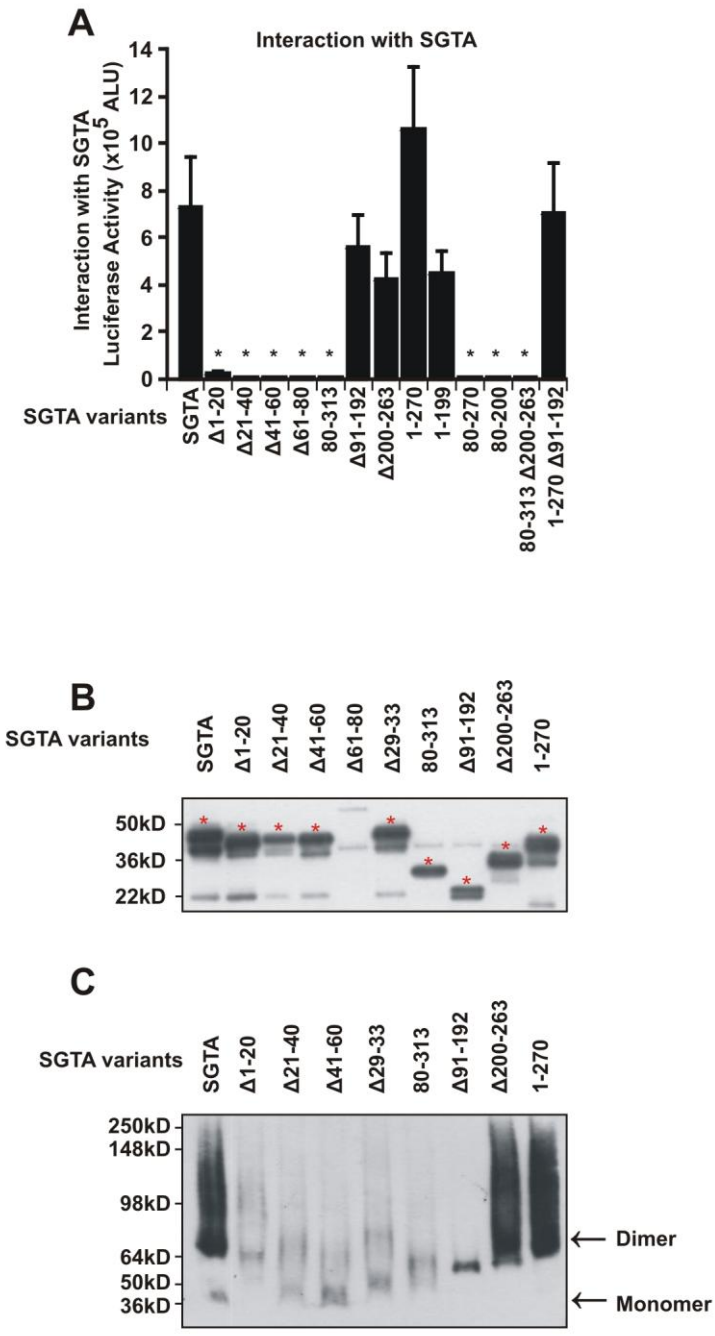
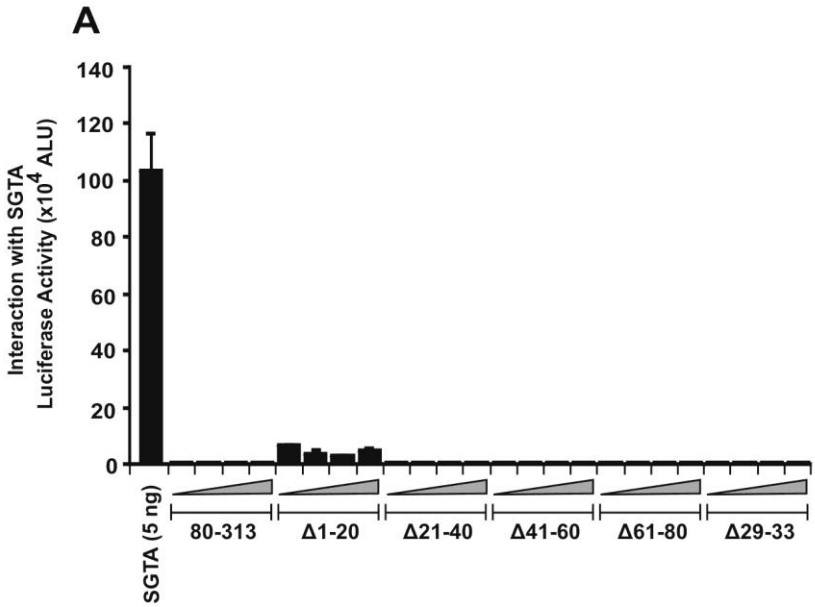
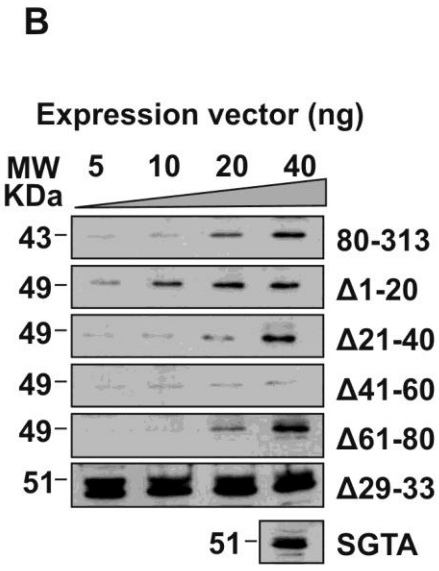

A
Interaction with SGTA
Interaction with SGTA
Luciferase Activity (x10^5 ALU)
14
12
10
8
6
4
2
0
SGTA variants
SGTA
Δ1-20
Δ21-40
Δ41-60
Δ61-80
80-313
Δ91-192
Δ200-263
1-270
1-199
80-270
80-200
80-313 Δ200-263
1-270 Δ91-192
B
SGTA variants
SGTA
Δ1-20
Δ21-40
Δ41-60
Δ61-80
Δ29-33
80-313
Δ91-192
Δ200-263
1-270
50kD
36kD
22kD
C
SGTA variants
SGTA
Δ1-20
Δ21-40
Δ41-60
Δ29-33
80-313
Δ91-192
Δ200-263
1-270
250kD
148kD
98kD
64kD
50kD
36kD
Dimer
Monomer

Figure 3.7: Deletion of amino acid segments within the first 80 amino acids of SGTA disrupts the formation of an SGTA homodimer. A: COS-1 cells (20,000/well) were transfected with 5 ng of GAL4-DBD-tagged SGTA deletion variant (or molar equivalent) and 5 ng of pVP16-tagged full length SGTA with 25 ng of the pGK-1 reporter plasmid. All wells were controlled for molar equivalent of expression plasmid. Total DNA concentration per well was kept constant with cotransfection of the prokaryotic expression vector pBS(sk-). Four wells were independently transfected for each variant and incubated for 24 hours. Cells were lysed in 30 µL passive lysis buffer and luciferase activity was measured on 10 µL of lysate. Data represent the mean ± SEM luciferase activity in arbitrary light units (ALU) of four individually transfected wells and is representative of at least 3 independently repeated experiments. *, $p < 0.01$ on Mann-Whitey U for differences between medians of full length SGTA and each of the variants. **B:** Immunoblot of COS-1 cells (100,000/well) transfected with 35 ng GAL4-DBD-tagged SGTA deletion variant for 24 hours. Cells were lysed in 150 µL RIPA buffer and cleared by centrifugation. Equal concentrations of lysate (25 µg) were loaded onto a 7.5% SDS-PAGE gel and resolved for SGTA by utilising anti-SGTA antibody. *, denotes specific SGTA band for each deletion construct. **C:** Immunoblot of COS-1 cell lysates created as described in B. Equal concentrations of lysate (25 µg) were loaded onto a 7.5% native PAGE gel and resolved for SGTA utilising anti-SGTA antibody.


A
Interaction with SGTA
Luciferase Activity (x10^4 ALU)
140
120
100
80
60
40
20
0
SGTA (5 ng)
80-313
Δ1-20
Δ21-40
Δ41-60
Δ61-80
Δ29-33


B
Expression vector (ng)
MW KDa
5
10
20
40
43
49
49
49
49
51
51
80-313
Δ1-20
Δ21-40
Δ41-60
Δ61-80
Δ29-33
SGTA

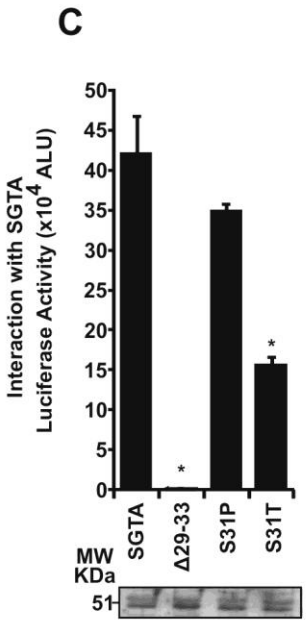

C
Interaction with SGTA
Luciferase Activity (x10^4 ALU)
50
45
40
35
30
25
20
15
10
5
0
SGTA
Δ29-33
S31P
S31T
MW KDa
51

Figure 3.8: Increasing the expression of SGTA deletion variants does not rescue SGTA homodimerisation. A: COS-1 cells were transfected with either GAL4-DBD SGTA or increasing molar concentrations of SGTA variants while controlling for molar concentrations of expression plasmid and DNA with pVP16 and the prokaryotic expression vector pBS(sk-) respectively. Cells were incubated for 24 hours and lysed as described in Figure 3.4. Data is representative of at least 3 independently repeated experiments. **B:** Immunoblot of transfected SGTA variants. The remaining lysate for each variant was pooled, cleared by centrifugation and an equal volume of lysate (25 μL) resolved for SGTA by immunoblot analysis utilising anti-SGTA antibody. **C:** SGTA point mutations S31P and S31T demonstrate an ability to form a homodimer similar to full length SGTA. COS-1 cells were plated, transfected and assayed as described in A. Data represent the mean ± SEM and is representative of at least 3 independently repeated experiments. *, $p < 0.01$ on Mann-Whitey U for differences between medians of full length SGTA and each of the variants.

3.3.5 Inhibition of SGTA homodimerisation by expression of a peptide sequence encompassing SGTA amino acids 1-80

As the SGTA amino acid sequence from 1-80 is necessary for homodimerisation, we then tested if this region alone is sufficient to form an interaction with full length SGTA or able to self associate. Mammalian two-hybrid expression plasmids were created to express only the first 80 amino acids of the SGTA amino terminus. Co-expression of SGTA 1-80 with full length SGTA did not result in an interaction, nor was SGTA 1-80 capable of self-association (Figure 3.9A and B). Nevertheless, co-expression of the 1-80 fragment potently and significantly inhibited SGTA dimerisation in a dose-dependent manner ($p<0.001$; Figure 3.9C and D). This effect was specific to residues 1-80, as co-expression of the remainder of the SGTA protein (amino acids 80-313) had little effect on dimerisation (Figure 3.9E).

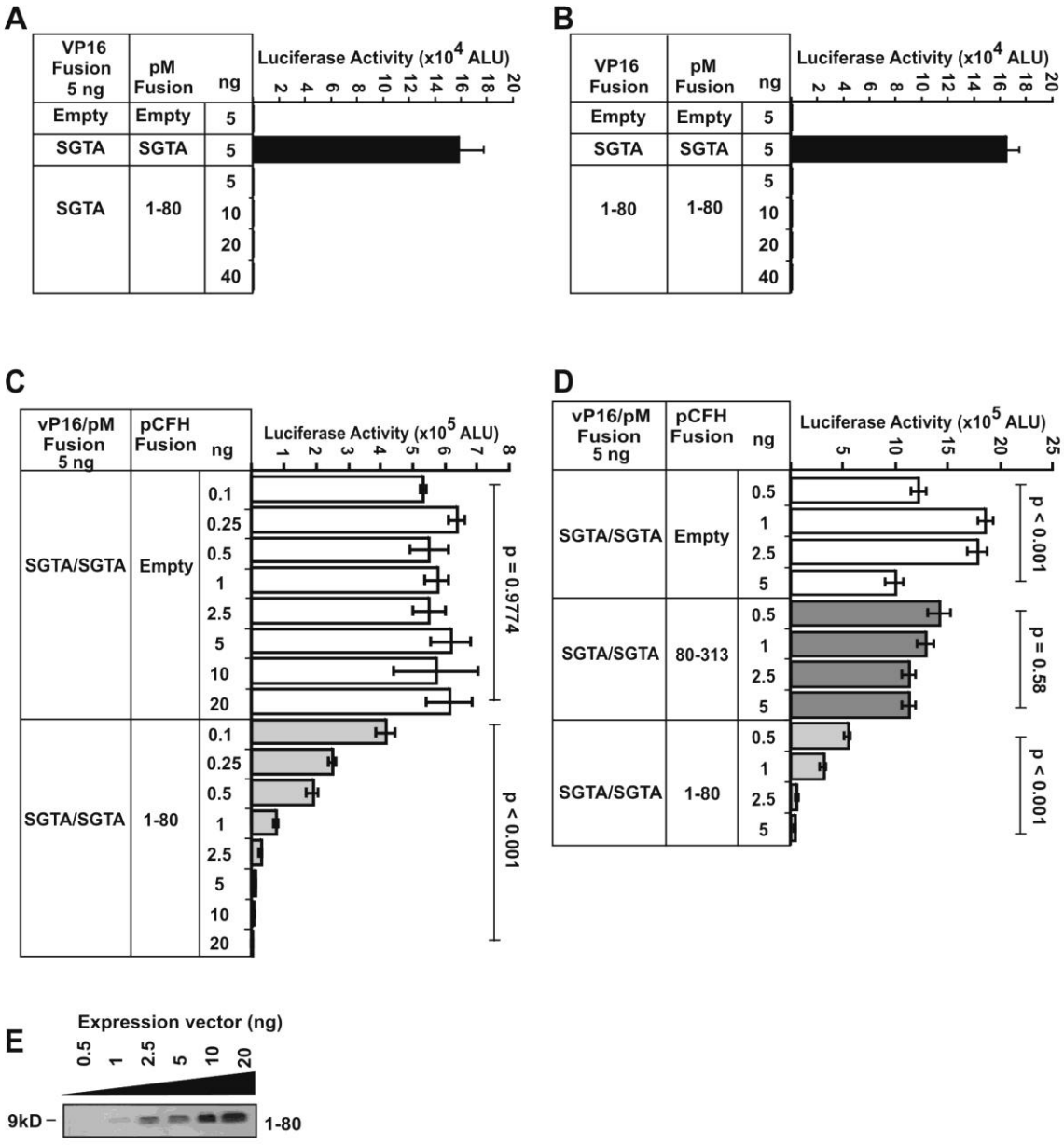

A
VP16 Fusion 5 ng
pM Fusion
ng
Luciferase Activity (x10^4 ALU)
Empty
Empty
5
SGTA
SGTA
5
SGTA
1-80
5
10
20
40
B
VP16 Fusion
pM Fusion
ng
Luciferase Activity (x10^4 ALU)
Empty
Empty
5
SGTA
SGTA
5
1-80
1-80
5
10
20
40
C
vP16/pM Fusion 5 ng
pCFH Fusion
ng
Luciferase Activity (x10^5 ALU)
SGTA/SGTA
Empty
0.1
0.25
0.5
1
2.5
5
10
20
p = 0.9774
SGTA/SGTA
1-80
0.1
0.25
0.5
1
2.5
5
10
20
p < 0.001
D
vP16/pM Fusion 5 ng
pCFH Fusion
ng
Luciferase Activity (x10^5 ALU)
SGTA/SGTA
Empty
0.5
1
2.5
5
p < 0.001
SGTA/SGTA
80-313
0.5
1
2.5
5
p = 0.58
SGTA/SGTA
1-80
0.5
1
2.5
5
p < 0.001
E
Expression vector (ng)
0.5
1
2.5
5
10
20
9kD
1-80

Figure 3.9: Co-expression of SGTA amino acids 1-80 can inhibit SGTA homodimerisation. COS-1 cells (20,000 cells/well) were transfected with equal molar amounts of empty pM and vP16 fusion expression plasmids. Total DNA was equal between wells. **A:** Effect of increasing molar amounts of pM1-80 is not sufficient to interact with full length SGTA. **B:** Effect of increasing molar amounts of pM/vP16 1-80 does not induce self-interaction. **C:** Effect of increasing molar amounts of empty pcFH or pcFH 1-80 expression plasmids on SGTA homodimerisation. **D:** Immunoblot analysis for SGTA in pooled lysates from replicate luciferase assays in C showing increasing pcFH 1-80 expression. **E:** Inhibition of SGTA dimerisation is specific to the first 80 amino acids. $p < 0.05$ by one-way ANOVA. Data represents mean ± SEM luciferase activity in 6 independently transfected wells. All data is representative of at least 3 independently repeated experiments.

3.3.6 Deletion of SGTA intra-molecular domains does not alter the capacity for SGTA to form a homodimer.

As the co-chaperone TPR domains are major binding sites for client molecules, including Hsp90 and Hsp70, it was next determined if a TPR deficient SGTA maintains homodimerisation in the context of other deletions. Deletion of the TPR domain did not alter the formation of homodimers compared to full-length SGTA (Figure 3.10A and B). To test if the carboxyl terminus is involved in intra-molecular actions that will facilitate SGTA homodimerisation, the carboxyl terminus was truncated of the linker region and glutamine-rich domain (SGTA 1-199) or the glutamine-rich domain only (SGTA 1-270). These truncated variants maintained the ability to form a homodimer, similar to that observed for the full length protein (Figure 3.10C and D). Together, these results demonstrate that any potential intra-molecular interactions provided by either the TPR domain or carboxyl terminus do not alter the ability for SGTA to form homodimers.

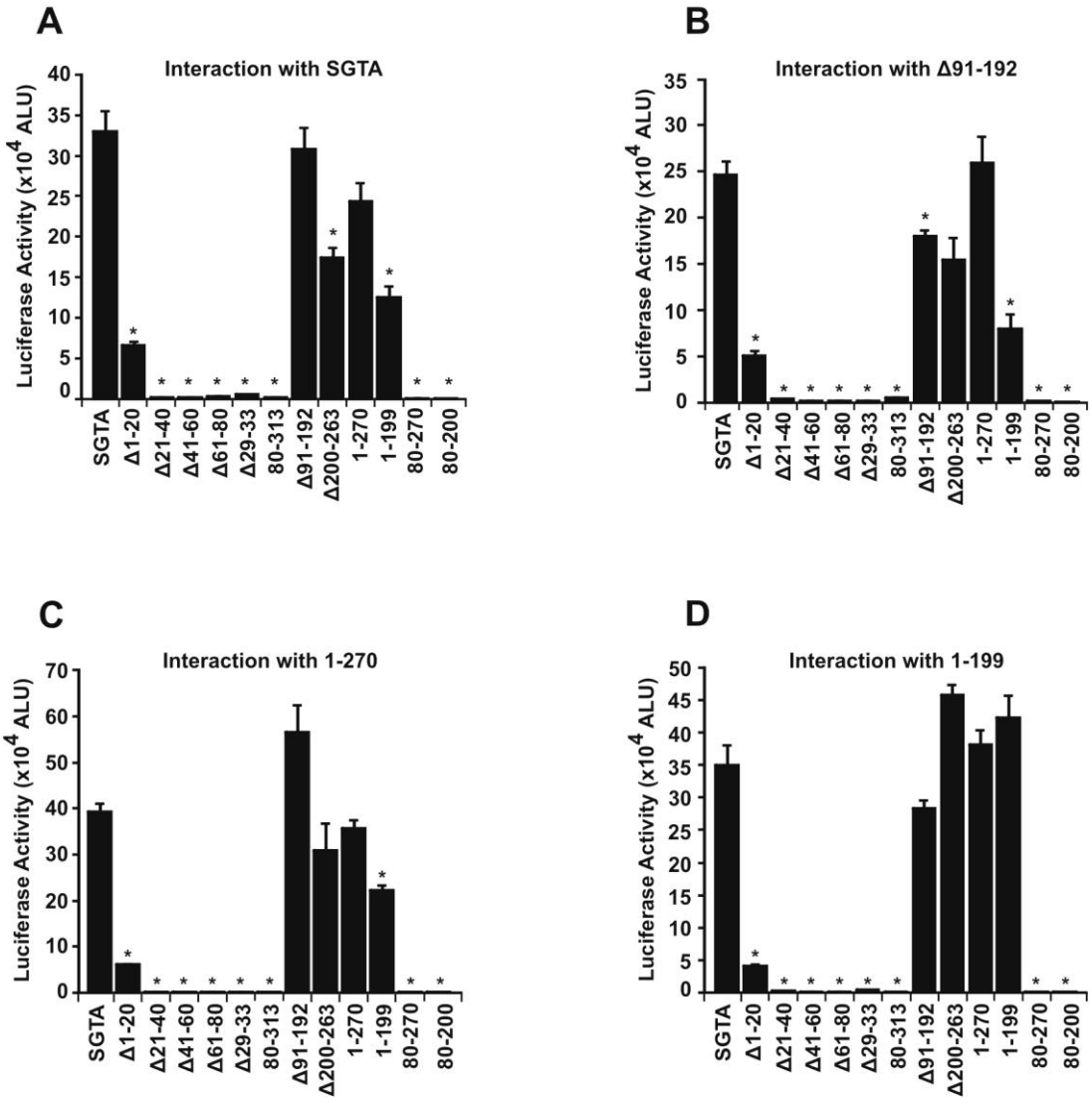

A
Interaction with SGTA
Luciferase Activity (x10^4 ALU)
B
Interaction with Δ91-192
Luciferase Activity (x10^4 ALU)
C
Interaction with 1-270
Luciferase Activity (x10^4 ALU)
D
Interaction with 1-199
Luciferase Activity (x10^4 ALU)
SGTA
Δ1-20
Δ21-40
Δ41-60
Δ61-80
Δ29-33
80-313
Δ91-192
Δ200-263
1-270
1-199
80-270
80-200

Figure 3.10: Deletion of SGTA TPR domain or truncation of the carboxyl terminus does not alter the formation of an SGTA homodimer. **A-D:** COS-1 cells were transfected with GAL4-DBD SGTA variants and co-expressed with pVP16-SGTA variants (SGTA, Δ91-192, 1-270 or 1-199) as described in Figure 3.4. All wells were controlled for molar equivalent of expression plasmid and total DNA transfected. Data represent the mean ± SEM of six independently transfected wells of at least 3 independently repeated experiments. *, $p < 0.05$ on Mann-Whitney U for differences between medians of full length SGTA and each of the variants within each panel.

3.3.7 Disruption of SGTA homodimerisation does not alter its ability to inhibit AR activity

Previously, it has been shown that full length SGTA reduces both the magnitude and sensitivity of AR transactivation activity in prostate cancer cells (Buchanan, Ricciardelli et al. 2007). In order to assess the role of SGTA homodimerisation on AR transcriptional activity, we utilised the inhibitory effects of the 1-80 peptide (Figure 3.9) to block the formation of SGTA homodimers. In prostate cancer cells, AR (pCMV-AR3.1) was co-expressed with either full length SGTA, SGTA 1-80 or a combination of both. Expression of SGTA significantly decreased AR activity at 0.1 nM DHT by 14% ($p<0.05$; Figure 3.11), whereas expression of 1-80 alone did not affect AR activity. In the presence of the homodimerisation inhibiting 1-80 peptide, AR activity was also decreased by SGTA expression to a similar extent as without the 1-80 peptide ($p<0.01$; Figure 3.11), which implies that the effect of SGTA on AR is independent of SGTA homodimerisation.

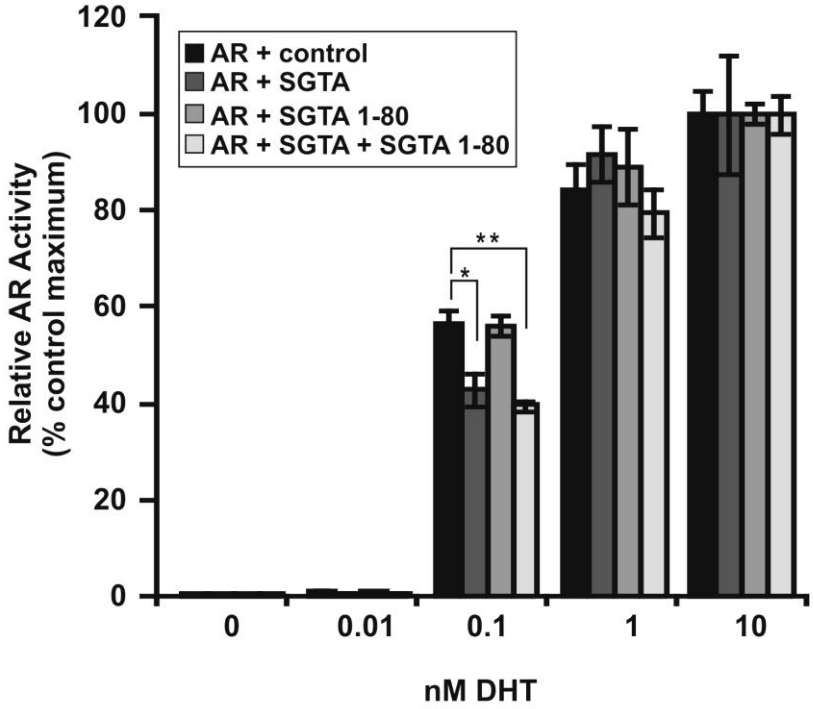


Figure 3.11: Inhibition of SGTA homodimerisation does not affect the inhibition of AR transactivation activity. PC3 cells (10,000/well) were transfected with 50 ng ARR3-tk-Luc reporter, 2.5 ng pCMV-AR3.1 and molar equivalent of pcFH-SGTA and/or pcFH-SGTA 1-80 or empty vector control. DNA concentration per well was kept constant with co-transfection of pBS(sk-). Six wells of each variant were treated with vehicle (ethanol), or increasing concentrations of DHT between 0.01 to 10 nM concentrations for 24 hours. Cells were lysed as described in Figure 3.6. Data represents the percent ± SEM maximum response for AR + control across all concentrations. *, $p < 0.05$, **, $p < 0.01$ on Mann-Whitney U for differences between medians of AR + SGTA compared to AR + control at each ligand concentration. Data is representative of at least 3 independently repeated experiments.

3.4 Discussion

The TPR domain of co-chaperone molecules remains one of the most evolutionarily conserved protein structures amongst species ranging from bacteria to humans (Andrade, Perez-Iratxeta et al. 2001; Schlegel, Mirus et al. 2007). In accordance, the evolutionary rate of the TPR domain has been slower when compared to the remaining co-chaperone sequence, most likely as a result of consistent favourable or essential protein-protein interactions. Previous reports have shown that proteins involved in the formation of complexes are on average more evolutionarily constrained than those that do not (Larsen, Olson et al. 1998; Aris-Brosou 2005). The contemporary role for TPR proteins in mammalian systems is highlighted by their ability to regulate steroid receptor signalling and intracellular protein transportation. These biological functions appears to have originated when the TPR proteins were integrated into the early chaperone system of the metazoan genera (Schlegel, Mirus et al. 2007). Around the same evolutionary time point, the immunophilins FKBP51, FKBP52 and the cyclophilin Cyp40 began to structurally differentiate from SGTA, and the other Hsp70 associated co-chaperones Hop and Hip (Schlegel, Mirus et al. 2007). In this chapter, analysis of SGTA protein sequences from *Xenopus* to *Homo sapiens* not only demonstrated good agreement with a validated species phylogeny (Ragan 2009), but also displayed an evolutionary distribution that is consistent with the phylogenetic trees for other steroid receptor TPR co-chaperones. This suggests that SGTA maintains an important biological function in eukaryotic systems, most likely relating to the regulation of the Hsp90 molecular chaperone complex (Johnson and Brown 2009).

While the TPR domain is conserved, SGTA is dissimilar from the other TPR containing co-chaperones through its ability to form homodimers. Despite a lack of evidence for the role of SGTA homodimerisation, it has been noted to decrease the binding affinity of the TPR domain for the human growth hormone receptor (Schantl, Roza et al. 2003). Conversely, homodimerisation has been found to be dispensable for other biological functions such as the effect of SGTA on the ATPase activity of Hsc70 or the effect on AR as demonstrated in this chapter, implying that SGTA homodimers may only impact on the biological activity of specific client proteins (Liu, Wu et al. 1999; Schantl, Roza et al. 2003).

While other studies have broadly defined the regions of SGTA that mediate homodimerisation, a comprehensive map of SGTA homodimerisation has yet to be compiled (Liou and Wang 2005; Buchanan, Ricciardelli et al. 2007). The findings in this thesis demonstrate that the entire 1-80 amino acid surface is necessary, but not sufficient for SGTA homodimerisation. Moreover, it appears that this region consists of a highly ordered secondary structure composed of non-polar hydrophobic amino acids and alpha helices, consistent with a complex binding surface. The finding that deletion of any region within the homodimerisation domain drastically altered native, but not denatured SGTA protein steady state levels, suggests that the ability of SGTA to form homodimers is directly affected by alterations within the amino acids 1-80, while the rest of the protein remains structurally sound. Indeed, this finding is consistent with studies that have found the formation of oligomeric complexes occurs as a result of selective pressures to improve overall protein stability (Larsen, Olson et al. 1998). Additionally, post-translational

modifications such as phosphorylation can serve as a regulatory mechanism in the formation of protein homodimers (Khokhlatchev, Canagarajah et al. 1998). In this chapter, an *in silico* screen was used to identify potential phosphorylation residues across the SGTA protein, including five within the homodimerisation domain. Although *in silico* phosphorylation screening approaches may be limited by the level of redundancy in the background data, potentially creating false positives, it nevertheless highlights specific sites that may be important for SGTA function. This has been recently demonstrated with the first experimentally confirmed SGTA phosphorylation site at serine residue 305, which acts to stabilise the interaction between SGTA and platelet derived growth factor receptor alpha (PDGFRα) (Moritz, Li et al. 2010).

Confirmation of the regions required for SGTA homodimerisation was initially attempted by co-immunoprecipitation. However, despite a series of optimisation steps, detection of SGTA homodimerisation was unsuccessful. The existence of several SGTA forms as demonstrated by native PAGE suggests that SGTA oligomeric complexes may be transient. It has been previously described that the formation of transient complexes is dependent on a number of physiochemical conditions, including the temporal and spatial positioning of the proteins in the cells, pH of the intracellular environment, ionic salt concentrations or changes in the relative concentration of interacting proteins (Nooren and Thornton 2003). Consequently, changes in these physiological conditions may shift the equilibrium of oligomeric formation. While steady state levels of both tagged SGTA proteins was not sufficient in some of the CoIP lysis buffers, it also remains possible that the pH and salt concentration for each of these buffers was not optimal to capture SGTA

homodimerisation. Nevertheless, several studies have demonstrated SGTA homodimerisation occurs via the amino terminus by using multiple techniques, including yeast and mammalian two hybrid assays, cross linking and dynamic light scattering (Tobaben, Varoqueaux et al. 2003; Liou and Wang 2005; Buchanan, Ricciardelli et al. 2007). Size exclusion chromatography, mass spectrometry or sedimentation velocity ultracentrifugation are several alternative methods that can be implemented in future experiments to investigate the specific amino acid residues required for SGTA homodimerisation. As SGTA has been known to interact with microtubule proteins of the cytoskeleton (Handley, Paddock et al. 2001), an additional consideration should be made that an intact cellular structure is required to maintain SGTA homodimerisation, which may possibly explain the success of cell based mammalian two-hybrid assay.

If we can assume the mammalian two-hybrid results are an accurate reflection of SGTA homodimerisation it was interesting to find that the TPR deficient SGTA variant was able to homodimerise to the same extent as full length SGTA, given that the SGTA TPR domain interacts with both Hsp70 and Hsp90 (Angeletti, Walker et al. 2002). This result suggests that the formation of SGTA homodimers is independent of the molecular chaperone complex, while it also appears that the SGTA carboxyl terminus is dispensable for SGTA homodimerisation, implying that intramolecular interactions outside of amino acids 1-80 are not require for SGTA to form homodimers or overall protein stability.

The existence of SGTA dimeric states opens the possibility of simultaneous interactions with multiple client proteins outside of the molecular chaperone complex. Indeed, it has been shown that SGTA homodimers are arranged as an elongated, non-spherical

structure, which can potentially generate a large surface area for protein interactions (Liou and Wang 2005). Studies demonstrating an association of SGTA with the human growth factor receptor, glucose transporter 1, viral capsule proteins Vpu and Gag, and PDGFRα collectively point to SGTA as a key mediator of client protein transport to the cell surface (Handley, Paddock et al. 2001; Schantl, Roza et al. 2003; Liou and Wang 2005; Moritz, Li et al. 2010). Therefore, the elongation structure of SGTA homodimers may provide the necessary requirements to simultaneously transport one or more client proteins to the cell surface. Conversely, the results presented here demonstrate that inhibition of SGTA homodimerisation does not alter its ability to affect AR transcriptional activity. This suggests that the existence of SGTA in either monomeric or dimeric states maintain the same biological efficacy and that regions outside of amino acids 1-80 most likely contribute to the effects of SGTA on AR activity. However, further studies are required in order to elucidate the requirement of SGTA homodimerisation for the biological function of other client proteins.

Regardless of the effect of SGTA homodimerisation domain on AR, the utilisation of the 1-80 peptide to disrupt the homodimerisation domain demonstrates a novel means of targeting SGTA. It had been previously reported by Liou and colleagues that the N-terminal region of SGTA was sufficient to homodimerise, but the authors did not further investigate if it was sufficient to interact with full length SGTA (Liou and Wang 2005). Conversely, the results presented here show that the homodimerisation domain alone was insufficient for either process, but that co-expression of SGTA amino acids 1-80 and full length SGTA potently blocked SGTA homodimerisation. Even though the underlying

mechanism remains unsolved, one might speculate that the 1-80 peptide transiently interacts with the homodimerisation interface, but does not contain the necessary residues to maintain a more stable interaction. Indeed, this phenomenon has been previously observed for peptide inhibitors of HIV-1 reverse transcriptase homo and heterodimerisation (Divita, Restle et al. 1994; Divita, Baillon et al. 1995). Given our findings that deletion of the TPR domain or the linker region/QRD maintains SGTA homodimerisation, it appears likely that residues between the homodimerisation and TPR domains (i.e. amino acids 81-90) are also necessary for the interaction between the 1-80 peptide and SGTA. Therefore, disruption to SGTA homodimerisation may occur through an unstable, transient interaction of the 1-80 peptide competitively inhibiting more stable interactions in the complete homodimerisation domain. An alternative explanation is that the existence of an indirect mechanism of destabilisation through interactions between the 1-80 fragment and secondary partners associate with SGTA homodimers.

In summary, this chapter demonstrates that the SGTA functional domains of SGTA are evolutionary conserved, which suggests that this co-chaperone has maintained an important biological function from amphibians to humans. The uniqueness of SGTA amongst the steroid receptor containing co-chaperones is in its ability to form a homodimer. While it was not possible to capture SGTA homodimerisation by CoIP experiments, an alternative assay was used to demonstrate that SGTA homodimerisation is mediated by the first 80 amino acids. These residues form a rigid, hydrophobic surface that allows the potential for protein-protein interactions. More importantly, SGTA is able to form homodimers independently of its TPR domain, which implies that SGTA

homodimerisation occurs outside of the Hsp70/90 chaperone complex. Furthermore, this chapter has shown that the homodimerisation domain in itself is insufficient for interactions, but acts as a potent inhibitor of SGTA homodimerisation and that disruption of homodimerisation does not interfere with the affect of SGTA on AR activity, suggesting that homodimerisation is not essential for SGTA biological function. In Chapter 4 of this thesis we investigate other regions of SGTA that may impact on AR activity.

CHAPTER 4

SGTA acts to restrict the sensitivity of Androgen Receptor activity

Chapter 4: SGTA acts to restrict the sensitivity of Androgen Receptor activity

4.1 Introduction

The findings from Chapter 3 of this thesis demonstrated that SGTA homodimerisation occurs through structurally conserved elements within the first 80 amino acids of the protein. However, homodimerisation was not required for SGTA to influence AR transcriptional activity, suggesting that regions outside of the SGTA homodimerisation domain are necessary to mediate the effects of SGTA on AR activity. The aim of this chapter was to examine the extent to which SGTA affects AR activity and to determine the requirement of individual SGTA domains have in mediating those effects.

Unliganded AR in normal cells is located predominately in the cytoplasm in association with the heat shock protein 70 (Hsp70) and/or 90 (Hsp90) chaperone complexes (Marcelli, Stenoien et al. 2006). While this association may facilitate AR ligand binding and transport (Thomas, Harrell et al. 2006), the biological necessity for active exclusion of the apo-AR from the nucleus remains unclear. One possibility is that the process of nuclear shuttling allows the cytoplasmic signalling environment to influence transcriptional responses in the nucleus (Ziegler and Ghosh 2005; Sun, Montana et al. 2007). Specifically, inducible transcription factors, such as the AR, in the absence of stimuli are retained in the cytoplasm due to the presence of various binding partners that mask a nuclear localisation signal (NLS). Upon ligand stimulation, these NLS masking factors are released from their

target protein, which allows the transcription factor to track through the nuclear pore complex and interact with the nuclear transportation machinery. The purpose of binding partners sequestering the majority of inducible transcription factors in the cytoplasm is to either prime the transcription factor to receive a transduction signal or target it for degradation and protein turnover (Ziegler and Ghosh 2005).

In the context of hormone activation, there is a need for steroid receptors to interact with the molecular chaperone complex in order to establish and maintain competent hormone responses (Pratt and Toft 1997). The incorporation of specific TPR containing co-chaperones into the molecular chaperone-steroid receptor complex is gaining momentum as a potentially important level of controlling steroid receptor activity. For example, the immunophilin FKBP52 acts to potentiate both GR and AR signalling by interacting with the cytoskeleton motor transport protein dynein (Cheung-Flynn, Prapapanich et al. 2005; Wochnik, Ruegg et al. 2005; Yong, Yang et al. 2007), whereas over expression of FKBP51 in squirrel monkeys is associated with lower GR ligand binding affinity and glucocorticoid resistance (Denny, Valentine et al. 2000; Scammell, Denny et al. 2001). Recently, it has been noted that FKBP51, along with Cyp40 enhances AR activity in androgen dependent prostate cancer cells (Periyasamy, Hinds et al. 2010), while a separate study identified that FKBP51 is capable of recruiting p23 to the Hsp90 complex, which leads to an increased total number of AR molecules competent to bind ligand (Ni, Yang et al. 2010). Collectively, these results highlight the potential diversity of mechanisms that the TPR co-chaperone system use to regulate the early stages of steroid receptor ligand binding and subsequent downstream transcriptional activity.

Recently, SGTA has been defined as a steroid receptor associated TPR containing co-chaperone, after being identified as an AR binding partner (Buchanan, Ricciardelli et al. 2007). SGTA over expression was found to promote cytoplasmic retention of the AR, subsequently decreasing the sensitivity of AR transcriptional activity (Buchanan, Ricciardelli et al. 2007). However, the effect of SGTA on AR was derived from a single synthetic reporter, and the ability of SGTA to control AR activity on multiple naturally occuring binding sites still remains unknown.

The implementation of contemporary genome-wide screening methods such as ChIP-chip or ChIP-sequencing has been used to investigate the dynamics of ligand dependent steroid receptor DNA binding. The complement of receptor binding sites across the genome, termed the steroid receptor cistrome, has been important in redefining the spatial and temporal placement of steroid receptors and how they regulate transcription. In the case of AR, these studies have revealed that the majority of AR binding sites lie distal from the transcriptional start site (Bolton, So et al. 2007; Massie, Adryan et al. 2007; Takayama, Kaneshiro et al. 2007; Wang, Li et al. 2007; Jia, Berman et al. 2008; Massie and Mills 2008; Wang, Li et al. 2009). Although, determining which distal AR binding region is involved in the regulation of gene expression remains elusive, it has been proposed that the use of luciferase reporter AR transactivation assays can be optimised to assess the functionality of these sites in isolation. By using multiple reporters, these assays may provide a closer surrogate of the diversity of AR responses than analysis of a single reporter alone (Jia, Berman et al. 2008; Jariwala, Cogan et al. 2009). To gain insight into the determinants and mechanisms by which SGTA might influence AR activity, the aims

addressed in this chapter are i) to investigate the effect of SGTA on AR activity on multiple androgen responsive loci and ii) identify the regions of SGTA that are necessary for an effect on AR activity.

4.2 Materials and Methods

4.2.1 Plasmids

Plasmids created specifically for AR transactivation assays conducted within this thesis have been described in chapter 3.2.1 and are listed in Appendix B2. Expression plasmids pCMV-AR3.1, pcFH-SGTA, pBS(sk-), and the androgen responsive reporter ARR3-tk-Luc have been previously described (Buchanan, Craft et al. 2004; Butler, Centenera et al. 2006; Buchanan, Ricciardelli et al. 2007; Need, Scher et al. 2009). The expression plasmid pSG5-ERα/HEGO was a gift from Professor Pierre Chambon (College de France, France). The pSG5-GR and pSG5-PGR expression vectors were a gift from Professor Michael Stallcup (University of Southern California, USA). The following androgen responsive reporters R01, R12, R16, R20, R22, R24, R26, R35, R42, R61, R62 were generated in our laboratory as previously described in our AR cistrome study on chromosomes 19 and 20 (Jia, Berman et al. 2008).

4.2.2 Quantitative real time PCR and Immunoblot

COS-1, PC3, C42B and LNCaP cells maintained as described in chapter 2.3.2.1 were seeded in 6 well plates (150,000 cell/well) and allowed to adhere for 24 hours. Cells were treated with either vehicle (ethanol) control or 10 nM DHT for 16 or 24 hours for mRNA or protein isolation respectively. RNA isolation and cDNA synthesis was performed as described in chapter 2.3.6 and 2.3.6.2 respectively. Quantitative real time PCR (QRT-PCR) was performed for *SGTA*, *FKBP51*, *FKBP52*, *Cyp40*, *PP5* and normalised to *GAPDH* using the delta delta ct method (Livak and Schmittgen 2001). Primer sequence and

cycle conditions used for real time PCR are listed in Appendix A3 and chapter 2.3.6.3 respectively. Protein lysates were prepared and quantified for immunoblot analysis as described in chapters 2.3.5.3 and 2.3.5.4 respectively. Immunoblot was performed as described in chapter 2.3.5. The following primary antibody dilutions were used: SGTA (Abnova) (1:1000), FKBP51 (1:1000), FKBP52 (1:1000), Tubulin (1:20,000).

4.2.3 Transient luciferase assay

AR transactivation assays were performed in cultured PC3 cell (10,000 cells/well in 96 well plates). Cells were transfected with 0.5 - 2.5 ng of pCMVAR-3.1, 5 - 20 ng of pcFH-SGTA, or equivalent molar amount of empty pcFH, and 50 ng of an AR responsive-luciferase reporter per well as described in chapter 2.3.3.2. Cells were treated with vehicle (ethanol) control or increasing concentrations of DHT for 24 hours in replicates of six and assayed for luciferase activity as described in chapter 2.3.3.1.

4.2.4 Chromatin integrated reporter luciferase assay

PC3 cells stably transfected with ARR3-tk-Luc were created by Dr. Eleanor Need as previously described (Need, Scher et al. 2009). These cells were used to assess whether SGTA modulates AR activity on a chromatin integrated reporter. *In vivo* luciferase assays were performed by transfection of 50 ng pCMV-AR 3.1 and 100 ng pcFH-SGTA or a molar equivalent of empty pcFH plasmid. Cells were treated with vehicle (ethanol) control or 0.01 – 1 nM DHT for 24 hours and assessed as described in chapter 2.3.3.2.

4.2.5 Statistical analyses

Statistical analyses were performed as indicated in figure legends using Graphpad Prism Version 5 software for Windows (GraphPad Software, California, USA). Non-parametric Mann-Whitney U tests were used to determine differences between groups where indicated in figure legends, while the non-parametric Spearman rho test was used to assess the linear association between two variables. A p-value < 0.05 was considered statistically significant.

4.3 Results

4.3.1 Tetratricopeptide repeat containing co-chaperones are expressed in prostate cancer cell lines

The relative cellular expression of the different TPR proteins is thought to determine which co-chaperones are preferentially bound to an Hsp90-steroid receptor complex (Smith and Toft 2008). In order to determine the most appropriate cell system for SGTA over expression experiments, the relative level of the five key steroid receptor associated co-chaperones was examined in four commonly available cell lines, C42B, LNCaP and PC3 prostate cancer cells along with transformed monkey kidney COS-1 cells. QRT-PCR analysis showed that SGTA expression is highest in COS-1 cells and lowest in PC3, while C42B and LNCaP cells contain relatively equal intermediate levels (Figure 4.1A). Relative levels of SGTA in the different cells lines was confirmed by immunoblot analysis (Figure 4.1F). Consistent with its putative role in promoting AR activity (Cheung-Flynn, Prapapanich et al. 2005), the immunophilin FKBP52 in the prostate, has the highest mRNA expression in the AR positive C42B and LNCaP cells compared to the AR negative COS-1 and PC3 cells, which was confirmed by immunoblot (Figure 4.1B and F). Treatment with DHT did not alter the expression of FKBP52 in any of the cell lines (Figure 4.1B and F). In contrast, expression of the related immunophilin FKBP51, a known AR regulated gene (Magee, Chang et al. 2006) was dramatically increased at both the mRNA and protein level (Figure 1.4C and F). Regulation by DHT was not observed in AR negative COS-1 and PC3 cells.

Cyp40 expression was relatively equal across the prostate cancer cell lines and lower in COS-1 cells (Figure 4.1D), while PP5 was highest in COS-1 cells. Confirmation of PP5 and Cyp40 protein steady state levels in these cell lines was not performed due to the lack of available antisera in our laboratory. From these data the low levels of endogenous SGTA and non functional AR in the prostate cancer PC3 cells makes it a good candidate for SGTA over expression transactivation assays, whereas C42B and LNCaP cells are excellent for SGTA knockdown experiments.

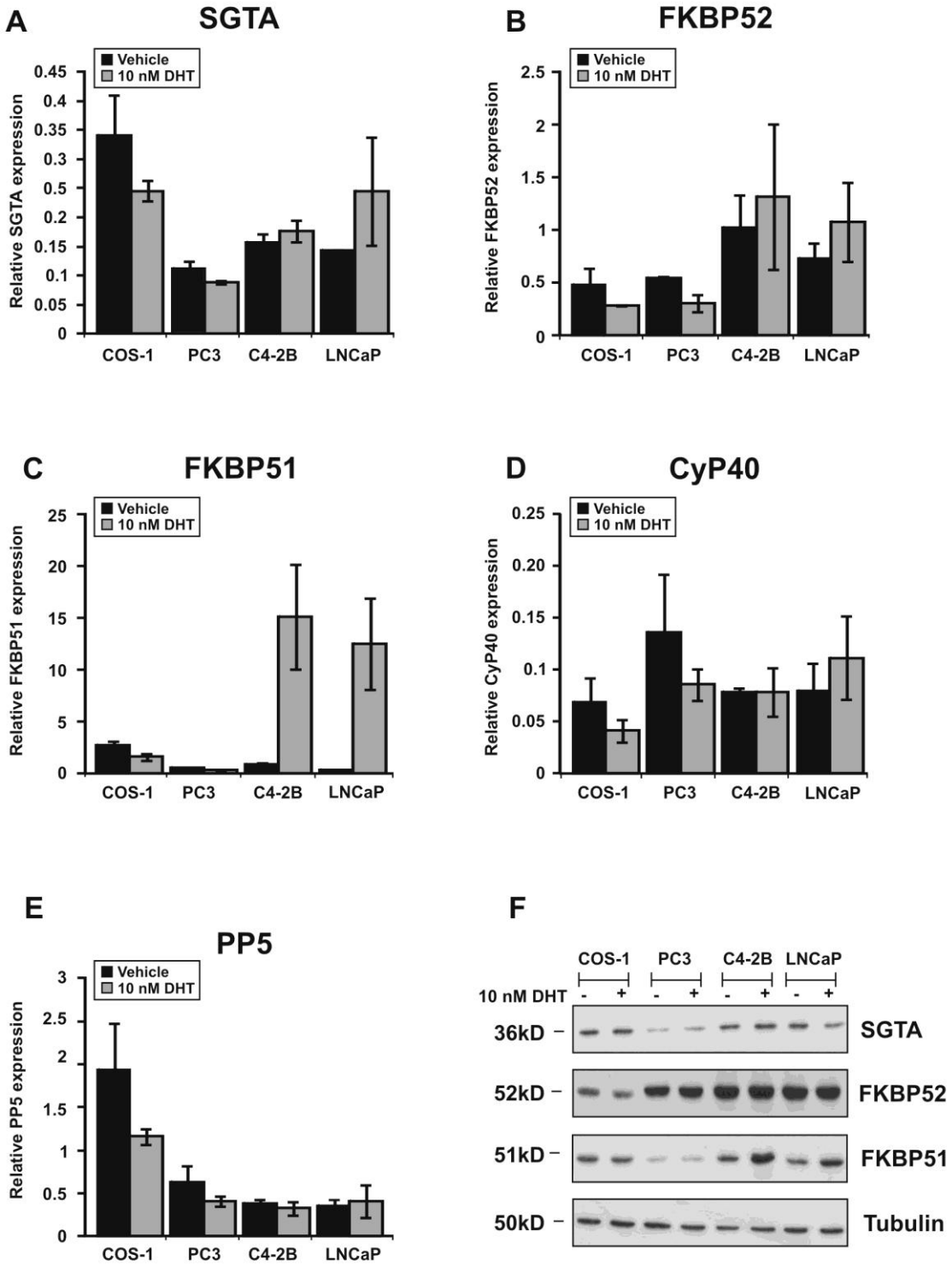

A
SGTA
Vehicle
10 nM DHT
Relative SGTA expression
0.45
0.4
0.35
0.3
0.5
0.2
0.15
0.1
0.05
0
COS-1
PC3
C4-2B
LNCaP
B
FKBP52
Vehicle
10 nM DHT
Relative FKBP52 expression
2.5
2
1.5
1
0.5
0
COS-1
PC3
C4-2B
LNCaP
C
FKBP51
Vehicle
10 nM DHT
Relative FKBP51 expression
25
20
15
10
5
0
COS-1
PC3
C4-2B
LNCaP
D
CyP40
Vehicle
10 nM DHT
Relative CyP40 expression
0.25
0.20
0.15
0.1
0.05
0
COS-1
PC3
C4-2B
LNCaP
E
PP5
Vehicle
10 nM DHT
Relative PP5 expression
3
2.5
2
1.5
1
0.5
0
COS-1
PC3
C4-2B
LNCaP
F
COS-1
PC3
C4-2B
LNCaP
10 nM DHT
- + - + - + - +
36kD
SGTA
52kD
FKBP52
51kD
FKBP51
50kD
Tubulin

Figure 4.1: Relative expression of TPR proteins in cell lines used within this thesis. A-E: COS-1, PC3, C42B and LNCaP cells were treated for 16 hours with either vehicle (ethanol) control or 10 nM DHT. RNA was isolated and analysed by QRT-PCR for expression of *SGTA*, *FKBP52*, *FKBP51*, *Cyp40* and *PP5* and normalised to the housekeeping gene *GAPDH*. Data are presented represent the mean (± SD) of two biological replicates for COS-1 and PC3 cells and three biological replicates for C42B and LNCaP cells. **F:** Immunoblot analysis of SGTA, FKBP52 and FKBP51 steady state protein levels. COS-1, PC3, C42B and LNCaP cells were treated for 24 hours with either vehicle (ethanol) control or 10 nM DHT. Tubulin was used as a loading control.

4.3.2 Optimisation of AR and SGTA transactivation assays

To determine the relative amount of AR required for optimal transactivation activity from the ARR3-tk-Luc reporter, the level of AR expression plasmid was titrated in PC3 cells. In agreement with a previously published report (Buchanan, Craft et al. 2004), increasing the concentration of AR expression vector transfected into PC3 resulted in an increase in response to DHT to a maximum of 2.5 ng of AR expression vector, while basal activity remained unaffected (Figure 4.2A). Next, transfection of increasing concentrations of SGTA expression plasmid or empty vector control were used to determine the level of transfected SGTA sufficient to influence AR activity without causing squelching of the general transcriptional machinery. Importantly, DNA toxicity effects in all transactivation assays in this thesis are controlled with an equivalent molar ratio of empty vector as well as an appropriate amount of non-specific prokaryotic plasmid DNA to maintain a constant amount of total DNA transfected into the cell. Transfection of 10 ng or greater empty pcFH plasmid resulted in a significant decrease in AR activity at 0.01 and 0.1 nM DHT ($p<0.01$; Figure 4.2B), suggesting that any effect of SGTA at these concentrations of vector will most likely be compounded by transcriptional squelching. Notably, transfection of 5 ng of pcFH-SGTA resulted in a significant decrease in AR activity at 0.01 and 0.1 nM DHT ($p<0.01$; Figure 4.2 C), consistent with a previous report (Buchanan, Ricciardelli et al. 2007), while pcFH-SGTA did not alter AR activity at 1 nM DHT ($p<0.01$; Figure 4.2B and C). Based on these observations, optimal transactivation conditions will consist of AR expression plasmid at a DNA concentration equivalent to 2.5 ng and either control empty or SGTA specific expression vectors at 5 ng.

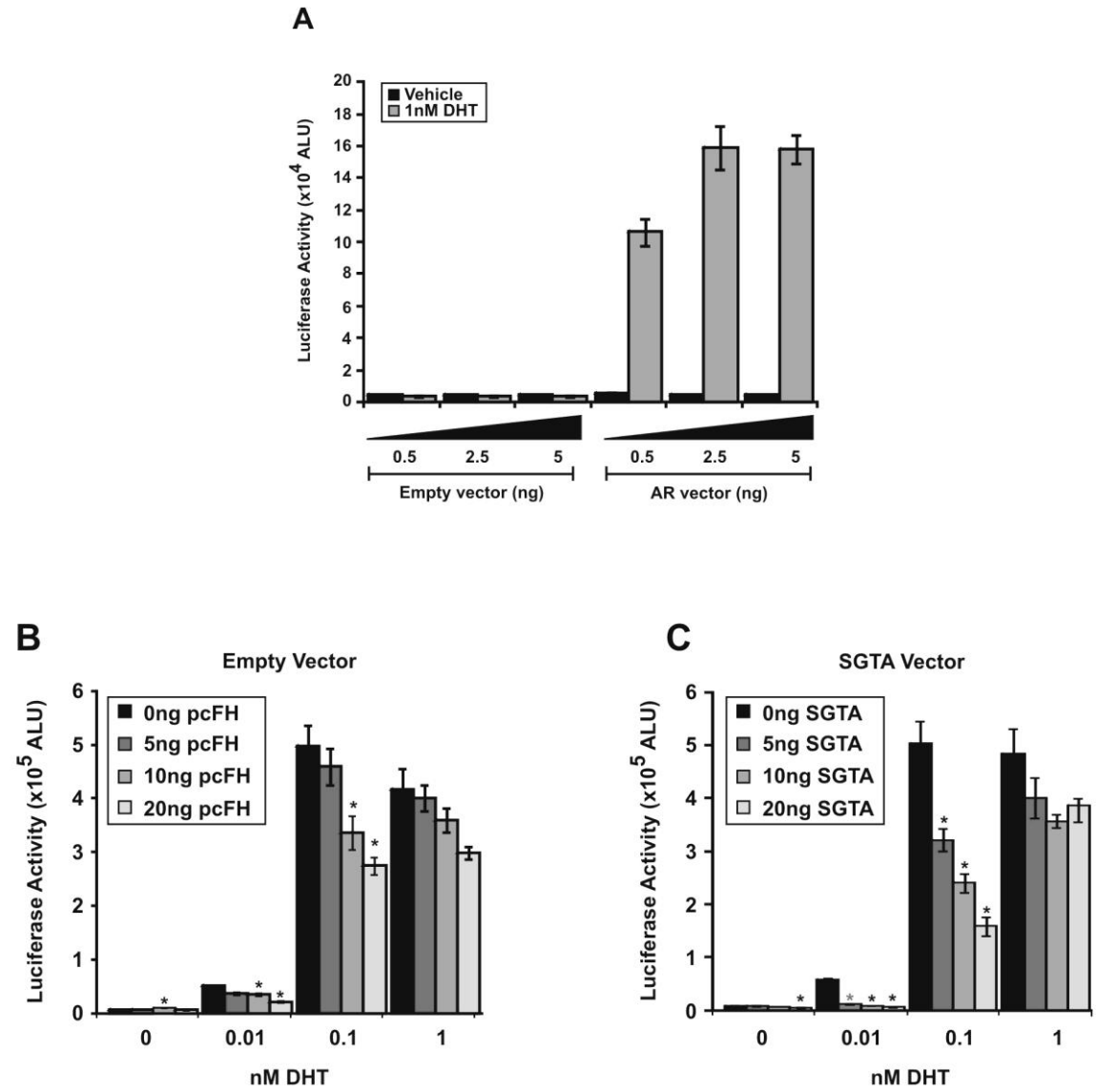

A
Vehicle
1nM DHT
Luciferase Activity (x10^4 ALU)
0.5
2.5
5
0.5
2.5
5
Empty vector (ng)
AR vector (ng)
B
Empty Vector
0ng pcFH
5ng pcFH
10ng pcFH
20ng pcFH
Luciferase Activity (x10^5 ALU)
0
0.01
0.1
1
nM DHT
C
SGTA Vector
0ng SGTA
5ng SGTA
10ng SGTA
20ng SGTA
Luciferase Activity (x10^5 ALU)
0
0.01
0.1
1
nM DHT

Figure 4.2: Optimisation of AR transactivation assays with over-expression of SGTA in PC3 cells. A: PC3 cells (10,000/well in 96 well plates) were transfected with increasing concentrations of AR (pCMV-AR3.1) while controlling for expression vector and DNA concentration per well with vectors pCMV and pBS(sk-), along with 50 ng ARR3-tk-Luc reporter per well. Six wells were transfected for 4 hours and then treated with either vehicle (ethanol) control or 1 nM DHT for 24 hours. Data represents the mean ± SEM luciferase activity in arbitrary light units (ALU) of 6 independently transfected wells, and is representative of at least 3 independently performed experiments. **B-C:** PC3 cells were transfected with 2.5 ng AR, 50 ng ARR3-tk-Luc reporter and increasing concentrations of pcFH-SGTA or empty vector control. Expression vector and total plasmid DNA concentration was controlled with the vectors pcFH and pBS(sk-). Cells were transfected for 4 hours and then treated with vehicle (ethanol) control or 0.01 – 1 nM DHT for 24 hours. *, $p < 0.01$ on Mann Whitney U between all vector concentrations *versus* no vector control (i.e.0 ng expression vector) for each ligand concentration. Data is representative of at least 3 independently repeated experiments.

4.3.3 SGTA decreases AR sensitivity to ligand

In order to determine the specificity of the effect of SGTA on AR activity, 13 different native AR responsive luciferase reporters generated in an AR cistrome study of chromosomes 19 and 20 were used in AR transactivation experiments (Jia, Berman et al. 2008). Combining the data from 2-5 independent transactivation experiments for each reporter (up to 30 biological replicates/reporter) revealed that SGTA over expression has an effect on basal activation of approximately 50% (7/13) of the reporters ($p<0.05$; Figure 4.3A), but a dramatic inhibitory effect on the ligand dependent AR activity of 12/13 reporters in the presence of 0.1 nM DHT, while SGTA had virtually no effect on AR activity with 1 nM DHT (Figure 4.3C and D). When AR transactivation data from all reporters was collated, SGTA over expression resulted in an average decrease of 16.8%, 21.8%, 32%, 6.7% for DHT concentrations of 0, 0.01, 0.1 and 1 nM respectively (Figure 4.3E). Further analysis revealed that the degree to which SGTA affected AR activity depended on the nature of the responsive loci. For example, SGTA significantly decreased AR activity on the R22 and R24 reporters at all ligand concentrations, whereas SGTA did not affect AR on the R35 reporter under any conditions (Figure 4.3A-D). To assess this more closely, the effect of SGTA on AR activity at 0.1 nM DHT for each reporter was ranked and compared to the strength of AR activity in the absence of SGTA. This correlation showed that SGTA had the greatest effect in reducing AR activity on those loci most responsive to DHT treatment ($p<0.006$; Figure 4.4).

Next, the potential effect of SGTA on AR responses in a chromatin context was assessed using a chromatin integrated ARR3 reporter in PC3 cells. SGTA over expression

maintained its inhibitory effect on AR at 0.1 nM DHT, which demonstrates that SGTA is still effective on AR regardless of the location of the reporter element and is applicable in the context of chromatin activation by the AR ($p<0.05$; Figure 4.3F).

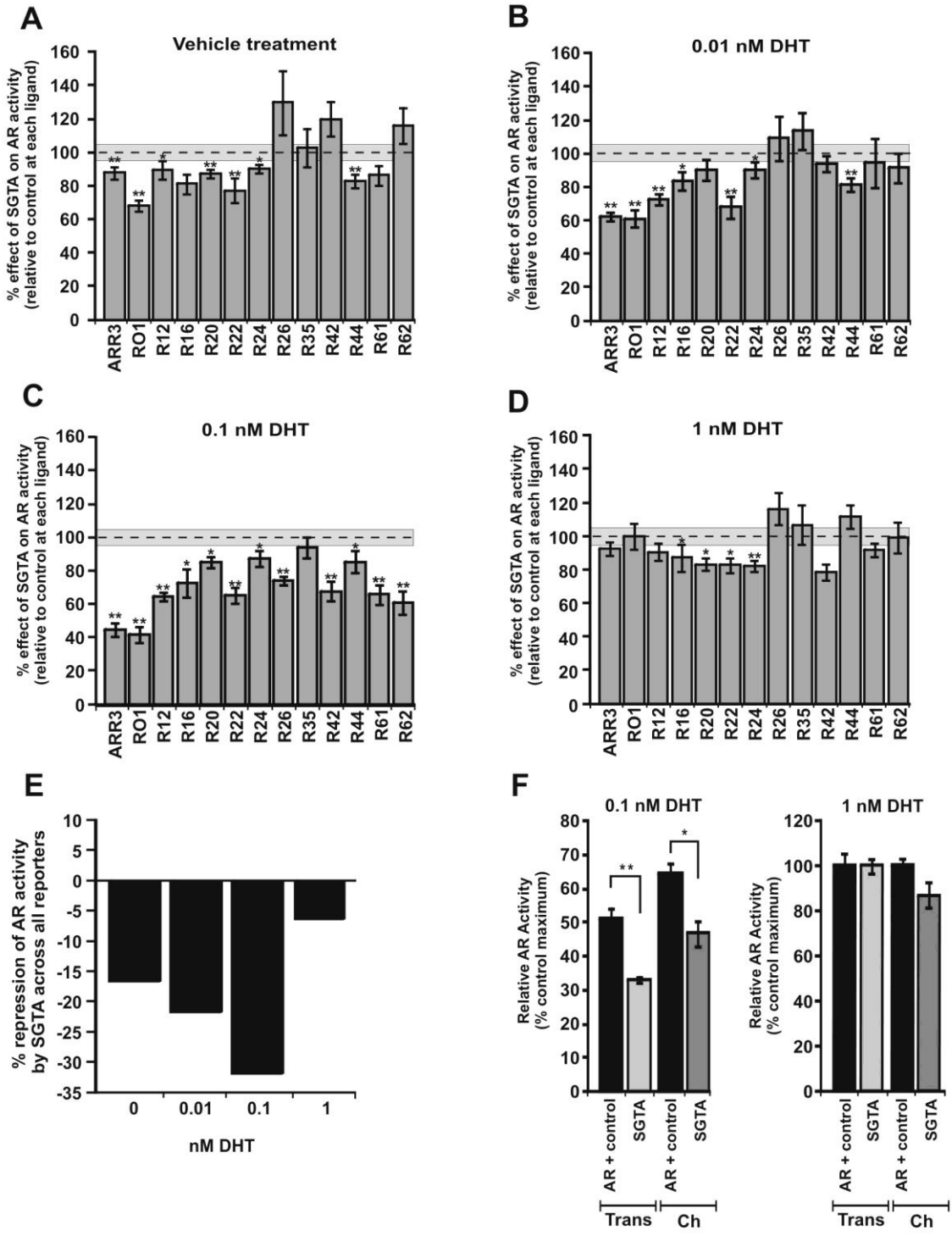

A
Vehicle treatment
% effect of SGTA on AR activity (relative to control at each ligand)
ARR3 RO1 R12 R16 R20 R22 R24 R26 R35 R42 R44 R61 R62
B
0.01 nM DHT
C
0.1 nM DHT
D
1 nM DHT
E
% repression of AR activity by SGTA across all reporters
0 0.01 0.1 1
nM DHT
F
0.1 nM DHT
1 nM DHT
Relative AR Activity (% control maximum)
AR + control
SGTA
Trans
Ch

Figure 4.3: Effect of SGTA on AR signalling on 13 different reporter constructs and on a chromatin integrated reporter. **A-D:** Effect of SGTA on AR ligand independent and dependent transactivation activity. PC3 cells were transfected with AR (2.5 ng), SGTA (5 ng) or empty plasmid control, and one of 13 AR reporter constructs (50 ng) then treated with vehicle (ethanol) or 0.01-1 nM DHT. Data represents combined results from 2-5 independent experiments (up to 30 replicates/reporter), and is presented as percent (±sem). Percentage effect of SGTA on AR activity is relative to AR + control (dotted line) at each ligand concentration. Horizontal grey bar at each ligand concentration represents ± median SEM for AR + control across all reporters. Significance denoted by *, is $p<0.05$; **, is $p<0.01$ on Mann-Whitney U for difference between medians of AR + SGTA in comparison to reporter-matched control. **E:** Mean effect of SGTA on AR activity on all reporters at each ligand concentration. Data from A-D presented as average percent decrease in AR activity by SGTA across all reporters at each ligand concentration **F:** Effect of SGTA on AR activation of a chromatin (Ch) integrated reporter using the PC3 ARR3 stable line compared to transiently transfected (Trans) ARR3 at 0.1 nM and 1 nM DHT respectively. * $p<0.05$; ** $p<0.01$ on Mann-Whitney U analysis for differences between medians as described in **A.**

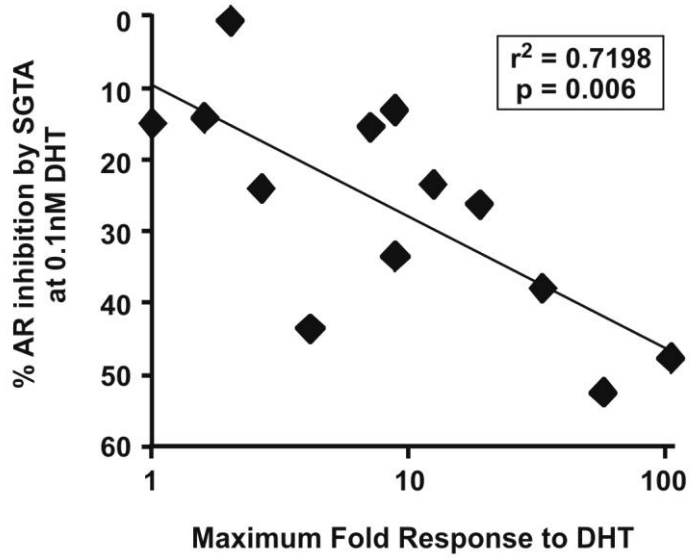


Figure 4.4: The greatest effect of SGTA on AR activity occurs on those loci that are most responsive to DHT. Data generated from Figure 4.4 A-D. Spearman r correlation between the percentage inhibition of AR with SGTA at 0.1 nM DHT and the maximal activation potential of AR over 0.01-1 nM DHT.

4.3.4 SGTA affects GR and PR transactivation activity

The effect of SGTA on AR activity is shared by various TPR co-chaperones that are also able to affect the transcriptional activity of other steroid receptors, implying that TPR proteins are able to simultaneously integrate into multiple Hsp90-steroid receptor complexes (Schulke, Wochnik et al. 2010). In order to determine if this is also true for SGTA, transactivation assays were designed to co-express SGTA with either AR, the glucocorticoid (GR), progesterone B isoform (PGR-B) or oestrogen alpha (ERα) receptors in PC3 cells. As previously demonstrated in this chapter, SGTA is able to significantly decrease AR activity at 0.01 and 0.1 nM DHT respectively (Figure 4.5A). Similarly, SGTA inhibits GR and PGR-B activity when in the presence of either the synthetic corticoid dexamethasone or progesterone respectively ($p<0.05$; Figure 4.5B and C), suggesting that SGTA may be able to constrain the ligand sensitivity of these receptors in a similar manner to AR. In agreement with results for other TPR co-chaperones (Schulke, Wochnik et al. 2010), SGTA did not alter the transcriptional activity of ERα (Figure 4.5D).

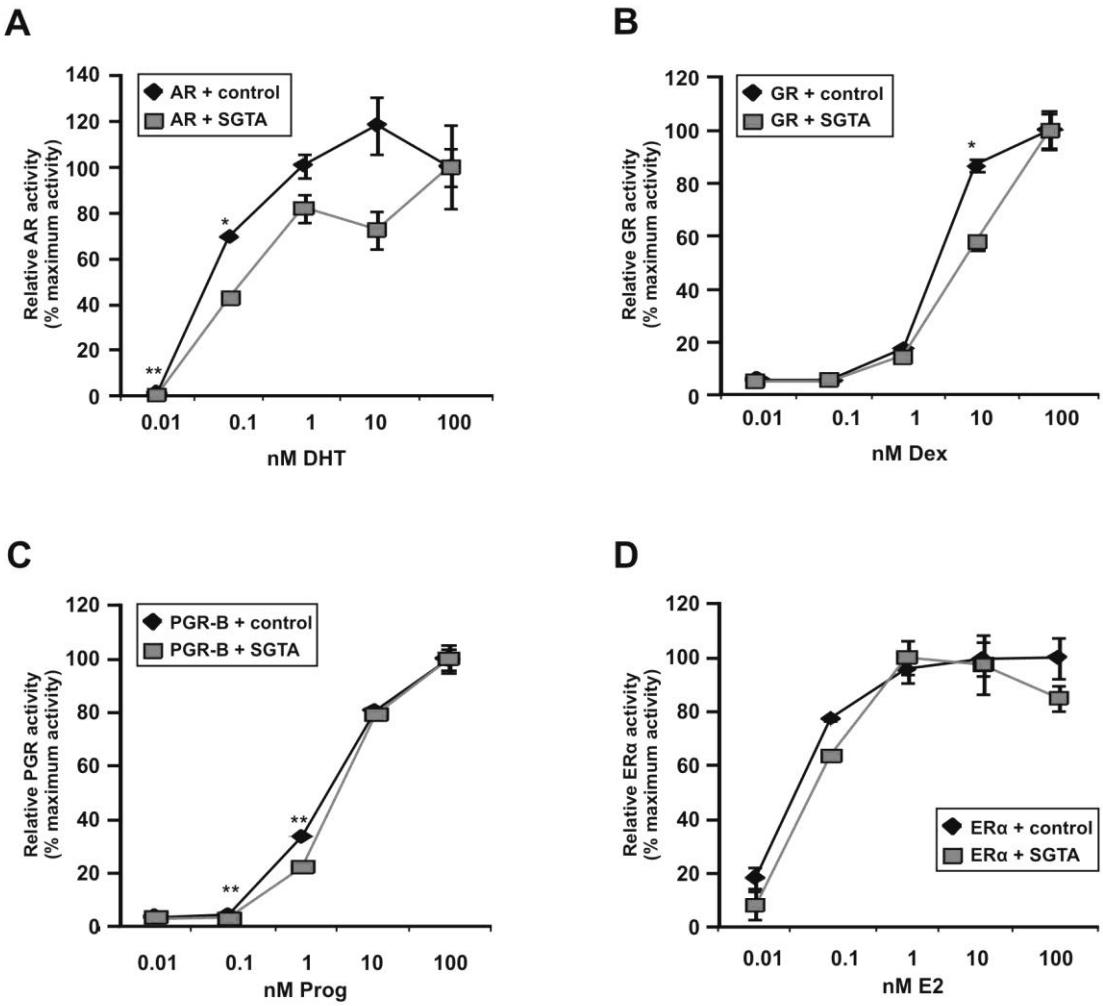

A
AR + control
AR + SGTA
Relative AR activity (% maximum activity)
nM DHT
B
GR + control
GR + SGTA
Relative GR activity (% maximum activity)
nM Dex
C
PGR-B + control
PGR-B + SGTA
Relative PGR activity (% maximum activity)
nM Prog
D
ERα + control
ERα + SGTA
Relative ERα activity (% maximum activity)
nM E2

Figure 4.5: SGTA maintains the strongest effect on the predominately cytoplasmic steroid receptors AR, GR and PGR-B. A-D: Effect of SGTA on steroid receptor ligand independent and dependent transactivation activity. PC3 cells were transfected with AR, GR, PGR-B or ERα (2.5 ng), SGTA (5 ng) or empty plasmid control. The ARR3-tk-Luc reporter was used in AR, GR and PGR-B transactivation assays, while the ERE-tk-Luc reporter was used for the ERα assay. Expression vector and total plasmid DNA concentration was controlled with the vectors pcFH and pBS(sk-). Cells were treated with 0.01 – 100 nM ligand (DHT, dexamethasone (Dex), progesterone (Prog) or estradiol (E2)) for 24 hours. Cells were lysed and luciferase activity measured as described in Figure 4.2A. Significance denoted by *, is $p<0.05$, **, is $p<0.01$ on Mann-Whitney U for difference between means of steroid receptor + SGTA *versus* the reporter-matched control. All data is representative of at least 3 independently repeated experiments.

4.3.5 Deletions within the SGTA homodimerisation domain variably alter AR transactivation activity

The results presented in Chapter 3 demonstrated that the entire 1-80 amino acid sequence in the SGTA amino terminus was required for homodimerisation. However, inhibition of this domain did not alter the ability of SGTA to decrease AR activity. To further investigate the precise requirement of the homodimerisation domain for the effect of SGTA on AR activity, SGTA variants were created with deletions along the first 80 amino acids. AR transactivation assays revealed that deletion of amino acid segments along the SGTA homodimerisation domain (SGTA Δ 1-20, Δ 41-60, Δ 29-33) or complete deletion of the entire domain (80-313) did not affect the capacity of SGTA to decrease AR activity at 0.1 nM DHT ($p<0.01$; Figure 4.6). However, deletion of amino acids 21-40 compromised the capacity of SGTA to affect AR at 0.1 nM DHT. Immunoblot analysis presented in chapter 3 (Figure 3.7B) demonstrates similar protein steady state levels across all SGTA deletion variants. Therefore, these results suggest there is either inherent variability within the SGTA homodimerisation domain to alter AR activity or alternatively, deletion of amino acids 21-40 could result in an altered protein conformation that prevents the interaction between SGTA and AR.

4.3.6 The SGTA linker region is necessary for an effect on AR activity

Given that the effects of SGTA on AR activity are independent of the homodimerisation domain (Figure 4.7A), deletion of the other functional domains was undertaken to examine if they are required for the inhibitory effect on AR. Deletion of the TPR (Δ 91-192) and

glutamine-rich domain (QRD; SGTA 1-270) did not alter the ability of SGTA to decrease AR activity at 0.1 nM DHT ($p<0.01$; Figure 4.7B and C), whereas removal of the linker region that separates the TPR and QRD was found to be necessary (Figure 4.7D).

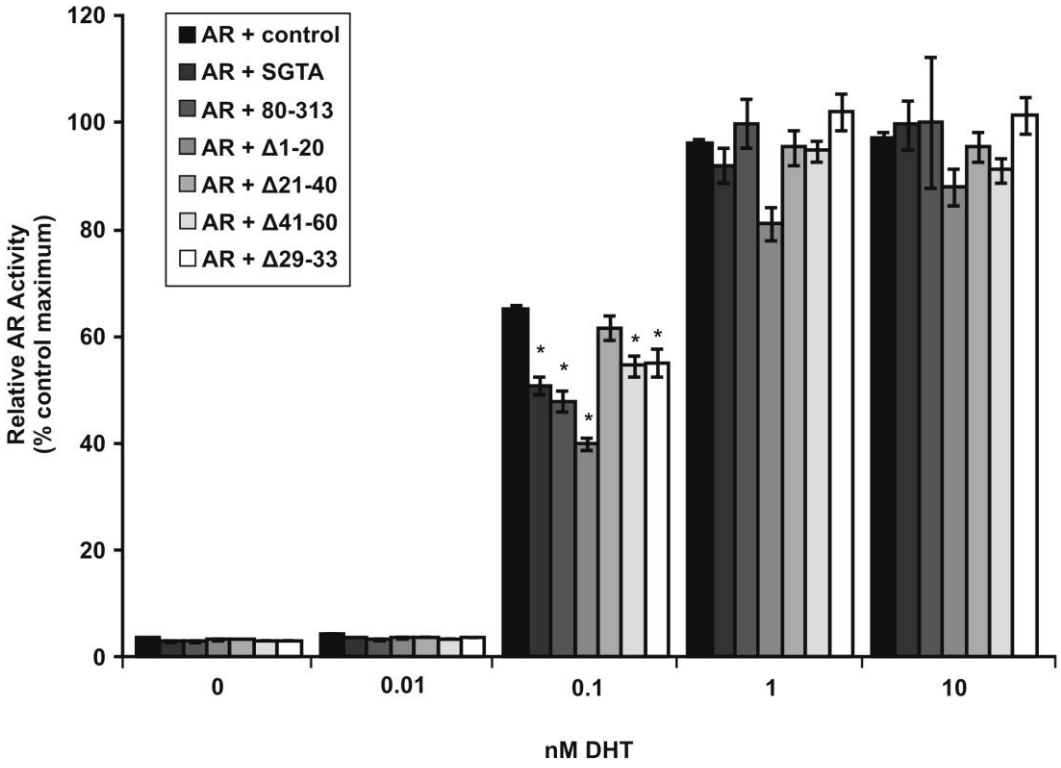


Figure 4.6: Effect of SGTA homodimerization deletion variants on AR activity. PC3 cells were transfected with AR, full length SGTA or SGTA homodimerisation deletion variant expression vectors and the ARR3-tk-Luc reporter. Cells were treated with 0 – 10 nM DHT for 24 hours. *, $p<0.01$ on Mann Whitney U analysis for AR + SGTA and variants compared to AR + control. Data is presented as percent (±sem) maximum response for AR + control across all concentrations. *, $p < 0.01$ on Mann Whitney U on AR + control at 0.1 nM DHT. Data is representative of at least 3 independently repeated experiments.

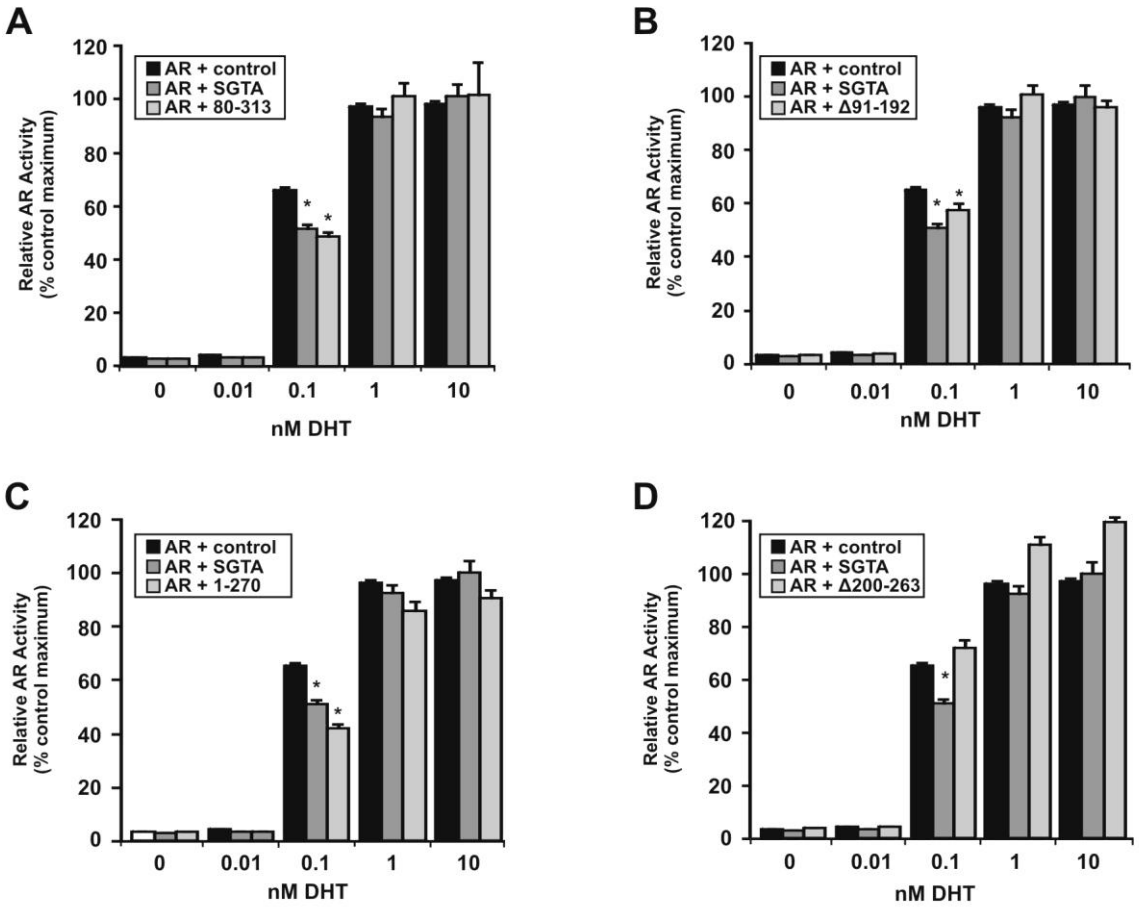


Figure 4.7: Effect of SGTA domain deletion variants on AR activity. A-D: PC3 cells were transfected with AR, full length SGTA or SGTA deletion variant expression vectors and the ARR3-tk-Luc reporter. Cells were treated with 0 – 10 nM DHT for 24 hours SGTA homodimerisation deletion (80-313), SGTA TPR deletion (Δ 91-192), SGTA linker region deletion (Δ200-263) and SGTA QRD deletion (1-270). Data is presented as percent (±sem) maximum response for AR + control across all concentrations. *, $p < 0.01$ on Mann Whitney U on AR + control at 0.1 nM DHT. All data is representative of at least 3 independently performed experiments.

4.4 Discussion

By regulating multiple stages of receptor action, including maturation, transport, degradation and the maintenance of transcriptional activity, the Hsp70 and Hsp90 molecular chaperone complexes are critical components of steroid receptor signalling. Nonetheless, the mechanisms underpinning chaperone control remain elusive. Emerging evidence for the AR suggests that the tetratricopeptide repeat (TPR) containing co-chaperones are dynamic modulators of steroid receptor function, and possibly support the interaction between the receptor and Hsp70 and/or Hsp90 complexes. Importantly, the relative abundance of those TPR proteins within a given cell or tissue type can dictate the heterogeneity of TPR-steroid receptor complexes (Smith and Toft 2008). Changes in TPR-steroid receptor heterogeneity can also occur upon ligand binding, whereby the receptor undergoes a series of conformational changes that results in an exchange of TPR proteins to allow receptor translocation. The exchange between SGTA and FKBP52 after the AR has bound DHT is one example (Cheung-Flynn, Prapapanich et al. 2005; Buchanan, Ricciardelli et al. 2007).

The results presented within this chapter demonstrated varying expression levels for five key steroid receptor associated TPR co-chaperones in prostate cancer cell lines, which not only provides formative information on the potential heterogeneity of TPR-steroid receptor complexes within the cell, but also on how those TPR proteins may influence steroid receptor signalling as hormone signals are received from the extracellular environment. In agreement with previously published reports, this study demonstrated that the LNCaP and C42B cell lines contained higher endogenous levels of the immunophilins FKBP51

and FKBP52 compared to PC3 cells, which may reflect the ability of these TPR proteins to more precisely control AR signalling in prostate cancer cells that are sensitive to androgen signals (Periyasamy, Warrier et al. 2007; Periyasamy, Hinds et al. 2010). The altered expression of SGTA, FKBP51 and Cyp40 observed with prostate cancer progression may therefore act to broaden AR responses when in the presence of low ligand concentrations (Buchanan, Ricciardelli et al. 2007; Periyasamy, Warrier et al. 2007; Ni, Yang et al. 2010; Periyasamy, Hinds et al. 2010).

The findings within this chapter demonstrated that the effect of SGTA on AR activity was most predominant at 0.01 and 0.1 nM DHT, but not higher concentrations. Moreover, the strongest inhibitory effects of SGTA were observed on those responsive loci that exhibited the greatest fold change to DHT. These results suggest that the presence of SGTA in prostate cells acts to constrict the magnitude of androgen responses, which implies a direct SGTA effect on AR activation rather than on the general transcriptional machinery. Additionally, this effect of SGTA on strong AR responses is further evidence that reflects the role TPR co-chaperones play in finely regulating both steroid receptor ligand sensitivity and gene expression. Therefore, the loss and/or gain of specific TPR co-chaperones may broaden the magnitude and scope of steroid receptor responses and aid in disease progression.

The actions of SGTA on AR ligand sensitivity are closely aligned with the historical model proposed for related TPR co-chaperones in steroid receptor activity. Specifically, the peptidylprolyl isomerase (PPIase) activities of Cyp40, FKBP52 and FKBP51 were thought to imply that TPR co-chaperones would be critical for receptor binding and the

acquisition of ligand binding competence (Pratt and Toft 1997). Indeed, FKBP51 catalyses the inclusion of the co-chaperone p23 into the Hsp90-AR complexes, increasing the affinity for androgens and the number of available ligand-competent AR molecules (Periyasamy, Warrier et al. 2007; Ni, Yang et al. 2010). However, it is the convergence of these diverse molecules on the process of nuclear translocation that has more recently become apparent. The exchange of FKBP51 for FKBP52 or PP5 in the dynein complex facilitates active transport of ligand bound AR to the nucleus (Davies, Ning et al. 2002). Similarly, the dynein-associated co-chaperones promote AR nuclear translocation, which can be blocked by the PPIase inhibitor cyclosporin A (Periyasamy, Warrier et al. 2007). SGTA does not exhibit PPIase activity, but acts to counter AR nuclear translocation, which is consistent with the observed decrease in the AR transactivation response at 0.1 nM DHT, a concentration where approximately 50% of receptors (EC_{50}) could be expected to be ligand bound (Wilson and French 1976; Buchanan, Ricciardelli et al. 2007). As SGTA acts to restrain the AR in the cytoplasm in a low hormone environment, the minimal effect of SGTA on AR activity observed at 1 nM DHT is mostly likely attributed to the majority of ligand bound AR overriding the inhibitory effects of SGTA, subsequently leading to an increase in AR nuclear translocation (Buchanan, Ricciardelli et al. 2007). Alternatively, the loss of SGTA during prostate cancer progression may explain the shift to predominantly nuclear AR localisation via increased interaction of AR with the dynein-linked co-chaperones (Zhang, Johnson et al. 2003).

The greatest effect of SGTA on PGR-B and GR transcriptional activity was at the EC_{50} for their respective ligands (Rohdewald, Mollman et al. 1986; Sarup, Rao et al. 1988).

Moreover, this predominant effect of SGTA on AR responses at 0.1 nM DHT, GR at 10 nM dexamethasone and PGR-B at 1 nM progesterone, instead of other ligand concentrations is consistent with a similar ligand-dependent result observed recently for other steroid receptor associated TPR proteins (Schulke, Wochnik et al. 2010). The PGR exists in most cell types as two isoforms (PGR-A and PGR-B), where PGR-A is homologous to PGR-B except for a 164 amino acid truncation at the amino terminus. It has been previously reported that the PGR isoforms have distinct subcellular distributions in the absence of ligand, whereby PGR-A is primarily localised to the nucleus while PGR-B is equally dispersed throughout the cell (Lim, Baumann et al. 1999). The PGR-B isoform was used in these studies as a PGR-A expression vector was unavailable in our laboratory. The lack of an effect by SGTA on ERα can therefore be explained by the subcellular localisation for each protein, as SGTA exclusively resides in the cytoplasm (Buchanan, Ricciardelli et al. 2007) while ERα maintains a constitutive nuclear localisation either in the absence or presence of agonist ligand (Kocanova, Mazaheri et al. 2010). These results suggest that SGTA actions are not exclusive to AR, rather SGTA acts to restrict the oxy-steroid receptors from the nucleus in the absence of ligand or in the presence of low hormone levels. Therefore, a potential biological role for SGTA is to act as a buffer against untoward hormone responses in specific tissue and cell types.

Studies demonstrating an association of SGTA with the human growth hormone receptor, glucose transporter 1, viral capsule proteins Vpu and Gag, and the platelet derived growth factor receptor (Handley, Paddock et al. 2001; Schantl, Roza et al. 2003; Liou and Wang 2005; Moritz, Li et al. 2010) collectively point to SGTA as a key mediator of client protein

transport to the cell surface. It is likely that the mechanism that drives this process, and potentially the cytoplasmic retention of the AR, is related to the association of SGTA with microtubules and actin filaments (Handley, Paddock et al. 2001; Liou and Wang 2005; Dutta and Tan 2008; Moritz, Li et al. 2010). Additionally, the findings within this chapter demonstrate the similar effect of SGTA to inhibit GR and PGR-B transcriptional activity, suggesting that the mechanism of action by SGTA on these other oxy-steroid receptors may be similar to that exhibited for AR. Therefore, the combined interaction between SGTA, the steroid receptor and microtubule proteins acts as a means of tethering the receptor to the cell cytoskeleton and limit its access to dynein-linked translocation machinery (Buchanan, Ricciardelli et al. 2007; Zhu, Horbinski et al. 2010)

Although the TPR domain may form the main interaction surface between SGTA and Hsp70, Hsp90 as well as other client proteins (Angeletti, Walker et al. 2002; Yin, Wang et al. 2006), deletion of the SGTA TPR region did not alter the capacity of SGTA to inhibit AR activity. This is also true of Cyp40, which retains its chaperone capacity without the TPR domain (Ratajczak and Carrello 1996). Collectively, those data imply that the effect of some co-chaperones on their client molecules may be independent of Hsp70 and Hsp90 (Mok, Allan et al. 2006), which is consistent with neither SGTA nor Cyp40 altering AR ligand binding, and also suggests a chaperone role in downstream activities such as transport. For both SGTA and Cyp40, chaperone capability potentially lies within a linker region adjacent to the TPR (Mok, Allan et al. 2006). The linker region within Cyp40 is enriched in hydrophobic amino acids that form a cleft that separates the PPIase and TPR domains. This unique amino acid composition provides the necessary structures to enable

protein-protein interactions with partially folded substrates (Mok, Allan et al. 2006). Importantly, this specific chaperone function may form part of the mechanistic actions of TPR co-chaperones to hold steroid receptors in a transcriptionally repressed state prior to ligand binding. Whether this is true for the effects of SGTA on AR requires further investigations. Undoubtedly, complex inter- or intra-molecular interactions of SGTA and other TPR chaperones are critical in their capacity to modulate steroid receptor responses.

In summary, the findings in this chapter highlight the effects of SGTA on steroid receptor transaction activity. Specifically, the results presented here have demonstrated that SGTA acts to constrain the sensitivity of AR ligand dependent activity across multiple responsive binding sites, which may represent a universal ability of SGTA to control AR signalling in prostate cancer cells. Importantly, this mechanism is not exclusive to AR; rather the effects of SGTA extend to other cytoplasmic steroid receptor, which implies that SGTA may constrain hormonal signalling in other tissue types. Furthermore, investigations presented in this chapter demonstrate that the biological actions of SGTA to desensitise the activity of AR in the presence of low ligand concentrations are independent of the homodimerization TPR and QRD domains. Rather, it appears that the effects of SGTA on AR are dependent on a linker region that separates the TPR and QRD regions. Nonetheless, the ability of SGTA to decrease the ligand sensitivity of AR and its activity on highly responsive loci may be an important mechanism in limiting spurious, high-level androgenic responses in the prostate.

CHAPTER 5

Global analysis of SGTA biological pathways identified

PI3 kinsae as a potential target in prostate cancer cells

Chapter 5: Global analysis of SGTA biological pathways identified PI3 kinase as a potential target in prostate cancer cells

5.1 Introduction

Until recently, the contribution of specific TPR containing co-chaperones to steroid receptor signalling pathways have largely been described as moderate effects on the regulation of receptor ligand binding affinity and sensitivity (Smith 2004). However, the generation of FKBP52 knockout mice demonstrated that the actions of TPR containing co-chaperone proteins can dramatically affect downstream genome-wide transcriptional outcomes and tissue physiology (Cheung-Flynn, Prapapanich et al. 2005; Yang, Wolf et al. 2006; Yong, Yang et al. 2007). Specifically, these studies revealed that both male and female mice display morphological and functional abnormalities predominantly in only androgenic and progestogenic sensitive tissues including, the prostate, testicles, penis and uterus. The loss of FKBP52 appears to alter hormonal signalling to a point whereby developmental programs are disrupted (Cheung-Flynn, Prapapanich et al. 2005; Yang, Wolf et al. 2006; Yong, Yang et al. 2007). Although FKBP52 has been thought to play a role in AR translocation, the loss of FKBP52 does not ultimately impair AR nuclear accumulation, but rather reduces the capacity of AR to induce gene expression (Yong, Yang et al. 2007). Results with FKBP51 are contradictory: while siRNA mediated knockdown in LNCaP prostate cells limits AR transcriptional activity on a subset of responsive genes, FKBP51 knockout mice exhibited normal tissue development

and function (Yong, Yang et al. 2007; Ni, Yang et al. 2010; Periyasamy, Hinds et al. 2010). It seems plausible from these results that the TPR co-chaperones are important for the effects on AR signalling in a cell and tissue specific manner (Yong, Yang et al. 2007).

Our previous study demonstrated that siRNA knockdown of endogenous SGTA in C42B and LNCaP cell lines increased both basal and DHT induced PSA expression, and that SGTA levels are lower in metastatic prostate cancer than in non-malignant or primary lesions (Buchanan, Ricciardelli et al. 2007). Although the physiological relevance of depleted SGTA levels in prostate cancer cells remains elusive, it has been previously shown that SGTA knockdown in HeLa cells results in cellular arrest in metaphase and subsequent apoptosis (Winnefeld, Rommelaere et al. 2004; Winnefeld, Grewenig et al. 2006), which suggests that the biological effects of SGTA may extend beyond steroid hormone signalling. Indeed, the interaction between SGTA and tyrosine kinases receptors, such as the human growth hormone receptor (hGHR) and the platelet derived growth factor receptor alpha (PDGFRα), suggests possible alternative mechanisms for the biological actions of SGTA in prostate cancer cells (Schantl, Roza et al. 2003; Moritz, Li et al. 2010). Given the potential range of client protein interactions, SGTA may play an important role as a modulator of intracellular signalling pathways that impact on cell viability. However, whether these effects are dependent or independent on AR as well as the broader biological function of SGTA in prostate cancer cells has not been investigated. Therefore, the objectives of this chapter were to investigate the biological effects of SGTA knockdown on the transcription profile of C42B cells in the absence of androgen signalling, and thereby to identify alternative pathways by which SGTA might affect cell proliferation.

5.2 Materials and Methods

5.2.1 Small Interfering RNA (siRNA) transfections and Immunoblot

C42B cells were seeded in 6 well plates (200,000 cells/well) for 24 hours. Cells were transfected with 5 nM non specific (NS) control siRNA or 1.67-5 nM SGTA specific siRNA according to the method described in chapter 2.3.3.4. Imunoblot was performed as described in chapter 2.3.5. The following primary antibody dilutions were used: SGTA (Abnova) (1:1000), Tubulin (1:20,000), AR (1:1000), FKBP51 (1:1000), Hsp90 (1:1000), p85 (1:1000), p110β (1:1000), Akt (1:300). Phosphorylated Akt antibodies were used at the following dilutions: Akt threonine 308 (Akt T308) (1:2000), Akt serine 473 (Akt S473) (1:1000).

5.2.2 RNA Isolation and QRT-PCR

C42B cells were transfected with NS control or SGTA specific siRNA according to the method described in section 5.2.1. RNA was isolated, quantified and synthesised into cDNA according to the methods described in chapter 2.3.6.1 and 2.3.6.2 respectively. QRT-PCR was performed on samples as described in chapter 2.3.6.3. Primer sequences are listed in Appendix A3.

5.2.3 Microarray and Gene Ontology Analysis

C42B cells were transfected with 5 nM NS control siRNA or three independent SGTA siRNA at a concentration of 1.67 nM each for 72 hours according to the method described in section 5.2.1. The transfection reagent was removed and cells were treated with either

vehicle (ethanol) control or 0.01, 0.1, 1 and 10 nM DHT for 16 hours. Five biological replicates were generated per treatment. RNA was harvested and validation of SGTA knockdown was conducted by QRT-PCR according to the method described in section 5.2.2. Vehicle treated samples were diluted to a concentration of 500 ng per biological replicate and were assessed for RNA quantity and integrity analysis using the Agilent Bioanalyser (Adelaide Microarray Centre, Adelaide). Three hundred nanograms of total RNA was linearly amplified and converted to biotinylated cDNA fragments utilising an Affymetrix GeneChip Whole Transcript Sense Target labelling Assay kit. Samples were hybridised to Affymetrix Human Gene 1.0 ST Arrays for 17 hours at 45°C prior to washing, staining and scanning (Adelaide Microarray Centre, Adelaide). Bioinformatics was performed on the raw transcript expression data using the Bioconductor Limma package implemented in R. Briefly, array data was normalised using variance stabilisation normalisation as previously described (Huber, von Heydebreck et al. 2002) and subjected to linear model regression. Heat maps were generated using either R or Heatmap Builder Version 1.0 (www.ashleylab.stanford.edu/tools_scripts.html). Gene pathway analysis was conducted using the Ingenuity Systems program to predict the enriched Molecular and Cellular Functions as well as the Canonical pathways significantly altered by SGTA knockdown.

5.2.4 Statistical analysis

Statistically significantly genes from the microarray were determined by an adjusted p value cut off of 0.05. The adjusted p value is generated by multiple testing corrections, which incorporates a Benjamini and Hochberg false discovery rate of 5%. Statistical

analyses for QRT-PCR experiments were performed using Graphpad Prism Version 5 software for Windows (Graphpad Software, California, USA). Mann-Whitney U tests were used to determine differences between groups as indicated in figure legends. A p-value < 0.05 was considered statistically significant.

5.3 Results

5.3.1 Knockdown of SGTA in C42B cells variably alters AR regulated genes

Three commercially available siRNAs directed against the SGTA mRNA sequence were independently transfected into C42B cells to assess for maximal SGTA knockdown. Immunoblot analysis demonstrated relative to non-specific (NS) control that the SGTA specific siRNA si3 displayed the highest efficacy in decreasing SGTA steady state protein levels after 24 hours compared to either of the other two SGTA siRNAs (Figure 5.1A), whereas after 48 hours, si1 and si3 displayed similar efficacies (Figure 5.1A). Differences in the potency of siRNA mediated knockdown can occur for multiple reasons including transfection efficiency, the degree of incorporation of the siRNA into the RNA-induced silencing complex (RISC) or off target effects on protein translation (Jackson and Linsley 2004). Nevertheless, this result demonstrates that SGTA siRNA si3 is the most proficient at reducing SGTA levels in the shortest time, and therefore was used for the remaining experiments in this chapter.

Observations from our previous study demonstrated that knockdown of SGTA for 3 days did not alter AR steady state protein levels in C42B cells, but did affect AR regulation of PSA (Buchanan, Ricciardelli et al. 2007). Here, long term (72 hours) SGTA deprivation using siRNA si3 decreased AR steady state protein levels in the absence of DHT compared to NS control (Figure 5.1B). Next, the effect of SGTA knockdown on the capacity of AR to regulate gene expression was investigated. QRT-PCR analysis demonstrated that transfection of si3 significantly decreased *SGTA* mRNA levels by 85% compared to NS control, but did not affect the levels of the related TPR protein *FKBP52*, which is

not androgen regulated ($p<0.01$; Figure 5.2A and B). Importantly, since FKBP52 and SGTA share homology in the TPR domain, the results from this experiment demonstrate that si3, which targets the region encoding the SGTA TPR domain, is unlikely to target the TPR of closely related proteins. The effect of SGTA knockdown on AR activity was analysed by *FKBP51* and *PSA* expression. As expected, treatment with 10 nM DHT increased both *FKBP51* and *PSA* mRNA levels; however there was no significant effect of SGTA siRNA compared to NS control transfected cells, although a slight decrease in PSA expression was observed (Figure 5.2C and D). Therefore, in contrast to our previous study, the data presented in this thesis imply that knockdown of SGTA may not alter AR transcriptional activity at high ligand concentrations. Indeed, this idea is supported by the *in vitro* studies presented in chapter 4, which suggests that the concentration of DHT used to activate the AR in these experiments (10 nM) was at a saturating level, and thus masked any subtle effects of SGTA.

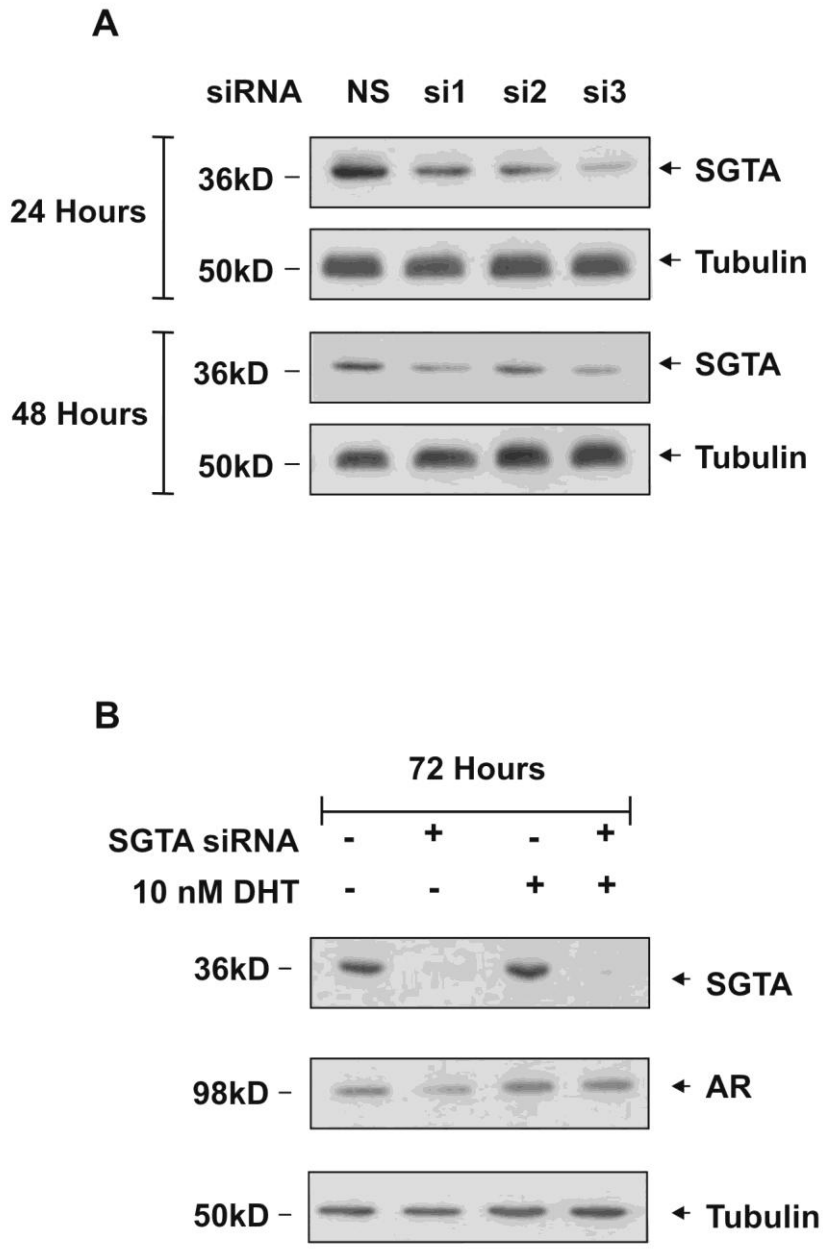

A
siRNA
NS
si1
si2
si3
24 Hours
36kD
SGTA
50kD
Tubulin
48 Hours
36kD
SGTA
50kD
Tubulin
B
72 Hours
SGTA siRNA
- + - +
10 nM DHT
- - + +
36kD
SGTA
98kD
AR
50kD
Tubulin

Figure 5.1: Transfection of three independent SGTA siRNA. A: C42B cells were transfected with either 5nM non specific (NS) control siRNA or 3 independent SGTA siRNA (si1, si2 and si3) for 4 hours. Transfection reagent was removed and replaced with RPMI + 5% DCC-FBS. Cell lysates were collected 24 and 48 hours after transfection and SGTA protein levels were analysed by immunoblot. **B:** C42B cells were transfected with 5 nM NS or SGTA specific siRNA si3 for 72 hours. Transfection reagent was removed and cells were treated with vehicle (ethanol) control or 10 nM DHT for 24 hours. Cell lysates were collected and analysed by immunoblot for SGTA and AR protein levels. Tubulin was used as a loading control.

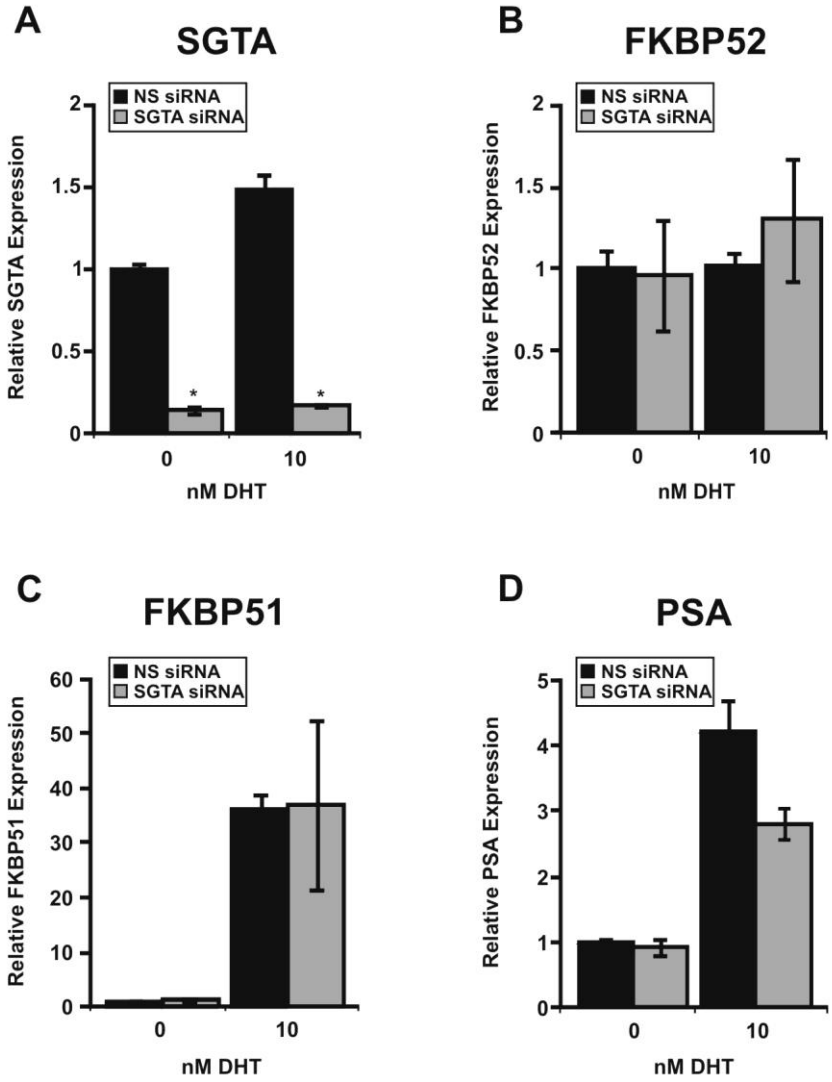

A
SGTA
NS siRNA
SGTA siRNA
Relative SGTA Expression
2
1.5
1
0.5
0
*
*
0
10
nM DHT
B
FKBP52
NS siRNA
SGTA siRNA
Relative FKBP52 Expression
2
1.5
1
0.5
0
0
10
nM DHT
C
FKBP51
NS siRNA
SGTA siRNA
Relative FKBP51 Expression
60
50
40
30
20
10
0
0
10
nM DHT
D
PSA
NS siRNA
SGTA siRNA
Relative PSA Expression
5
4
3
2
1
0
0
10
nM DHT

Figure 5.2 A-D: Effect of SGTA siRNA on the relative gene expression of SGTA, FKBP51, PSA and FKBP52 in C42B cells. Cells were transfected with 5 nM NS control siRNA or SGTA specific siRNA si3 as described in Figure 5.1B. Cells were treated with vehicle (ethanol) or 10 nM DHT for 16 hours. RNA was isolated and analysed by QRT-PCR for expression of *SGTA* and the androgen regulated genes *FKBP51* and *PSA*. *FKBP52* mRNA levels were also analysed as a control for potential off target siRNA effects. Gene expression was normalised to the housekeeping gene *GAPDH*. Data are presented as relative to vehicle control (set to 1) and represent the mean (± SD) of three biological replicates. All data presented were assessed for significance at $p<0.05$ by Mann-Whitney U for difference between medians of SGTA siRNA versus NS siRNA, as indicated by *.

5.3.2 SGTA knockdown does not alter AR transcriptional activity at low ligand concentrations

In order to determine if the effect of SGTA knockdown was masked by high ligand concentration we next used a range of DHT concentrations to eliminate this as a factor in our initial experiments. QRT-PCR analysis showed *SGTA* mRNA levels decreased by 70% across all samples transfected with si3 (Figure 5.3A). Increasing DHT concentrations resulted in an expected dose-dependent increase in *FKBP51* and *PSA* expression, but knockdown of SGTA did not result in any consistent difference in expression when compared to NS control (Figure 5.3B and C). This was further confirmed by immunoblot analysis of FKBP51 protein levels (Figure 5.3D).

Given the conflicting results between these and previous studies, we decided to focus on the consequences of long-term SGTA depletion on the transcriptional profile of prostate cancer cells in the absence of androgen signalling. In order to generate the most robust RNA samples for microarray analysis we first sought to reduce potential off-target effects exhibited by siRNA knockdown. Previous reports have demonstrated that transfection of multiple distinct siRNAs at lower concentrations results in a synergistic reduction of the target mRNA, while also reducing the non-specific effects for each individual siRNA (Jackson and Linsley 2004). The three commercially available SGTA specific siRNAs, which target the SGTA mRNA sequence at exons 5, 8 and 9 respectively, were transfected alone (5 nM) or in combination (1.67 nM each) into C42B cells (Figure 5.4A). Immunoblot analysis showed a relatively equal decrease in SGTA protein steady state levels for individual siRNAs at 72 hours that was recapitulated by low-dose combination

of the individual siRNAs (Figure 5.4B). We therefore generated 5 independent biological RNA replicates from cells treated with the pool of three SGTA specific siRNAs, or with NS control siRNA, for microarray studies. To eliminate any bias from androgen signalling, and to sufficiently determine the effect of SGTA on other cellular pathways, C42B cells were maintained in stripped serum throughout the 72 hour knockdown period. Signalling pathways were reactivated by the addition of 5% stripped serum for 16 hours prior to RNA collection. QRT-PCR analysis demonstrated that the combination of siRNAs reduced *SGTA* mRNA levels by approximately 85% in all biological replicates (Figure 5.4C).

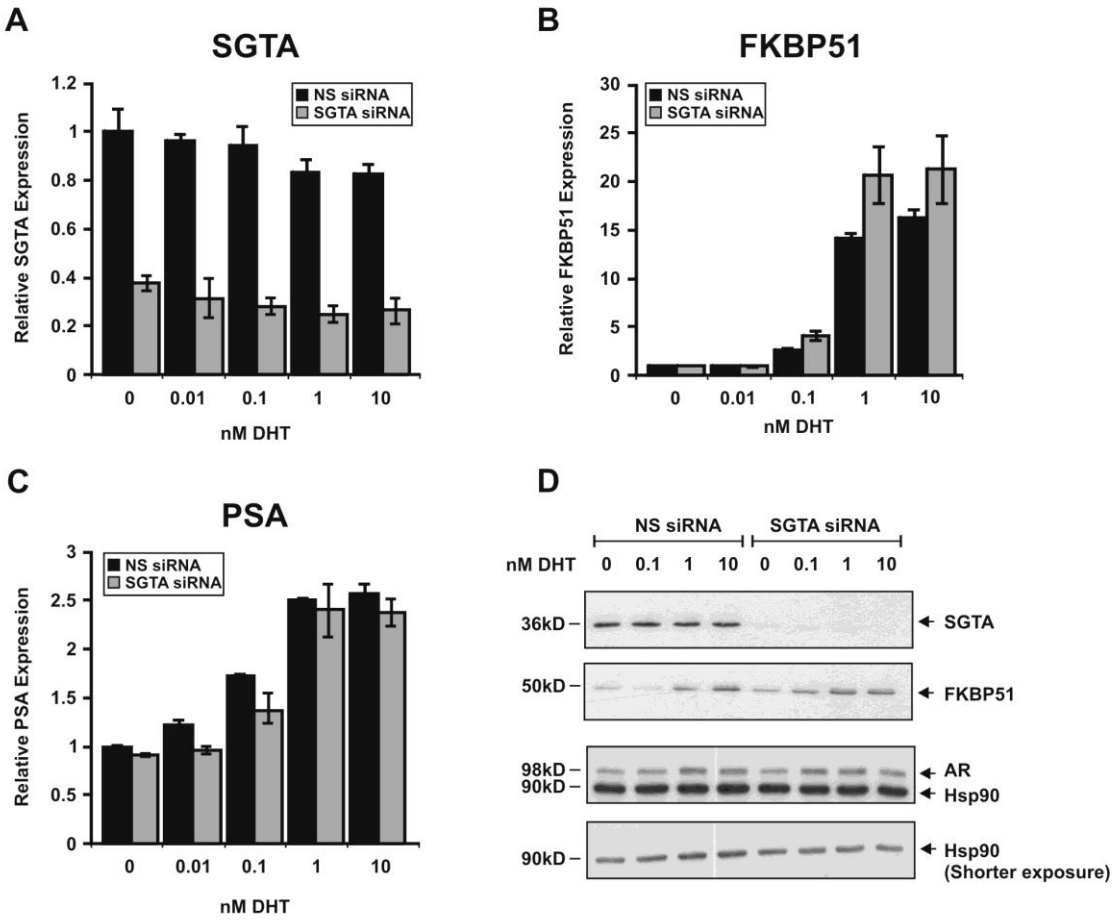


Figure 5.3 A-C: Effect of SGTA knockdown on AR regulated genes FKBP51 and PSA with increasing dose of DHT. C42B cells were transfected with NS or SGTA specific siRNA as described in Figure 5.2. Cells were treated with either vehicle (ethanol) control or 0.01-10 nM DHT for 16 hours. RNA was isolated and analysed for *SGTA*, *FKBP51* and *PSA* gene expression as described in Figure 5.2. Data represent the mean (± SD) of two biological replicates. **D:** C42B cells were transfected and treated as described in A-C. Cell lysates were collected and analysed by immunoblot for SGTA, FKBP51 and AR protein levels. Hsp90 was used as a loading control.

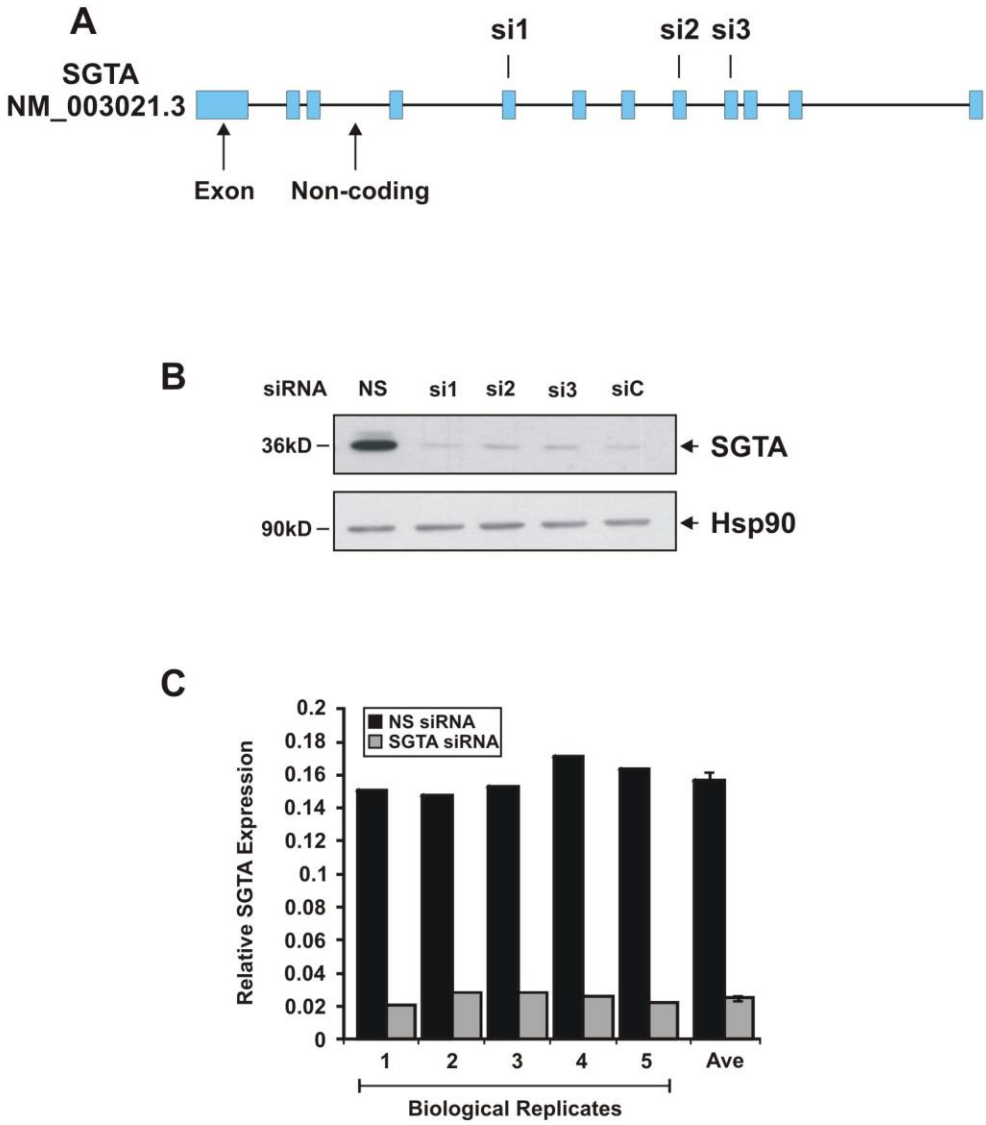

A
si1
si2 si3
SGTA
NM_003021.3
Exon
Non-coding
B
siRNA NS si1 si2 si3 siC
36kD
SGTA
90kD
Hsp90
C
NS siRNA
SGTA siRNA
Relative SGTA Expression
0.2
0.18
0.16
0.14
0.12
0.1
0.08
0.06
0.04
0.02
0
1 2 3 4 5 Ave
Biological Replicates

Figure 5.4: Three independent SGTA siRNAs pooled to reduce off target effects. A: Schematic of SGTA gene located on chromosome 19. Blue boxes represent exons, separated by non coding regions. SGTA siRNA1, 2 and 3 (si1, si2 and si3) target exons 5, 8 and 9 respectively. **B:** C42B cells were transfected with 5 nM of either NS siRNA, SGTA specific siRNA (si1, si2 or si3) or a combination of all SGTA siRNAs (siC) each at a final concentration of 1.67 nM. Cells were transfected for 72 hours as described in Figure 5.1B. Cell lysates were collected and analysed as described in Figure 5.3D. Hsp90 was used as a loading control. **C:** Five independent biological replicates of C42B cells were transfected as described in B. The transfection reagent was removed and cells were treated with either vehicle (ethanol) control or 0.1-1 nM DHT for 16 hours. RNA was isolated and analysed by QRT-PCR for expression of *SGTA* normalised to the housekeeping gene *GAPDH*. Data is representative of either individual replicates or the average of all five (± SEM).

5.3.3 SGTA knockdown alters the genome-wide expression profile of C42B cells.

Affymetrix microarray analysis from the 5 biological replicates demonstrated that SGTA knockdown altered the expression of 1955 genes ($p<0.05$), with 62.9% (1230/1955) of genes lower, and 37.7% (725/1955) higher than the NS control (Figure 5.5). The complete list of genes significantly altered by SGTA depletion is reported in Appendix C. A literature search was conducted on the most differentially regulated genes to determine their general biological properties and if they have been previously reported in prostate cancer. The top 10 down and up-regulated genes with known biological properties are presented in Tables 5.1 and 5.2 respectively. Of those, 7 of the down-regulated genes have been implicated in prostate cancer, compared to 5 out of the top 10 up-regulated genes. Moreover, it was noted that 2 out of the top 10 down-regulated genes (*S100A10* and *TNFSF10*) are involved in cell cycle progression, while 4 of the top 10 up-regulated genes (*IGFBP3*, *PLD1*, *BCAT1* and *CCND3*) are involved in anti proliferative and/or pro-apoptotic processes. These results demonstrated that the loss of cytoplasmic SGTA affects the transcriptional profile of prostate cancer cells and suggests that SGTA may play a role in prostate cancer proliferation and cell survival pathways.

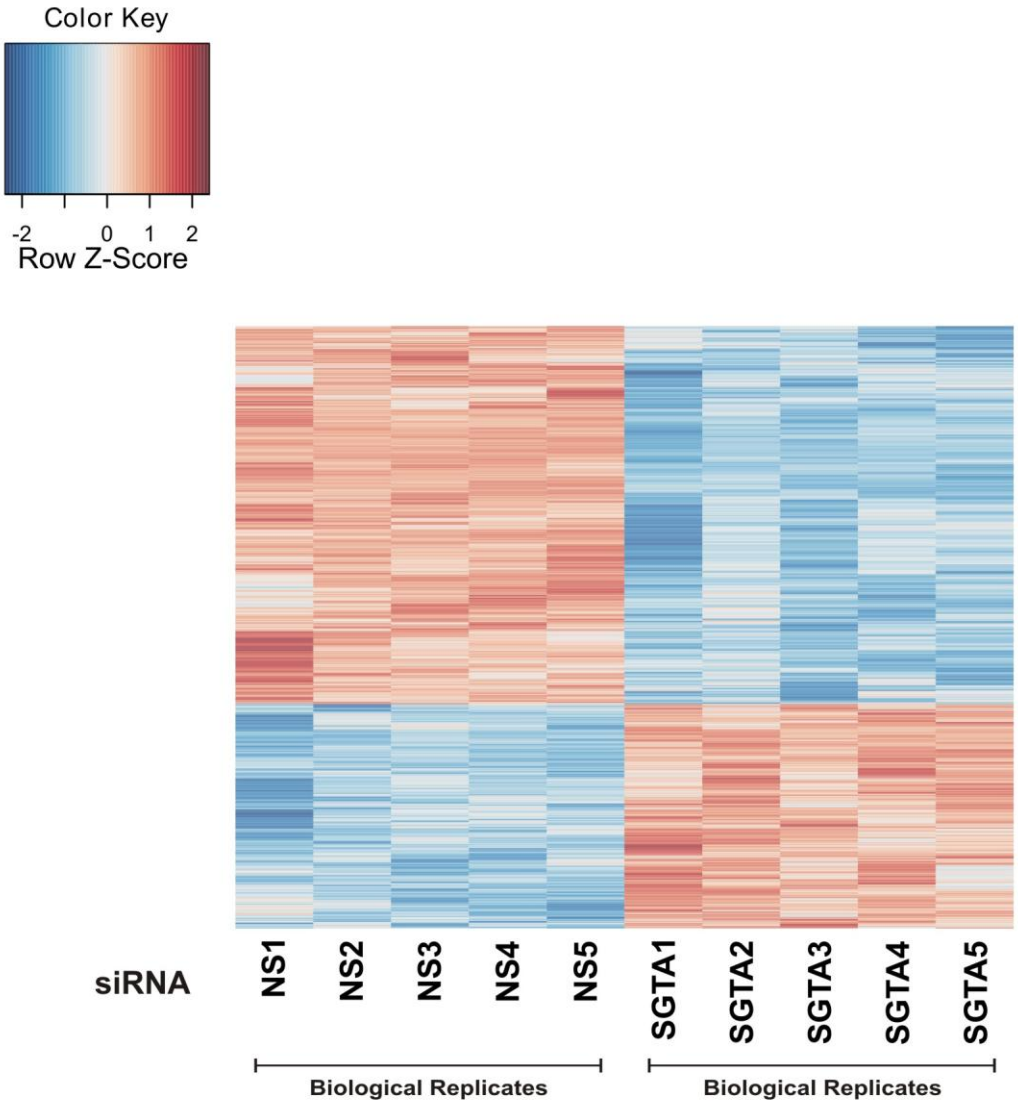


Figure 5.5: SGTA knockdown Microarray Heatmap of genes differentially regulated by SGTA. Biological replicates generated as described in Figure 6.4C were run on an Affymetrix GeneChip Human Gene 1.0 ST array. Heatmap demonstrated genes differentially regulated by SGTA knockdown significance was determined by an adjusted p-value of 0.05. A colour change from blue to red represents an up-regulation of gene expression.

Gene Symbol	Probe ID	Average Expression	Fold Change	Adj. p value	Reported in prostate cancer (PCa)	Biological Properties
SGTA	8032530	8.09	- 4.10	1.99E-08	Yes (Buchanan, Ricciardelli et al. 2007)	• TPR co-chaperone • ↓ AR activity • ↓ with PCa progression
S100A10	7920123	8.08	- 4.10	1.71E-06	Yes (Romanuik, Wang et al. 2010)	• Membrane trafficking, cell cycle progression • ↑ with PCa progression
KCNJ13	8059776	6.50	- 4.10	2.69E-05	No	• Potassium channel
TNFSF10	8092169	5.94	- 2.90	0.000208	No	• Pro-apoptotic tumour necrosis factor ligand
SLC22A3	8123246	7.18	- 2.71	1.71E-06	Yes (Tomlins, Mehra et al. 2007)	• Cation transporter • ↓ with PCa progression
PLA2G2A	7913216	6.88	- 2.56	2.75E-05	Yes (Schmidt, Murillo et al. 2004)	• Fatty acid metabolism • ↓ with androgens
MYLK	8090098	8.52	- 2.54	1.42E-06	Yes (Leveille, Fournier et al. 2009)	• Phosphorylation and stabilisation of muscle fibres • ↓ with androgens
NAPELPD	8141872	8.32	-2.38	4.89E-06	Yes (Wang, Zhao et al. 2008)	• Phospholipase that acts of phospholids in the cell membrane
STEAP1	8134030	8.40	-2.20	3.10E-06	Yes (Hubert, Vivanco et al. 1999)	• Increases cellular adhesion of mesenchemal stem cells • ↑ in PCa
RCAN3	7898957	8.12	-2.17	9.02E-05	No	• Inhibits calcineurin serine/threonine phosphatase activity
TLL2	7935296	7.04	-2.13	3.58E-05	No	• zinc-dependent metalloprotease activity that processes pro-lysyl oxidases

Table 5.1: Top 10 down-regulated genes in SGTA knockdown microarray. Average expression is determined by the relative probe intensity for each gene across all biological replicates. Fold change represents SGTA siRNA/NS siRNA. The adjusted p value is generated by multiple testing corrections, which incorporates a Benjamini and Hochberg false discovery rate of 5%. The biological properties of each gene were determined by PubMed literature searches. Those genes reported to be associated with prostate cancer are indicated along with the specific references.

Gene Symbol	Probe ID	Average Expression	Fold Change	Adj. p value	Reported in prostate cancer (PCa)	Biological Properties
IGFBP3	8139488	6.99	2.55	1.71E-06	Yes (Massoner, Colleselli et al. 2009; Ingermann, Yang et al. 2010)	• Anti-proliferative and pro-apoptotic to PCa cells • Inhibits PCa cell migration and invasion
CYP1A2	7984862	8.20	2.30	0.000617	Yes (Sterling and Cutroneo 2004)	• Cytochrome p450 metabolism, steroid synthesis • Constitutively expressed in PCa
LRRC31	8092921	5.43	1.99	0.00088	No	• Transmembrane receptor
PLD1	8092134	7.62	1.93	0.000151	Yes (Rumsby, Schmitt et al. 2011)	• Tyrosine kinase signalling, regulation of mitosis • ↑ activity in PCa
BCAT1	7961829	5.65	1.92	4.89E-06	No	• Amino acid metabolism • Cell growth
SNORD115-11	7982084	5.70	1.85	0.000161	No	• mRNA splicing
CCDN3	8126371	7.60	1.72	9.86E-05	Yes (Olshavsky, Groh et al. 2008)	• G1/S cell cycle progression • Interacts with AR and ↓ AR activity
CHAC1	7982868	6.77	1.71	0.000164	No	• Regulator of cation transport
CD24	8177222	5.41	1.68	0.0055	Yes (Nagy, Szendroi et al. 2009)	• Glycoprotein cell surface marker • ↑ in PCa
FAM129A	7922846	6.19	1.68	0.00011	No	• Regulator of eIF2α and S6K1/4E-BP1 phosphorylation

Table 5.2: Top 10 up-regulated genes in SGTA knockdown microarray. Average expression is determined by the relative probe intensity for each gene across all biological replicates. Fold change represents SGTA siRNA/NS siRNA. The adjusted p value is generated by multiple testing corrections, which incorporates a Benjamini and Hochberg false discovery rate of 5%. The biological properties of each gene were determined by PubMed literature searches. Those genes reported to be associated with prostate cancer are indicated along with the specific references.

5.3.4 Validation of SGTA knockdown microarray

Validation of the microarray results was conducted by QRT-PCR on a set of independently generated RNA samples. Simultaneously, we tested the impact on androgen signalling on the expression of these candidate genes by using NS or SGTA siRNA transfected cells treated with either 0.1 or 1 nM DHT. Consistent with previous knockdowns, this experiment yielded an 85% reduction in *SGTA* mRNA compared to NS control across all treatment groups ($p<0.01$; Figure 5.6A). QRT-PCR validation of the down-regulated gene set verified that knockdown of SGTA significantly decreased the expression of *S100A10*, *PLA2G2A* and *MYLK* compared to NS transfected cells ($p<0.05$; Figure 5.6 B-D). Additionally, the expression of *IGFBP3*, *LRRC31* and *PLD1* were significantly up-regulated in SGTA depleted cells ($p<0.05$; Figure 5.7 A-C).

An interesting finding from the microarray data set was that SGTA knockdown significantly decreased *AR* gene expression by a linear fold change of 1.2 (Appendix C). However, analysis of *AR* mRNA levels from the validation set revealed the expression of *AR* remained relatively unchanged either in the absence or presence of SGTA at vehicle control (Figure 5.7D). Regardless, treatment with 1 nM DHT resulted in a significant increase in AR expression in SGTA depleted cells ($p<0.05$; Figure 5.7D). Surprisingly, 6 out of the 7 candidate genes (*S100A10*, *PLA2G2A*, *MYLK*, *LRRC31*, *PLD1* and *AR*) investigated for microarray validation were significantly down-regulated by androgens (ANOVA $p<0.05$; Figure 5.6 B-D and Figure 5.7 B-D), whereas DHT treatment resulted in

the significant up-regulation of *IGFBP3* (ANOVA $p<0.05$; Figure 5.7A). Although previous results suggested that the loss of SGTA did not affect the expression of classical AR regulated genes such as *PSA* and *FKBP51*, these findings imply that there is a convergence of SGTA activity and AR signalling on a subset of AR regulated genes. Mechanistically, it appears that SGTA acts to either increase or decrease the basal expression of these genes, which subsequently alters their ability to respond to androgen signalling. Taken together, these data suggest that the loss of SGTA may disrupt the expression of a subset of androgen regulated genes, and thus create and entirely new transcriptional profile in prostate cancer cells.

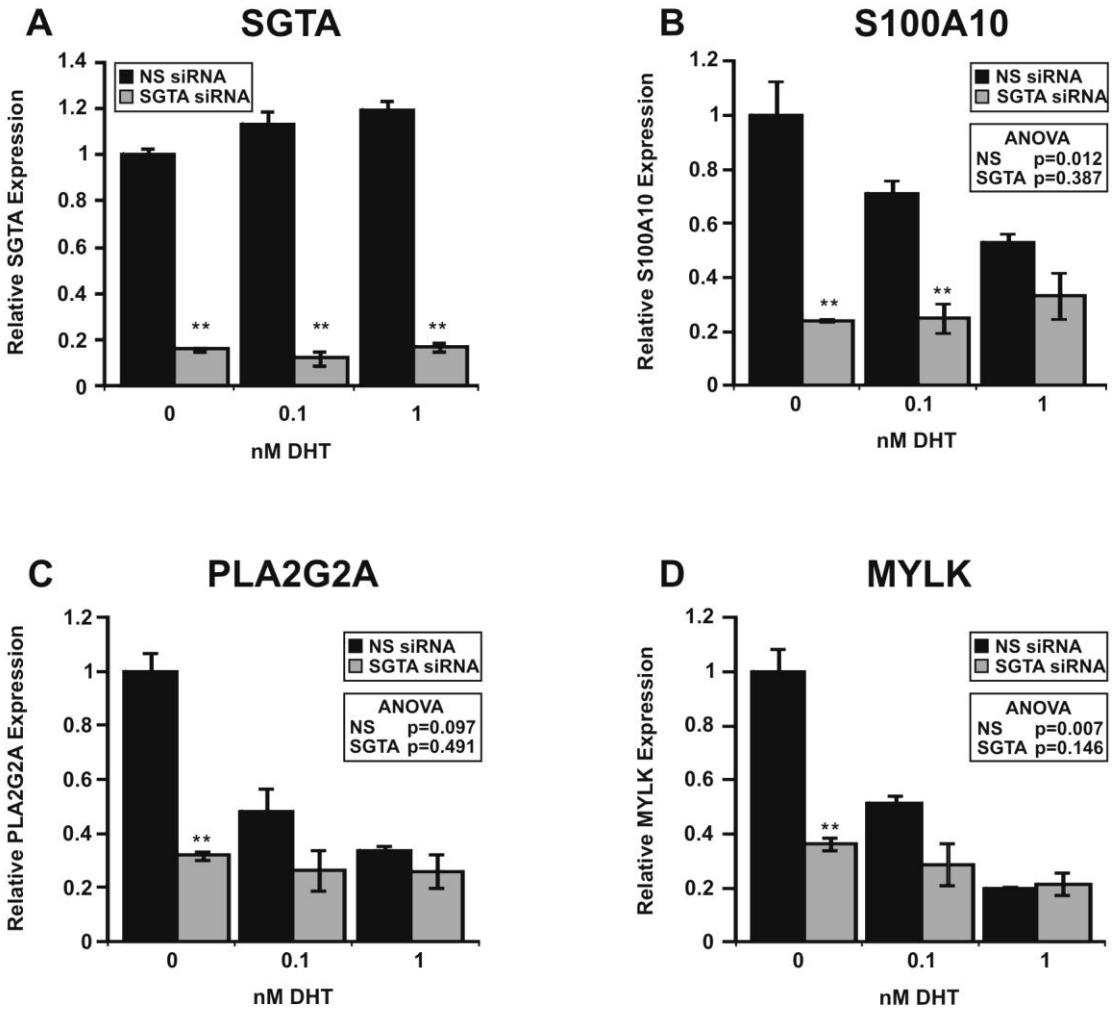

A
SGTA
Relative SGTA Expression
NS siRNA
SGTA siRNA
nM DHT
B
S100A10
Relative S100A10 Expression
ANOVA
NS p=0.012
SGTA p=0.387
C
PLA2G2A
Relative PLA2G2A Expression
ANOVA
NS p=0.097
SGTA p=0.491
D
MYLK
Relative MYLK Expression
ANOVA
NS p=0.007
SGTA p=0.146

Figure 5.6 A-D: Validation of genes down-regulated by SGTA knockdown. A microarray validation sample set was created with C42B cells transfected with NS or SGTA specific siRNA according to Figure 5.4C. RNA was isolated and analysed by QRT-PCR for expression of *SGTA*, *S100A10*, *PLA2G2A* and *MYLK* and normalised to the housekeeping gene *GAPDH*. Data are presented represent the mean (± SEM) of four biological replicates and is representative of 2 independently repeated experiments. One-way ANOVA was used to determine dose dependent effect of DHT treatment. *, is $p<0.05$, **, is $p<0.01$ on Mann-Whitney U for difference between medians of SGTA siRNA in comparison to NS siRNA.

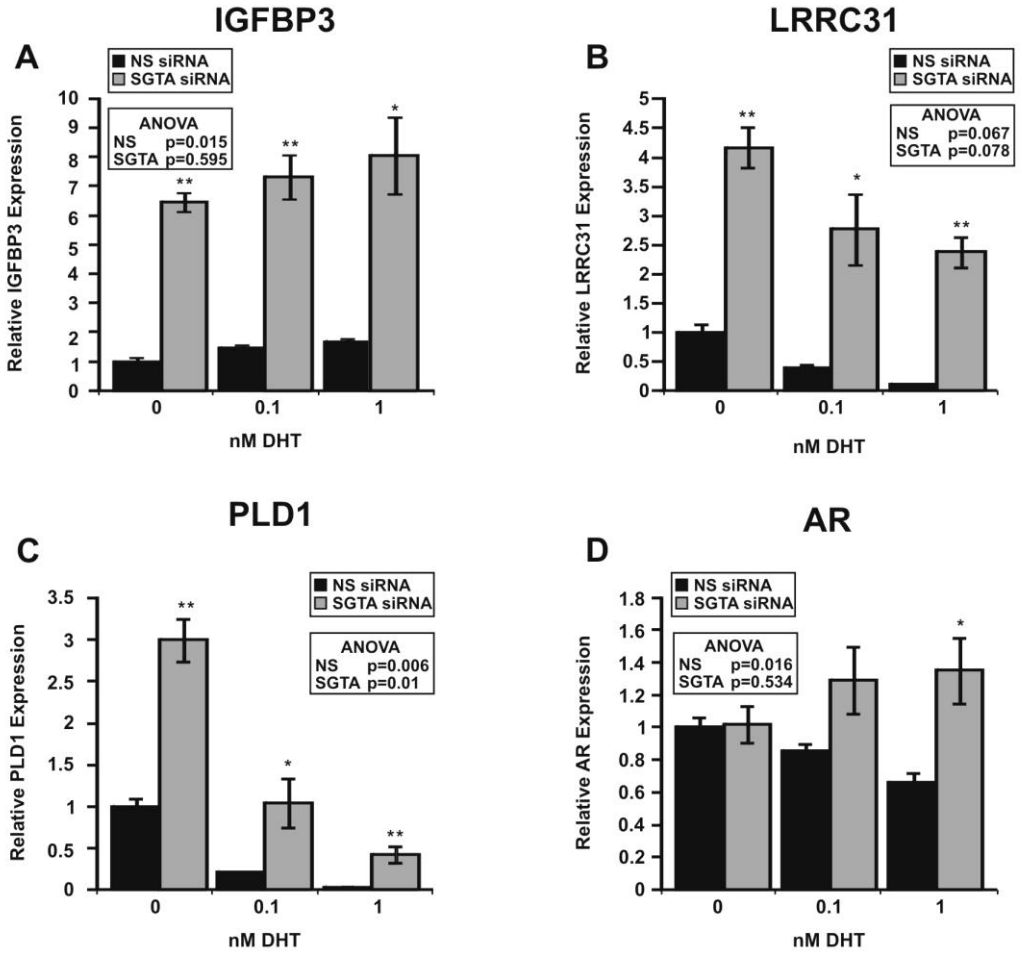


Figure 5.7 A-D: Validation of genes up-regulated by SGTA knockdown. Data is representative of samples created as described in Figure 5.6. RNA was isolated and analysed by QRT-PCR for expression of *IGFBP3*, *LRRC31*, *PLD1* and *AR* and normalised to the housekeeping gene *GAPDH*. Data are presented represent the mean (± SEM) of four biological replicates and is representative of 2 independently repeated experiments. One-way ANOVA was used to determine dose dependent effect of DHT treatment. *, is $p<0.05$, **, is $p<0.01$ on Mann-Whitney U for difference between medians of SGTA siRNA in comparison to NS siRNA.

5.3.5 SGTA knockdown affects cell proliferation gene ontology categories

To broaden our analysis from candidate genes to the global consequences of SGTA knockdown in prostate cancer cells, Ingenuity Pathway Analysis (IPA) was used to investigate cellular networks and pathways. The top 5 gene ontology categories significantly altered by SGTA knockdown are listed in Tables 5.3 and 5.4 respectively. All canonical pathways significantly altered by SGTA knockdown are presented in Appendix D. The top 2 most enriched Molecular and Cellular Function categories were Cell Death and Cell Cycle (Table 5.3), whereas Prostate Cancer Signalling was ranked as the 16th most significantly altered (Appendix D). Moreover, the most enriched canonical pathway is p53 signalling (Table 5.4), which is a pro-apoptotic pathway that is functionally inhibited in essentially all cancers, including prostate cancer (Bourdon 2007). The effect of SGTA knockdown on p53 signalling was examined in more detail by assessing the changes in individual genes in this pathway (Figure 5.8). With SGTA knockdown there was an increase in p53 expression, and a paradoxical decrease in the expression of p53 positively regulated target genes that play a role in apoptosis (i.e. *CASPASE 6*, *CABC1*, *APAF1* and *TEAP*) and cell cycle arrest (i.e. *CYCLINK* and *GADD45*) (Figure 5.8). Interestingly, this analysis revealed that several genes in the phosphoinositide 3-kinase (PI3 kinase) pathway were down-regulated in response to SGTA knockdown (Figure 5.8). The PI3 kinase signalling pathway has previously been documented as a dominant pathway for the maintenance of prostate cancer proliferation (Vivanco and Sawyers 2002).

Table 5.3: Effect of SGTA knockdown on Molecular and Cellular Functions as determined by IPA.

Molecular and Cellular Functions	p value range
Cell Death	$4.99x10^{-7} – 1.08x10^{-2}$
Cell Cycle	$3.42x10^{-6} – 1.08x10^{-2}$
Cell Morphology	$8.04x10^{-6} – 1.08x10^{-2}$
Cellular Function and Maintenance	$8.04x10^{-6} – 1.08x10^{-2}$
Cellular Development	$6.16x10^{-5} – 1.08x10^{-2}$

Table 5.4: Top 5 canonical pathways altered by SGTA knockdown as determined by IPA.

Top Canonical Pathways	p value
p53 Signalling	$1.78x10^{-6}$
Valine, Leucine and Isoleucine Degradation	$4.94x10^{-5}$
Molecular Mechanisms of Cancer	$2.51x10^{-5}$
Butanoate Metabolism	$6.7x10^{-4}$
Aryl Hydrocarbon Receptor Signalling	$7.97x10^{-4}$

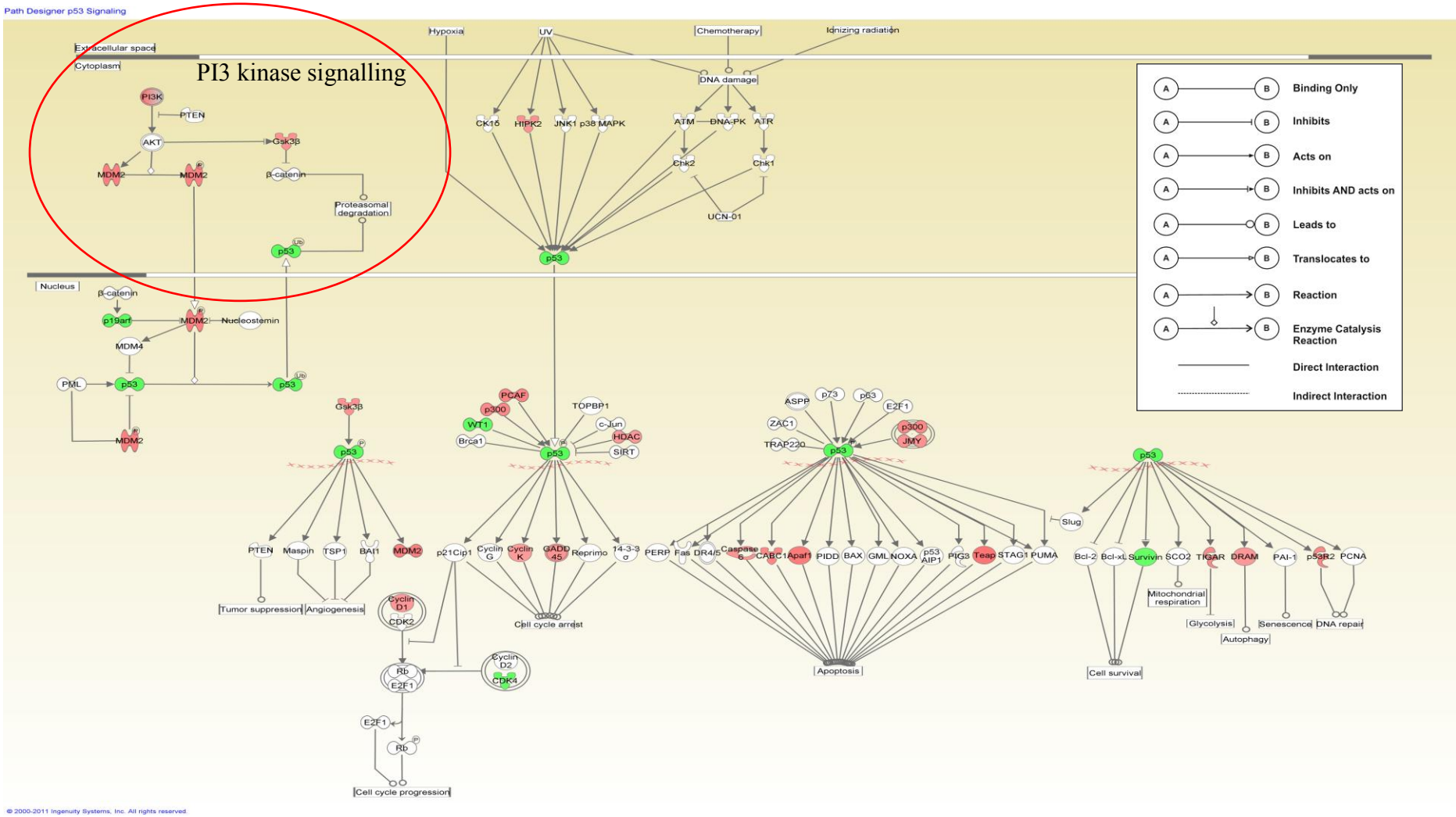

Path Designer p53 Signaling
PI3 kinase signalling
Extracellular space
Cytoplasm
Nucleus
Hypoxia
UV
Chemotherapy
Ionizing radiation
DNA damage
PI3K
PTEN
AKT
Gsk3β
MDM2
β-catenin
Proteasomal degradation
p53
CK1δ
HIPK2
JNK1
p38 MAPK
ATM
DNA-PK
ATR
Chk2
Chk1
UCN-01
p19arf
Nucleostemin
MDM4
PML
PCAF
p300
WT1
Brca1
TOPBP1
c-Jun
HDAC
SIRT
ASPP
p73
p63
E2F1
ZAC1
TRAP230
JMY
Slug
PTEN
Maspin
TSP1
BAI1
MDM2
p21Cip1
Cyclin G
Cyclin K
GADD 45
Reprimo
14-3-3 σ
PERP
Fas
DR4/5
Caspase 6
CABC1
Apaf1
PIDD
BAX
GML
NOXA
p53 AIP1
PIG3
Teap
STAG1
PUMA
Bcl-2
Bcl-xL
Survivin
SCO2
TIGAR
DRAM
PAI-1
p53R2
PCNA
Tumor suppression
Angiogenesis
Cyclin D1
CDK2
Cell cycle arrest
Rb
E2F1
Cyclin D2
CDK4
Cell cycle progression
Apoptosis
Cell survival
Mitochondrial respiration
Glycolysis
Autophagy
Senescence
DNA repair
Binding Only
Inhibits
Acts on
Inhibits AND acts on
Leads to
Translocates to
Reaction
Enzyme Catalysis Reaction
Direct Interaction
Indirect Interaction
© 2000-2011 Ingenuity Systems, Inc. All rights reserved.

Figure 5.8: Effect of SGTA knockdown on p53 signalling. Effects of SGTA knockdown on the expression of genes implicated in the p53 signalling pathway. Pathway was generated in IPA using Path Designer. Genes up and down-regulated by SGTA knockdown in C42B cells are highlighted in green and red respectively. Red circle highlights the proteins in the PI3 kinase pathway that are affected by SGTA knockdown and how they contribute to p53 signalling. Figure legend describes the actions of interaction between each protein in the pathway.

5.3.6 SGTA down-regulates Class I phosphoinositide 3-kinase genes

Given the functional importance of PI3 kinase signalling in prostate cancer (Li, Ittmann et al. 2005), we next investigated the outcomes of SGTA knockdown from the microarray onto the PI3 kinase signalling pathway using the Path Designer program in IPA (Figure 5.9). The PI3 kinase proteins are comprised of three Class IA catalytic subunits (p100α, p110β, and p110δ), a Class IB catalytic subunit (p110γ) and three regulatory subunits (p85α, p85β and p55γ). SGTA knockdown resulted in the down-regulation of the *p110* and *p85* Class IA PI3 kinase subunit genes as well as the plasma membrane adapter kinase *GRB2* (Figure 5.9). Importantly, of the 3 Class IA catalytic and 3 regulatory PI3 kinase subunit genes present on the microarray, a significant decrease occurred in 4 (*p85α*, *p55γ*, *p110β* and *p110δ*) with SGTA knockdown (Figure 5.10A). It has been previously reported that expression of these PI3 kinases is influenced by steroid hormones, such as estradiol (Lee, Park et al. 2005). Here we show that expression of *p85α*, *p55γ*, *p110β* and *p110δ* is significantly decreased with DHT treatment (ANOVA $p<0.05$; Figure 5.10 B-E). Although validation of the effect of SGTA knockdown was confirmed on *p110δ* expression (vehicle treatment Figure 5.10E), the addition of DHT to SGTA depleted cells resulted in the reversal of AR mediated down regulation (Figure 5.10 B-E). These data provide further evidence to suggest that there is a convergence of SGTA onto a specific subset of AR regulated genes that then modulates the transcriptional profile of prostate cancer cells.

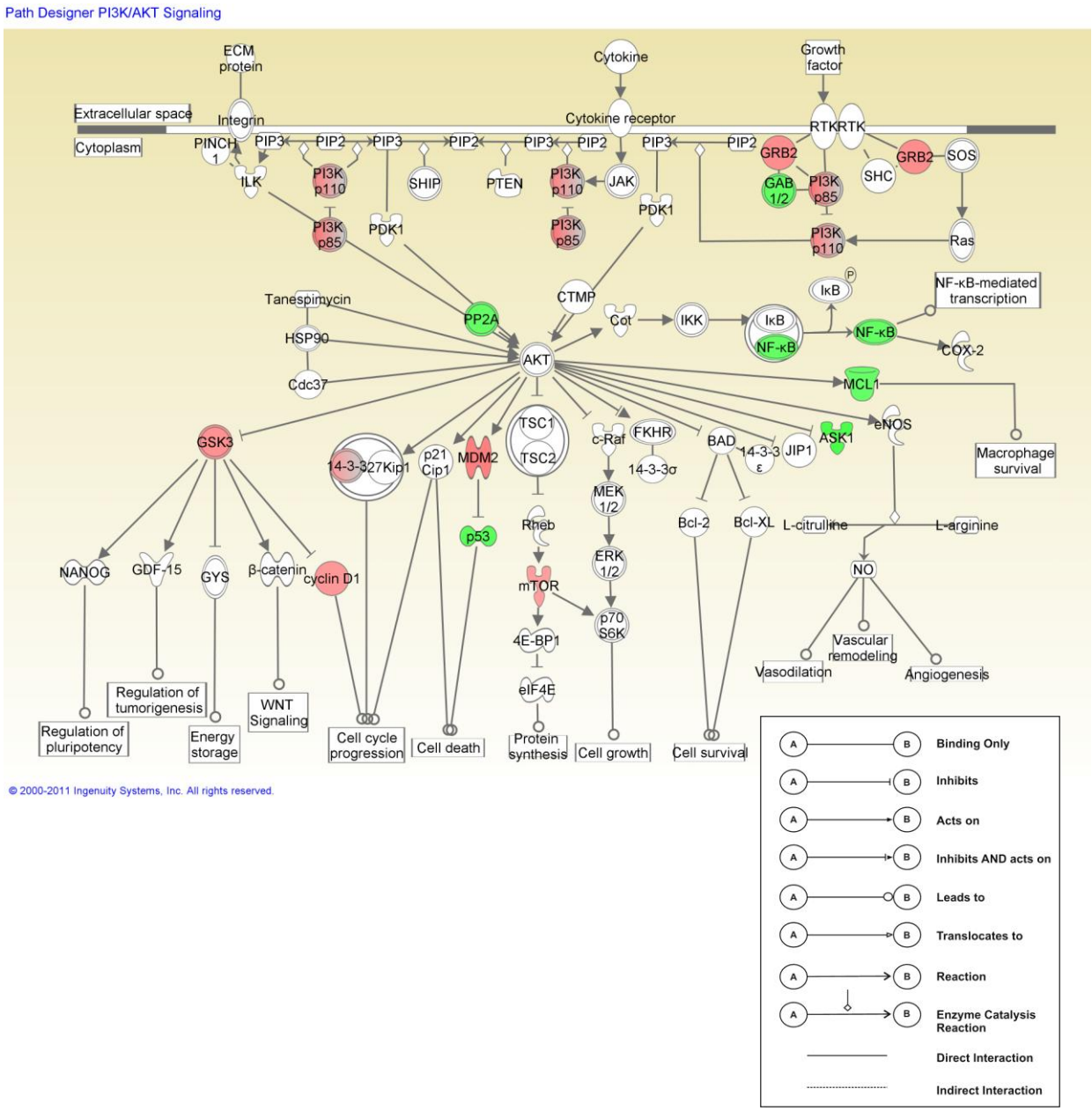
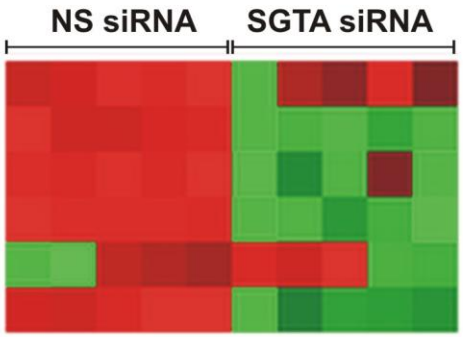

Path Designer PI3K/AKT Signaling
ECM protein
Cytokine
Growth factor
Extracellular space
Integrin
Cytokine receptor
RTK
RTK
Cytoplasm
PINCH 1
PIP3
PIP2
PIP3
PIP2
PIP3
PIP2
PIP3
PIP2
GRB2
GRB2
SOS
ILK
PI3K p110
SHIP
PTEN
PI3K p110
JAK
GAB 1/2
PI3K p85
SHC
PI3K p85
PDK1
PI3K p85
PDK1
PI3K p110
Ras
Tanespimycin
CTMP
IkB
NF-κB-mediated transcription
PP2A
Cot
IKK
IkB
NF-κB
NF-κB
COX-2
HSP90
AKT
Cdc37
MCL1
GSK3
TSC1
TSC2
c-Raf
FKHR
BAD
14-3-3 ε
JIP1
ASK1
eNOS
Macrophage survival
14-3-3σ
p21 Cip1
MDM2
MEK 1/2
Rheb
Bcl-2
Bcl-XL
L-citrulline
L-arginine
NANOG
GDF-15
GYS
β-catenin
cyclin D1
p53
ERK 1/2
mTOR
NO
4E-BP1
p70 S6K
Vascular remodeling
Vasodilation
Angiogenesis
eIF4E
Regulation of tumorigenesis
WNT Signaling
Regulation of pluripotency
Energy storage
Cell cycle progression
Cell death
Protein synthesis
Cell growth
Cell survival
© 2000-2011 Ingenuity Systems, Inc. All rights reserved.
Binding Only
Inhibits
Acts on
Inhibits AND acts on
Leads to
Translocates to
Reaction
Enzyme Catalysis Reaction
Direct Interaction
Indirect Interaction

Figure 5.9: Phosphoinositide 3-kinase signalling pathway. Effects of SGTA knockdown on the expression of genes implicated in the PI3 kinase signalling. Pathway was generated in IPA using Path Designer. Genes up and down-regulated by SGTA knockdown in C42B cells are highlighted in green and red respectively. Figure legend describes the actions of interaction between each protein in the pathway.



Gene	Fold Change	Adj. p value
p110α	-1.14	0.146
p110β	-1.44	0.0002
p110δ	-1.41	0.0012
p85α	-1.62	9.65E-05
p85β	1.04	0.645
p55γ	-1.25	0.0042

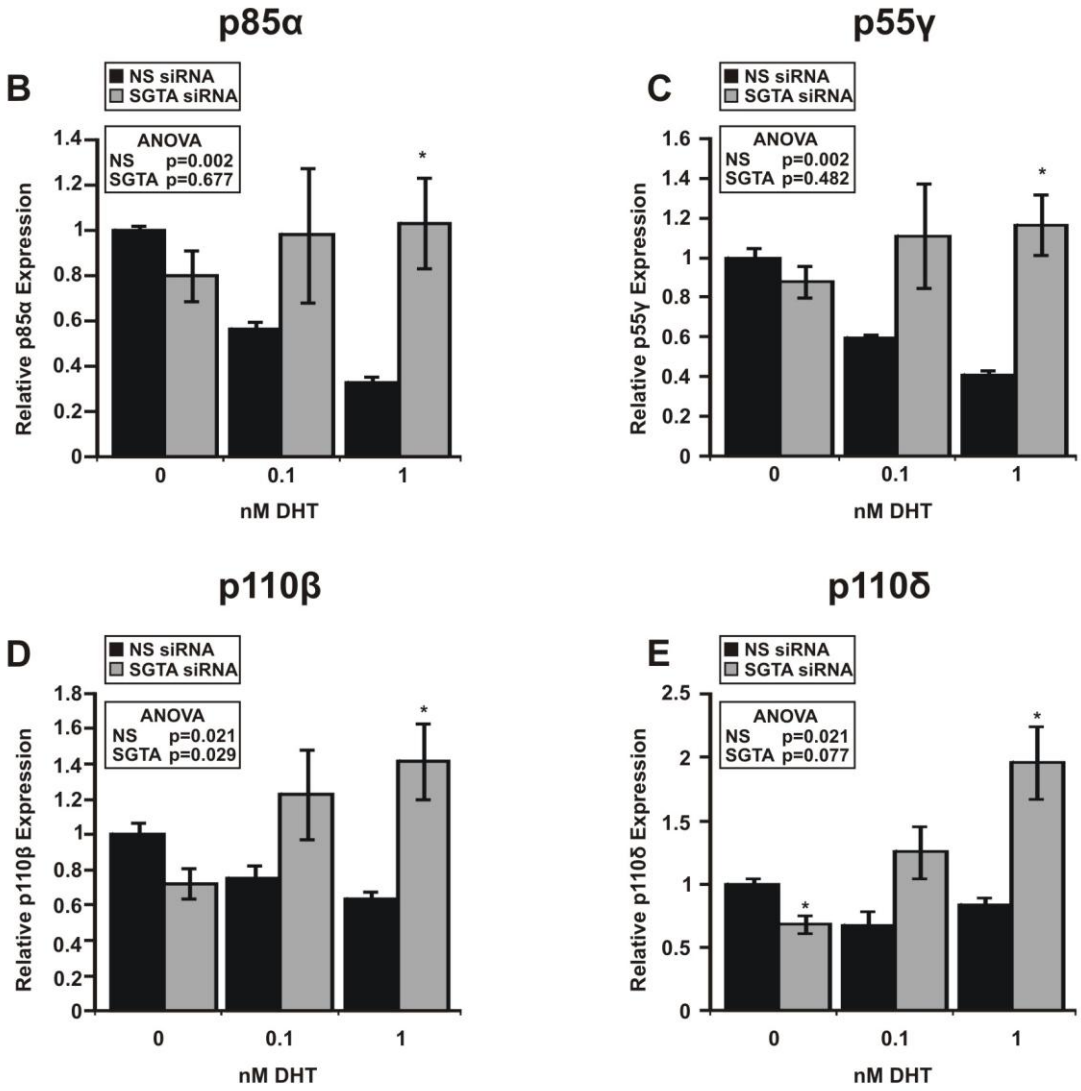


Figure 5.10: SGTA knockdown in C42B cells alters androgen mediated regulation of PI3 kinase genes. A: Heatmap of PI3 kinase genes from the microarray data presented in Figure 5.5 was generated using Heatmap Builder Version 1.0. A colour change from red to green represents a down-regulation of gene expression. **B-D:** Data is representative of samples created as described in Figure 6.6. RNA was isolated and analysed by QRT-PCR for expression of *p85α*, *p55γ, p110β* and *p100δ* and normalised to the housekeeping gene *GAPDH*. Data represent the mean (± sem) of four biological replicates and is representative of 2 independently repeated experiments. One-way ANOVA was used to determine dose dependent effect of DHT treatment. *, is $p<0.05$, on Mann-Whitney U for difference between medians of SGTA siRNA in comparison to NS siRNA.

5.3.7 SGTA knockdown modulates PI3 kinase-Akt activity

SGTA has been previously implicated as a positive modulator of PI3 kinase signalling by maintaining the activity of the downstream PI3 kinase target protein Akt (Moritz, Li et al. 2010). Therefore, we next investigated how knockdown of SGTA would affect PI3 kinase signalling and Akt activity in prostate cancer cells. SGTA knockdown did not affect either vehicle or DHT treated p85 protein steady state levels (Figure 5.11). However, the antibody used in this study detects both α and β subunits and therefore the effect of SGTA knockdown on individual subunits may be masked. Consistent with the QRT-PCR data presented in Figure 5.9D, basal p110β protein steady state levels were decreased with knockdown of SGTA, while treatment with 1 nM DHT resulted in a slight recovery in protein steady state levels (Figure 5.11). It has been recently reported that a reduction in p110β protein levels alone by siRNA knockdown reduced Akt activity in prostate cancer cells as measured by dephosphorylation of the threonine 308 (T308) and serine 473 (S473) residues respectively (Jiang, Chen et al. 2010). We investigated the effect of SGTA knockdown on the status of Akt phosphorylation in C42B cells. Indeed, the loss of SGTA resulted in reduced phosphorylation at both sites either in the absence or presence of DHT, although treatment with 1 nM DHT stabilised Akt phosphorylation levels (Figure 5.11). The decrease in Akt T308 and S473 phosphorylation could not readily be attributed to a decrease in total Akt levels, particularly in the presence of DHT (Figure 5.11). In the absence of other evidence, it is possible that the loss of Akt activity is directly mediated by a decrease in p110β levels. Collectively, these findings support a preliminary argument that

SGTA may act to modulate both a specific AR transcriptional program and PI3 kinase signalling in prostate cancer cells.

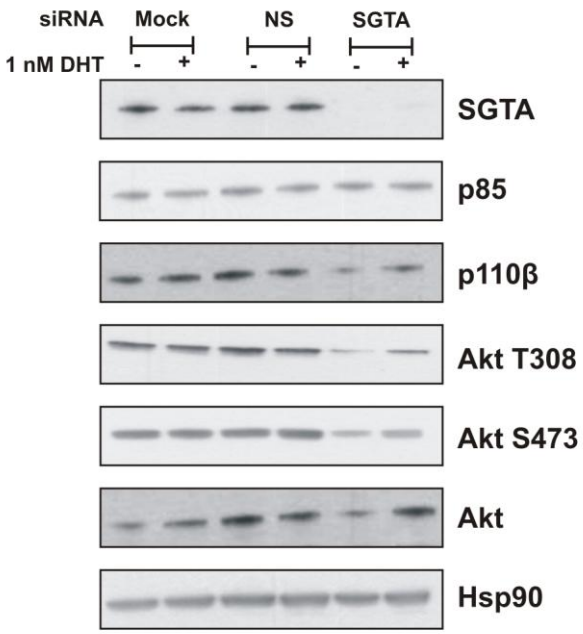


Figure 5.11: Knockdown of SGTA in C42B cells reduces Akt activity. Immunoblot analysis of cells transfected as described in Figure 5.6. Cells were treated with vehicle (ethanol) control or 1 nM DHT for 24 hours and lysates were harvested using RIPA buffer containing both protease and phosphatase inhibitors. Immunoblot analysis of SGTA, p85, p110β, and Akt protein steady state levels. Analysis of active Akt signalling was determined by phosphorylation status of the threonine 308 (T308) and serine 473 (S473) residues respectively. Hsp90 was used as a loading control.

5.4 Discussion

To date the role of SGTA in prostate cancer cells has been thought to primarily reflect its interaction with AR. However, as multiple SGTA client proteins have now been identified, including the tyrosine kinase receptors PDGFRα and hGHR (Schantl, Roza et al. 2003; Moritz, Li et al. 2010), it is unquestionable that the biological role of SGTA extends beyond AR signalling in prostate cancer. One of the aims of this chapter was to determine the effects of SGTA in the absence of androgen signalling. The findings presented here demonstrate that long-term SGTA deprivation culminates in substantial transcriptome changes in prostate cancer cells. Specifically, there was a deregulation of genes involved in a number of key biological networks that affect both the cell cycle and cell viability, including p53 and PI3 kinase signalling pathways.

The tumour suppressor gene p53 is a transcription factor that regulates genes required to block DNA replication and promote cell cycle arrest and apoptosis (el-Deiry, Tokino et al. 1993; Harper, Adami et al. 1993; Chipuk and Green 2006). Like many cancers, clinical samples of prostate cancer are often characterised by loss or mutation of p53, which contributes to the progression of the tumour to a castrate resistant state (Chi, deVere White et al. 1994; Eastham, Stapleton et al. 1995). The C42B cells utilised in this study are a model of castrate resistance and express low levels of wild type p53 (Ko, Gotoh et al. 1996). SGTA knockdown resulted in a small, but significant 1.3 fold increase in *p53* expression, implying that the presence of SGTA may exert some direct or indirect control over *p53* expression, which possibly might affect the outcomes of p53 signalling.

Indeed, a previous report has demonstrated that over expression of exogenous wild type p53 in C42B cells decreases cell proliferation by 2 fold compared to controls (Ko, Gotoh et al. 1996). However, the level of p53 required to achieve this effect has not been determined.

More detailed analysis of the p53 pathway revealed that SGTA knockdown caused down-regulation of several Class IA phosphatidylinositol-3 kinase (PI3 kinase) subunit genes. Like p53 signalling, the PI3 kinase pathway has also been associated with prostate cancer pathogenesis and progression (Vivanco and Sawyers 2002; Li, Ittmann et al. 2005). The Class 1A PI3 kinases are a group of enzymes comprised of regulatory (p85α, p85β, p55α, and p55γ) subunit proteins that interact with the catalytic (p110α, p110β and p110δ) subunits to form heterodimeric complexes that can be activated by receptor tyrosine kinases at the cell surface (Figure 5.12). Alternatively, receptor tyrosine kinases can also indirectly activate PI3 kinase subunits via RAS interactions with p110 (Figure 5.12). The findings from this chapter demonstrated that knockdown of SGTA decreased the mRNA expression of *p85α, p55γ, p110β* and *p110δ* respectively. Although the precise mechanisms by which SGTA affects PI3 kinase gene expression are unknown.

Emerging evidence indicates that cumulative changes to PI3 kinase gene expression can occur under various physiological settings, leading to persistent alterations in PI3 kinase activity (Kok, Geering et al. 2009). It has been shown that short term induction of *p85* mRNA expression can occur upon cell stimulation by various ligands such as retinoic acid or estradiol (Lee, Park et al. 2005; Bastien, Plassat et al. 2006), whereas *p110* expression is

induced by the phosphodiesterase inhibitor 3-isobutyl-1-methylxanthine and dexamethasone (Asano, Kanda et al. 2000). The studies from this chapter further highlight the potential role steroid receptors, in particular the AR, play in regulating the expression of PI3 kinase genes (Figure 5.11). Moreover, there is evidence to suggest that regulation of PI3 kinase genes may extend to other members of the nuclear receptor family, such as RAR, PPARα/β/γ and RXR (Rieusset, Roques et al. 2001). Additionally, it has been demonstrated that various Hsp90-TPR complexes are able to interact with and control their transcriptional activity. For example, the incorporation of PP5 into PPAR complexes acts to increase PPAR transactivation activity, whereas the inclusion of CHIP results in the inhibition of PPAR (Sumanasekera, Tien et al. 2003). Similarly, the incorporation of SGTA into Hsp90-AR and possibly other steroid receptor complexes, such as the GR may be a mechanism through which SGTA is able to modulate the expression of PI3 kinase genes (Figure 5.12). Indeed, the results presented in this chapter show that knockdown of SGTA is sufficient to antagonise the androgenic effects on PI3 kinase gene expression; implying that there may be a direct mechanism through which SGTA acts on AR signalling to regulate the expression of PI3 kinase genes.

Regulation of steroid receptor transcriptional activity is achieved on multiple levels. One area that has gathered significant interest is the impact that cytoplasmic chaperones might have on the stabilisation of the steroid receptor/ligand interaction. However, few attempts have been made to evaluate how this might translate to altered steroid receptor transcriptional profiles. Given the findings from our previous study, which demonstrated

that knockdown of SGTA enhanced the capacity for AR to up-regulate *PSA* mRNA expression (Buchanan, Ricciardelli et al. 2007), it was surprising not to observe a similar effect on *PSA* or *FKBP51* expression in this chapter, even though potent knockdown of *SGTA* mRNA and protein steady state levels was achieved. The discrepancy in results between the two studies can be attributed to a number of factors, including the use of different siRNAs, the possibility of off-target effects that feed forward onto AR signalling as well as potential differences in transfection and cell culturing methods. Additional sources of variation can occur between independently cultured strains of the same cell line over a long period of time (Bahia, Ashman et al. 2002; Watson, Bahia et al. 2004). Given that the initial study was conducted several years ago in the laboratory of Professor Coetzee (University of Southern California), it is possible that characteristic changes occurred in the C42B cell line that has now precluded SGTA from producing an observable effect of AR activity on these genes.

Nevertheless, one of the more intriguing findings from this chapter was that the vast majority of candidate genes chosen from the SGTA knockdown microarray were also found to be down-regulated by androgens, which implies that the actions of SGTA may be enriched in a specific subset of androgen regulated genes. Indeed, it appears that the effect of SGTA on AR may manifest itself at a transcriptional level in three ways. Firstly, SGTA acts to maintain the ability of the AR to down-regulate genes. Second, SGTA synergises with AR to suppress gene expression altogether and thirdly, SGTA antagonises AR mediated gene induction. While the precise mechanism by which SGTA co-ordinates these

different transcriptional responses is unknown, our data broadly suggests that SGTA either acts with or against the AR to suppress the expression of a large subset of genes in prostate cancer cells. Therefore, the loss of SGTA expression with prostate cancer progression may hold important biological consequences for the regulation of transcriptional profile of prostate cancer cells in both an intact and androgen depleted environment. However, further analysis of the effects of SGTA knockdown on a larger subset of known androgen regulated genes in multiple AR positive prostate cancer cells lines is required to confirm these observations.

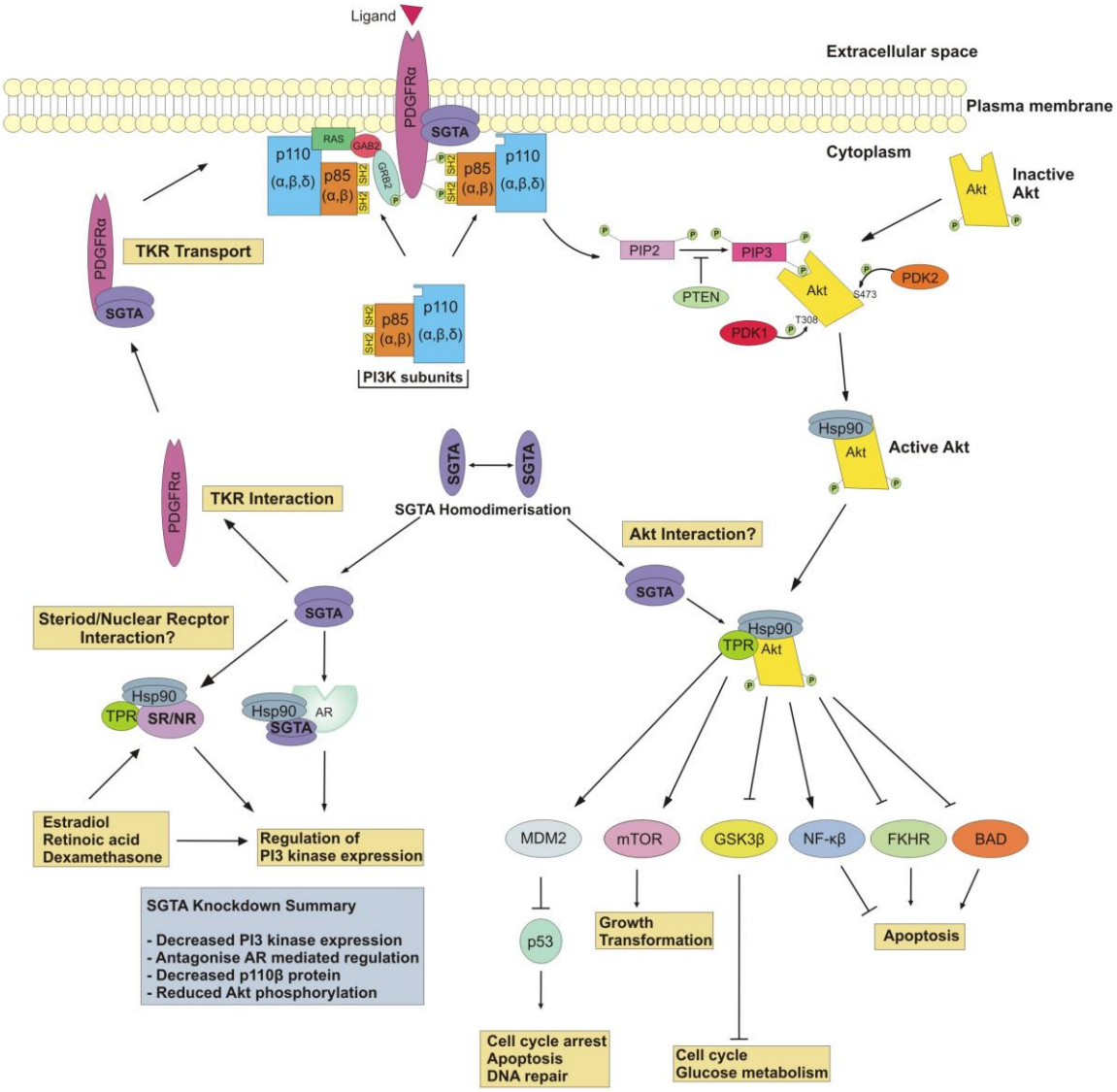


Figure 5.12: Proposed model for the effect of SGTA on tyrosine kinase receptor (TKR) - PI3 kinase signalling in prostate cancer cells.

The findings in this chapter, along with a previous study, have implicated SGTA as a positive regulator of Akt activity in cancer (Moritz, Li et al. 2010). The serine/theronine kinase Akt is a central component of the PI3 kinase pathway (Figure 5.12). Upon

ligand stimulation and tyrosine kinase receptor activation, the molecule PIP2 is phosphorylated and converted to PIP3, which then acts to recruit an inactive form of Akt to the cell surface (Figure 5.12). There, maximal activation of Akt can be achieved by phosphorylation of the threonine residue 308 (T308) and serine residue 473 (S473) by the kinases PDK1 and PDK2 respectively (Vivanco and Sawyers 2002) (Figure 5.12). Activated (phosphorylated) Akt functions downstream of the PI3 kinase subunits to regulate many biological processes, including promoting proliferation and growth, while inhibiting apoptosis. In this study, knockdown of SGTA results in decreased phosphorylated levels at both the T308 and S473 residues of Akt, implying that SGTA plays a role in maintaining Akt activity in prostate cancer cells, possibly via enabling normal expression of the PI3 kinase subunit p110β. Indeed, a recent study has demonstrated that reducing the levels of p110β and p110δ catalytic subunits decreases Akt phosphorylation (Jiang, Chen et al. 2010). Moreover, the same study showed that serum starvation for 72 hours (the same length of time as SGTA knockdown in this thesis) did not alter PI3 kinase activity, which supports a specific rather than experimental effect of SGTA on Akt activity and that prostate cancer maintains a constitutively active PI3 kinase pathway in a castrate resistant environment (Jiang, Chen et al. 2010). Conversely, other TPR co-chaperones, such as FKBP51 have been shown to act as a negative regulator of PI3 kinase activity by promoting the dephosphorylation of Akt at S473 via the phosphatase PHLPP, whereby knockdown of FKBP51 results in enhanced Akt activity through hyperphosphorylation of the S473 site (Brognard, Sierecki et al. 2007; Pei, Li et al. 2009; Mulholland, Tran et al. 2011). Future studies that investigate the potential roles

different TPR co-chaperones play as regulators of PI3 kinase signalling may help decipher the mechanism by which SGTA maintains PI3 kinase/Akt signalling and therefore potentially provide a novel means of disrupting this pathway in prostate cancer cells.

In summary, the findings presented in this chapter have uncovered novel biological actions of SGTA in prostate cancer cells. Due to its ability to restrict AR subcellular localisation and transcriptional activity, it was presumed that knockdown of SGTA would enhance AR activity. Surprisingly, this thesis demonstrated that SGTA does not affect the expression of the canonical AR regulated genes *PSA* and *FKBP51*, but rather appears to have generated a unique transcriptional profile in prostate cancer cells that affects androgen down-regulated genes. Additionally, cytoplasmic SGTA affects the transcriptional regulation of genes within critical cell signalling pathways that may contribute to the pathophysiological phenotype of excessive prostate cancer cellular proliferation and survival. The findings within this chapter demonstrate that loss of SGTA may inhibit PI3 kinase signalling in both intact and an androgen depleted environment potentially leading to a loss of Akt phosphorylation. The loss of SGTA with prostate cancer progression may therefore significantly alter the regulatory mechanisms controlling cellular events such as proliferation and survival in metastatic disease.

CHAPTER 6

The effect of SGTA on prostate cancer cell proliferation

Chapter 6: The effect of SGTA on prostate cancer cell proliferation

6.1 Introduction

The previous chapters of this thesis discussed the ability of SGTA to control the sensitivity of ligand dependent AR activity in prostate cancer cells, whereas cells depleted of SGTA display an altered expression profile of genes involved in key signalling pathways that affect cell proliferation. However, the functional consequences of this effect as well as the more broader biological role of SGTA in prostate cancer cells remain elusive. One of the key effects of AR signalling in prostate cancer is the promotion of cellular proliferation and survival. Indeed, enhanced AR activity that is generated either through increased AR levels and/or gain of function mutations has been associated with increased tumour growth during the progression of the disease to a castrate resistant state (Chen, Welsbie et al. 2004; Dehm and Tindall 2007; Haapala, Kuukasjarvi et al. 2007). The presence of circulating androgens that stimulates AR activity and tumour growth underpins the use of androgen deprivation therapy (ADT) for prostate cancer, which initially induces cell cycle arrest and/or apoptosis and a reduction in tumour burden (Huggins and Hodges 1972; Denmeade, Lin et al. 1996; Agus, Cordon-Cardo et al. 1999). However, the beneficial effects of ADT

are temporary, as the majority of patients relapse with recurrent disease (Feldman and Feldman 2001; Chen, Welsbie et al. 2004).

It is now clear that the AR continues to signal and be a mediator of cell proliferation, even in an androgen depleted environment or during treatment with anti-androgens. Therefore, as an alternative means of blocking AR actions in prostate cancer cells there is increasing interest in targeting critical co-mediators of cell cycle regulation on which the AR may rely. In this context, several TPR containing co-chaperones have been identified as co-activators of AR activity and subsequent prostate cancer cell proliferation. For example, a recent report demonstrated that elevated levels of FKBP51 and Cyp40 in prostate cancer samples compared to normal prostate tissue contributed to an increase in both AR signalling and cell proliferation (Periyasamy, Hinds et al. 2010). The immunophilin targeting compounds FK506 and cyclosporine A (CsA) are able to inhibit the activities of FKBP51/FKBP52 and Cyp40 respectively (Periyasamy, Warrier et al. 2007; Kozany, Marz et al. 2009). Consequently, these inhibitors have been a useful tool in demarcating the role of TPR co-chaperones in AR function and prostate cancer proliferation. For example, inhibition of Cyp40 by CsA is effective at reducing the cell proliferation of both AR positive (i.e. LNCaP) and negative (i.e. PC3, DU145) cell lines, whereas FK506 suppressed the growth of only AR positive cells, suggesting that some of the physiological effects of specific TPR co-chaperones may be AR dependent (Periyasamy, Warrier et al. 2007). Indeed, evidence provided by FKBP51 and FKBP52 mouse knockout studies have demonstrated that only FKBP52-deficient mice display aberrant morphology in selective

androgen sensitive tissues (Cheung-Flynn, Prapapanich et al. 2005; Yong, Yang et al. 2007).

Currently, only two studies have investigated the biological role of SGTA in the proliferation of HeLa cells, both of which were conducted in the Cziepluch laboratory (Winnefeld, Rommelaere et al. 2004; Winnefeld, Grewenig et al. 2006). These investigations showed that depletion of SGTA by siRNA knockdown causes a misalignment of chromosomes along the metaphase plate, which then results in mitotic arrest and cell death (Winnefeld, Rommelaere et al. 2004; Winnefeld, Grewenig et al. 2006), suggesting that SGTA plays an important role in the maintenance of the cell cycle and proliferation. Although the effects of altered SGTA levels on prostate cancer cell proliferation have yet to be determined, the consequences may be clinically important given the observed loss of SGTA during prostate cancer progression from our previous study (Buchanan, Ricciardelli et al. 2007). Moreover, this thesis has extensively discussed the ability of SGTA to control the sensitivity of ligand dependent AR activity as well as the regulation of PI3 kinase signalling in prostate cancer cells, and thus an additional consequence of decreased SGTA levels may be to affect the potency of AR and/or PI3 kinase signalling in a low hormone environment. However, the implications this alteration has on disease outcomes remains unknown. Therefore, the aims for this chapter are to i) determine if SGTA plays a role in prostate cancer cell proliferation *in vitro* and ii) determine if the levels of SGTA in prostate cancer cells compared to benign tissue are related to disease outcome.

6.2 Materials and Methods

6.2.1 Cell proliferation assays, siRNA knockdown and immunoblot

Parental or stably transfected LNCaP cells were seeded in 24 well plates (25,000/well) in 1 mL RPMI-1640 medium containing 10% FBS. For knockdown experiments C42B cells were seeded in 24 well plates (25,000/well) in 1 mL of RPMI-1640 medium containing 5% FBS. After 24 hours the medium was removed and the cells were mock transfected or transfected with 5 nM non specific (NS) or three independent SGTA siRNA each at a concentration of 1.67 nM according to the method outlined in chapter 2.3.3.4. Cells were transfected in medium containing either 5% dextran charcoal stripped fetal bovine serum (DCS-FBS) or 5% FBS. Cells were harvested using trypsin at the indicated time points and counted using a haemocytometer. Viable cells were assessed by trypan blue exclusion, while the number of dead cells was assessed by uptake of trypan blue. For immunoblot analysis, LNCaP or C42B cells were seeded in 6 well plates (200,000 cells/well). LNCaP cells were harvested and lysates collected to analyse for AR, HA, PSA, calnexin and tubulin protein levels according to the method described in chapter 2.3.5. C42B cells were transfected with NS or SGTA specific siRNA as described above. Cell lysates were collected and analysed by immunoblot for SGTA and beta actin protein levels according to the method described in chapter 2.3.5.

6.2.2 Cloning of SGTA into two independent stable integration mammalian expression vectors

Two independent stable cells lines were created in the laboratory to over express SGTA in the LNCaP prostate cancer cell line. Either a HA-SGTA or GFPiresSGTA expression vector was integrated into the chromatin of LNCaP cells. All expression vectors were created by Dr. Jeffery Barrett.

The commercially available plasmid pIRESpuro3 was selected for the creation of a constitutively expressing HA tagged SGTA (HA-SGTA) vector. The pIRESuro3 vector contains an internal ribosomal entry site (IRES) sequence that separates the gene conferring antibiotic resistance from the multiple cloning site. The pIRES-EGFP vector was utilised to constitutively express both SGTA and green fluorescent protein (GFP) as independent proteins from the same transcript (GFPiresSGTA). The position of the IRES sequence is positioned in between the multiple cloning site and the GFP coding region. The primers IRSSGTs and IRSGTas were used to amplify HA-SGTA from the pSG5:HA-SGTA expression vector according the PCR parameters listed in Appendix A1. The amplified region was gel purified and digested using *NheI* and *AgeI* according to the method outlined in chapter 2.3.1.6. To subclone the SGTA gene into the pIRES-EGFP expression vector, SGTA was amplified from the pSG5:HA-SGTA expression vector using the forward primer SGTGFPs, which contains an *EcoRI* restriction site, Kozak sequence and start codon to amplify the SGTA gene without the HA tag, and a reverse primer SGTGFPas, which contains a *BamHI* restriction site and stop condon. Primer sequences and PCR parameters are listed in Appendix A1. The PCR product was gel purified and

digested with *EcoRI* and *BamHI* respectively using the method outlined in chapter 2.3.1.6. The restricted HA-SGTA or SGTA fragments were ligated into digested pIRESspuro3 or pIRES-EGFP vectors respectively overnight at 16°C utilising TA DNA polymerase. The amplified regions were sequenced verified in both directions along the entire length and over the ligation sites of the PCR product according to the method outlined in chapter 2.3.1.7.

6.2.3 Creation of stable transformants

LNCaP cells were harvested at log phase by trypsinisation, resuspended in growth medium and pelleted by centrifugation at 2000 g for 5 mins. Cells were washed once with double the volume of room temperature PBS and pelleted as above. Viable cells were counted using a haemocytometer with trypan blue exclusion and resuspended at approximately $1x10^7$ cells/ml in PBS. An aliquot of 0.5 mL of cells was mixed with 20 μg of the pIRESpuro3-HA, pIRESpuro3-HA-SGTA, pIRESpuro-EGFP or pIRESpuro-EGFPiresSGTA and 400 μL of the samples were transferred to a 4 mm gap cuvette (BTX International, Massahusetts, USA) and electroporated on a square wave electroporator ECM 630 (BTX International) at 170 V for 70 msec. The cell mixture was immediately resuspended in 15 mL of charcoal stripped growth medium and plated on 100 mm tissue culture plates.

6.2.4 Selection of stable transformants

Twenty four hours after transfection, growth medium containing 1 μg/mL puromycin (Sigma-Aldrich, St Louis, MO, USA) in charcoal stripped growth medium was placed on

plates containing cells transfected with pIRESpuro3 vectors, while 800 μg/mL geneticin (Invitrogen, San Diego, CA, USA) was used for pIRESpuro-EGFP vectors. Growth medium was changed every 48 hours and plates left until visible colonies had formed. Single colonies were transferred to each well on 24 well plates utilising sterile cloning cylinders, vacuum grease and gentle trypsinisation. Colonies were subsequently propagated into T25 then T75 flasks and cell lines were frozen in normal growth medium utilising the method outlined in chapter 2.3.2.3.

6.2.5 Clinical cohort and creation of tissue microarrays

Of the men whom underwent transurethral resection of the prostate (TURP) for BPH between 2000 and 2007 at the Repatriation General Hospital (RGH), a total of 66 patients had an incidental diagnosis of prostate cancer, a Gleason grading, and >5% cancer on histology. Areas of BPH and cancer were identified in each by hematoxylin and eosin staining, mapped onto archived paraffin embedded material by one pathologist. All protocols were approved by the Flinders Medical Centre and RGH ethics committee (Protocol #042/10). A series of 6 tissue microarrays were constructed by insertion of the paraffin embedded donor block into the donor block holder of the tissue microarrayer. A standard plastic cassette, containing a blank paraffin block (recipient block) was placed into the recipient block place holder. Duplicate 1.5 mm diameter by 3 mm deep cores were extracted from the pathologist defined areas of BPH and prostate cancer and embedded across 6 recipient paraffin blocks with 46 samples per block. Two additional prostate cancer samples and one liver sample were included as controls for each recipient block.

6.2.6 Immunohostochemistry

The following immunostaining protocol was used by Mr Damien Leach for the detection of AR and SGTA expression in the patient cohort described above. Tissue sections 2 μM in thickness were cut from the tissue microarray blocks using an XYZ microtome and placed onto treated Menzel-Glaser Superfrost Ultra-Plus glass slides, which were then baked at 60°C for 1 hour prior to staining. The slides were dewaxed in xylene and rehydrated in ethanol washes and PBS. The slides were treated with 3% H_20_2 in PBS for 2 minutes to block for endogenous peroxidise. To counteract the epitope masking effect of formalin fixation, sections were immersed in 0.01 M citrate buffer (pH 6.0) and heated on HIGH Watts in a microwave oven for 4 minutes or until boiling, and then on LOW Watts for 10 minutes. Sections were placed in a cold water bath and allowed to cool for 20 minutes and then washed in PBS for 2 minutes. Once sections were washed, a 1 % skim milk block was added and the sections were incubated for 20 minutes at room temperature in a humid chamber. The blocking solution was removed and the primary antibody was diluted in milk block at the following dilutions AR (1:100) and SGTA (ProteinTech, Chicago, USA) (1:1000). Primarily antibodies were added to the sections and then incubated overnight in a humid chamber at 4°C. Following overnight incubation the slides were washed 3 times in PBS for 5 minutes each. Primary antibody was detected using the Dako Envision LSAB system plus HRP kit according to the manufacturer's instructions. Briefly, the sections were incubated in secondary antibody solution for 30 minutes at room temperature in a humid chamber. The sections were washed once in PBS and then incubated in streptavidin solution for 30 minutes at room temperature in a humid chamber, and washed again in PBS

and then incubated in freshly prepared diaminobenzidine (DAB) solution for 8 minutes. The sections were washed in distilled water and then counterstained with Lillie Mayer's haematoxylin for 3 seconds and rinsed in tap water. The slides were dehydrated and cleared in ethanol and xylene, and PIX mounting medium was used to adhere coverslips onto the slides.

Immunohistochemistry staining for each antisera was quantified independently by Mr. Damian Leach and myself. The immunoreactivity for AR and SGTA was scored in a minimum of 3 independent fields in both BPH and cancer regions. An arbitrary score from 0-3 was used to determine the intensity of immunoreactivity for each antisera, whereby 0 = no staining and 3 = intense staining. The scores for each area were added to produce a representative scale ranging from 0-9 and statistics were performed on the score mean to determine differences in immunoreactivity between BPH and cancer regions.

6.2.7 Statistical analysis

The Wilcox rank sum test was used to determine a difference in medians across patient parameters at the time of follow up after diagnosis. The Wilcox rank sum test was also used to determine a difference between means for AR or SGTA immunoreactivity in BPH specimens compared to patient matched cancer samples. Two-way ANOVA was used to compare the difference in means for *in vitro* cell proliferation. Significance was confirmed at $p<0.05$.

6.3 Results

6.3.1 Knockdown of SGTA in C42B cells reduces cell proliferation

The results presented in chapter 5 demonstrated that knockdown of SGTA levels affected the expression of genes involved in key signalling pathways, such as PI3 kinase, which can influence cell proliferation. Therefore, we first assessed the functional effects of decreasing cellular levels of SGTA on prostate cancer cell proliferation. C42B cells were either mock transfected or transfected with a non specific (NS) or SGTA specific siRNA for 6 days in stripped serum. Immunoblot analysis demonstrated that expression of SGTA protein was depleted for the duration of the experiment (Figure 6.1C). However, the loss of SGTA did not affect cell viability (Figure 6.1A and B).

Although C42B cells are the androgen independent derivative of LNCaP cells, they remain responsive to hormone signals. Therefore, we examined the effect of SGTA knockdown on C42B cell proliferation in the presence of normal growth medium. Interestingly, the loss of SGTA significantly decreased C42B cell proliferation compared to both mock and NS transfected controls after a period of 6 days ($p<0.05$; Figure 6.2A). Immunoblot analysis demonstrated that SGTA protein levels were depleted throughout the duration of the experiment, while the percentage of dead cells remained relatively consistent across all treatment groups (Figure 6.2B and C). Collectively, these findings demonstrate that the effects of SGTA on cell proliferation are dependent on growth factors, in full serum. As the process of stripping serum removes many factors including steroid hormones, it is difficult to determine which ones may be important. Nevertheless, given the sensitivity of

C42B cells to androgens we can speculate that SGTA may act as an important mediator of androgen signalling, which contributes to the maintenance of cell proliferation. Indeed, the rate of growth of C42B cells in stripped serum appears to be severely retarded compared to those in normal serum (Figure 6.1A and Figure 6.2A). Thus, the depletion of androgens from the serum may mask the effects of SGTA knockdown on cell proliferation.

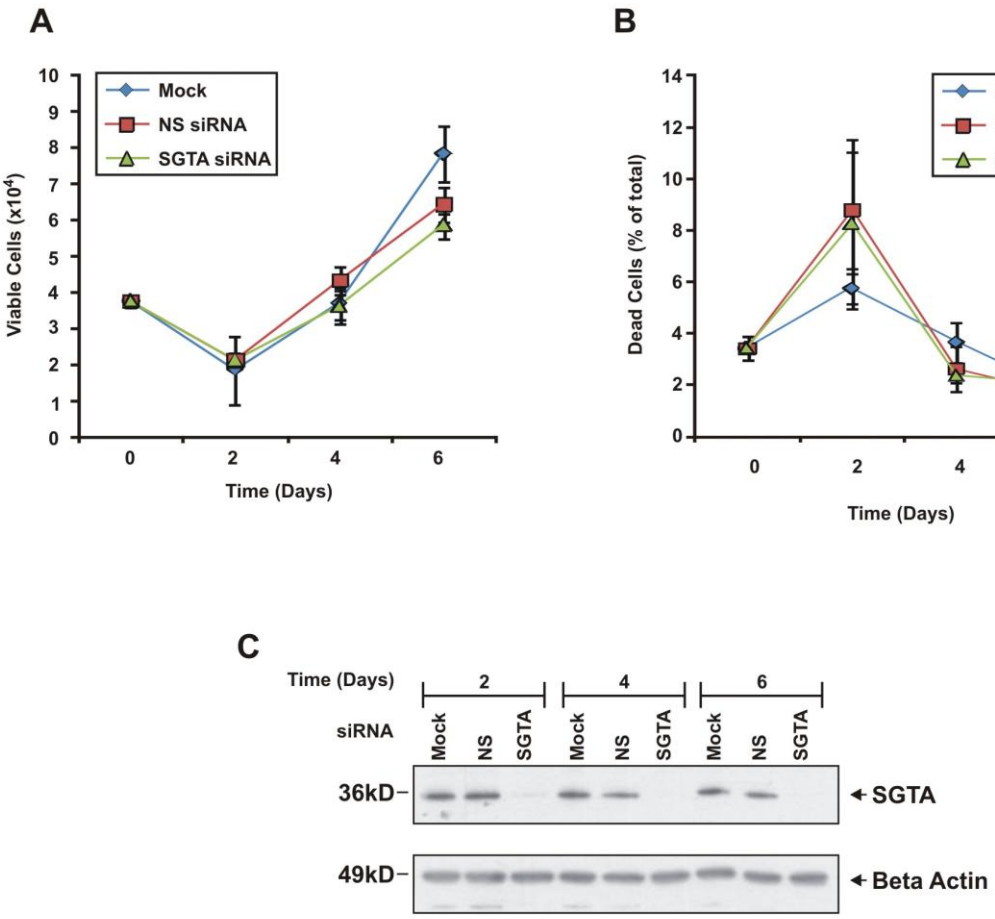

A
Viable Cells (x10⁴)
Time (Days)
Mock
NS siRNA
SGTA siRNA
B
Dead Cells (% of total)
Time (Days)
Mock
NS siRNA
SGTA siRNA
C
Time (Days)
2
4
6
siRNA
Mock
NS
SGTA
36kD
SGTA
49kD
Beta Actin

Figure 6.1: Knockdown of SGTA in C42B cells in stripped serum does not alter cell proliferation. A-B: C42B cells were either mock transfected or transfected with non specific (NS) siRNA or SGTA specific siRNA in serum free medium for 4 hours and then supplemented with 5% DCS-FBS. Cells were cultured for 6 days and counted every 2 days using a haemocytometer and cell viability was assessed by Trypan blue exclusion. The number of dead cells is expressed as a percentage of the total cells counted. Data is presented as the mean (±SEM) of triplicate wells in an experiment. Results are representative of 2 independent experiments. **C:** Cell lysates were collected after each count and analysed by immunoblot for SGTA protein levels. Beta actin was used as a loading control.

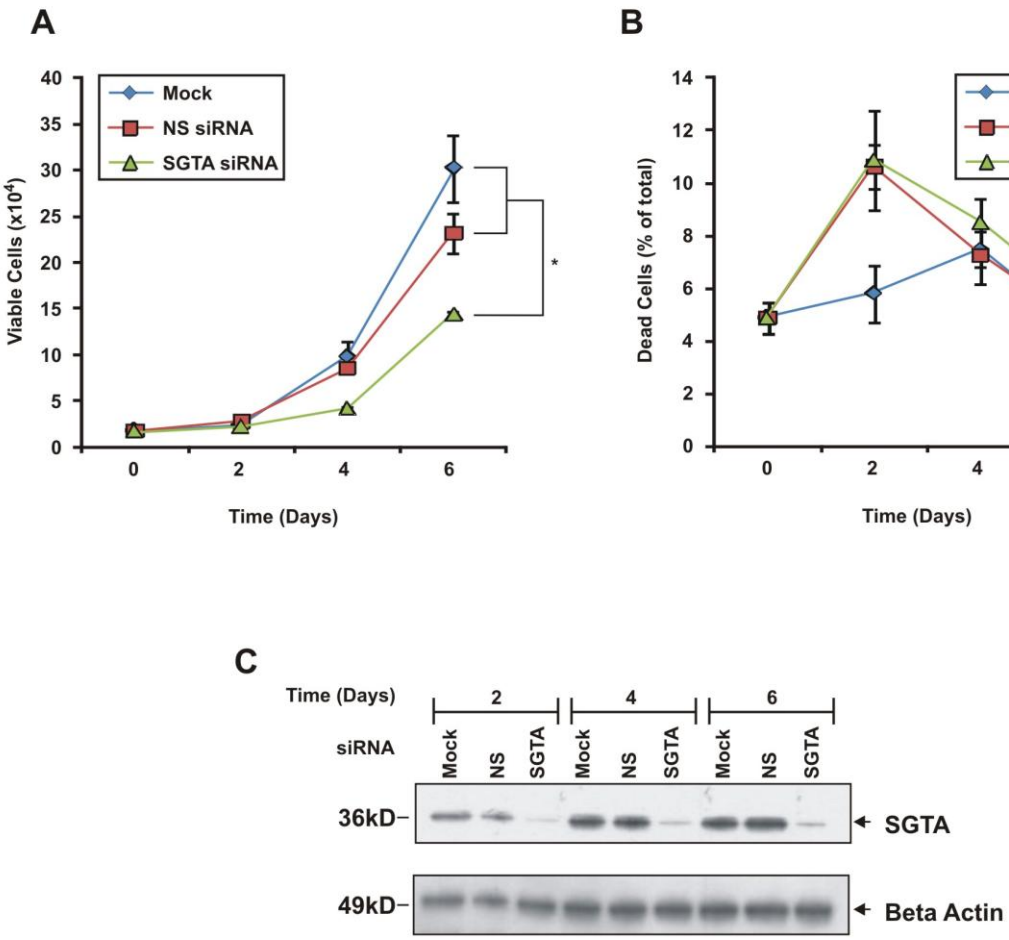

A
Mock
NS siRNA
SGTA siRNA
Viable Cells (x10⁴)
Time (Days)
*
B
Mock
NS siRNA
SGTA siRNA
Dead Cells (% of total)
Time (Days)
C
Time (Days)
2
4
6
siRNA
Mock
NS
SGTA
36kD
SGTA
49kD
Beta Actin

Figure 6.2: Knockdown of SGTA in C42B cells in normal serum reduces cell proliferation. A-B: C42B cells were either mock transfected or transfected with non specific (NS) siRNA or SGTA specific siRNA in serum free medium for 4 hours and then supplemented with 5% FBS. Cells were cultured for 6 days and counted every 2 days as described in Figure 6.1A-B. Data are presented as the mean (±SEM) of triplicate wells in an experiment. Results are representative of 2 independent experiments. Two-way ANOVA was used to determine the difference in cell growth between groups *, $p<0.05$ differences between mock/NS transfected cells versus SGTA siRNA. **C:** Cell lysates were collected after each count and analysed by immunoblot for SGTA protein levels. Beta actin was used as a loading control.

6.3.2 Stable SGTA over expression in LNCaP cells does not alter AR activity

Next, in order to determine if increasing the levels of SGTA protein levels also affects prostate cancer cell proliferation, two different LNCaP stable cell lines were developed to constitutively over express either HA tagged SGTA protein or an untagged SGTA that is jointly expressed with GFP (GFPiresSGTA). Immunoblot analysis was conducted on two independently generated LNCaP clones for each cell line, which demonstrated equal expression of HA-SGTA and GFPiresSGTA respectively (Figure 6.3A and B). Given that this thesis has demonstrated that over expression of SGTA inhibits AR signalling, we next investigated if HA-SGTA or GFPiresSGTA maintain a similar effect. Immunoblot analysis revealed that AR and PSA protein steady state levels remained constant either in the presence or absence of HA-SGTA or GFPiresSGTA (Figure 6.3A and B). GFPiresSGTA clone #2 cell lines appeared to have reduced AR and PSA protein levels, although immunoblot analysis of tubulin revealed unequal loading of this sample. Collectively, these results suggest that the level of SGTA expressed in these cells is not sufficient to inhibit AR activity.

6.3.3 Stably transfected LNCaP cells display reduced cell proliferation

The functional effects of SGTA over expression were then assessed on prostate cancer cell proliferation. Expression of either empty HA or HA-SGTA significantly reduced cell proliferation compared to parental LNCaP control cells over a period of 7 days ($p<0.05$; Figure 6.3C). Equally, HA-SGTA clone #2 cells grew at a significantly slower rate than to HA control or HA-SGTA clone #1 cells ($p<0.05$; Figure 6.3C). The difference in cell

growth observed between parental LNCaP and the stable cell line was not due to an increase in cell death (Figure 6.3D). These data indicate that only one of the two stable SGTA cell lines (HA-SGTA #2) was capable of affecting cell proliferation compared to HA control cells. However, the suppressed growth of the HA control cells compared to the parental LNCaP cell line may be suggestive that the expression of the HA tag induces cytotoxic effects. Consequently, it is difficult to draw conclusions of the specific effects of HA-SGTA expression on prostate cancer cell proliferation. Nevertheless, we used an alternative approach by using the GFPiresSGTA expression vector, which expresses an un-tagged SGTA and GFP protein from the same transcript.

Cell proliferation analysis showed that SGTA over expressing cells grew at a significantly slower rate compared to either parental or GFP control #2 LNCaP cell lines ($p<0.05$; Figure 6.3E). Additionally, these experiments demonstrated that the GFP only control cell lines also displayed a reduced rate of proliferation compared to the parental LNCaP controls. Although it has been previously documented that expression of GFP induces cell apoptosis (Liu, Jan et al. 1999), no difference in cell death was observed between the cell lines in this study (Figure 6.3F). Alternatively, the severely reduced growth rate of the GFP control #1 could be attributed to the integration of the GFP vector in a region of chromatin that is required for cell proliferation. These results suggest that while SGTA may reduce prostate cancer cell proliferation *in vitro*, the potential cytotoxic effects of either the HA or GFP tags may also act as a contributing factor.

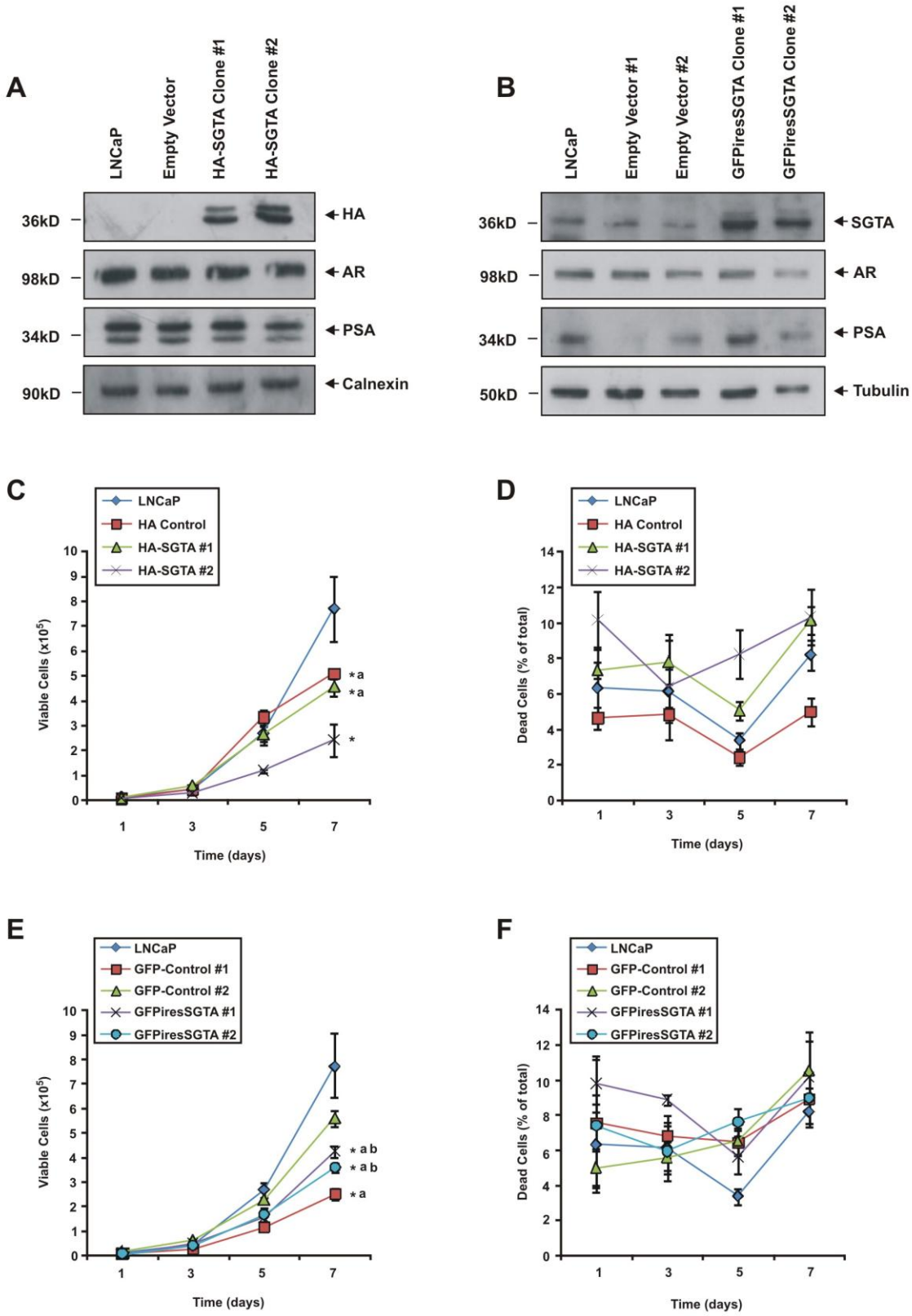

A
LNCaP
Empty Vector
HA-SGTA Clone #1
HA-SGTA Clone #2
36kD
98kD
34kD
90kD
HA
AR
PSA
Calnexin
B
LNCaP
Empty Vector #1
Empty Vector #2
GFPiresSGTA Clone #1
GFPiresSGTA Clone #2
36kD
98kD
34kD
50kD
SGTA
AR
PSA
Tubulin
C
LNCaP
HA Control
HA-SGTA #1
HA-SGTA #2
Viable Cells (x10^5)
Time (days)
*a
*a
*
D
LNCaP
HA Control
HA-SGTA #1
HA-SGTA #2
Dead Cells (% of total)
Time (days)
E
LNCaP
GFP-Control #1
GFP-Control #2
GFPiresSGTA #1
GFPiresSGTA #2
Viable Cells (x10^5)
Time (days)
* a b
* a b
* a
F
LNCaP
GFP-Control #1
GFP-Control #2
GFPiresSGTA #1
GFPiresSGTA #2
Dead Cells (% of total)
Time (days)

Figure 6.3 Validation of stable SGTA over-expressing LNCaP cells and its effects on cell proliferation. A: Cell lysates were harvested from parental LNCaP cells, or cells stably transfected with either empty HA or HA tagged SGTA expression plasmid. Immunoblot analysis of SGTA protein levels was conducted using HA antisera, while AR and PSA steady state levels were also analysed. Calnexin was used as a loading control. **B:** Lysates were harvested from parental LNCaP cells or from cells that were stably transfected with either empty green fluorescent protein (GFP) or GFPiresSGTA expression plasmids. Immunoblot was used to analyse the protein steady state levels of SGTA, AR and PSA, while tubulin was used as a loading control. All immunoblots were performed by Ms Elisa Cops. **C-D:** LNCaP cells stably transfected with empty HA or HA tagged SGTA were cultured in fresh growth medium for 7 days. Cells were counted every 2 days using a haemocytometer and cell viability was assessed by Trypan blue exclusion. The number of dead cells is expressed as a percentage of the total cells counted. Data is presented as the means (±SEM) of triplicate wells in an experiment. Results are representative of 2 independent experiments. Two-way ANOVA was used to determine differences in cell growth between groups over 7 days. *****; $p<0.05$ differences between parental LNCaP cells *versus* HA control, HA-SGTA #1 and HA-SGTA #2 cells. **a;** $p<0.05$ differences between HA-SGTA #2 cells *versus* HA control and HA-SGTA #1 cells. **E-F:** LNCaP cells stably transfected with empty GFP or GFPiresSGTA were cultured in fresh growth medium for 7 days. Cells were counted as described for A-B. Data is presented as the means (±SEM) of triplicate wells in an experiment. Results are representative of 2 independent experiments. Two-way ANOVA analysed difference in cell growth between groups over 7 days. *****; $p<0.05$ differences between parental LNCaP cells *versus* GFP control #1, GFPiresSGTA

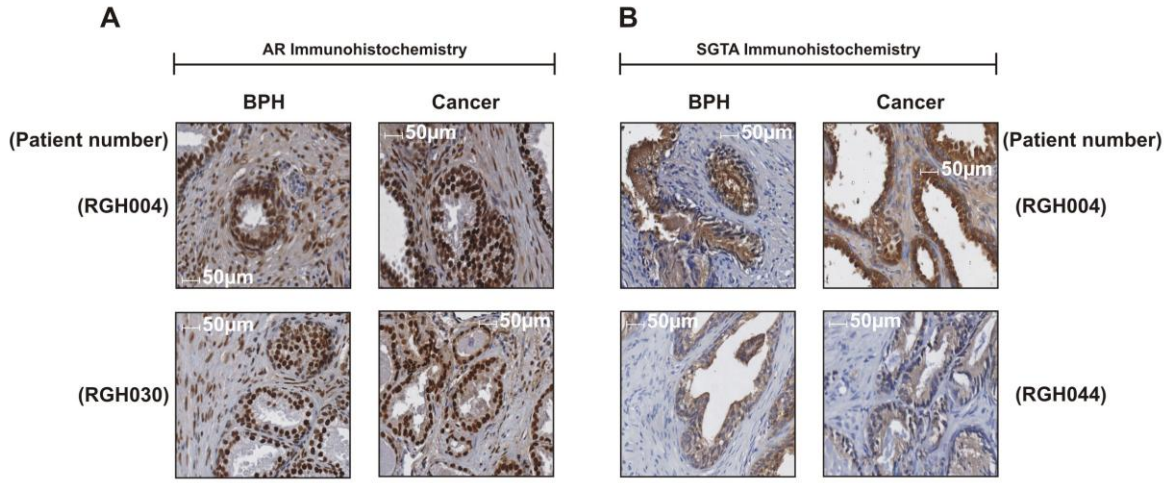
#1 and GFPiresSGTA #2 cells. **a**; $p<0.05$ differences between GFP control #2 cells *versus* GFPiresSGTA #1, GFPiresSGTA #2 and GFP control #1 cells. **b**; $p<0.05$ differences between GFP control #2 cells *versus* GFPiresSGTA #1 and GFPiresSGTA #2 cells. All cell viability assays were performed by Dr. Jeffrey Barrett.

6.3.4 Expression of AR and SGTA does not change in patient matched BPH and prostate cancer samples.

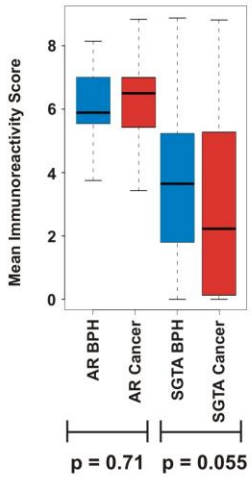
The data presented so far in this chapter suggests that the relative level of SGTA plays a biologically important role in prostate cancer proliferation. Together with the evidence from our previous study that demonstrated a decrease in SGTA levels with prostate cancer progression (Buchanan, Ricciardelli et al. 2007), these data imply that SGTA may be a clinically relevant marker of either AR activity and/or the ability of prostate cancer cells to proliferate in an androgen depleted environment. However, one of the limitations of the cohort from our latter study was the lack of clinical outcome data. Therefore, in order to further assess the clinical significance of SGTA in prostate cancer, a pilot study was conducted in this thesis to investigate the levels of AR and SGTA with Gleason grade, PSA levels and survival from a cohort of 66 different clinical samples of patient matched benign prostatic hyperplasia (BPH) and incidental prostate cancer.

Immunohistochemistry analysis of incidental prostate cancer samples demonstrated that AR protein is predominately localised in the nucleus of luminal epithelial and stromal cells of both BPH and prostate cancer samples (Figure 6.4A). In agreement with the observations from our previous study, the expression of SGTA was mainly confined to the cytoplasm of luminal epithelial cells, although SGTA protein was detected in the stroma of some cancer samples (Figure 6.4B). Analysis of AR and SGTA immunoreactivity revealed that AR expression was slightly higher in cancer samples compared to BPH, while the overall level of SGTA expression was lower in cancerous regions compared to benign (Figure 6.4C), although these data did not reach significance (p=0.055). Analysis of the

follow-up patient data revealed no significant differences between patient age or PSA levels with survival, whereas a significantly higher Gleason grade was recorded in those patients who died from their disease compared to those who are still alive ($p<0.0007$; Figure 6.4D). No correlation was observed between either AR or SGTA levels and survival, nor was there any difference in the AR:SGTA ratio in patient matched BPH and cancer samples (Figure 6.4D). Collectively, these findings demonstrate that SGTA levels tended to be lower in cancerous regions compared to non-malignant tissue, which remains consistent with our previous study. Although no significant difference was observed between SGTA levels and any of the outcome data, it remains plausible that a decrease in SGTA levels in prostate cancer cells may impact on AR activity and affect cell proliferation, however further analysis on a greater number of samples is required.



C



D

					Minimum and Maximum ranges for each parameter					
Parameters	Median all Patients	Median Alive	Median Dead	p value	Min all patients	Max all patients	Min Alive	Max Alive	Min Dead	Max Dead
Age	86.5	86	88.5	0.185	60	100	67	98	60	100
Gleason Grade	8	7	9	0.0007	4	10	4	10	7	10
PSA (mg/ml)	16.5	22.4	16.1	0.721	0.5	83.00	0.5	83.00	0.9	26.17
AR BPH	5.89	6.3	5.86	0.489	3.17	8.14	3.17	8.14	3.75	7.4
AR CaP	6.5	6.5	6.36	0.477	0.67	8.83	3.43	8.14	0.67	8.83
SGTA BPH	3.65	4.03	3.5	0.590	0	8.88	0	8.88	0.5	7
SGTA CaP	2.23	2.42	1.56	0.721	0	8.83	0	8.83	0	7.31
BPH ratio	1.56	1.54	1.54	0.553	0.636	36.57	0.794	36.57	0.821	11.4
Cancer ratio	1.90	1.84	2.98	0.793	0.794	122.14	0.636	122.14	0.848	86.9

Figure 6.4: Expression of AR and SGTA in patient matched clinical samples of BPH and prostate cancer. A-B: Immunohistochemistry with SGTA or AR antisera. Two examples of AR and SGTA expression in patient matched benign prostatic hyperplasia (BPH) and prostate cancer samples. Patient samples RGH004 and RGH030 were stained for AR, while patient samples RGH004 and RGH044 were stained for SGTA. All images are at 40x magnification. **C:** Immunoreactivity of each antisera was scored in a minimum of 3 independent fields by two researchers in both BPH and cancer regions. The scores were collapsed into a representative scale ranging from 0-9. Box plots represent the mean AR and SGTA immunoreactivity score. Wilcox ranked sum statistics were used to determine differences of the AR and SGTA mean immunoreactivity score between BPH and cancer samples respectively. **D:** Table represents patient follow-up data collected at the RGH. Median age, Gleason grade, PSA levels and AR and SGTA immunoreactivity scores in BPH and cancer samples were recorded. BPH and cancer ratios represent the mean AR:SGTA pair wise ratio for patient matched BPH and cancer sample respectively. Minimum and maximum ranges for all parameters are also presented. Wilcox rank sum test was used to determine the difference in medians or means between alive and dead patients for each parameter.

6.4 Discussion

The process of prostate cancer cell proliferation is dependent on many intracellular proteins, but none more so than the AR. Understanding the mechanisms that control AR signalling is essential in determining how it regulates the cell cycle and promotes prostate cancer cell proliferation and survival. The role of the molecular chaperone system as a regulator of AR activity in prostate cancer is evident through *in vitro* and *in vivo* experiments that utilise Hsp90 inhibitors such as 17-AAG, which collectively demonstrate a reduction in both AR activity and cancer cell growth (Saporita, Ai et al. 2007; Williams, Tabios et al. 2007). Meanwhile, the role of the TPR co-chaperones FKBP51, FKBP52 and Cyp40 as modulators of AR ligand binding affinity, subcellular localisation and transcriptional activity appears to be of significant importance for maintenance of prostate cancer cell proliferation (Periyasamy, Warrier et al. 2007; Ni, Yang et al. 2010; Periyasamy, Hinds et al. 2010). Given the failure of several Hsp90 inhibitors in clinical trials (Trepel, Mollapour et al. 2010), the TPR co-chaperones have been identified as a possible alternative means of either targeting the AR or improving the efficacy of Hsp90 inhibitors. Indeed, several studies have already used selective inhibitors to demonstrate that these TPR proteins can be used as a direct means of inhibiting AR activity and preventing prostate cancer proliferation (Periyasamy, Warrier et al. 2007; Periyasamy, Hinds et al. 2010; Trepel, Mollapour et al. 2010; Horibe, Kohno et al. 2011).

Considering the inhibitory effects of SGTA over expression on AR signalling, this study investigated the functional consequences of altered SGTA protein levels on prostate cancer cell proliferation. While expression of both HA and GFPiresSGTA appeared to have

reduced LNCaP cell proliferation *in vitro*, the empty HA and GFP control vectors also displayed a very predominant effect on cell viability. At this stage there are two plausible reasons for this observation i) that expression of the HA and GFP tags exhibit a cytotoxic effect on LNCaP cells, a phenomenon that has been previously documented for other cell lines (Hall, Young et al. 2002; Holzbeierlein, Lal et al. 2004) and/or ii) the HA and GFP vectors integrated into regions of chromatin that are critical for cell proliferation. Despite many laboratories successfully creating stable cell lines that express tagged proteins, it is clear that both of these tags may pose significant limitations on the interpretation of the impact SGTA has on cell proliferation. Nonetheless, several studies have successfully utilised cell lines that over express TPR co-chaperones as a means of gaining greater insight of the effects of TPR proteins on client protein activity, the efficacy of drug compounds and the impact of TPR co-chaperones on cell viability (Urban, Golden et al. 2001; Shirane and Nakayama 2003; Febbo, Lowenberg et al. 2005; Pei, Li et al. 2009; Chambraud, Sardin et al. 2010; Ni, Yang et al. 2010). Therefore, future studies that utilise a stable cell line that exclusively expresses an untagged SGTA and no other protein will be useful to further understanding the biological importance of SGTA to prostate cancer physiology.

Regardless of the complications posed by the SGTA over expression experiments, the role of SGTA in cell proliferation was evaluated in this thesis by SGTA knockdown. Interestingly, the findings presented in this chapter demonstrate that knockdown of SGTA reduces cell proliferation only in the presence of full serum. While the C42B cells used in this study remain sensitive to androgen signalling, they also have the ability to maintain

cell growth in an androgen depleted environment, albeit at a greatly reduced rate compared to cells grown in normal serum (Liu, Brubaker et al. 2004). Therefore, the lack of an effect by SGTA knockdown on C42B cell proliferation in stripped serum is most likely to be an artefact of severe growth suppression. Taken together, these results imply that SGTA may potentially play a homeostatic role in maintaining the integrity of intracellular signalling pathways. As the presence of androgens in the serum is likely to provide a potent signal to the cell, one might speculate that the loss of SGTA may act to disrupt AR signalling, which results in a reduction in cell growth. However, it is difficult to discount the contribution of other growth factors present in the serum to prostate cancer cell proliferation. Alternatively, as both the SGTA over expression and knockdown data suggests that SGTA plays an anti-proliferative role in prostate cancer cells, it is possible that a balanced level of SGTA protein is required to prevent the negative effects on cellular proliferation.

Aside from the data presented in chapter 5 of this thesis, the underlying mechanism for SGTA mediated cell proliferation has been previously investigated in two independent cell lines revealed that SGTA knockdown resulted in mitotic arrest and cell death (Winnefeld, Rommelaere et al. 2004; Winnefeld, Grewenig et al. 2006). Those studies demonstrate that although SGTA steady state protein levels are maintained during all stages of the cell cycle, cells depleted of SGTA begin to arrest during the transition from prometaphase into metaphase (Winnefeld, Rommelaere et al. 2004). Mechanistically, it appears that cell arrest is a consequence of a misalignment of at least 2-3 chromosomes located close to the spindle poles during metaphase, implicating SGTA acts as a limiting factor of the spindle

assembly checkpoint and progression into anaphase (Winnefeld, Rommelaere et al. 2004; Winnefeld, Grewenig et al. 2006). Furthermore, an interaction was detected between SGTA, Hsc70, Hsp70 and the cytosolic complex Bag6/Bat3 at the spindle poles during prometaphase, suggesting the incorporation of SGTA into this complex is essential for the progress of the cell cycle (Winnefeld, Grewenig et al. 2006). Given these previous findings, a similar mechanism may explain how an alteration in SGTA levels reduces cell proliferation in prostate cancer cells. It is possible that the interaction between SGTA and Hsc/Hsp70 is vital for the efficacy of intracellular signalling pathways critical to cell proliferation. Therefore, depletion or over expression of SGTA may compromise the cell's ability to correctly process the growth promoting signals received from the extracellular environment, thereby resulting in a reduction in cell proliferation. Given the potential for SGTA to modulate multiple signalling pathways, further understanding the biological role of SGTA in prostate cancer cells may underscore the important benefits of utilising SGTA as a novel therapeutic target.

The regulatory ability of SGTA to restrain the AR in the cytoplasm and thereby reducing its transcriptional activity signifies SGTA as a potentially important intracellular marker of AR signalling and prostate cancer outcomes, such as cell proliferation and progression. In this chapter, we conducted a pilot study that investigated the clinical significance of SGTA expression in a cohort of patient matched BPH and incidental prostate cancer samples. Despite reports that have dismissed incidental prostate cancer as an indolent form of the disease and therefore should remain untreated (Cantrell, DeKlerk et al. 1981), a recent study has documented that incidental tumours represent a clinically important subset of

prostate cancers as approximately 27% of men with incidental prostate cancer will die from their disease (Andren, Garmo et al. 2009). The re-evaluation of incidental prostate cancer suggests that it represents a clinically significant subset of the disease. The findings presented in this chapter demonstrated that while SGTA levels tended to be lower in cancer related samples compared to benign regions, there was no correlation between SGTA levels and patient outcomes. Taken together with the results from our previous study, these findings suggest that SGTA expression is lost in range of different prostate cancer subtypes and implies that SGTA levels and prostate cancer incidence and progression may be inversely related. Future studies involving a larger number of samples would be required to definitively determine if SGTA levels do indeed correlate with disease outcomes.

In summary, while further optimisation is required to accurately assess the effects of SGTA over expression on prostate cancer cell proliferation *in vitro*, these studies suggest that SGTA may play an important homeostatic role in regulating cell proliferation. Additionally, this study provides evidence that knockdown of SGTA in the presence of full serum is able reduce prostate cancer cell proliferation, suggesting that SGTA may act as a mediator of intracellular signalling that promotes cell proliferation. Collectively, these findings imply that SGTA plays an anti-proliferative role and that there appears to be an inherent level of SGTA that is important to maintain normal cell proliferation. Therefore, SGTA remains a novel therapeutic target as an effective means of disrupting either AR or other signalling pathways critical for prostate cancer cell proliferation. This provides a

basis for further investigations into the mechanisms of how SGTA may affect prostate cancer cell proliferation.

CHAPTER 7

General Discussion

Chapter 7: General Discussion

Molecular chaperone complexes that incorporate tetratricopeptide repeat (TPR) containing co-chaperone proteins are potentially critical regulators of AR signalling in prostate cancer. One of these TPR proteins, SGTA, has been reported to inhibit AR activity by retaining the receptor in the cytoplasm (Buchanan, Ricciardelli et al. 2007). In clinical samples of metastatic prostate cancer, SGTA levels are lower compared to non-malignant tissue. Together, these data suggest that the loss of SGTA may contribute to continued AR activity in castrate resistant prostate cancer. However, many aspects of the biological actions of SGTA in prostate cancer cells are unknown. This thesis examined the key regions of SGTA required for its inhibitory effects on AR activity, with a specific emphasis on the nature and contribution of SGTA homodimerisation to overall AR signalling. Additionally, this thesis explored more broadly the biological effects of SGTA action on the transcription profile of prostate cancer cells, and the functional implications this might have on cell proliferation.

7.1 Major Findings of this thesis

7.1.1 Characterisation of the SGTA homodimerisation domain and its effects on AR activity.

The findings in thesis indicate that structural elements within the first 80 amino acids of SGTA are not only required for the formation of SGTA homodimers, but also provide stability to the overall protein structure. Importantly, this thesis demonstrates that the

SGTA homodimerisation domain is not essential for the inhibitory effects on AR activity. Given the similarities between these results and previous studies, which also showed SGTA homodimerisation is not required for client protein function (Liu, Wu et al. 1999; Angeletti, Walker et al. 2002; Liou and Wang 2005), it appears that the most likely role for SGTA homodimerisation is to provide additional stability of the SGTA structure. However, more broadly the requirement of SGTA homodimerisation may be to enable maximal interaction between SGTA and its client proteins, such as the human growth hormone receptor (Schantl, Roza et al. 2003), without directly affecting client protein activity.

7.1.2 The linker region of SGTA is required for its inhibitory effects on AR activity

Further studies undertaken in this thesis to delineate the regions of SGTA required for an effect on AR activity identified the linker region that separates the central TPR domain from the glutamine-rich carboxyl terminus as necessary. As previous studies have identified the SGTA TPR domain as the major determinant of protein-protein interactions and/or the regulation of client protein activity (Liu, Wu et al. 1999; Angeletti, Walker et al. 2002; Schantl, Roza et al. 2003; Liou and Wang 2005), this thesis provides the first evidence that the mechanism of SGTA action on AR is independent of its TPR domain. Consequently, these findings challenge our previously proposed model that the inhibitory effects of SGTA are mediated by the TPR domain interacting with the AR hinge region (Buchanan, Ricciardelli et al. 2007). Rather, it appears that the SGTA linker region may provide the necessary structural elements required for the biological effects of

SGTA on AR transactivation activity. A role for the SGTA linker region is supported by reports that demonstrate that the analogous region in Cyp40 is required for the interaction between the Cyp40 TPR domain and Hsp90 as well as its chaperone/protein folding capabilities (Ratajczak and Carrello 1996; Mok, Allan et al. 2006). Therefore, a similar mechanism may exist for SGTA, whereby SGTA utilises amino acid residues flanking the TPR domain and linker region to enable the TPR domain to interact with Hsp90, while the linker region forms a complex with the AR. Given the transient or weak interaction between SGTA and Hsp90 (Angeletti, Walker et al. 2002; Winnefeld, Grewenig et al. 2006), a stable interaction between the SGTA linker region and the AR may be essential in order to maintain the inhibitory effects of SGTA on AR activity. Although the actions of SGTA remain consistent with the effects of other TPR co-chaperones on AR signalling (Schulke, Wochnik et al. 2010), the discovery of the predominant effects of the SGTA linker region on AR activity distinguishes SGTA from the actions of FKBP51, FKBP52 and PP5, which use their TPR domains as the dominant mode of interaction with Hsp90-steroid receptor complexes (Barent, Nair et al. 1998; Das, Cohen et al. 1998; Sinars, Cheung-Flynn et al. 2003). Therefore, targeting the SGTA linker region may have the potential to select for SGTA-AR complexes over other TPR proteins in order to disrupt AR signalling in prostate cancer.

7.1.3 SGTA acts to restrain the sensitivity of AR activity in prostate cancer cells.

This thesis demonstrated that SGTA inhibits AR activity across an extensive set of native androgenic responsive loci. Specifically, SGTA constrained the sensitivity of AR

responses by inhibiting the majority of AR activity at ligand concentrations of 0.1 nM DHT or lower, which represents a sub-physiological ligand concentration in prostate tissue (Salerno, Moneti et al. 1988), which would result in approximately 50% of AR molecules being ligand bound (Wilson and French 1976). However, following androgen deprivation therapy, intracellular ligand concentrations will be reduced to a level that allows the inhibitory effects of SGTA to become more pronounced such that SGTA further excludes the AR from the nucleus (Locke, Guns et al. 2008). Importantly, several recent reports suggest that intracellular ligand conversion of adrenal androgens and *de novo* androgen synthesis in prostate cancer compared to normal cells significantly contributes to continued AR activity during the progression of a castrate resistant state (Montgomery, Mostaghel et al. 2008; Knudsen and Penning 2010). In this context, the accumulation of intracellular androgens above the 0.1 nM concentration threshold would be predicted to override the SGTA effect, while also complementing the lower levels of SGTA in prostate cancer cells to favour continued AR signalling in a castrate environment (Scher, Buchanan et al. 2004; Scher and Sawyers 2005; Hendriksen, Dits et al. 2006; Buchanan, Ricciardelli et al. 2007; Chmelar, Buchanan et al. 2007; Wang, Li et al. 2009). Therefore, by either increasing the level of SGTA, as shown in this thesis, or modulating the interaction of SGTA with AR in prostate cancer cells, it may be possible to control the sensitivity of AR activity in an androgen deprived environment. However, validation of this system would require further investigations in both *in vitro* and *in vivo* models of prostate cancer.

7.1.4 SGTA acts as a regulator of intracellular signalling pathways critical for prostate cancer cell proliferation

The results presented in chapter 6 of this thesis indicate that both SGTA protein over expression and knockdown were sufficient to reduce cell proliferation, implying that the relative balance of SGTA and AR levels within a cell, rather than their absolute levels, are important for cell proliferation. Indeed, several lines of evidence from previous studies have implicated SGTA in the maintenance of cell cycle checkpoints and chromosomal positioning during metaphase (Winnefeld, Rommelaere et al. 2004; Winnefeld, Grewenig et al. 2006). Any alteration in the levels of SGTA might be sufficient to disrupt these biological processes. In addition, studies conducted in this thesis demonstrated that long term depletion of cellular SGTA alters the transcriptional profile of prostate cancer cells that includes the regulation of genes within key signalling pathways, such as p53 and several members of the Class IA PI3 kinase family. In addition, the data presented in chapter 5 indicate that SGTA has a direct effect on both the basal and androgen dependent expression of a subset of AR regulated genes, which further implicates SGTA as a modulator of androgen signalling. This suggests that the SGTA mediated suppression of these genes may be important in normal prostate physiology that is disrupted when SGTA expression is lost in metastatic disease, but further studies would be needed to confirm this.

Collectively, the above findings imply that SGTA may act to modulate both androgen and PI3 kinase signalling in prostate cancer and that the loss of SGTA with prostate cancer progression to metastatic disease may have repercussions on the activity of these pathways. Androgen and PI3 kinase signalling represent two of the most active pathways in

prostate cancer, and a recent study has demonstrated that both of these pathways regulate each other via a reciprocal negative feedback mechanism, whereby the inhibition of one pathway activates the other (Carver, Chapinski et al. 2011). In this context, the loss of SGTA expression during the progression of prostate cancer, may act to restrict PI3 kinase signalling and reinforce a specific AR transcriptional program. Future investigations may decipher the precise mechanistic effect of SGTA on PI3 kinase signalling and their role in prostate cancer.

7.2 Future Directions

7.2.1 Identifying the regions of SGTA that determine AR cytoplasmic retention

The current study identified regions of SGTA that are able to influence AR activity, but further investigations are necessary to understand the involvement of these regions in the modulation of AR subcellular localisation and gene mediated transcriptional responses. While multiple *in vitro* techniques, such as co-immunoprecipitation and affinity chromatography have been previously utilised to identify the domains of proteins that are involved in these interactions, these systems do not provide any information on the spatial and temporal organisation of these proteins in a cellular system. Therefore, future studies that utilise fluorescence resonance energy transfer (FRET) technology might be able to map the regions required for interaction between SGTA and AR *in vivo*. In addition, FRET technology can be readily combined with fluorescence lifetime imaging microscopy (FLIM) techniques, which would allow investigations on the subcellular localisation of

both AR and SGTA to be tracked within a cell in real time. As this thesis identified the SGTA linker region as being necessary for the inhibitory effects of SGTA on AR activity, further characterising the amino acids encompassing this domain will be an important next step in understanding the mechanisms of SGTA action.

7.2.2 Identification of SGTA client proteins in prostate cancer

To more precisely define the biological actions of SGTA in prostate cancer cells, it remains important to determine the overall complement of SGTA client proteins. Several studies have previously attempted to identify SGTA client proteins either through yeast two-hybrid screens or affinity chromatography combined with mass spectrometry (Schantl, Roza et al. 2003; Liou and Wang 2005; Winnefeld, Grewenig et al. 2006). However, these approaches include the limited capacity to capture weak or transient protein-protein interactions with high dissociation constants. To overcome some of these issues, it has been proposed that protein-protein crosslinking, followed by immunoaffinity chromatography and tandem mass spectrometry offers a unique approach to identify SGTA protein interactions *in vivo* under a range of different physiological conditions (Vasilescu, Guo et al. 2004). The utilisation of stable cells lines expressing the different SGTA deletion variants presented in this thesis will also provide an ideal platform to define the specific requirement of each of the different SGTA domains for interaction with client proteins and activity.

7.2.3 Further investigations into the effects of SGTA on PI3 kinase signalling in prostate cancer

One of the most novel findings in this thesis was the potential for SGTA to modulate PI3 kinase signalling. A recent study has demonstrated that both the AR and PI3 kinase pathways in prostate cancer regulate each other by reciprocal negative feedback mechanisms (Carver, Chapinski et al. 2011). Critically, the combinatorial inhibition of both AR and PI3 kinase signalling pathways acts to profoundly reduce tumour growth (Carver, Chapinski et al. 2011). This thesis presents a case where the loss of SGTA in prostate cancer cells converges on both androgen signalling and PI3 kinase/Akt activity, which may then influence the ability of the cell to proliferate. Future studies that determine the prolonged effects of SGTA knockdown on both the androgen and PI3 kinase pathways could utilise stable cell lines that produce an SGTA specific small hairpin RNA (shRNA) under the control of an inducible promoter. Importantly, that system would enable high-throughput analysis of the functional effects of SGTA knockdown on the maintenance of the cell cycle, cell proliferation and survival of prostate cancer cells both *in vitro* and *in vivo*. The LNCaP xenograft model presented in this thesis has been established in our laboratory as means of investigating the potential of therapeutic agents (Gleave, Tolcher et al. 1999; Cheng, Snoek et al. 2006). The introduction of the stable SGTA knockdown cells as a xenograft model could be initially used to evaluate the effects of SGTA on tumour growth and AR function in a castrate and non-castrate environment.

7.3 Summary & Conclusions

The work completed for this thesis has provided novel insights into the mechanism of SGTA action in prostate cancer cells. Importantly, the findings presented here have defined the SGTA linker region as being necessary for the inhibitory effects of SGTA on AR activity, which implies that SGTA utilises the linker region instead of its TPR domain as a means of incorporating into Hsp90-AR complexes. By identifying the SGTA linker region as the critical mediator for the inhibitory effects of SGTA on AR action, this thesis has differentiated the molecular actions of SGTA from other AR associated TPR containing co-chaperones, which subsequently may allow for the specific targeting of SGTA-AR complexes as a means of disrupting AR activity in prostate cancer cells. This extensive examination of SGTA has also revealed that this chaperone is able to fine tune the sensitivity of AR transcriptional activity, which suggests that SGTA acts as a buffer of hypersensitive AR responses that may occur in an androgen depleted environment. Through studying SGTA, this thesis has also provided new information into the biological actions of SGTA in prostate cancer cells, in particular the convergence of SGTA on multiple oncogenic pathways that are essential to prostate cancer cell proliferation and possibly cancer progression. The results generated in this thesis provide a framework for future investigations that look at the underlying molecular mechanisms of SGTA action on intracellular signalling pathways *in vivo*, utilising SGTA as a means of controlling both the specificity and magnitude of both AR and PI3 kinase signalling in prostate cancer cells may be well worth investigating.

Appendices

Appendix A: Primers and PCR conditions

Appendix A1: Cloning primers
Chapter 3:

Construct Name	Sense Primer Name – Sequence (5' to 3')	Antisense Primer Name – Sequence (5' to 3')	PCR conditions (°C/seconds)	Restriction Endonuclease
pM-SGTA Δ1-20	SGTdel1-20s GTATCGCCGGAATTCCACGGGGGGCCTCTCG	SGTdel1-20as CGAGAGGCCCCCGTGGAATTCCGGCGATAC	96/300 then [96/20, 66/30,72/120] 40 times	*XhoI/SacI*
PCR product from above	pMS2 -AGGTCTCCGCTGACTAGGGCACATCTGA	SGT188as GTCCAGCTCCAGAGCCTTCTTGTAGTAAGC	96/300 then [96/20, 65/30,72/120] 40 times	
pM-SGTA Δ21-40	SGTdel21-40s - ACCAGCTCCGGACTGCGTTTGGGGTGACG	SGTdel21-40as ACCCCAAACGCAGTCCGGAGCTGGTCATGCAG GAA	96/300 then [96/20, 66/30,72/120] 40 times	*XhoI/SacI*
PCR product from above	pMS2 AGGTCTCCGCTGACTAGGGCACATCTGA	SGT188as GTCCAGCTCCAGAGCCTTCTTGTAGTAAGC	96/300 then [96/20, 65/30,72/120] 40 times	
pM-SGTA Δ41-60	SGTdel41-60s GTCGCCATCCAGTGCCTGGAGATATTTGAAGCG GCTGCCACG	SGTdel41-60as CGTGGCAGCCGCTTCAAATATCTCCAGGCACT GGATGGCGAC	96/300 then [96/20, 66/30,72/120] 40 times	*XhoI/SacI*
PCR product from above	pMS2 AGGTCTCCGCTGACTAGGGCACATCTGA	SGT188as GTCCAGCTCCAGAGCCTTCTTGTAGTAAGC	96/300 then [96/20, 65/30,72/120] 40 times	
pM-SGTA Δ61-80	SGTdel61-80s CTCCCTCAGACTCTGCCGGAGACCCCGCCTTCC GAGGAGGAC	SGTdel61-80as GTCCTCCTCGGAAGGCGGGGTCTCCGGCAGAG TCTGAGGGCG	96/300 then [96/20, 66/30,72/120] 40 times	*XhoI/SacI*

PCR product from above	pMS2 AGGTCTCCGCTGACTAGGGCACATCTGA	SGT188as GTCCAGCTCCAGAGCCTTCTTGTAGTAAGC	96/300 then [96/20, 65/30,72/120] 40 times	
pM-SGTA Δ29-33	SGTdel29-33s - TCCGATGCTGTCGCCATCCAGT	SGTAdel29-33as ACTGGATGGCGACAGCATCGGA	96/300 then [96/20, 65/30,72/120] 40 times	*XhoI/SacI*
PCR product from above	pMS2 AGGTCTCCGCTGACTAGGGCACATCTGA	SGT188as GTCCAGCTCCAGAGCCTTCTTGTAGTAAGC	96/300 then [96/20, 65/30,72/120] 40 times	
pM-SGTA S31P	SGTAS31PF GCTCAGGAGCCCTTGGAAGTCGCCATCCAGTGC CTG	SGTAS31PR GGCGACTTCCAAGGGCTCCTGAGCATCGGACG	94/180 then [94/60, 52/60, 78/720] 12 times then 68/3600	-
pM-SGTA S31T	SGTA S31TF GCTCAGGAGACCTTGGAAGTCGCCATCCAGTGC CTG	SGTAS31TR- GGCCTGTTCCAAGGTCTCCTGAGCATCGGACG	94/180 then [94/60, 52/60, 71/720] 12 times then 68/3600	-
pcH	pCHs AATTCGCCGCCACCATGGAATACCCATACGATG TTCCTGACTATGCGGCGGCCGCTT	pCHas CTAGAAGCGGCCGCCGCATAGTCAGGAACATC GTATGGGTATTCCATGGTGGCGGC	-	*EcoRI /XbaI*
pcF	pcFs AATTCGCCGCCACCATGGAAGATTATAAAGATG ATGATGATAAAGCGGCCGCTTCTAGAG	pCFas GATCCTCTAGAAGCGGCCGCTTTATCATCATCA TCTTTATAATCTTCCATGGTGGCGGC	-	*EcoRI/BamHI*
pcFH-SGTA 1-80	pcFHs AATTAATACGACTCACTATAGGG	PcFHSGT1-80as GACTGGATCCTCGCGCGGGGCTCCTCA	96/300 then [96/20, 60/30,72/120] 40 times	*XbaI/BamHI*

Chapter 4:

Construct Name	Sense Primer Name – Sequence (5' to 3')	Antisense Primer Name – Sequence (5' to 3')	PCR conditions (°C/seconds)	Restriction Endonuclease
pCFH-SGTA Δ1-20	pCFH-SGTAs GACTTCTAGAATGGACAACAAGAAGCGCCTG	pCFH-SGTAas GACTGGATCCTCATCACTCCTGCTGGTCGTC	96/300 then [96/20, 65/30,72/120] 40 times	*XbaI/BamHI*
pCFH-SGTA Δ21-40	pCFH-SGTAs GACTTCTAGAATGGACAACAAGAAGCGCCTG	pCFH-SGTAas GACTGGATCCTCATCACTCCTGCTGGTCGTC	96/300 then [96/20, 65/30,72/120] 40 times	*XbaI/BamHI*
pCFH-SGTA Δ41-60	pCFH-SGTAs GACTTCTAGAATGGACAACAAGAAGCGCCTG	pCFH-SGTAas GACTGGATCCTCATCACTCCTGCTGGTCGTC	96/300 then [96/20, 65/30,72/120] 40 times	*XbaI/BamHI*
pCFH-SGTA Δ29-33	pCFH-SGTAs GACTTCTAGAATGGACAACAAGAAGCGCCTG	pCFH-SGTAas GACTGGATCCTCATCACTCCTGCTGGTCGTC	96/300 then [96/20, 65/30,72/120] 40 times	*XbaI/BamHI*
pCFH-SGTA Δ91-192	pCFH-SGTAs GACTTCTAGAATGGACAACAAGAAGCGCCTG	pCFH-SGTAas GACTGGATCCTCATCACTCCTGCTGGTCGTC	96/300 then [96/20, 65/30,72/120] 40 times	*XbaI/BamHI*
pCFH-SGTA Δ200-263	pCFH-SGTAs GACTTCTAGAATGGACAACAAGAAGCGCCTG	pCFH-SGTAas GACTGGATCCTCATCACTCCTGCTGGTCGTC	96/300 then [96/20, 65/30,72/120] 40 times	*XbaI/BamHI*
pCFH-SGTA 1-270	pMSGTA(80-313)pCFHs GACTTCTAGAACCCCGCCTTCCGAGGAGGACT	pMSGT(1-270)pCFHas GACTGGATCCCAGGTCGTTCTGCGAGGGGCT	96/300 then [96/20, 65/30,72/120] 40 times	*XbaI/BamHI*
pCFH-SGTA 80-313	pMS2 AGGTCTCCGCTGACTAGGGCACATCTGA	pCFH-SGTAas GACTGGATCCTCATCACTCCTGCTGGTCGTC	96/300 then [96/20, 65/30,72/120] 40 times	*XbaI/BamHI*

Chapter 6

Construct Name	Sense Primer Name – Sequence (5' to 3')	Antisense Primer Name – Sequence (5' to 3')	PCR conditions (°C/seconds)	Restriction Endonuclease
pIRESpuro3-HA-SGTA	IRSSGTs TAAGCTAGCATGGGCTACCCATACGATGTTC	IRSSGTas ATTACCGGTTCACTCCTGCTGGTCGTCGT		*NheI/AgeI*
pIRES2-SGTA-EGFP	SGTGFPs TAAGAATTCATTATGGACAACAAGAAGCGCCTGGC	SGTGFPas GGATCCTCACTCCTGCTGGTCGTCGT		*EcoRI/BamHI*

Appendix A2: Sequencing primers
Sense sequencing primers

Primer Name	Primer Name – Sequence (5' to 3')	Position
pMS1	AGCATAGAATAAGTGCGACA	Nucleotides -80 to -61 of pM-SGTA
pMS2	AGGTCTCCGCTGACTAGGGCACATCTGA	
pVP16S1	TCTGGATATGGCCGACTTCGA	Nucleotides -76 to -56 of pVP16-SGTA
pCFHs	AATTAATACGACTCACTATAGGG	
pCMVS3	ATTGACGCAAATGGGCGGTA	Nucleotides -149 to-130 of pcDNA3.1

Antisense sequencing primers

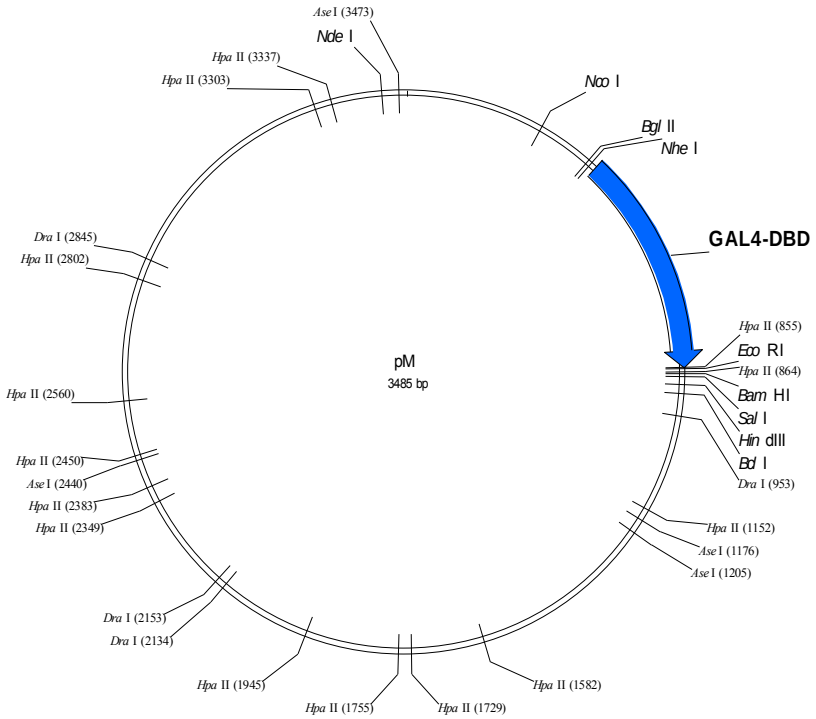
Primer Name	Primer Name – Sequence (5' to 3')	Position
pMAS1	AGCAAGTAAAACCTCTACAAAT	Nucleotides +57 to +36 of pM-SGTA
SGT188as	GTCCAGCTCCAGAGCCTTCTTGTAGTAAGC	
pVP16AS1	ACCTCTACAAATGTGGTATGGCT	Nucleotides +47 to +25 of pVP16
pCFHas	TAGAAGGCACAGTCGAGG	
pIPUROAS	CCACCCTCAAAGGCATCACC	
pIESGTAS	GAATCCTCACTCCTGCTGGTCGTCGT	

Appendix A3: Quantitative real time PCR primers

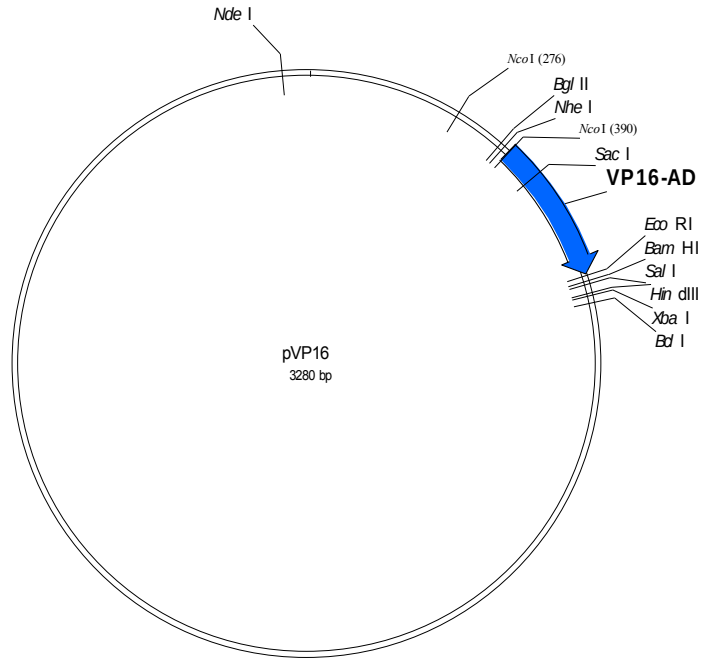
Gene Name	Sense Primer Name – Sequence (5' to 3')	Antisense Primer Name – Sequence (5' to 3')	Amplicon Size (bp)	mRNA position (bp)
GAPDH	TGCACCACCAACTGCTTAGC	GGCATGGACTGTGGTCATGAG	144	556-642
SGTA	TGCCTGGAGACTGCGTTTGG	TGCTGTAGGCTGCGGCTCTGTTGCA	298	259-556
PSA	ACCAGAGGAGTTCTTGACCCCAAA	CCCCAGAATCACCCGAGCAG	161	524-684
FKBP51	AAAAGGCCAAGGAGCACAAC	TTGAGGAGGGGCCGAGTTC	236	1345-1580
FKBP52	GAATACAGACTCGCGGTGAA	CAGTGCAACCTCCACGATAG	65	656-720
AR	CCTGGCTTCCGCAACTTACAC	GGACTTGTGCATGCGGTACTCA	168	3285-3452
S100A10	AAAGGCTACTTAACAAAGGAGGACC	GTCCTTCATTATTTTGTCCACAGC	108	575-682
PLA2G2A	CATCTGCATTTGTCACCCAAGA	GATCATTCTGTGGAAATTCACCAA	118	265-382
MYLK	AGCTTGGTCAGCCTGTTGTTT	AGCAAACTTTGGTGGGCACT	104	671-774
IGFBP3	CCCAACTGTGACAAGAAGGGAT	AGAGGCTGCCCATACTTATCCA	104	862-965
LRRC31	GAATAACTGTGGATTAACAACAGCG	CCTACAAAACCATTCCAGGAGATA	105	356-460
PLD1	CAGCGATCCCAAGATACAAGAA	TTTATTGGACAGCCGGAGAGA	103	254-361
p85α	ACTCTCTGAAATTTTCAGCCCTATG	CGTTCATTCCATTCAGTTGAGATTA	114	831-944
p55γ	AGGTGATGATGCCCTATTCGA	TTGGAACTGCTGAAGTCATTGG	102	805-886
p110β	CTCGGGAAGCTACCATTTCTTATA	AGTCTGATTCACACATGCAAACATA	119	140-258
p110δ	AATGCCAACCTCAGCACCAT	TCTGGTTGATGCAGGTGAACA	112	328-434

Appendix B: Plasmids

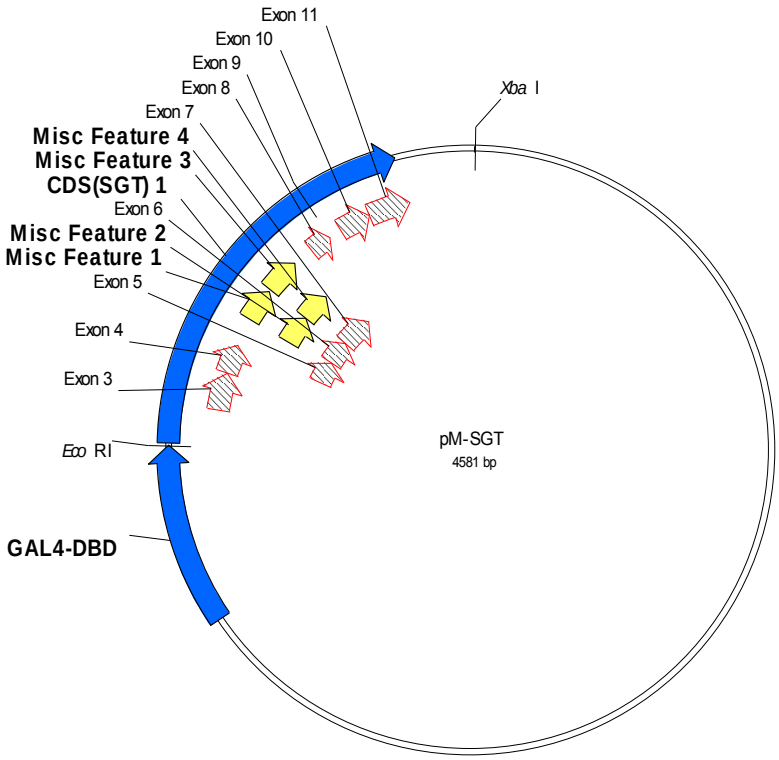
Appendix B1: Plasmids for mammalian 2-hybrid interaction assays



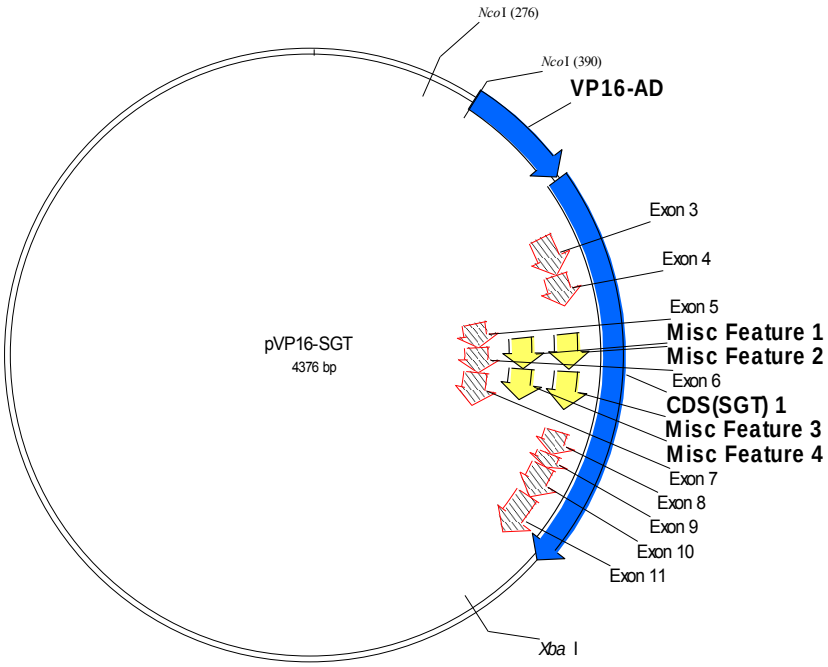
pM



pVP16



pM-SGTA

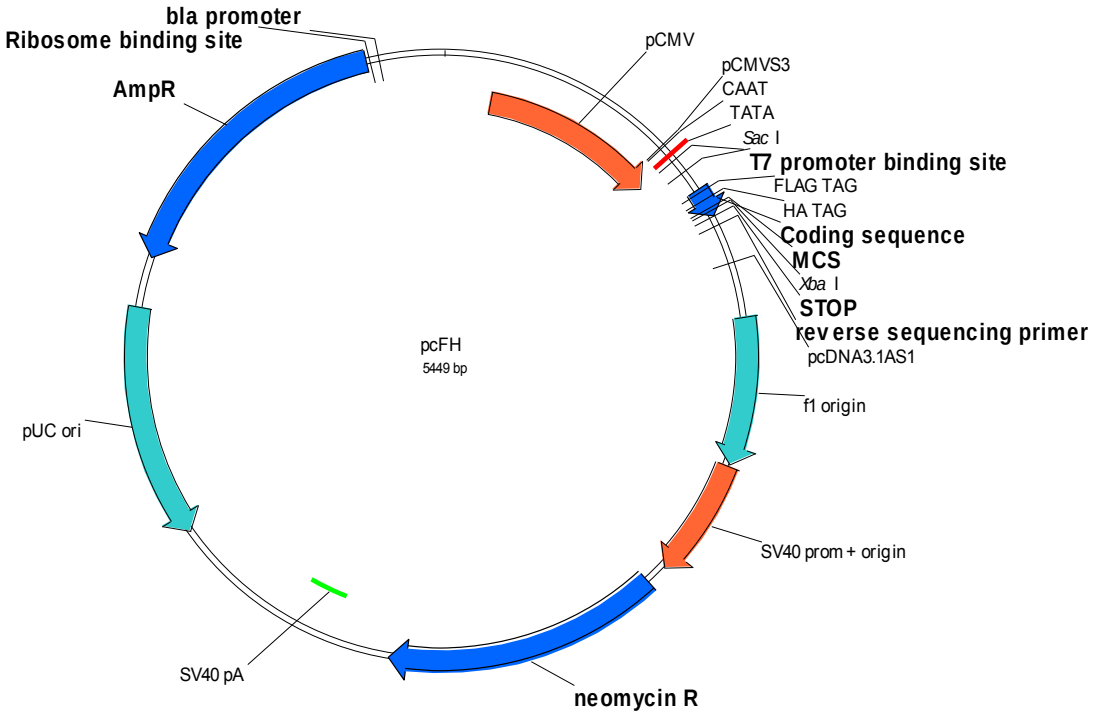


pVP16-SGTA

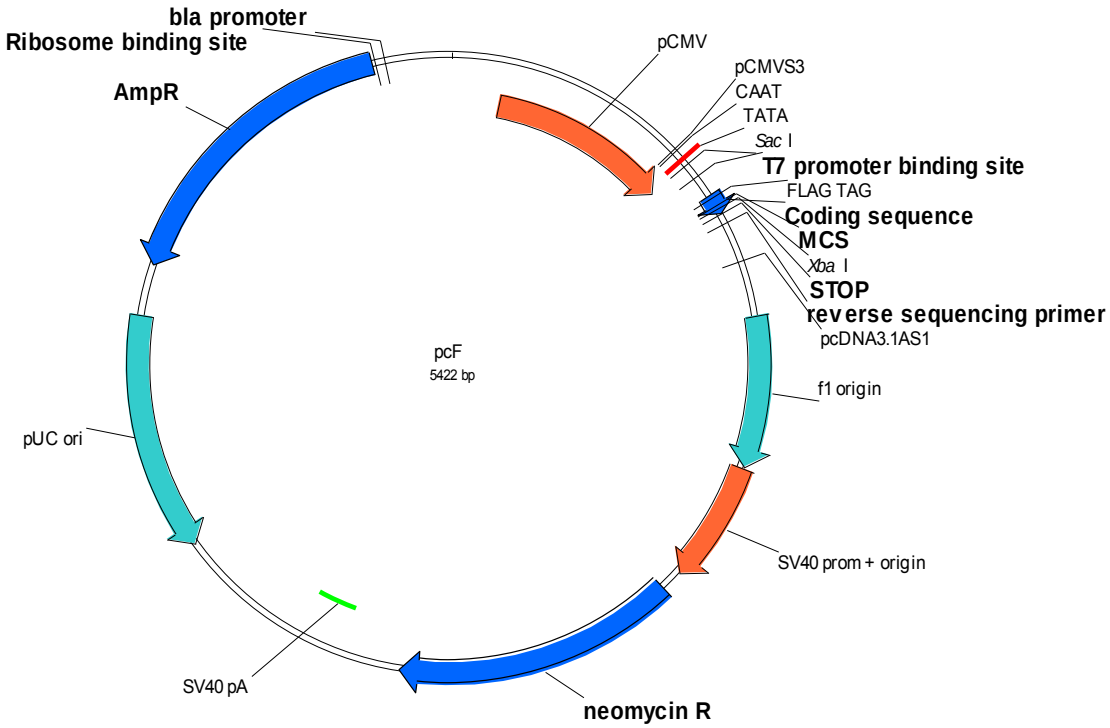
Plasmids constructed for this thesis for mammalian 2-hybrid interaction assays
The following plasmids are variants of the pM-SGTA plasmids depicted above:

pM-SGTA Δ 1-20
pM-SGTA Δ 21-40
pM-SGTA Δ 41-60
pM-SGTA Δ 61-80
pM-SGTA Δ 29-33
pM-SGTA S31P
pM-SGTA S31T

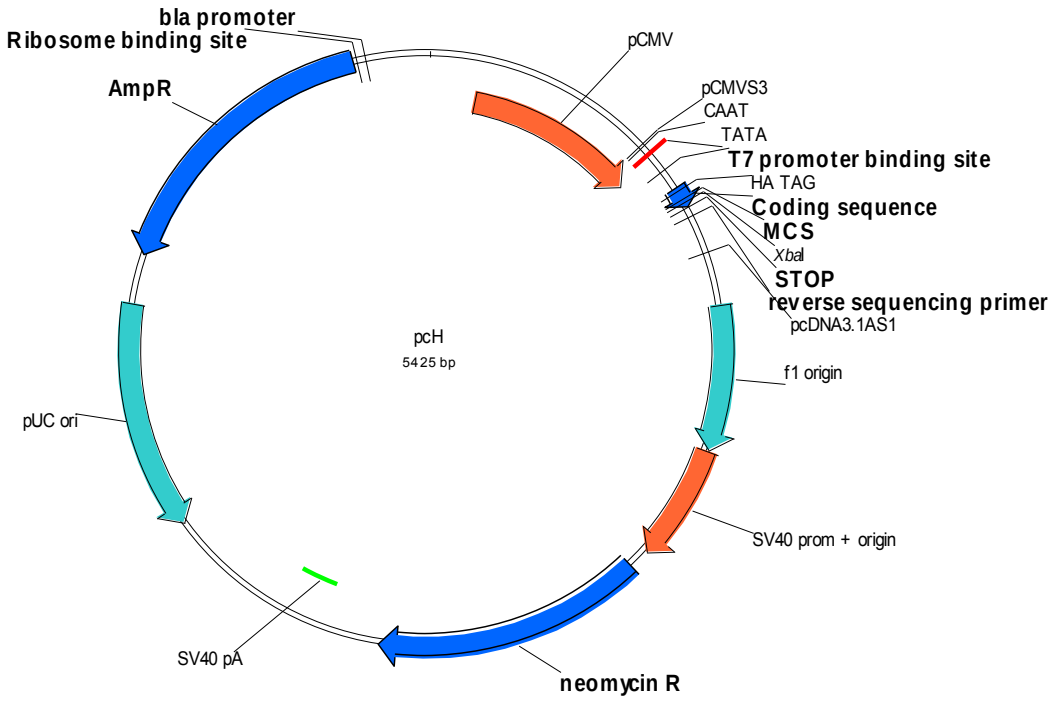
Appendix B2: Plasmids for transactivation assays


bla promoter
Ribosome binding site
AmpR
pCMV
pCMVS3
CAAT
TATA
Sac I
T7 promoter binding site
FLAG TAG
HA TAG
Coding sequence
MCS
Xba I
STOP
reverse sequencing primer
pcDNA3.1AS1
pcFH
5449 bp
f1 origin
pUC ori
SV40 prom + origin
SV40 pA
neomycin R

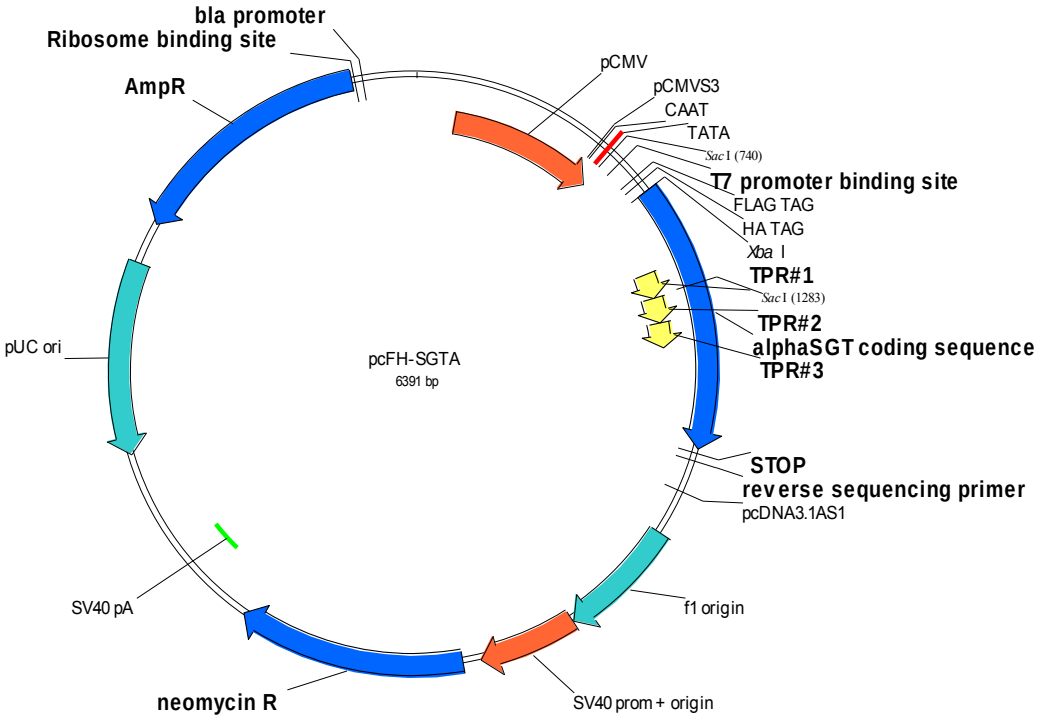
pcFH


bla promoter
Ribosome binding site
AmpR
pCMV
pCMVS3
CAAT
TATA
Sac I
T7 promoter binding site
FLAG TAG
Coding sequence
MCS
Xba I
STOP
reverse sequencing primer
pcDNA3.1AS1
pcF
5422 bp
f1 origin
pUC ori
SV40 prom + origin
SV40 pA
neomycin R

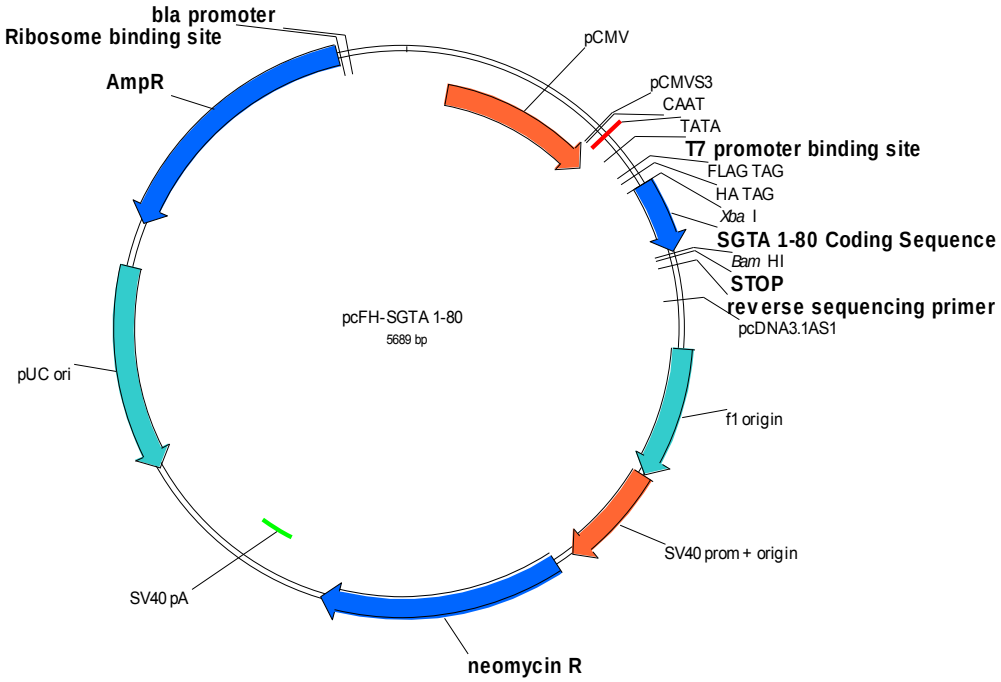
pcF


bla promoter
Ribosome binding site
AmpR
pCMV
pCMVS3
CAAT
TATA
T7 promoter binding site
HA TAG
Coding sequence
MCS
XbaI
STOP
reverse sequencing primer
pcDNA3.1AS1
pcH
5425 bp
f1 origin
pUC ori
SV40 prom + origin
SV40 pA
neomycin R

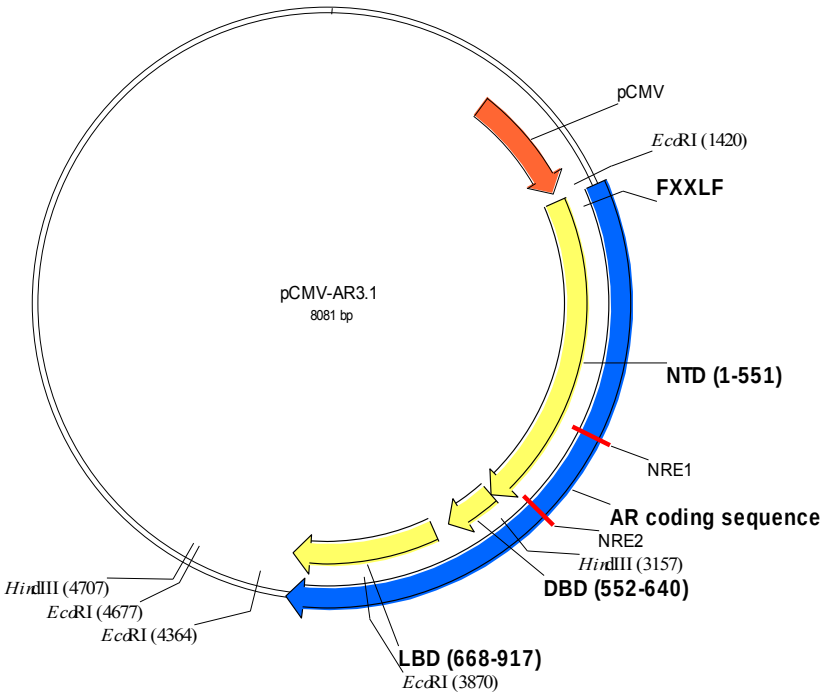
pcH


bla promoter
Ribosome binding site
AmpR
pCMV
pCMVS3
CAAT
TATA
SacI (740)
T7 promoter binding site
FLAG TAG
HA TAG
XbaI
TPR#1
SacI (1283)
TPR#2
alphaSGT coding sequence
TPR#3
pcFH-SGTA
6391 bp
pUC ori
STOP
reverse sequencing primer
pcDNA3.1AS1
f1 origin
SV40 pA
neomycin R
SV40 prom + origin

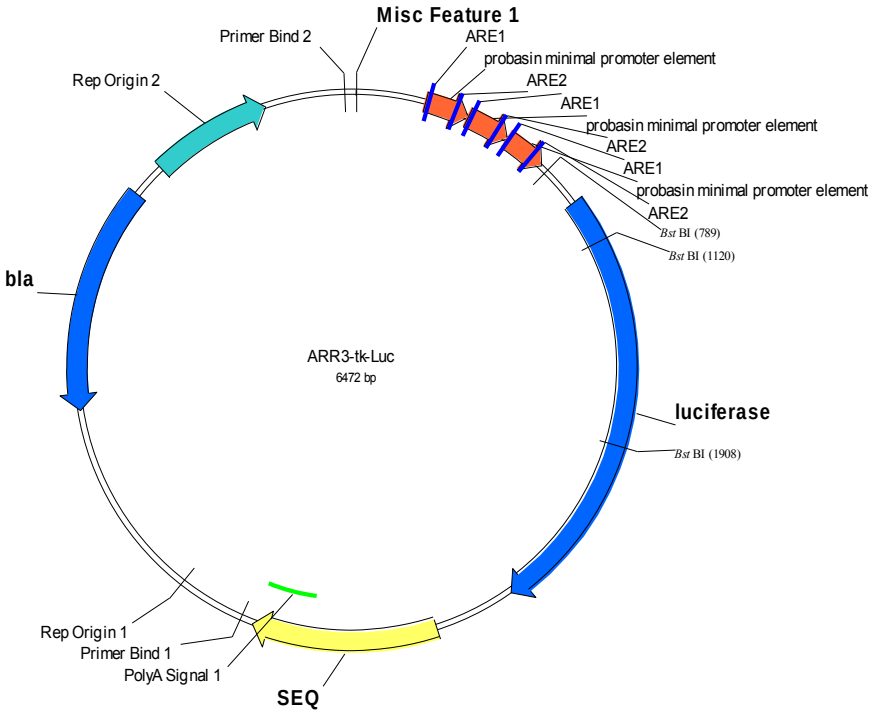
pcFH-SGTA



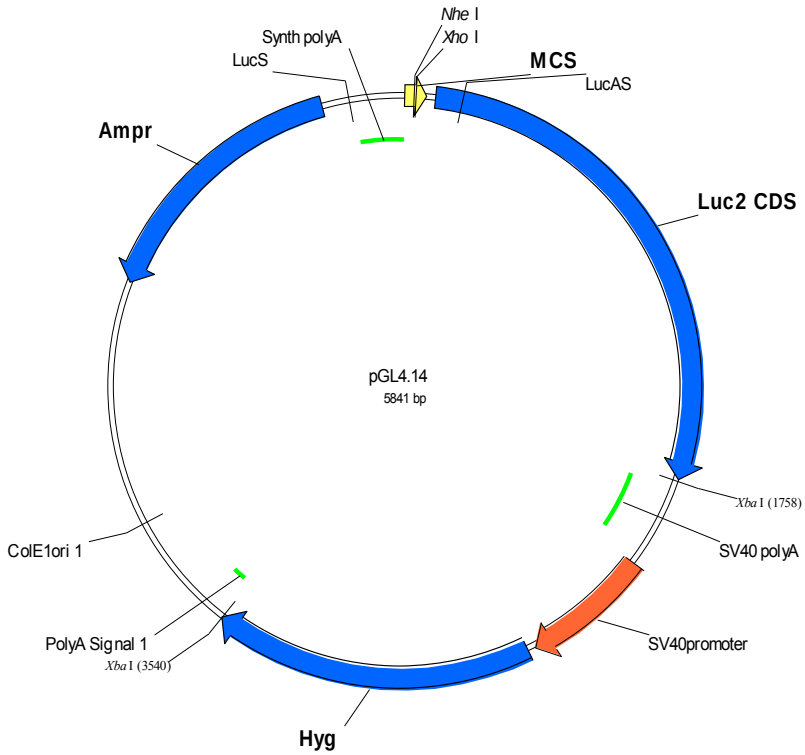
pcFH-SGTA 1-80



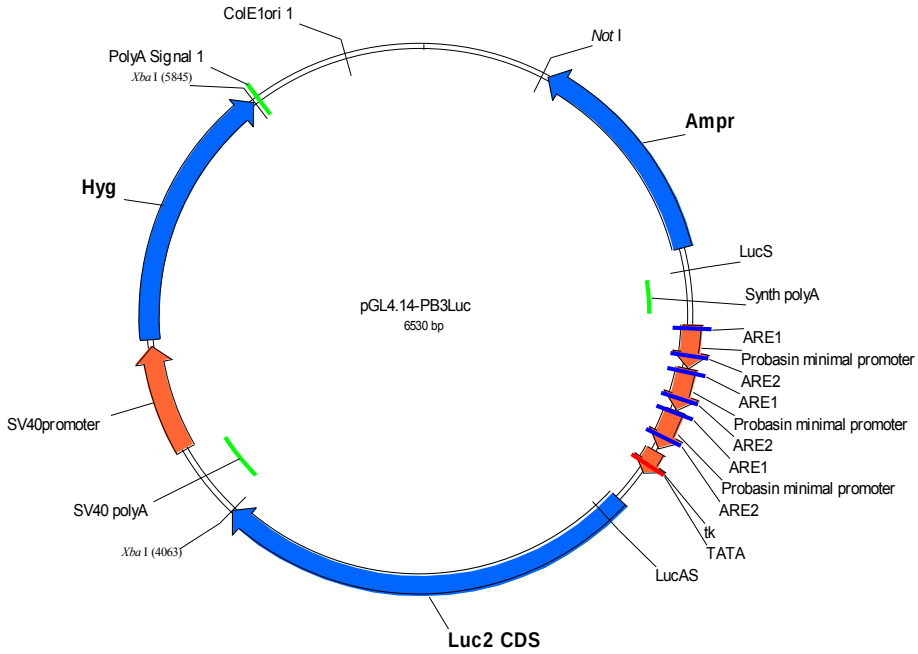
pCMV-AR3.1



ARR3-tk-Luc



pGL4.14



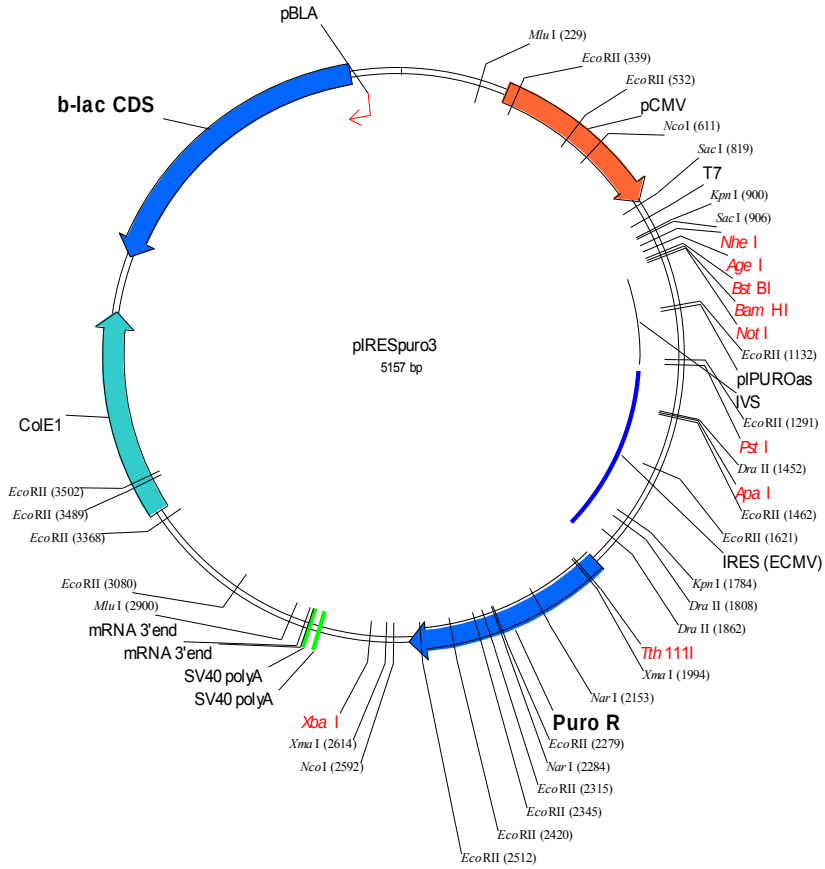
pGL4.14-PB3Luc

Plasmids constructed for this thesis for transactivation assays

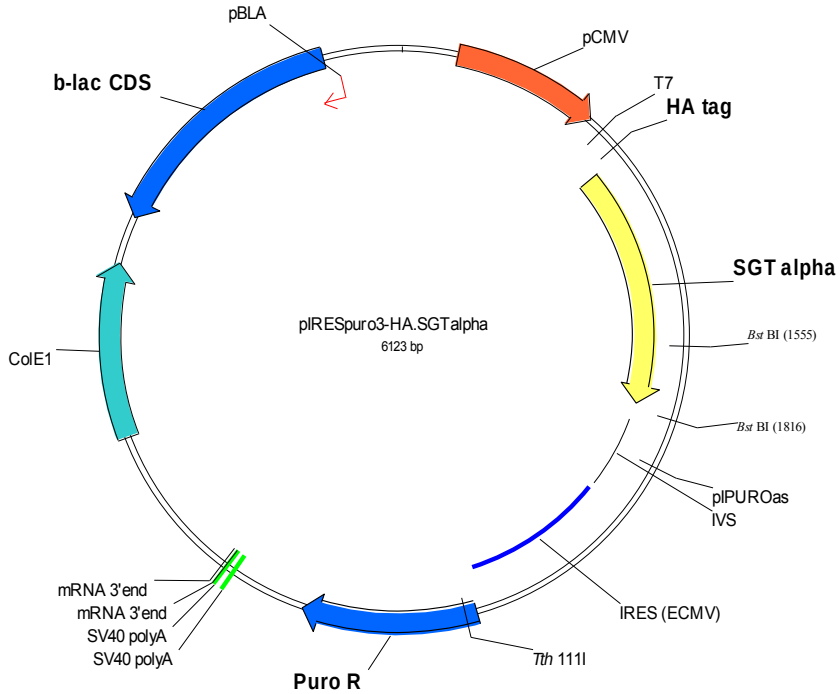
The following plasmids are variants of the pcFH-SGTA plasmids depicted above:

pcFH-SGTA Δ 1-20
pcFH-SGTA Δ 21-40
pcFH-SGTA Δ 41-60
pcFH-SGTA Δ 91-192
pcFH-SGTA Δ200-263
pcFH-SGTA 80-313
pcFH-SGTA 1-270

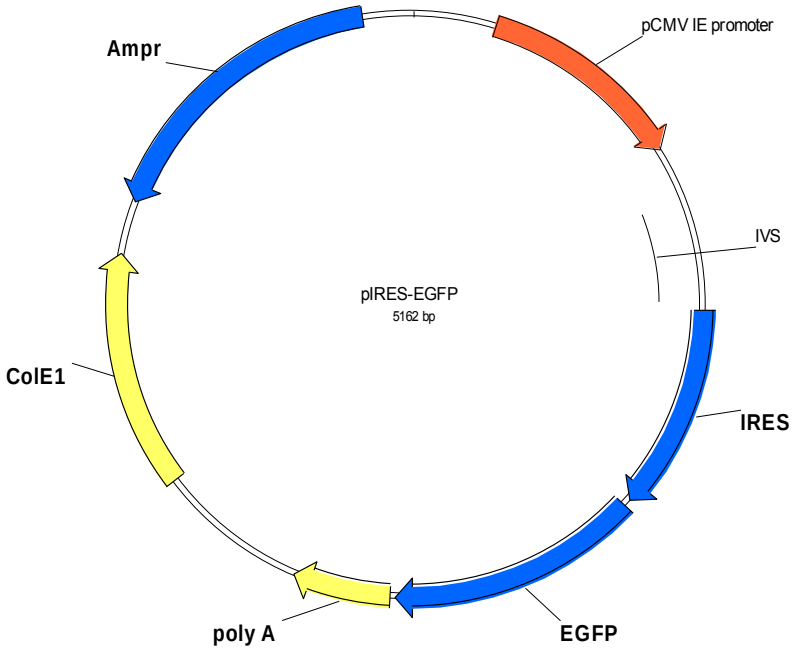
Appendix B3: Plasmids for stable SGTA over expression


pBLA
b-lac CDS
Mlu I (229)
Eco RII (339)
Eco RII (532)
pCMV
Nco I (611)
Sac I (819)
T7
Kpn I (900)
Sac I (906)
Nhe I
Age I
Bst BI
Bam HI
Not I
Eco RII (1132)
pIPUROas
IVS
Eco RII (1291)
Pst I
Dra II (1452)
Apa I
Eco RII (1462)
Eco RII (1621)
IRES (ECMV)
Kpn I (1784)
Dra II (1808)
Dra II (1862)
Tth 111I
Xma I (1994)
Nar I (2153)
Puro R
Eco RII (2279)
Nar I (2284)
Eco RII (2315)
Eco RII (2345)
Eco RII (2420)
Eco RII (2512)
pIRESpuro3
5157 bp
ColE1
Eco RII (3502)
Eco RII (3489)
Eco RII (3368)
Eco RII (3080)
Mlu I (2900)
mRNA 3'end
mRNA 3'end
SV40 polyA
SV40 polyA
Xba I
Xma I (2614)
Nco I (2592)

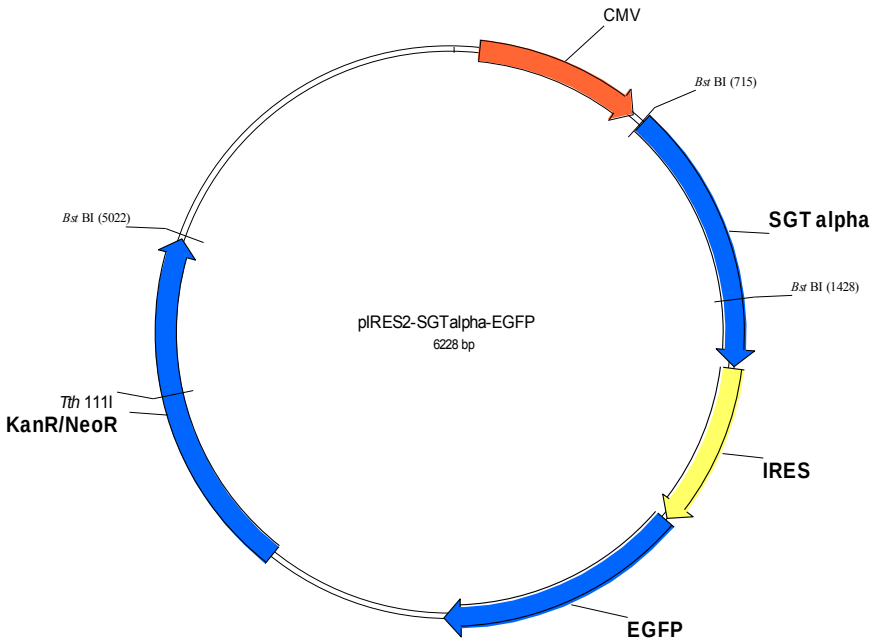
pIREpuro3


pBLA
b-lac CDS
pCMV
T7
HA tag
SGT alpha
Bst BI (1555)
Bst BI (1816)
pIPUROas
IVS
IRES (ECMV)
Tth 111I
Puro R
mRNA 3'end
mRNA 3'end
SV40 polyA
SV40 polyA
pIRESpuro3-HA.SGTalpha
6123 bp
ColE1

pIREpuro3-HA-SGTA



pIRES-EGFP



pIRES2-SGTA-EGFP

Appendix C: Microarray Dataset

Gene Name	ID	Log2 Fold Change	Average expression	Adj. p value
SGTA	8032530	-2.0365	8.0774	1.99E-08
S100A10	7920123	-2.0361	8.0750	1.71E-06
KCNJ13	8059776	-2.0357	6.4971	2.69E-05
C7orf63	8134051	-1.5373	5.8744	1.42E-06
TNFSF10	8092169	-1.5365	5.9389	0.000208194
SLC22A3	8123246	-1.4407	7.1795	1.71E-06
C1orf161	7904244	-1.3659	6.2592	7.52E-05
PLA2G2A	7913216	-1.3562	6.8821	2.75E-05
IGFBP3	8139488	1.3487	6.9878	1.71E-06
MYLK	8090098	-1.3428	8.5244	1.42E-06
ARPM1	8092002	-1.2692	6.1972	3.53E-05
NAPEPLD	8141872	-1.2512	8.3196	4.89E-06
CYP1A2	7984862	1.2046	8.2023	0.000617411
STEAP1	8134030	-1.1383	8.3972	3.10E-06
RCAN3	7898957	-1.1156	8.1170	9.02E-05
TLL2	7935296	-1.0947	7.0373	3.58E-05
DGKH	7968800	-1.0805	6.8407	2.17E-05
ABCG2	8101675	-1.0755	5.6393	2.76E-05
SLC38A9	8112121	-1.0751	9.0072	1.55E-05
STARD4	8113491	-1.0439	7.7454	1.37E-05
ZC3H12A	7900146	-1.0017	7.8335	8.25E-06
OCLN	8105908	-0.9944	9.9783	9.86E-05
LRRC31	8092021	0.9933	5.4295	0.000880375
C11orf92	7951593	-0.9924	7.1206	3.58E-05
GPX8	8105348	0.9912	5.9508	0.001524444
NFIB	8160138	-0.9643	6.4892	1.62E-05
DPY19L1	8138977	-0.9517	6.8002	0.000310816
PLD1	8092134	0.9462	7.6157	0.000151049
BCAT1	7961829	0.9399	5.6536	4.89E-06
PFKFB3	7926037	-0.9334	6.9329	0.007594649
LIN7C	7947221	-0.9235	8.5707	8.66E-06
IL6ST	8112139	-0.9174	8.2276	0.000241499
ACOX1	8018558	-0.9028	8.2296	1.37E-05
ANKRD28	8085628	-0.9001	7.3589	2.97E-05
NPR3	8104746	-0.8989	5.8304	0.000108122
KLF7	8058477	-0.8979	7.7452	7.52E-05
SLPI	8066493	-0.8963	10.7871	0.000241499
DPP4	8056222	-0.8935	9.1321	3.40E-05
UPK1A	8027938	0.8884	6.5130	9.87E-05
SNORD115-11	7982084	-0.8833	5.6970	0.000160584
GPR63	8128316	-0.8761	6.8935	6.86E-05
MYO1B	8047127	-0.8647	7.1144	1.71E-06
GPR126	8122365	-0.8608	8.4426	3.10E-06
NIPAL3	7898939	-0.8589	9.3875	1.42E-06
P4HA1	7934278	-0.8570	10.1623	0.000362476
PCMTD1	8150714	-0.8411	8.6277	7.91E-06
CLU	8149927	-0.8410	7.9306	2.97E-05
DMXL1	8107474	-0.8392	7.7624	3.72E-05
TMEM140	8136388	-0.8344	7.3113	2.69E-05
SLC35A5	8081667	-0.8272	8.3961	8.11E-06
ITGAV	8046861	-0.8189	8.7098	2.96E-05
ENDOD1	7943293	-0.8113	9.0100	2.03E-05
BTD	8078147	-0.7939	7.8003	1.15E-05
NEDD9	8123936	-0.7914	6.1293	4.12E-05
AHCYL1	7903803	0.7859	10.3827	2.97E-05
CCND3	8126371	-0.7851	7.6024	9.86E-05
TMEM45B	7945169	0.7832	8.9145	0.000336873
CHAC1	7982868	0.7781	6.7718	0.000164137
TOMM20	7925174	-0.7740	8.3605	0.003096602
MYNN	8083794	-0.7734	8.2803	2.25E-05
LRRN1	8077366	-0.7566	5.9140	0.004083127

Gene Name	ID	Log2 Fold Change	Average expression	Adj. p value
DICER1	7981111	-0.7530	8.7672	1.15E-05
VPS13A	8155946	0.7458	7.8680	0.000441249
C5orf23	8104758	-0.7457	5.2628	0.000238905
CD24	8177222	-0.7450	5.4120	0.005562387
HACL1	8085608	0.7445	8.5202	1.37E-05
DAAM1	7974697	-0.7439	7.4484	2.66E-05
FAM129A	7922846	-0.7428	6.1915	0.000114134
WNT5A	8088180	-0.7407	7.2120	0.00022265
FAM63B	7983940	-0.7397	7.0369	0.00145096
RDH11	7979743	-0.7375	9.9144	8.11E-06
UTRN	8122464	-0.7374	7.3943	0.000188863
REPS2	8166243	0.7374	8.2575	0.000142089
GK5	8091120	-0.7371	7.6319	8.99E-05
SNORD115-26	7982058	-0.7369	4.7644	4.12E-05
TBRG1	7944850	0.7344	9.2765	2.54E-05
STC1	8149825	0.7344	4.9635	0.001191312
SELT	8154305	0.7344	10.3363	0.001779005
MCM9	8129214	0.7344	5.7786	0.000668898
C14orf143	7980690	-0.7330	7.7723	6.98E-05
FOXN3	7980680	-0.7202	7.9305	0.000142089
REXO2	7944011	-0.7197	10.0891	5.70E-05
TRERF1	8126428	-0.7163	7.9671	0.00019223
LNX2	7970716	-0.7163	10.5900	8.11E-06
PLEKHH1	7975238	-0.7161	7.3744	8.11E-06
WDR26	7924582	-0.7147	8.8595	9.86E-05
ACPP	8082673	-0.7130	7.5686	0.000129198
KLF4	8163002	-0.7118	6.0916	0.000463254
ARHGAP29	7917850	-0.7077	7.6595	0.000693157
NF2	8072242	-0.7066	8.8122	6.86E-05
FAT1	8104079	-0.7046	7.8439	7.52E-05
PIK3R1	8105778	-0.6986	9.1291	9.65E-05
GLYATL2	7948354	-0.6977	7.2408	0.000812594
STEAP2	8134036	0.6935	11.4029	8.66E-06
CD164	8128716	-0.6911	10.7264	0.00022265

Gene Name	ID	Log2 Fold Change	Average expression	Adj. p value
NGRN	7985983	-0.6900	9.3045	0.00022265
ACADSB	7931168	0.6889	9.0772	5.46E-05
EIF2C4	7900009	-0.6880	7.1147	1.37E-05
MATN2	8147516	-0.6867	6.6329	4.38E-05
DIO1	7901565	-0.6866	5.1398	0.00025146
ARID5B	7927732	-0.6862	8.6156	0.00022265
PTPMT1	7939818	-0.6858	8.5566	0.000870286
TOR1AIP2	7922637	0.6840	8.3098	0.000897395
RAB3B	7916112	-0.6829	6.0262	0.007023562
MID1	8171297	-0.6774	6.5016	6.86E-05
PFKFB4	8086961	-0.6773	6.6017	0.014182169
TP53INP1	8151890	-0.6736	9.3968	0.000202802
BHLHE40	8077441	-0.6710	7.5230	0.001524444
ASNS	8141150	-0.6697	9.3392	4.10E-05
CBLN2	8023822	0.6689	9.2299	3.01E-05
SELK	8088167	0.6681	8.1355	0.000142483
BANK1	8096617	-0.6661	6.0141	0.000182534
MT1F	7995825	-0.6649	8.8099	9.86E-05
CYBASC3	7948565	0.6636	9.7058	0.000266537
FUT11	7928395	-0.6630	7.5366	0.003692646
FRK	8129071	-0.6628	5.6224	0.000340978
LPL	8144917	-0.6627	6.2618	0.00105819
APC	8107330	0.6611	5.9776	0.000142483
MALL	8054479	-0.6599	6.5373	0.000225378
ROD1	8163402	-0.6581	8.5550	0.000199009
C10orf104	7928300	-0.6570	8.1836	3.72E-05
UBA6	8100615	-0.6531	8.1381	0.00049428
CENPH	8105842	0.6517	5.5876	0.007690666
TMPRSS2	8070467	-0.6516	8.7774	0.000246552
PDXDC1	7993433	-0.6503	8.9616	8.66E-06
RMND5A	8043310	-0.6450	8.5968	0.001377088
SSFA2	8046726	0.6444	9.2441	0.0002235
SLC7A11	8102800	0.6415	8.8021	0.000618565
DEGS1	7910001	-0.6394	10.8223	0.000694001

Gene Name	ID	Log2 Fold Change	Average expression	Adj. p value
RRAGC	7915160	-0.6383	8.3192	3.58E-05
ENPP5	8126750	-0.6374	6.3744	0.010336048
HOXC9	7955865	-0.6373	7.6387	4.31E-05
C2orf43	8050608	-0.6373	6.8552	0.000121849
RCN1	7939120	0.6352	9.3395	0.000596362
NAIP	8112521	-0.6342	8.3456	0.000417369
LCOR	7929596	-0.6315	7.7454	7.03E-05
KGFLP1	8155487	-0.6310	6.0737	0.002244502
TPRM8	8049394	-0.6310	5.5504	0.001111568
SESN3	7951077	-0.6310	10.2221	3.27E-05
SGTB	8112409	-0.6308	6.5260	0.000982419
COMMD2	8091432	0.6298	8.6126	0.001904173
AHNAK	7948667	-0.6293	7.6436	0.001298465
KIF13A	8124088	-0.6283	7.1499	9.86E-05
MEAF6	7914996	-0.6272	8.4881	0.000851104
PMS2	8138030	-0.6264	9.5925	3.69E-05
GRIN3A	8162908	-0.6246	5.4424	0.000505569
SLC1A3	8104930	-0.6222	5.7974	0.006716952
CPEB2	8094169	0.6220	5.5525	0.000835301
ITPR2	7961900	0.6200	6.0732	0.000180125
REV3L	8128894	-0.6192	6.7813	9.93E-05
FAM96A	7989611	-0.6165	8.5109	0.001405953
TULP4	8123044	-0.6159	6.1228	0.000637383
NAIP	8112478	-0.6151	8.4705	0.000243738
TLE3	7990033	-0.6135	8.3583	0.000417369
NCEH1	8092177	-0.6134	8.3694	3.80E-05
APAF1	7957759	-0.6130	6.3092	0.00017802
COLEC12	8021946	-0.6120	9.2513	3.58E-05
DHRS4	7973448	-0.6119	8.2791	0.000341074
PTGFR	7902527	-0.6103	7.5254	0.000130984
AMMECR1	8174496	0.6091	7.9097	0.000900582
NKX3-1	8149811	-0.6088	8.4876	0.000121849
COBLL1	8056343	0.6073	6.9284	0.000449277
FAM169A	8112649	-0.6053	5.7657	0.000344197

Gene Name	ID	Log2 Fold Change	Average expression	Adj. p value
IL1RN	8044574	-0.6016	5.2269	0.00011905
CDH3	7996819	-0.5958	7.5762	6.08E-05
MAP3K13	8084589	-0.5958	6.7751	0.002692917
CD55	7909332	-0.5957	6.0865	0.001779005
NDRG1	8153002	-0.5954	8.9623	0.01419127
COL12A1	8127563	-0.5920	5.1643	0.000886922
TRERF1	8126402	-0.5896	7.2145	0.000238905
NCOA3	8063211	-0.5846	8.0998	5.54E-05
RWDD2A	8120927	-0.5838	8.4689	2.76E-05
SLC2A12	8129666	-0.5835	6.4833	2.17E-05
PDE8A	7985662	-0.5826	6.6828	0.000129198
CCDC14	8090133	-0.5805	8.8523	0.00030757
CDKL5	8166289	-0.5792	5.3551	0.000202802
FERMT2	7979204	-0.5784	6.8481	0.003105126
KIAA2018	8089647	-0.5755	6.3899	0.00132309
RANBP2	8044263	-0.5752	8.9411	0.00148074
OSBPL9	7901385	-0.5738	7.7544	6.38E-05
RNF144B	8117106	-0.5736	7.6965	6.86E-05
FAM162A	8082066	-0.5721	9.3075	0.000129198
GPD1L	8078386	-0.5713	7.9657	0.00022265
NCRNA00219	8107321	-0.5706	8.4216	0.000897395
RNF160	8069711	-0.5674	6.6361	0.000144901
MYB	8122202	-0.5670	6.8615	0.000257888
BTG1	7965423	-0.5667	11.0278	7.52E-05
HIPK1	7904137	-0.5656	7.8848	8.97E-05
DHRS4L2	7973458	-0.5654	7.9000	8.97E-05
DNASE2B	7902623	0.5651	6.6023	0.00038923
CUL5	7943580	-0.5647	8.0357	0.000338225
SPAST	8041236	-0.5643	7.4794	0.000833514
MDM2	7956989	-0.5641	9.5548	9.65E-05
HMOX1	8072678	0.5636	7.8877	0.012917097
HOXC6	7955873	-0.5621	7.3458	0.000405001
CYTSB	8005661	-0.5590	7.7672	3.58E-05
KIAA1467	7954077	-0.5588	8.3086	0.000586531

Gene Name	ID	Log2 Fold Change	Average expression	Adj. p value
HSD17B14	8038213	0.5580	6.7426	0.001111568
ELAC2	8012856	-0.5578	9.4516	0.00011609
SIAE	7952408	-0.5572	8.9669	2.76E-05
TTC39B	8160213	-0.5570	5.9280	0.003355662
GDE1	7999889	-0.5568	8.2682	0.000142089
RAB8B	7984112	-0.5562	7.4830	0.002133006
SGPL1	7928171	-0.5551	9.6375	8.97E-05
SKAP2	8138689	-0.5539	8.4491	0.000268924
SLC30A4	7988426	-0.5522	11.1213	4.12E-05
ALDH3A2	8005638	-0.5509	9.2927	2.97E-05
IBTK	8127787	-0.5504	8.4627	0.00059864
KGFLP1	8067839	-0.5489	5.2776	0.002075344
ATG2B	7981192	-0.5461	7.7098	0.000241499
HTATSF1	8170166	-0.5454	8.3327	0.000471923
ZNF292	8120992	-0.5442	6.4575	0.00045853
TAB2	8122672	-0.5385	8.0705	0.000160584
GCLC	8127158	-0.5373	9.4713	0.000241499
C18orf45	8022514	0.5362	7.7544	0.001436944
ZDHHC5	7940051	0.5348	9.1658	0.00105819
CASP4	7951372	-0.5334	6.8823	0.001485715
JHDM1D	8143341	0.5333	6.2613	0.002165375
GARS	8132070	-0.5329	10.2754	0.000618258
S1PR3	8156278	-0.5328	7.7057	0.000154675
PPIL4	8130087	-0.5315	7.1357	0.012332424
MYH10	8012475	-0.5309	8.9536	4.99E-05
C5orf22	8104680	-0.5303	8.6577	0.00059864
PIK3CB	8091009	-0.5301	9.7311	0.000184859
TM9SF3	7935320	-0.5299	11.7631	7.52E-05
VPS13D	7897890	-0.5289	7.1860	0.000294084
PIGB	7983811	-0.5283	7.1721	0.000433694
CHM	8173892	-0.5278	6.6926	0.001748692
SELT	8083352	-0.5270	10.3284	0.000241499
EXPH5	7951545	-0.5253	7.2281	0.005197424
KALRN	8082165	-0.5253	5.7036	6.94E-05

Gene Name	ID	Log2 Fold Change	Average expression	Adj. p value
AGR2	8138381	-0.5242	5.2432	0.009764937
IGF2R	8123181	-0.5236	8.9683	0.000241499
SLC22A23	8123658	-0.5224	7.1102	0.001371947
MAP4K5	7978997	-0.5223	6.9017	0.002887138
NEDD4L	8021376	-0.5219	9.8695	0.000124917
CAB39L	7971590	0.5215	8.2636	0.009848714
ACP5	8034304	-0.5213	4.9043	0.013119491
BNIP3	7937079	-0.5205	10.6127	0.028378012
HGD	8089851	-0.5205	5.7212	0.002215754
PDE6B	8093360	0.5192	5.8991	0.000549155
HIVEP2	8129953	-0.5176	6.7207	0.006295647
ARHGAP6	8171313	-0.5176	7.4883	0.000280023
GALNTL4	7946641	-0.5173	6.3003	9.39E-05
NFAT5	7996954	-0.5171	7.5460	0.001619792
STX3	7940191	-0.5169	7.8176	0.001328849
RFK	8161857	-0.5155	8.4023	0.000726774
EHHADH	8092523	0.5152	5.6990	0.010708259
BANF1	8180260	-0.5149	10.2451	8.44E-05
TAX1BP1	8131975	-0.5137	10.1630	0.00042557
BCAP29	8135422	0.5124	7.1573	0.000871597
FAM198B	8103415	-0.5124	7.4660	0.00134578
ZNF654	8081069	-0.5123	6.9415	0.007076485
NBEAL1	8047606	-0.5122	5.8862	0.024589335
ANKRD44	8057990	-0.5119	6.1624	8.97E-05
CHCHD7	8146517	-0.5116	6.0528	0.000541982
PPM1K	8101701	-0.5115	6.0316	0.000544168
LSM5	8138912	0.5113	6.8857	0.014240395
MAP2K4	8005029	-0.5110	7.9430	0.002165375
EPAS1	8041781	-0.5100	6.0871	0.001191312
KCTD10	7966202	-0.5094	7.4358	0.000596362
SLC4A4	8095585	-0.5085	8.1524	0.000182534
CLMN	7981142	0.5077	6.8624	0.00038076
SNORD3A	8005547	0.5077	10.1611	0.043254783
UBE3B	7958532	0.5077	7.9286	0.000596362

Gene Name	ID	Log2 Fold Change	Average expression	Adj. p value
SORBS1	7935188	0.5077	5.5792	0.003111267
BRP44L	8130732	0.5077	8.6543	0.031088724
KAT2B	8078227	-0.5053	6.7801	0.000982419
SACS	7970569	0.5046	7.3802	0.005652097
KIAA1324L	8140709	-0.5037	8.7132	0.001411635
RBL2	7995631	-0.5018	8.5367	0.000186233
LYSMD3	8113064	-0.5014	8.6347	0.000897395
LYPD6B	8045664	-0.4998	5.8241	0.003360326
TTC6	7974029	-0.4986	5.0125	0.010597199
PIK3CD	7897482	-0.4952	7.4892	0.001191312
CLDN12	8134091	-0.4951	9.6925	0.000208861
GRLF1	8029856	-0.4941	8.9940	0.000208194
MEIS1	8042356	-0.4922	5.3273	0.005155841
DHRS3	7912537	-0.4912	6.6419	0.004537469
ERLIN1	7935692	-0.4909	8.4786	0.008537904
ST6GAL1	8084717	-0.4899	6.2592	0.000588256
METTL14	8097066	-0.4899	7.7233	0.001124685
FAM126B	8058182	0.4896	7.5037	0.000125795
MCCC2	8177601	-0.4893	7.0265	0.001589524
C9orf41	8161829	-0.4892	8.0225	0.006800435
MBTPS1	8003089	-0.4889	9.1769	0.00022265
RNMT	8020323	-0.4889	7.7470	0.00453731
BEST1	7940582	-0.4879	5.0716	0.003174233
EIF5A2	8092073	0.4879	6.4436	0.003073591
PTPRG	8080810	-0.4862	6.1674	0.000417369
RBKS	8051215	0.4861	6.2280	0.004874973
MCFD2	8051998	-0.4856	8.1951	0.000138177
TIFA	8102362	-0.4851	6.2603	0.013468137
EDEM1	8077458	-0.4846	7.8329	0.0002235
ESYT2	8144184	0.4840	7.9176	0.000302971
ATF4	8180337	0.4835	10.5008	0.000244096
CAMK2D	8102415	-0.4828	6.2403	0.011570622
LRRC37B	8006336	0.4820	5.5153	0.00682399
WDR7	8021312	0.4820	7.8435	0.000362251

Gene Name	ID	Log2 Fold Change	Average expression	Adj. p value
FSTL1	8089835	0.4817	7.2533	0.001612308
ICK	8127109	-0.4811	8.4119	0.011693437
KIAA0247	7975361	-0.4803	7.0880	0.00149588
C19orf48	8038624	-0.4792	9.0139	0.000339812
CYR61	7902687	-0.4790	5.8940	0.002306129
TBCEL	7944623	-0.4786	8.3843	0.000308855
POM121L8P	8105989	0.4779	6.4179	0.011735808
DUS3L	8033025	-0.4778	7.2252	0.00049428
CABC1	7910164	-0.4770	7.9108	0.000639965
UBXN2B	8146544	0.4759	7.9573	0.021609061
TAF13	7918284	-0.4750	8.6082	0.001524444
C11orf80	7941714	-0.4746	7.0314	0.000129198
VEZT	7957613	-0.4735	7.8911	0.002054766
CECR1	8074237	-0.4735	4.9642	0.004433757
FRYL	8100251	-0.4731	7.4093	0.002380204
ARHGEF3	8088247	-0.4729	5.8906	0.001014526
FBXO9	8120251	-0.4726	9.4805	0.000260142
HOXC13	7955845	-0.4726	9.0992	6.51E-05
CCNYL1	8047854	-0.4723	7.2130	0.001260191
C9orf172	8159439	-0.4717	5.9458	0.009907601
C10orf118	7936419	-0.4717	8.4990	0.001407833
LGALS8	7925361	0.4713	5.7282	0.006315289
CRYBG3	8081171	-0.4711	7.0050	0.012171738
CD58	7918902	-0.4711	6.1352	0.004203122
NAMPT	8142120	-0.4700	9.7770	0.004083127
AKTIP	8001410	-0.4697	8.2429	0.002718492
FAM177B	7909946	-0.4695	5.1629	0.006796703
ENTPD7	7929750	-0.4690	6.1543	0.00022265
SYTL2	7950810	-0.4683	7.7539	0.001251665
ALDH3B2	7949882	-0.4679	7.8980	0.004261106
C6orf192	8129649	-0.4676	7.2022	0.000703721
FAM47E	8095819	0.4674	5.6246	0.019531213
LOC646214	7986603	0.4666	5.5834	0.033093148
SLC6A6	8078014	-0.4664	7.1896	0.007870086

Gene Name	ID	Log2 Fold Change	Average expression	Adj. p value
MAP3K5	8129804	-0.4664	6.4670	0.005082035
SPOPL	8045514	-0.4661	7.6694	0.019992724
BIRC3	7943413	0.4656	5.3669	0.001779005
SMARCC1	8086810	-0.4654	8.5533	0.000307766
GSTA4	8127094	-0.4651	6.6713	0.003459973
ACER3	7942679	-0.4646	7.2953	0.006320354
ATP8B1	8023497	-0.4644	8.0007	0.001873784
FRRS1	7917954	-0.4629	7.5637	0.001657948
ACER2	8154563	-0.4618	6.5937	0.01835909
CSNK1A1	8115022	-0.4613	10.3023	0.002389871
HELZ	8017776	-0.4603	7.6825	0.000405001
ADARB1	8069178	-0.4601	7.5346	0.000364183
ZNF778	7997904	-0.4595	9.5626	0.00146865
MARS	7956443	-0.4586	9.8016	0.00030757
CFL2	7978586	0.4576	8.1734	0.00308751
SIDT2	7944049	-0.4573	9.1863	0.000458543
PRKAA1	8111796	-0.4571	9.6104	0.000844037
BDP1	8177560	-0.4570	8.7438	0.002165375
RASL11A	7968236	-0.4565	5.9042	0.002211896
BCOR	8172088	-0.4556	8.3496	0.000266537
MAPKAP1	8164177	-0.4549	9.2505	0.000637383
NELF	8165552	0.4549	7.5020	0.019752498
C12orf57	7953564	0.4543	9.7057	0.000904839
ZBTB34	8157947	0.4533	6.4577	0.000202802
RGPD1	8043324	0.4531	8.3104	0.002777838
PDE3B	7938629	-0.4530	5.8556	0.002437485
GLI3	8139212	-0.4529	4.9764	0.025518136
CDC25A	8086880	-0.4529	7.2617	0.004407518
RRM2B	8152133	-0.4523	8.3983	0.000972946
TRIB3	8060344	-0.4523	7.2025	0.002133006
PHLDA1	7965040	0.4521	5.9800	0.003018945
BDP1	8106025	-0.4517	8.7273	0.002341757
DGKE	8008629	0.4512	6.1332	0.000972946
FBXO9	8120269	0.4509	5.0752	0.035556833

Gene Name	ID	Log2 Fold Change	Average expression	Adj. p value
AKAP9	8134122	-0.4505	7.2102	0.002776768
KIDINS220	8050128	-0.4504	8.5091	0.001833515
OTUD4	8103011	-0.4499	5.8701	0.016947308
GRHL2	8147697	-0.4496	9.8062	0.000238837
RGPD3	8054414	-0.4481	9.5394	0.001750232
METT10D	8011275	-0.4479	8.6370	0.001743213
BCL9L	7952116	-0.4478	7.7909	0.003995567
YAP1	7943398	0.4477	8.9931	0.002819031
ZDHHC21	8160151	-0.4463	8.0284	0.005105589
PLCB4	8060897	-0.4462	7.7130	0.003313816
NAMPT	7933084	-0.4461	10.8760	0.001612308
SLC5A1	8072587	-0.4451	5.5119	0.007099157
KGFLP2	8161362	-0.4449	6.7235	0.000505569
SNORA48	8004506	-0.4446	9.4992	0.019531213
FASTKD1	8056693	-0.4441	8.2692	0.004861112
TRMT112	7949075	0.4434	11.4958	0.004433768
C1QTNF3	8111443	-0.4433	6.4499	0.043605931
SNORA16A	7914216	0.4429	7.1222	0.001654064
NRBF2	7927775	-0.4423	6.2997	0.019118941
ZFP36L2	8051814	0.4420	7.8133	0.001622189
PCDHB2	8108683	0.4418	5.0866	0.003634519
HOMER2	7991034	-0.4418	7.2129	0.024589335
ATG2B	7981217	0.4416	6.8410	0.002154295
MRGPRE	7945859	-0.4412	6.0650	0.001498022
DENND4C	8154531	-0.4409	7.9798	0.000164242
SNORD45C	7902396	0.4409	6.0444	0.014035955
DUSP2	8053882	-0.4398	7.6458	0.001638189
USP32	8017212	0.4397	7.8927	0.001589524
EP300	8073345	0.4391	7.3038	0.006790834
KIAA0232	8093961	-0.4387	7.3026	0.003502009
TAPT1	8099506	-0.4386	7.0770	0.017621631
SLC6A9	7915543	-0.4379	7.4087	0.007285424
EGLN3	7978544	0.4379	6.9654	0.005618738
POM121L8P	8105935	0.4376	6.3485	0.048409273

Gene Name	ID	Log2 Fold Change	Average expression	Adj. p value
GABPA	8133030	-0.4372	7.8353	0.015437209
NUCB2	7938687	0.4353	11.2205	0.003106571
RPS6KC1	7909661	-0.4350	7.7453	0.000336875
BIRC6	8041283	-0.4347	7.6390	0.001287848
ATF5	8030557	-0.4346	7.0641	0.0002716
KITLG	7965322	0.4344	5.3242	0.014616995
LIFR	8111677	-0.4336	7.3945	0.002514277
SNORD30	7948900	-0.4334	9.0248	0.001191312
RGPD4	8044161	0.4332	9.4207	0.001416024
SNORD35A	8030366	-0.4329	8.2206	0.015467423
H2AFJ	7954124	0.4327	6.6378	0.000208194
THRSP	7942793	-0.4325	5.6971	0.000824088
CENPN	7997381	-0.4324	8.6721	0.00022265
FLII	8013191	0.4322	9.2371	0.00016384
CALU	8135955	-0.4321	9.1507	0.000982419
JAG1	8064978	0.4317	7.5608	0.000596362
ZNF680	8139820	-0.4315	6.4279	0.04507466
HINT3	8121886	-0.4312	8.2835	0.003056383
PAK1	7950578	-0.4310	5.2727	0.002718492
CAP2	8117054	-0.4309	8.4446	0.001055667
DHRS7	7979473	-0.4306	10.2867	0.000142483
USP34	8052443	-0.4304	7.8833	0.002819031
MLLT4	8123407	-0.4296	6.4442	0.002602854
STK38	8126018	-0.4293	7.7400	0.000154675
HERC1	7989516	-0.4292	6.8837	0.004261106
DNAJC27	8050790	-0.4286	5.4624	0.028690578
CHD9	7995583	-0.4278	6.7138	0.005309221
NBEAL1	8047596	-0.4274	6.4853	0.043989688
BNIP3L	8145454	-0.4274	10.0607	0.005689869
MLKL	8002778	-0.4269	6.9527	0.000904839
KBTBD7	7971218	0.4269	7.5444	0.001595165
CAMK2N1	7913237	-0.4256	10.6376	0.000883258
MLL3	8143988	-0.4253	7.8110	0.003678478
TNRC6B	8073214	-0.4252	7.9877	0.001638189

Gene Name	ID	Log2 Fold Change	Average expression	Adj. p value
ARFGAP3	8076515	-0.4252	8.4237	0.005008879
INSIG2	8044766	-0.4246	8.3616	0.014035955
MOSPD1	8175288	-0.4244	6.2478	0.024775747
ZNF217	8067113	-0.4232	9.8255	0.000545484
TRMT61A	7977105	0.4223	6.2186	0.001371947
C12orf5	7953211	-0.4219	7.2624	0.002513767
KLF9	8161648	-0.4217	8.1862	0.005981612
LRTOMT	7942315	-0.4208	6.5061	0.002513767
CDC42BPB	7981387	-0.4206	8.2058	0.001025165
NSMAF	8150928	-0.4206	7.4207	0.000241051
ADD3	7930380	-0.4203	9.7546	0.002798379
KDELR3	8073015	-0.4200	8.6888	0.003686546
TMEM144	8098041	0.4199	8.1244	0.00842909
HBP1	8135392	-0.4194	8.7958	0.009093117
DSP	8116780	-0.4194	8.7430	0.004547799
ETNK2	7923596	-0.4185	5.3181	0.000328423
RGPD5	8054676	-0.4183	9.4289	0.001963293
SLC16A10	8121515	-0.4180	7.9233	0.007689861
MLL5	8135277	-0.4158	8.5293	0.000328423
SNORD32A	8030360	0.4158	7.6294	0.001255217
P4HA2	8113981	-0.4156	7.9390	0.014368072
TACR2	7934074	0.4155	6.4515	0.005155841
HIVEP1	8116910	-0.4152	7.1672	0.00308751
TGFBR1	8156826	-0.4149	8.2104	0.000956819
LDHA	7938777	-0.4148	12.2860	0.002513767
DENND1B	7923131	-0.4141	7.5912	0.000543107
GRWD1	8030035	0.4133	7.9597	0.000243131
USP24	7916443	-0.4133	7.3786	0.001260191
PTK7	8119689	-0.4127	6.6534	0.002380204
CDC14B	8162610	-0.4124	5.2282	0.018804535
GCC2	8044236	-0.4124	8.7076	0.002122047
KIAA1217	7926679	-0.4106	6.9190	0.000467315
FAM69A	7917728	-0.4105	6.9890	0.004185704
ABTB2	7947462	-0.4104	6.2581	0.000417369

Gene Name	ID	Log2 Fold Change	Average expression	Adj. p value
DYNLT1	8130499	-0.4103	6.9411	0.01168015
SLITRK3	8091863	-0.4099	5.2129	0.018686451
SLC26A2	8109194	-0.4096	6.6989	0.008602471
ETFDH	8098084	0.4094	9.2023	0.004164072
SNORD57	8060503	0.4094	8.8056	0.01282664
SRCRB4D	8140403	-0.4093	5.4762	0.025961152
ZFYVE16	8106602	0.4092	7.1929	0.00605817
ARMC6	8027117	-0.4084	8.0567	0.003031508
PPP1R14C	8122734	-0.4084	7.6582	0.000972946
DHX29	8112081	-0.4082	8.7438	0.002276164
PTCH1	8162533	-0.4082	7.2615	0.00066405
C1QTNF6	8075897	-0.4081	5.6575	0.026327571
XG	8165808	-0.4080	6.5235	0.011591732
TMSB4X	8158240	-0.4076	7.4238	0.023572734
IDH2	7991374	-0.4074	10.2210	0.00176934
TMEM194A	7964347	0.4072	8.5736	0.001708727
SHMT2	7956401	-0.4069	10.4353	0.000471923
DOCK4	8142345	0.4069	5.8844	0.021852625
MC1R	7998055	0.4065	6.0335	0.001400957
P2RX5	8011415	-0.4064	6.1434	0.007793275
SIK2	7943760	-0.4063	7.2662	0.006174131
ZNF462	8157105	0.4057	8.4672	0.003005735
TSPAN5	8101828	0.4056	5.5401	0.010597199
GNAI1	8133860	-0.4056	5.2641	0.023947498
RGPD6	8044304	-0.4056	8.9409	0.002524254
HIST1H3E	8117415	-0.4044	6.8426	0.023567292
ANKRD13C	7916928	-0.4042	8.2344	0.000639434
ATXN1	8124040	0.4041	6.1558	0.008464216
DUSP12	7906810	0.4041	6.9631	0.002640135
SFTPA2	7934698	-0.4036	6.8700	0.001055667
C6orf211	8122818	-0.4033	7.4209	0.048409273
SLC44A4	8179861	-0.4033	11.3253	0.000972946
DCP2	8107356	-0.4033	8.0537	0.004450664
HBEGF	8114572	-0.4032	6.7704	0.025700072

Gene Name	ID	Log2 Fold Change	Average expression	Adj. p value
DFFB	7897210	-0.4028	6.5190	0.00134578
PSD4	8044584	0.4020	7.1640	0.009212472
BZW1L1	8047339	-0.4020	10.5071	0.000482638
EMB	8112007	-0.4019	7.7879	0.035321534
KCNK5	8126153	-0.4018	7.2828	0.005915447
CPEB4	8110055	-0.4017	7.4891	0.014153369
PTPN21	7980616	-0.4016	5.6175	0.026917423
DMXL2	7988789	0.4015	7.8606	0.001750232
IDH1	8058552	-0.4013	11.9211	0.002099462
ARHGAP28	8019964	-0.4012	6.6286	0.006841267
PLEKHM1	8016239	-0.4005	6.5159	0.046983922
DIRC2	8082120	-0.4004	8.4638	0.001995466
GCNT2	8116835	-0.4002	5.1082	0.017341678
SLC1A5	8037835	-0.4001	8.2413	0.001375807
SNORA61	7914212	0.4000	8.1187	0.005155841
AP1S2	8017210	0.3999	6.1485	0.013070467
MYO1E	7989277	-0.3998	7.1436	0.00456168
IFRD1	8135514	-0.3998	7.5843	0.011093574
BMF	7987454	0.3991	6.1563	0.005527065
KRTCAP3	8040949	-0.3985	7.9284	0.004938082
SNORD1C	8010078	0.3980	8.2433	0.017063158
MIA3	7909898	0.3978	9.2498	0.000471923
GRHL1	8040190	-0.3973	6.8062	0.000216716
ZSCAN5A	8039577	0.3966	5.9343	0.010385872
HMGCS2	7919055	-0.3964	10.8856	0.000516441
SLC16A13	8004266	-0.3940	6.9880	0.000767482
ROCK2	8050302	-0.3933	8.1116	0.000340943
CYP2E1	7931643	0.3928	6.1941	0.002684439
QSER1	7939158	0.3923	7.5993	0.002515774
YOD1	7923967	-0.3920	6.9968	0.034835838
WWP2	7996976	-0.3918	7.4546	0.000829415
SNORD116-21	7981990	0.3912	9.5333	0.026603781
SSBP2	8112940	-0.3907	6.1076	0.012155462
BOD1	8115865	0.3905	8.0437	0.027623943

Gene Name	ID	Log2 Fold Change	Average expression	Adj. p value
PCK2	7973530	0.3899	7.5305	0.000922414
AP4E1	7983679	-0.3899	6.2058	0.008537904
FZD3	8145611	-0.3896	7.5771	0.005155841
TMEM167A	8112967	-0.3893	9.2581	0.017884907
SPIRE1	8022356	0.3892	7.4362	0.015417415
RPL13	7997933	0.3889	7.6568	0.036974673
KATNAL1	7970844	-0.3889	7.1549	0.02906207
FAM135A	8120552	-0.3888	5.7577	0.005618738
FAM125A	8026751	0.3886	8.0791	0.00234862
ZNFX1	8066905	-0.3885	7.4209	0.006150047
KIAA0415	8131265	0.3884	6.7076	0.005364435
GNPAT	7910520	-0.3882	7.9835	0.003346945
DDHD1	7979223	-0.3881	7.0032	0.012500618
NSL1	7924172	-0.3876	9.3012	0.007060106
LGALS8	7910706	-0.3874	7.9697	0.000646352
KTELC1	8081853	-0.3872	6.9013	0.028465534
ADM2	8074063	0.3865	7.1105	0.008503983
FKBP11	7962895	0.3861	7.5447	0.000639965
UBN2	8136516	-0.3859	7.4672	0.000593615
CHML	7925500	-0.3856	7.3689	0.001667914
BMPR2	8047538	0.3855	7.9631	0.011089069
SNORD116-8	7981964	-0.3851	8.9209	0.01775324
KIAA0494	7915882	-0.3851	9.2405	0.000938098
HCCS	8165995	-0.3850	8.9726	0.002396771
RALB	8044919	0.3849	8.9715	0.000951702
NPTX2	8134463	0.3845	7.0501	0.021881697
TFR2	8141560	0.3844	6.3311	0.015048195
ARL1	7965789	0.3843	8.5317	0.01235511
CCNC	8128429	-0.3840	8.2754	0.01024282
ERRFI1	7912157	-0.3837	7.3245	0.014368072
NSD1	8110289	-0.3835	8.4879	0.001136292
GRB2	8018364	-0.3834	8.6392	0.000292399
ZBTB34	8157941	0.3831	7.1018	0.000904839
HIST1H2AK	8124524	-0.3830	7.7932	0.008327237

Gene Name	ID	Log2 Fold Change	Average expression	Adj. p value
NVL	7924558	-0.3829	8.9290	0.008512498
PIKFYVE	8047865	-0.3820	7.5793	0.001750232
PTPRJ	7939839	0.3814	7.1322	0.005618738
DDX10	7943690	0.3812	7.7326	0.006030487
ZAK	8046461	0.3812	5.9887	0.01470731
C5orf4	8115397	0.3812	6.0873	0.006030487
GATSL1	8140249	0.3812	7.8810	0.000904839
GPR161	7922108	0.3811	6.4143	0.001454854
KIAA1109	8097148	-0.3803	6.8413	0.018804535
HTT	8093685	-0.3798	7.2139	0.00234862
NSF	8007885	-0.3790	10.2956	0.000596362
ZBTB37	7907486	-0.3789	6.7132	0.007285424
SCARNA16	8010137	0.3787	6.6002	0.012171738
PCNX	7975416	-0.3786	7.2653	0.002808122
SNORA49	7960052	0.3786	6.1569	0.029127419
KDM5B	7923453	-0.3781	9.1437	0.001497616
FKBP14	8138834	-0.3777	7.2056	0.001377088
NCOA6	8065776	-0.3776	7.2634	0.009093117
PLEKHM3	8058512	-0.3770	6.6060	0.012892319
SNX13	8138401	-0.3770	8.1526	0.004313876
ALG11	7969228	0.3769	8.6777	0.001612308
NSUN5	8140020	0.3769	9.1533	0.00093374
CIDEB	7978272	0.3767	5.6376	0.010067054
RABGGTB	7902382	0.3763	9.6553	0.001090203
SNHG12	7914202	-0.3760	7.9755	0.003493468
ABCD1	8170704	-0.3756	8.1025	0.016172585
ACOX3	8099304	-0.3755	6.9213	0.025424694
PDCD4	7930454	0.3754	10.1867	0.016947308
LOC100133075	7919582	-0.3754	5.9618	0.006320354
MAP3K1	8105436	0.3753	7.4146	0.00605817
NUPR1	8000574	0.3753	10.0815	0.000709827
EIF2S2	8065730	-0.3753	8.8896	0.001642189
TMEM14A	8120239	0.3751	9.0430	0.026343585
PSPH	8137464	-0.3750	8.8780	0.016784986

Gene Name	ID	Log2 Fold Change	Average expression	Adj. p value
TRAPPC6B	7978739	-0.3747	8.7839	0.001120321
HERC4	7933947	0.3745	7.9925	0.005381707
GCLM	7917779	-0.3745	7.4644	0.012956028
GBAS	8132929	-0.3744	9.1354	0.013574157
INADL	7901804	-0.3744	8.3099	0.00132309
DENND1B	7923141	0.3744	7.1306	0.005572223
NCRNA00176	8064242	-0.3744	6.0236	0.004243856
SCD	7929816	-0.3744	11.0593	0.004861112
MLLT6	8014702	-0.3742	5.5374	0.015021849
ANKRD56	8101207	-0.3737	6.9688	0.001050155
TMEM138	7940473	-0.3737	8.9231	0.007139309
STAT3	8015607	-0.3736	10.3964	0.00151056
EFNA5	8113433	-0.3732	10.4219	0.001476492
MTHFR	7912496	-0.3727	6.6486	0.00578388
TMEM164	8169365	-0.3726	7.7143	0.007429302
XPR1	7907861	-0.3721	8.4806	0.001964278
ZNF827	8103025	0.3720	6.4176	0.003201753
POLR3G	8106820	-0.3719	7.5986	0.010067054
LRG1	8032834	-0.3716	5.5835	0.016880098
VIPR2	8165658	0.3715	10.3986	0.013208818
KLRAQ1	8041913	0.3713	7.0739	0.027962692
WDR1	8099340	-0.3713	9.6553	0.002165375
NCRNA00094	8159109	0.3710	6.2021	0.011864184
ZNF778	7997896	-0.3703	6.4018	0.010135892
ACTR3C	8143766	-0.3700	5.8355	0.025424694
CPEB3	7935011	-0.3698	5.8736	0.012171738
STRN	8051443	-0.3698	7.0023	0.004878192
PITPNC1	8009353	-0.3695	6.6933	0.002887138
YPEL5	8041197	-0.3695	6.5207	0.000520025
PRRC1	8107750	-0.3692	9.6757	0.002819031
SLC39A10	8047174	0.3690	8.2475	0.003629423
PBX3	8157890	0.3689	5.3899	0.01316682
METTL11A	8158544	0.3689	7.9956	0.029474036
PILRB	8134789	-0.3689	7.5915	0.026319327

Gene Name	ID	Log2 Fold Change	Average expression	Adj. p value
CXorf40A	8170393	-0.3689	6.5885	0.022699848
RLF	7900395	0.3685	8.0879	0.00234862
KPNA5	8121632	0.3685	5.6563	0.030796727
ERCC5	7969935	0.3681	8.0458	0.026343585
SMYD2	7909689	-0.3678	6.0930	0.01282664
EIF3B	8131111	0.3675	9.8419	0.002946139
LRBA	8103106	-0.3675	9.9221	0.004624311
RCC1	7899462	0.3674	10.5020	0.000703721
SECISBP2	8156295	-0.3673	7.4315	0.007149819
PPAN-P2RY11	8025563	-0.3664	7.9144	0.001050155
SNX11	8008096	-0.3661	7.2986	0.005699376
TTC39A	7916024	0.3652	7.5856	0.003173893
COCH	7973797	-0.3651	6.0341	0.004926083
PHF12	8013812	0.3648	9.1779	0.000972946
IKZF3	8014891	-0.3648	6.8436	0.005155841
C20orf112	8065612	-0.3647	5.7143	0.012221529
GAGE12B	8167575	-0.3643	10.1794	0.041954878
C10orf12	7929609	0.3639	6.8083	0.005336078
FUT8	7975136	-0.3639	7.2582	0.000526349
COX11	8117696	-0.3638	7.5093	0.038808416
CDCA5	7949364	-0.3635	7.6897	0.015848543
TMPPE	8086048	0.3626	6.1493	0.009605693
CEP350	7907790	0.3625	6.6133	0.007285424
ARHGAP5	7973840	0.3625	8.1457	0.002464568
PHTF1	7918634	0.3622	5.1793	0.025547433
OSR2	8147573	0.3622	8.5365	0.000505361
CYFIP2	8109528	-0.3611	7.1128	0.004028296
SHC4	7988563	-0.3609	5.7552	0.038263821
IFRD2	8087576	-0.3606	7.8849	0.002819031
DZIP3	8081503	0.3603	5.2115	0.003629423
MKL2	7993310	-0.3601	7.1797	0.001407064
MPP5	7975203	0.3593	8.8518	0.003313816
ESPNL	8049598	0.3592	5.5863	0.036455623
C4orf29	8097373	-0.3586	6.8240	0.01024282

Gene Name	ID	Log2 Fold Change	Average expression	Adj. p value
MTHFD2	8084064	-0.3585	9.4142	0.001910699
PYGO2	7920594	-0.3581	6.7466	0.001988129
KGFLP2	8155530	0.3581	5.9771	0.005625748
MYRIP	8078933	-0.3580	6.5657	0.013192557
PPFIA2	7965166	-0.3580	8.9384	0.00753292
USE1	8026679	0.3578	9.0162	0.000940227
TMSB4X	8166072	0.3576	8.5934	0.005686787
MLL	7944223	0.3574	7.2137	0.005040271
DDIT3	7964460	-0.3573	8.1272	0.003130397
H1FX	8090555	0.3573	8.0394	0.006229099
HIBCH	8057719	0.3571	8.0851	0.024811368
IPO4	7978132	0.3567	8.0454	0.00045767
TMSL3	8101774	-0.3566	9.0016	0.003250482
CHST10	8054297	0.3565	7.3040	0.003370796
UGCG	8157216	0.3565	6.8541	0.004537469
TRIM4	8141363	0.3563	7.5587	0.013919664
CERK	8076792	-0.3563	6.6495	0.001769414
SNORD116-3	7981966	0.3562	9.2832	0.027927135
ZNF211	8031792	-0.3557	5.7647	0.026068651
FRYL	8100292	-0.3556	6.7157	0.036860673
LGTN	7923889	-0.3554	7.7094	0.002630632
SYNJ1	8070010	-0.3551	6.4925	0.010418148
C9orf72	8160531	-0.3550	6.9847	0.00682399
SCO1	8012823	0.3549	8.4392	0.017388287
LRSAM1	8158028	0.3547	7.1450	0.001213806
RP2	8167006	0.3540	7.6782	0.003219915
MTAP	8154635	0.3540	6.6979	0.003045239
LANCL2	8132897	0.3535	8.6561	0.01069969
NAP1L1	7965048	-0.3534	10.8187	0.009291479
RTN1	7979455	-0.3534	7.0842	0.003310067
OGFOD2	7959535	-0.3533	6.4581	0.007381221
ZFYVE20	8085537	-0.3533	6.7151	0.011512922
SPATA18	8095021	-0.3532	6.9669	0.01532307
USP9X	8166826	0.3527	8.7070	0.001671556

Gene Name	ID	Log2 Fold Change	Average expression	Adj. p value
SMG1	7999841	0.3521	7.1728	0.026105838
ZDHHC20	7970524	0.3518	8.6151	0.002165375
PCDHGB4	8180282	-0.3515	6.7926	0.049425232
RNF187	7910372	-0.3513	8.9515	0.006052171
MNS1	7989146	-0.3510	6.4570	0.014368072
NCOR2	7967493	-0.3506	6.6153	0.001920444
WNK3	8173059	-0.3503	5.9283	0.015416009
TMSB4X	8067007	0.3503	7.6247	0.024328568
ALDH1A3	7986446	-0.3502	7.1474	0.003539238
SLC9A7	8172280	-0.3499	8.4496	0.001840538
LCP1	7971461	-0.3497	8.6392	0.012673788
GXYLT1	7962349	0.3496	7.0980	0.008753538
ACTR3	8044686	-0.3495	10.8002	0.001873784
RNF19A	8152041	0.3489	8.3711	0.007661799
NPM3	7935903	0.3488	7.7205	0.016484623
AQP3	8160670	0.3487	8.5857	0.013412813
PHF10	8123463	0.3486	7.6866	0.005434447
AGT	7924987	-0.3486	5.3331	0.014616995
BTN3A2	8117435	-0.3481	6.2324	0.02418934
LOC100130274	8153486	0.3475	5.4770	0.007285424
LRRC58	8089830	-0.3470	8.5339	0.018559265
POFUT1	8061706	0.3467	8.3697	0.00234862
FAM69B	8159373	-0.3465	7.4352	0.007759789
TAOK3	7966851	0.3459	8.0242	0.001191312
CYTH2	8030064	-0.3458	6.5055	0.010010053
AGPS	8046604	0.3458	8.0598	0.014337228
EPHA6	8081138	0.3458	5.4365	0.009721367
ALDOC	8013660	0.3458	10.0504	0.025475646
KLF15	8090343	-0.3456	6.6833	0.013051547
NOVA1	7978391	-0.3455	7.2070	0.004141984
CDK5R1	8006409	0.3453	6.8621	0.008905804
GSK3B	8089801	-0.3452	9.3061	0.00151856
MTUS1	8149500	-0.3451	6.4161	0.007931533
VWA2	7930663	-0.3449	5.9040	0.006790834

Gene Name	ID	Log2 Fold Change	Average expression	Adj. p value
ERBB2	8006906	-0.3448	9.1768	0.000784639
ERBB2IP	8105681	-0.3444	9.0392	0.008250925
PDK1	8046408	-0.3439	8.7594	0.018686451
NCAM2	8067985	0.3437	11.1930	0.000598218
MAGEA2	8170562	-0.3436	8.5606	0.002396771
CYTSA	8071881	-0.3436	10.0361	0.005512883
C12orf23	7958346	0.3436	7.1746	0.01069969
MAGEA2	8175732	-0.3429	8.4798	0.002227263
PLA2G7	8126784	-0.3428	7.0012	0.01607103
TANC1	8045889	0.3426	9.3663	0.003261162
SLC39A3	8032525	-0.3425	7.7389	0.00661849
KCTD11	8004360	0.3424	6.7425	0.027754575
BRWD1	8070341	0.3422	7.2032	0.006030487
TMEM147	8027876	-0.3420	9.5743	0.044319155
UVRAG	7942626	0.3418	7.4790	0.0163819
HOXD13	8046524	0.3418	6.3884	0.022799939
MTHFD2	8042830	0.3416	9.9406	0.001021242
FCHO2	8106141	-0.3415	7.5365	0.000699941
MRPL20	7911566	0.3411	6.3816	0.024902174
PYCR1	8019316	0.3411	9.5457	0.001454854
ATP8A1	8100026	0.3410	5.0662	0.011936774
CD97	8026300	0.3405	7.6293	0.009795947
C10orf41	7928531	0.3405	5.6778	0.038349582
GPNMB	8131844	0.3401	8.4437	0.017894987
FJX1	7939365	-0.3390	5.5839	0.003799446
C6orf81	8118981	-0.3387	5.2745	0.034887168
SARS2	8036656	-0.3386	7.4098	0.002887138
CA1	8151592	-0.3380	5.6147	0.040068616
ATP2B4	7908940	0.3380	7.8183	0.004789986
FLNB	8080714	0.3379	10.2785	0.003266784
NKRF	8174684	-0.3379	6.4281	0.017482234
SLC43A1	7948249	0.3377	9.1968	0.007735184
C16orf93	8000932	-0.3370	6.1461	0.000885072
NOTCH3	8034940	-0.3370	7.8765	0.008142095

Gene Name	ID	Log2 Fold Change	Average expression	Adj. p value
HMHB1	8108900	-0.3370	5.3999	0.009919961
LRRC14	8148923	0.3369	7.3344	0.021939645
UBE2G2	8070799	-0.3366	8.3641	0.001524444
SLC12A7	8110755	-0.3364	7.5130	0.001748692
VLDLR	8154100	-0.3364	7.0570	0.027183052
MSTO1	7906021	0.3363	8.5414	0.002227263
NETO1	8023828	0.3362	10.2119	0.004537469
C12orf60	7954132	-0.3360	5.1512	0.007247485
SETDB2	7969114	0.3359	6.5652	0.040809988
EEF1B2	8047771	0.3356	7.3641	0.008945048
DHPS	8034454	-0.3356	8.7212	0.020672791
ACSF2	8008321	-0.3355	6.3764	0.015345078
C14orf79	7977331	0.3354	6.5709	0.006296535
CTSC	7950906	-0.3349	8.0601	0.000563157
YPEL1	8074780	-0.3346	6.1336	0.035174679
PNPLA8	8142307	-0.3344	8.1010	0.0212636
ALOX12B	8012309	-0.3343	5.4556	0.01128801
JMY	8106516	-0.3341	7.0447	0.003502009
FAM105A	8104570	-0.3340	6.3215	0.030216582
TBC1D20	8064336	-0.3337	7.8549	0.005851699
SMA5	8105937	-0.3336	10.0346	0.019448351
GNPTAB	7965812	0.3336	7.9163	0.019448351
ABCC4	7972297	-0.3335	9.0914	0.002227263
KIF3A	8114030	-0.3332	7.6475	0.015472566
C14orf128	7978538	0.3328	6.0405	0.008765532
IMPA2	8020183	-0.3324	8.0403	0.001653372
SRBD1	8051963	-0.3324	7.2583	0.013532891
SMA5	8112491	-0.3324	10.1240	0.023978539
RBPJ	8094460	-0.3321	9.0332	0.012743957
ARMC8	8082940	-0.3320	7.7133	0.003126075
SPRY1	8097282	-0.3318	7.0354	0.025961152
CDK8	7968199	0.3317	10.2096	0.014974676
PVRL4	7921773	0.3316	6.4195	0.010418148
OPN3	7925492	-0.3316	5.2547	0.016755883

Gene Name	ID	Log2 Fold Change	Average expression	Adj. p value
RSF1	7950606	0.3315	8.1371	0.0032579
ARID2	7955019	-0.3314	7.7899	0.005246565
NEIL1	7985001	-0.3312	5.4970	0.014462985
ZNF266	8033754	0.3311	8.4284	0.005944076
ARF3	7962904	-0.3306	11.0169	0.001298465
FAM32A	8026541	0.3306	7.9693	0.03039818
KLHL1	7971937	-0.3301	5.3558	0.031088724
CASC5	7982757	-0.3297	7.6579	0.011086293
KAT5	7941382	0.3293	7.8985	0.001441817
TAF9	8112458	-0.3292	8.2376	0.000829588
ZNF367	8162601	0.3290	7.5384	0.003077036
ELMO2	8066716	-0.3288	7.5607	0.003845138
ZNF175	8030831	0.3286	6.3892	0.021166358
SNORA21	8014755	-0.3285	8.0112	0.049171321
SLC45A2	8111417	0.3281	5.7800	0.015411017
NR2F1	8106923	-0.3280	6.5514	0.012001927
RIMS1	8120613	0.3280	6.2512	0.002390066
ALDH16A1	8030321	0.3279	7.4114	0.003313816
CCDC109A	7928318	0.3278	7.7725	0.0236154
CD99L2	8175647	-0.3277	6.9962	0.019531213
EIF2C1	7900030	0.3277	7.8409	0.003073591
TP53	8012257	-0.3274	10.3049	0.005119972
SNORD55	7901046	-0.3273	7.7993	0.032007101
OSBPL1A	8022572	0.3272	7.5239	0.010396103
ANKRD13A	7958600	-0.3271	8.8376	0.002555277
RRP7B	8076449	-0.3267	9.7245	0.00308751
TMEM30A	8127637	-0.3266	9.1298	0.042976315
LPCAT3	7960730	-0.3263	11.2598	0.001111568
ZNF692	7925773	0.3263	8.4341	0.0212636
DENND4A	7989849	0.3252	7.5409	0.012138969
RAB18	7926836	0.3250	9.7404	0.023310173
FXYD5	8027778	0.3250	6.0003	0.025487183
PPM1A	7974781	-0.3250	7.0293	0.012221529
TBC1D22B	8119169	0.3249	6.4191	0.00187409

Gene Name	ID	Log2 Fold Change	Average expression	Adj. p value
DLL3	8028719	-0.3248	6.1300	0.043933078
RCAN2	8126760	0.3248	6.1494	0.017854555
VARS	8178609	-0.3247	9.5113	0.001307001
LATS2	7970498	-0.3245	7.1050	0.015411017
TRMT2A	8074541	-0.3243	7.8479	0.002408141
PACSIN2	8076533	-0.3241	9.4843	0.002211896
SLC38A1	7962516	-0.3237	10.4035	0.000904839
PIK3R3	7915787	0.3236	10.1957	0.004197016
USP28	7951752	0.3235	8.2823	0.001967674
TMEM87B	8044417	-0.3235	8.3808	0.006790834
HIPK2	8143307	-0.3234	8.5105	0.005572223
LZIC	7912292	-0.3228	8.7269	0.004624311
PRKAR1B	8137675	-0.3227	7.7577	0.00308751
CHPT1	7958000	-0.3227	10.8198	0.003244426
RFX3	8159876	0.3227	5.1800	0.009278333
HMGCL	7913682	-0.3226	7.8547	0.012138969
ETFA	7990566	0.3224	10.5371	0.017894987
TBCK	8102171	-0.3222	7.5237	0.014617458
SERINC5	8112865	0.3220	10.7509	0.001979601
LRTM2	7953032	0.3219	5.0521	0.038713492
RYR2	7910792	-0.3218	5.1324	0.011086293
CARS	7945803	-0.3216	8.6160	0.016025874
GAPVD1	8157858	0.3212	8.5531	0.001524444
DYNLT3	8172035	-0.3209	8.0132	0.007138067
CHKB-CPT1B	8077123	-0.3207	7.2030	0.012334564
ETFB	8038792	-0.3207	9.0669	0.005197424
MXD1	8042503	-0.3206	6.2511	0.013319224
CCDC48	8082465	0.3204	7.8337	0.011325323
HCFC2	7958158	0.3203	7.6184	0.007759789
GDPD1	8008802	-0.3203	7.4562	0.025719009
TAOK1	8006030	0.3202	8.1599	0.014368072
APLP2	7945182	-0.3196	10.9900	0.004239338
GLRX	8113214	0.3195	6.5977	0.038966251
LIPT2	7950420	-0.3194	6.2287	0.0333824

Gene Name	ID	Log2 Fold Change	Average expression	Adj. p value
FAR2	7954631	0.3194	5.3091	0.010826403
RICTOR	8111698	-0.3194	6.5976	0.015204148
SNORA44	7914214	-0.3192	6.2061	0.00592218
BBS4	7984686	0.3185	8.1687	0.01069969
C7orf55	8136535	-0.3185	7.7763	0.027623943
KIAA1161	8160786	-0.3184	6.4120	0.017341678
C1D	7934731	-0.3184	7.5328	0.007108908
TPRS1	8152453	0.3184	7.4426	0.011799869
CHD6	8066303	0.3182	8.4241	0.004125747
MRPS12	8028563	-0.3181	7.6366	0.018686451
NT5DC3	7965918	0.3181	5.5860	0.015837229
SNX25	8098581	-0.3181	6.6682	0.012090663
CORO2A	8162744	-0.3178	7.2378	0.019868769
GLYATL1	7940135	-0.3178	8.0252	0.00682399
SLCO4A1	8063923	-0.3177	7.5912	0.023169548
ACSL4	8174474	-0.3176	5.2705	0.009093117
FAM173A	7992043	0.3175	8.2530	0.042280941
CYP39A1	8126770	-0.3170	6.6180	0.011078127
NIPAL1	8094938	-0.3167	7.4611	0.010979794
CNIH4	7910014	0.3165	9.5306	0.002714738
PIK3AP1	7935337	0.3162	7.3788	0.008404168
LRP10	7973352	-0.3159	8.2393	0.008240899
MRRF	8157638	-0.3159	8.6472	0.005173554
DNASE1	7992934	-0.3157	6.2445	0.011078127
UBR3	8046213	-0.3155	7.2817	0.042775487
RHOB	8040473	0.3154	9.3316	0.022786269
MCTP2	7986293	-0.3154	8.8313	0.011654353
SOCS7	8006768	-0.3148	6.5978	0.005967545
KIAA0802	8020037	-0.3147	5.6304	0.034278474
HOXC12	7955852	-0.3147	7.6240	0.006997155
CDK17	7965652	-0.3146	5.5513	0.013967679
KCNMA1	7934570	0.3144	6.1354	0.010437318
PRR3	8117922	0.3140	7.0225	0.011900175
IGSF3	7918913	-0.3140	6.3878	0.02809177

Gene Name	ID	Log2 Fold Change	Average expression	Adj. p value
GPR107	8158597	-0.3138	7.7084	0.003393082
MACF1	7900235	-0.3136	6.6792	0.017708249
CGN	7905406	-0.3132	6.7669	0.012201433
CPT1A	7949971	-0.3131	10.5176	0.006424342
KRT6C	7963410	-0.3127	6.3243	0.010979794
SNORD116-14	7981976	-0.3126	9.8353	0.019951571
QKI	8123315	0.3126	5.9262	0.019531213
PTPLB	8090091	0.3124	10.0636	0.001436944
SPEN	7898278	-0.3123	7.0482	0.010418148
C14orf129	7976571	0.3122	7.5294	0.0056833
INTS8	8147396	0.3119	8.1270	0.030500909
SMG7	7908097	-0.3117	8.2210	0.004903004
KDM5A	7960221	0.3115	7.6944	0.022103359
IER3	8178435	-0.3113	5.3498	0.046408553
SNORA70	8170863	-0.3108	9.9488	0.008014363
IQGAP1	7986010	0.3103	8.4928	0.002133006
RUNX3	7913805	0.3102	5.2123	0.009979044
BAMBI	7926875	-0.3100	9.9501	0.019819643
C12orf51	7966517	-0.3096	6.3585	0.018297681
MZF1	8039809	-0.3094	6.7289	0.021976731
RNF144A	8040090	-0.3092	6.4390	0.046402966
NRP1	7932985	-0.3091	9.1893	0.003266784
DNASE1L1	8176076	-0.3087	7.5387	0.007401013
ISOC1	8107814	0.3086	8.3768	0.002634715
NKPD1	8037502	-0.3086	5.9986	0.007285424
ATXN7L1	8142100	0.3082	6.9792	0.014033183
SECISBP2L	7988581	0.3082	8.7153	0.028690578
CDK14	8134098	0.3079	8.4629	0.006086447
NDUFS1	8058428	-0.3078	10.1959	0.001371947
PLEKHM3	8058509	-0.3074	6.3881	0.048069062
NDUFAF1	7987642	0.3073	8.8866	0.043672149
KIAA0040	7922474	-0.3070	5.4021	0.022760241
DNAJC13	8082688	0.3068	8.5422	0.012568924
C6orf48	8179326	-0.3068	9.6560	0.023688612

Gene Name	ID	Log2 Fold Change	Average expression	Adj. p value
STMN1	7913869	0.3066	9.3255	0.008605613
AGPHD1	7985192	0.3066	7.2346	0.01470731
TTC21B	8056426	-0.3065	7.5338	0.007542939
PSMG4	8116655	0.3065	5.4502	0.043254783
CREB1	8047839	0.3058	9.8736	0.005930282
UFSP1	8141643	-0.3056	7.7409	0.019575033
HOXC5	7955887	0.3055	5.3165	0.04405872
SNORD116-17	7981986	0.3054	10.6604	0.009093117
TBC1D7	8123961	0.3053	7.3285	0.005364435
PABPC1L	8062890	0.3053	6.6008	0.017894987
ALDH2	7958784	0.3053	7.6902	0.014577339
RAPGEF6	8113881	-0.3053	7.9294	0.007897615
C9orf156	8162706	-0.3052	5.7982	0.011192906
GAL	7942064	-0.3052	8.7447	0.023332362
RP1-199H16.1	8076113	-0.3050	6.1484	0.027865691
DUT	7983594	-0.3041	7.3825	0.007931533
MOCOS	8020955	-0.3040	7.2295	0.003073591
SEMA3C	8140534	-0.3038	8.1355	0.035005786
TAGLN2	7921487	-0.3037	7.8177	0.014196112
ZBTB16	7943984	-0.3036	7.1508	0.002208722
KGFLP2	8155490	-0.3036	8.1180	0.005476891
TAF9	8177635	0.3036	8.0948	0.001140391
C11orf67	7942783	0.3035	6.1404	0.045152046
PINK1	7898663	-0.3034	7.0388	0.005430124
ATP2B1	7965359	-0.3033	10.4808	0.001888122
CDC42SE1	7919888	-0.3031	8.1640	0.007688672
SGK196	8146278	-0.3030	9.6248	0.005246565
C5orf42	8111584	0.3029	5.9041	0.038808416
FLAD1	7905831	-0.3026	6.8886	0.001691909
ARHGAP10	8097717	-0.3024	6.4467	0.018794393
POLQ	8089875	-0.3023	7.0543	0.008332397
GTF2A2	7989315	-0.3023	7.6584	0.042635666
VAPA	8020129	-0.3023	7.6891	0.018066495
LGMN	7980958	-0.3021	9.9147	0.001055667

Gene Name	ID	Log2 Fold Change	Average expression	Adj. p value
TUBA4A	8059177	-0.3019	9.8663	0.008603586
PFN2	8091446	-0.3016	8.7036	0.027131451
CANT1	8018982	-0.3012	9.1055	0.015848543
ZBTB10	8147040	0.3011	7.8617	0.002779486
ZMYM1	7899943	-0.3011	7.9985	0.017894987
RPGRIP1L	8001423	-0.3011	6.6893	0.018755253
CASP6	8102311	0.3010	6.8817	0.035277921
LYN	8146500	-0.3010	7.3401	0.013192557
DOCK5	8145365	-0.3009	6.2078	0.049931536
SGEF	8083471	0.3008	9.6077	0.004537469
FTL	8030171	0.3007	8.8325	0.014196112
ERI1	8144516	-0.3004	7.4082	0.005040271
VASN	7992967	0.3003	7.1767	0.045749557
SNORA70	8025498	0.3002	10.0184	0.010071347
CD46	7909400	-0.3000	9.3151	0.011693437
FGFR3	8093518	-0.3000	5.5704	0.031088724
MPZL3	7952036	-0.2998	8.3037	0.005406161
PQLC2	7898556	0.2996	6.3426	0.003747901
PARVA	7938528	-0.2993	7.4224	0.031988553
SLC44A3	7903144	0.2992	7.1184	0.012286269
TNPO2	8034482	-0.2992	9.3756	0.003200652
PSMC3IP	8015642	0.2992	8.6359	0.005618738
CNNM2	7930194	-0.2990	7.2321	0.002158623
ANO10	8086467	-0.2989	8.1681	0.00654007
SMC5	8155770	-0.2987	8.4818	0.033105396
ZNF136	8025998	0.2987	6.7418	0.042331575
PRKAB2	7919305	0.2986	7.3626	0.018804535
LRP8	7916282	-0.2984	7.6087	0.007429302
NPC1	8022531	-0.2983	9.6402	0.005434447
RSL24D1	7989013	-0.2976	9.3153	0.00513864
ADAM9	8146000	0.2973	10.7615	0.009473448
ZCCHC6	8162147	0.2973	7.7452	0.005276616
ADD1	8093643	-0.2971	9.1945	0.005267881
GEMIN4	8010946	-0.2970	8.7903	0.031853927

Gene Name	ID	Log2 Fold Change	Average expression	Adj. p value
DDX23	7962869	0.2970	9.1961	0.014904689
ABAT	7993126	-0.2967	7.6228	0.006035822
TMEM63C	7975932	-0.2965	6.8139	0.00234862
USP53	8097098	-0.2965	7.5767	0.005477583
CDKN2A	8160441	0.2963	6.4707	0.025317743
MEST	8136248	-0.2961	9.1622	0.008976636
PPP1R3B	8149264	-0.2958	7.2811	0.002968353
ZNF652	8016546	-0.2957	7.4354	0.010597199
ZNF3	8141380	0.2955	7.9668	0.002486037
RNF213	8010454	0.2953	7.6511	0.02027519
IGF2BP3	8138566	0.2953	7.1875	0.032908817
NDRG3	8066051	0.2951	9.0985	0.003788361
SCLY	8049582	0.2947	7.6677	0.002416696
ASB1	8049657	-0.2946	7.0944	0.004831664
MFSD6	8047078	-0.2946	7.9082	0.00444811
TNRC6C	8010188	0.2945	6.0589	0.005406161
HOXA5	8138735	-0.2944	6.1398	0.043253664
SDR39U1	7978335	0.2943	7.7530	0.006710886
TMEM65	8152750	0.2942	6.9764	0.008345769
TTL	8044462	0.2941	8.0983	0.003136056
LCNL1	8159531	-0.2939	5.7236	0.034729404
SRPR	7952557	-0.2936	10.2641	0.005197424
USP32	8013262	-0.2934	7.3418	0.012201433
GABPB1	7988687	0.2932	8.2875	0.004734767
P4HTM	8079677	-0.2932	8.1301	0.007270608
POLR2A	8004431	-0.2929	8.2606	0.005377917
PDIA2	7991815	0.2929	5.5403	0.021805508
C7orf27	8137847	0.2926	7.9117	0.012138969
MAN2B1	8034420	-0.2924	8.5579	0.007955593
NOTCH2	7919095	0.2924	7.7535	0.042082121
SLC37A1	8068810	0.2923	7.7487	0.036333365
TXLNA	7899703	0.2921	8.9886	0.005336078
RRP7A	8076455	-0.2918	9.3331	0.003626422
BTAF1	7929201	-0.2916	8.5062	0.008537904

Gene Name	ID	Log2 Fold Change	Average expression	Adj. p value
COX15	7935647	-0.2913	8.1295	0.008834948
DPM2	8164336	0.2911	7.8137	0.037129632
TRUB2	8164428	0.2910	9.6617	0.004674985
CD276	7984743	0.2907	8.1562	0.003788854
YRDC	7915084	0.2906	8.6512	0.013028902
BUD31	8134589	-0.2905	8.1462	0.015509961
CRYAB	7951662	-0.2904	5.9818	0.011461854
PPFIBP2	7938231	0.2904	7.5640	0.003247537
UBR1	7987981	-0.2903	7.7031	0.013384723
BAZ2A	7964203	0.2902	8.1183	0.005618738
RAD9A	7941865	0.2900	8.0173	0.034887168
CENPM	8076393	0.2899	8.0141	0.008240899
YARS	7914563	-0.2897	9.5170	0.001269454
LPAR2	8035703	-0.2897	6.8878	0.021839038
INO80D	8058415	-0.2894	6.8978	0.036333365
RECK	8155169	-0.2894	6.3506	0.027786909
SMCR7L	8073135	-0.2892	8.1026	0.00321537
C1orf43	7920492	0.2892	11.0458	0.00456168
STK33	7946365	0.2891	7.5924	0.019130605
PRMT1	8030437	-0.2891	9.0507	0.011192906
SNORD14C	7952339	-0.2889	8.3048	0.013384723
BRD3	8164995	-0.2888	7.5118	0.015204148
EPCAM	8098439	-0.2885	10.0053	0.049598476
ADRBK2	8072015	0.2882	7.3045	0.011797386
OVOL1	7941401	-0.2882	6.7323	0.015116855
CBWD3	8155422	0.2880	9.0049	0.01172401
CD3EAP	8029688	0.2879	6.6425	0.018831808
UTP6	8014081	0.2879	9.7426	0.004053203
KIAA0922	8097867	0.2879	7.4728	0.002259281
RIOK3	8020508	0.2879	8.8347	0.006150047
TIMP2	8018966	-0.2878	9.3504	0.001850635
SGK3	8146717	-0.2878	7.6590	0.029155209
CMBL	8110971	0.2878	9.2175	0.007076485
OSTF1	8155883	0.2877	9.3751	0.010598481

Gene Name	ID	Log2 Fold Change	Average expression	Adj. p value
NOP56	8060484	-0.2873	7.9887	0.027183052
SLC25A6	8177003	-0.2872	11.1179	0.005290066
STRA13	8019350	0.2871	8.5215	0.022086872
DTL	7909568	0.2871	8.7905	0.013621424
MARVELD2	8177498	-0.2870	8.4655	0.013384723
TELO2	7992271	-0.2866	6.7164	0.008240899
SLC25A19	8018352	0.2865	6.6753	0.008905889
RAPGEF2	8098121	-0.2864	6.4170	0.035135997
SUGT1	7969271	-0.2864	8.1780	0.018559265
ARID4A	7974621	0.2864	6.7143	0.02716489
TAF9B	8176263	-0.2863	8.8089	0.006199916
UBA2	8027650	-0.2861	8.8520	0.007594649
FLJ41484	7972932	-0.2861	6.8674	0.043420001
PANK1	7934945	0.2860	7.3777	0.006030487
GAS2L1	8072216	-0.2859	7.5057	0.011900175
CAST	8107005	-0.2858	8.0535	0.012171738
ARL6IP5	8080926	-0.2857	11.2053	0.006977808
MKX	7932733	0.2857	5.9077	0.025626863
DISP1	7909954	-0.2856	6.2068	0.012975614
C7orf60	8142415	0.2854	7.6296	0.016784986
GDF11	7956026	-0.2853	6.7556	0.035931146
RNF11	7901376	-0.2853	8.5513	0.019049754
C11orf51	7950128	0.2852	8.3148	0.042385278
WDR3	7904364	-0.2852	8.3287	0.005515469
GGCX	8053429	0.2852	7.8079	0.002714738
LYRM7	8107859	0.2852	7.0454	0.007897615
SLC7A5	8003298	-0.2850	9.4031	0.006150047
CHMP2B	8081055	0.2850	7.9906	0.027962692
DGCR14	8074364	-0.2845	6.0563	0.033054274
MTFR1	8146649	-0.2841	9.8809	0.00632222
BSDC1	7914530	-0.2837	8.5917	0.004883169
RRP1	8068938	-0.2836	8.0167	0.004028296
CLDN4	8133360	0.2836	8.5360	0.00861356
SDCCAG3	8165156	0.2834	7.9841	0.017894987

Gene Name	ID	Log2 Fold Change	Average expression	Adj. p value
KTI12	7916130	0.2833	8.5685	0.006547923
ATP11C	8175492	-0.2833	7.7271	0.012192018
CDK20	8162194	0.2833	6.5531	0.042023075
SCOC	8097521	-0.2832	7.9947	0.00456168
UBE4A	7944195	0.2832	9.6232	0.017095761
SLC35A3	7903281	-0.2831	8.8971	0.003065029
FBXO28	7909992	0.2829	10.0941	0.048633412
HDHD3	8163505	-0.2828	7.6698	0.007982084
THOC5	8075239	-0.2828	8.7039	0.002113552
NUFIP1	7971361	-0.2828	7.4423	0.014226323
GADD45G	8156309	-0.2825	7.5612	0.025961152
NSUN5P1	8133633	-0.2825	7.9828	0.022547153
FPGT	7902308	-0.2824	8.3370	0.007302344
C1D	7934729	-0.2823	7.1568	0.013967679
C10orf46	7936596	-0.2820	7.6339	0.014618841
MYC	8148317	0.2817	10.1339	0.045042823
ZMYND8	8066786	-0.2815	7.4306	0.005173554
ADCY9	7999079	0.2814	6.6931	0.049431491
GNAQ	8180344	0.2813	6.1855	0.049718232
OSBPL11	8090277	0.2813	6.6856	0.011078127
FBXO45	8084947	0.2812	8.1383	0.006638336
ARMC1	8151066	0.2809	8.7069	0.036593402
ANKRD50	8102720	-0.2808	7.2037	0.007853617
C1orf198	7924996	0.2808	7.3036	0.041605393
SLC19A1	8070912	0.2807	7.3045	0.025943062
C17orf63	8013776	-0.2807	7.5295	0.026418148
ATG12	8113651	-0.2806	6.8472	0.008765532
SAT1	8166469	0.2804	8.7546	0.021394491
TRAIP	8087513	-0.2798	6.3013	0.005381707
ZNF358	8025179	0.2796	8.5282	0.023310173
QTRT1	8025728	0.2795	8.4507	0.012109876
PGM2	8094556	-0.2795	9.5627	0.014616995
APCDD1	8020141	-0.2794	5.9045	0.036825871
LOC349196	8149216	0.2793	6.6561	0.021718883

Gene Name	ID	Log2 Fold Change	Average expression	Adj. p value
SLC35F5	8054771	0.2793	9.0164	0.001619792
KIAA0319L	7914809	-0.2791	9.1116	0.003266784
TSPYL2	8167763	-0.2783	7.7257	0.011408058
MAP3K3	8009183	0.2783	7.2784	0.01129947
C14orf33	7979351	-0.2782	6.3625	0.010289096
RNF4	8093590	0.2780	7.3282	0.010176629
USP47	7938448	-0.2778	8.7207	0.008537904
SH3BP5	8085556	-0.2775	6.1387	0.005243182
GNG4	7925250	0.2774	7.0231	0.043359579
MDK	7939665	0.2773	8.8993	0.004463234
SLC38A6	7974816	-0.2772	7.3599	0.049431491
NF1	8006239	-0.2770	8.1740	0.021194224
MCM5	8072687	0.2770	9.5309	0.039748821
RBM9	8075673	-0.2768	8.5398	0.003130397
GAS8	7998103	-0.2768	7.7086	0.029474036
EPS15	7916045	0.2767	9.3581	0.004239338
MON2	7956697	-0.2767	8.3344	0.007858229
FAM50B	8116658	-0.2766	7.5215	0.035321534
CCDC82	7951157	-0.2766	4.9548	0.045749557
MED13	8017312	-0.2765	9.2935	0.007982084
TMEM181	8123062	-0.2764	7.5982	0.01144763
ECSIT	8034286	-0.2763	7.8097	0.022750316
LMLN	8085033	-0.2760	7.3722	0.007136575
GNAI3	7903703	0.2757	8.9540	0.036350628
EEF1D	8153457	0.2756	6.2941	0.046149159
TMEM50A	7899005	0.2756	8.7951	0.038375505
IPCEF1	8130408	0.2755	5.2730	0.0212636
PIAS2	8023133	0.2754	9.3254	0.042331575
C1orf9	7907404	0.2752	8.2613	0.009071449
TOM1L2	8013159	-0.2750	8.9738	0.044458667
RC3H1	7922432	-0.2747	8.2225	0.041471756
GTPBP10	8134079	0.2747	9.0431	0.014368072
ANKRD13B	8006063	0.2746	6.7508	0.034928402
CLIP2	8133459	0.2737	5.7281	0.029342703

Gene Name	ID	Log2 Fold Change	Average expression	Adj. p value
MAT1A	7934755	0.2736	5.8652	0.019128608
WT1	7947363	0.2736	6.1063	0.024001826
C1orf69	7910261	-0.2734	6.5122	0.011850527
ATF4	8073148	0.2734	8.4156	0.015848543
AIDA	7924491	-0.2733	6.8871	0.018508345
SEC23IP	7930956	-0.2732	10.2544	0.002968353
NES	7921088	-0.2731	6.2606	0.03473996
SGPP1	7979574	-0.2728	8.3878	0.002819031
FBXO6	7897728	-0.2727	5.9225	0.019819643
NOL6	8160682	-0.2726	8.4510	0.01463774
BLMH	8014008	0.2726	8.2153	0.01496286
UXS1	8054395	0.2725	8.1051	0.006865497
ZNF276	7998002	-0.2724	6.9315	0.019531213
ZMIZ1	7928558	-0.2724	7.3041	0.004795769
ERCC6	7933509	0.2721	7.4220	0.017894987
PSEN1	7975545	-0.2720	9.0238	0.025547433
AP1B1	8075217	0.2720	9.0158	0.006843708
SMA5	8177544	-0.2717	10.6413	0.03547257
USP3	7984132	-0.2717	8.5056	0.017341678
JUB	7977854	-0.2717	6.5932	0.028552318
UPF3A	8180302	-0.2713	7.5003	0.007108908
LONRF1	8149399	-0.2712	7.4694	0.007650816
SRR	8003722	0.2706	8.0330	0.014675072
CDK4	7964522	-0.2705	10.3134	0.004450684
GUSBL1	8112469	0.2704	10.6945	0.036974911
FAM46B	7914015	0.2700	5.4119	0.045122233
ACAT2	8123137	0.2698	8.7770	0.007450941
TMOD3	7983744	-0.2697	8.9927	0.018747194
TET2	8096675	0.2696	7.2852	0.048243543
SMCHD1	8019885	-0.2696	9.1786	0.0224293
SLC2A5	7912224	-0.2695	6.7986	0.023169463
GOLGA4	8086183	-0.2694	5.3885	0.031547925
RAB1A	8052680	-0.2693	10.2341	0.046128514
GAB1	8102982	0.2692	5.6250	0.01070449

Gene Name	ID	Log2 Fold Change	Average expression	Adj. p value
SNORD45A	7902398	0.2689	8.7050	0.017477594
RRP9	8087790	0.2688	7.9416	0.014943287
TTC3	8068522	0.2687	8.4107	0.03015746
RFXAP	7968653	0.2684	5.8311	0.023310173
NCRNA00174	8139873	-0.2684	6.1427	0.048301943
LNX1	8100362	-0.2684	6.6918	0.016947308
TLCD1	8013771	-0.2684	9.0047	0.012235495
REEP6	8024323	-0.2682	9.1489	0.021839038
LOC554249	8161353	0.2681	7.7324	0.035174679
G3BP2	8101043	-0.2680	9.4600	0.00308751
MTHFR	7897753	0.2677	5.0531	0.010437318
BTNL9	8110631	0.2677	6.4169	0.044022883
DUSP4	8150076	-0.2677	5.4235	0.032951204
MTMR2	7951112	-0.2676	8.3461	0.01880313
ALS2	8058295	0.2676	6.6473	0.033538697
C21orf33	8069026	-0.2673	8.5038	0.046802833
KPNA4	8091764	0.2673	8.4799	0.048243543
THOC6	7992795	0.2670	8.0684	0.049912669
BLNK	7935270	0.2668	5.6680	0.00872038
IL17RB	8080562	0.2668	6.8352	0.023310173
LRRC45	8010719	-0.2667	7.0125	0.047700052
MLH3	7980246	0.2666	6.7767	0.031186334
MYO6	8120783	0.2663	9.8588	0.010394182
HOOK2	8034521	0.2656	8.7438	0.021394491
LACTB	7984103	-0.2656	6.9444	0.045152046
KCNQ5	8120654	0.2656	6.4073	0.009762714
DDX54	7966570	0.2651	8.5387	0.01099229
MRM1	8006668	-0.2645	6.6783	0.014462985
RTN4RL2	7940022	-0.2644	7.1682	0.048819637
CRIPT	8041813	-0.2644	8.0263	0.034088428
NOSTRIN	8046099	0.2644	6.6284	0.037138117
SULT1A3	7994582	-0.2643	8.0822	0.029554579
C17orf106	8010012	-0.2642	7.9947	0.015848543
NOTCH2NL	7904702	-0.2640	8.3413	0.011303912

Gene Name	ID	Log2 Fold Change	Average expression	Adj. p value
ZNHIT2	7949373	-0.2639	6.6733	0.018649001
PRPF3	7905171	0.2638	9.0882	0.044959998
KLHL13	8174654	0.2638	6.2627	0.010979794
SC5DL	7944656	-0.2637	9.0486	0.042413342
ZDHHC6	7936346	-0.2637	8.4821	0.002408141
UBXN8	8145691	-0.2636	6.7175	0.042775487
LRP6	7961339	0.2636	8.6571	0.02144598
ARHGEF9	8173217	0.2633	7.2870	0.005246565
SETX	8164701	-0.2630	8.2720	0.014616995
FADS2	7940565	0.2629	11.6806	0.00229712
PRAF2	8172531	0.2625	7.4120	0.03911949
DULLARD	8012116	0.2622	8.0701	0.032985412
UROS	7936937	-0.2622	9.4505	0.002321192
RAB21	7957177	0.2618	9.3662	0.02245544
GUSBL1	8112564	0.2618	10.7094	0.03859898
AARSD1	8015741	0.2617	7.9609	0.04471436
NAT8L	8093578	0.2611	5.8506	0.037640292
AP1G1	8002592	-0.2611	9.5654	0.008108999
RNASEH2A	8026051	0.2610	9.8064	0.007982084
H2AFX	7952179	0.2606	8.8098	0.037114811
MAGEA3	8175747	0.2606	9.5385	0.004169145
AIDA	7917148	0.2606	11.5300	0.049598476
HBM	7991758	-0.2605	6.2128	0.014789253
PDZRN3	8088848	0.2604	5.7120	0.044213313
UAP1L1	8159554	-0.2603	8.0896	0.004574961
SNORD116-15	7981978	0.2603	10.8202	0.014093331
GDAP2	7918955	-0.2601	8.3364	0.030313517
UNC119B	7959212	-0.2601	8.3716	0.012128205
DHX16	8178377	0.2601	8.4247	0.003751588
SRM	7912374	0.2601	9.7425	0.007738901
THG1L	8109576	-0.2601	7.6747	0.03373804
GRK4	8093665	0.2599	5.3475	0.041028741
TUB	7938269	0.2598	6.8343	0.013532891
RPS20	8150872	0.2595	11.6576	0.046389307

Gene Name	ID	Log2 Fold Change	Average expression	Adj. p value
SULT1A3	7994781	0.2594	8.0576	0.030143089
UBE2G1	8011626	0.2594	9.5896	0.004203122
ZNF470	8031669	0.2590	6.0087	0.034886732
PHF7	8080306	-0.2585	5.7513	0.046372108
COQ4	8158214	-0.2582	8.0387	0.005119972
SNX9	8122986	-0.2581	6.8808	0.024775747
INPP5K	8011062	-0.2581	7.8058	0.005008016
ALG14	7917896	-0.2580	7.7619	0.005151216
TKT	8088106	-0.2579	9.5557	0.014450725
NCL	8059689	-0.2578	11.3763	0.005155841
RINL	8036622	0.2577	5.1521	0.048433359
TOE1	7901091	0.2576	7.9082	0.045541889
BMP2K	8096004	-0.2576	6.3906	0.042532444
CXADR	8067955	0.2574	8.4258	0.019236907
GIGYF2	8049199	-0.2573	8.5669	0.013319224
SCYL2	7957806	-0.2572	8.3388	0.045506883
PRPF40A	8055913	-0.2571	9.2421	0.043254783
SMAP2	7900426	0.2568	9.1786	0.016036595
INPP5F	7930927	0.2567	5.7695	0.021780908
ZNF239	7933180	-0.2567	7.0994	0.011591258
TPRM2	8069085	-0.2564	5.8775	0.041080824
CCDC28A	8122327	-0.2563	6.4909	0.012332424
FAM49B	8152845	0.2563	7.0154	0.02441179
ZNF277	8135497	0.2563	7.3369	0.044367777
CCDC125	8112439	-0.2561	8.1739	0.023863979
DNAJC24	7939093	0.2561	6.6632	0.045541889
TYSND1	7934114	-0.2560	7.7189	0.012138969
IRX4	8110865	0.2560	8.0182	0.012128205
SPAG1	8147661	-0.2559	6.8205	0.022449134
HOOK3	8146243	-0.2558	7.9058	0.034278474
TMF1	8088700	0.2556	8.1285	0.008834948
NSUN4	7901219	-0.2554	9.1490	0.022386166
LOC650293	8144496	-0.2552	5.7185	0.008905804
CBWD3	8161587	-0.2552	9.5945	0.016030978

Gene Name	ID	Log2 Fold Change	Average expression	Adj. p value
CCDC137	8010629	0.2552	7.2171	0.03533115
NFE2L1	8008087	0.2551	9.6385	0.034286833
PTPN13	8096176	-0.2549	6.9205	0.025104625
KIAA1919	8121525	0.2545	6.7547	0.022596245
DRAM1	7958019	-0.2542	6.4178	0.044756658
DHFRL1	8089029	-0.2539	7.9449	0.012090663
CEP78	8156026	-0.2539	7.6921	0.0126222
R3HDM1	8045425	0.2538	7.5597	0.021224937
TMEM131	8054092	0.2538	7.7336	0.006199916
TFAP4	7999102	-0.2537	6.8725	0.00865826
CEP55	7929334	-0.2537	8.3357	0.049425232
CBWD3	8155636	-0.2536	9.5063	0.019531213
SPAG7	8011765	0.2534	7.2491	0.008014363
UBE2J1	8128111	-0.2533	6.5944	0.03796369
RPS27L	7989493	0.2529	7.3624	0.003899023
CA12	7989501	0.2528	8.7011	0.005652803
TRIM65	8018502	-0.2527	7.3217	0.013574157
CCNA2	8102643	0.2526	8.6801	0.023984032
FADS1	7948612	0.2525	9.4716	0.008864352
CLSTN1	7912257	0.2521	9.6485	0.008537904
ANKRD17	8100902	-0.2521	8.8606	0.009093117
LOC650293	8144422	0.2520	5.5807	0.011461854
AKAP11	7968835	-0.2519	7.0384	0.045403237
UPF3A	8180301	-0.2519	7.4933	0.019721459
OAT	7936871	-0.2514	8.3072	0.034505519
YLPM1	7975725	-0.2513	7.5608	0.016107821
C8orf30A	8148799	-0.2510	7.8914	0.032684434
ZNF561	8033795	-0.2506	6.8007	0.020932362
ANAPC13	8090866	0.2505	8.9268	0.004020068
UBR5	8152148	0.2505	8.7096	0.013161574
ARFGEF1	8151149	-0.2504	7.8671	0.018814422
HECTD1	7978449	0.2504	9.0299	0.012989885
OTUD3	7898602	-0.2502	6.8216	0.012334564
SLFN5	8006531	0.2501	9.5141	0.046128514

Gene Name	ID	Log2 Fold Change	Average expression	Adj. p value
FXYD3	8027748	0.2501	8.1751	0.011864184
KIAA1737	7975926	-0.2501	7.6176	0.024732712
LOC100288413	8100338	0.2497	6.8242	0.030671366
C9orf16	8158177	-0.2497	6.9627	0.035842339
HEATR5A	7978492	0.2496	7.7313	0.034611634
VGLL4	8085340	0.2495	8.2299	0.042601829
NIPA1	7986675	-0.2495	8.3359	0.012332424
NSUN5P2	8139947	-0.2494	8.2813	0.038361725
FKBP10	8007154	0.2494	8.9751	0.030246356
RRBP1	8065136	0.2493	8.3766	0.011685856
TARBP1	7925130	0.2492	8.3543	0.043429126
DCBLD2	8089082	-0.2490	6.8851	0.021737448
SNORD74	7922418	0.2490	9.6087	0.046402966
IFI30	8026971	0.2490	6.0996	0.029474036
UBAP2L	7905700	-0.2487	10.3902	0.025943062
CBWD3	8161537	-0.2486	9.5053	0.018567984
MCM2	8082350	0.2485	9.3528	0.029383162
MAGEA6	8170553	-0.2484	8.5854	0.008014363
CEBPG	8027566	-0.2483	7.8089	0.044389955
RNF10	7959173	0.2478	9.2741	0.005944076
LOC349196	8149151	-0.2474	6.6468	0.033865906
LOC349196	8149214	-0.2473	6.6468	0.033865906
GRIPAP1	8172504	-0.2472	7.1153	0.039306784
CLIP1	7967255	-0.2472	7.4586	0.046268101
BTN3A3	8117476	-0.2471	6.4837	0.033865906
UGGT1	8045090	-0.2468	8.9797	0.029528047
HUWE1	8172914	0.2468	8.7457	0.034887168
SMPDL3B	7899407	-0.2468	8.4994	0.024775747
MOSC2	7909866	-0.2465	7.4695	0.017703117
MFSD9	8054356	0.2464	6.3741	0.049431491
POLH	8119858	0.2462	8.1064	0.033428718
HSDL2	8157233	-0.2462	9.2480	0.016025874
NIN	7979044	-0.2461	6.9196	0.005099765
MBD2	8023382	-0.2461	8.8069	0.031476575

Gene Name	ID	Log2 Fold Change	Average expression	Adj. p value
TK2	8001818	-0.2459	7.7481	0.04471436
DCUN1D4	8095009	-0.2457	7.6798	0.043971377
KIAA1033	7958216	0.2457	8.0922	0.043139762
EXO1	7910997	0.2456	8.2892	0.029207104
IMPDH2	8087254	0.2455	10.2437	0.013071309
HDAC8	8173531	0.2454	7.3261	0.010069405
ZNF160	8039034	-0.2453	7.4599	0.021794469
C6orf162	8121002	0.2453	6.9284	0.03354684
RNF2	7908169	0.2452	7.2590	0.035381215
RUNDC1	8007435	-0.2452	8.3764	0.020687483
PIH1D1	8038382	-0.2452	8.1431	0.010499982
KCTD15	8027584	-0.2452	8.3151	0.014616995
PLP2	8167449	-0.2451	9.0993	0.03533115
C16orf80	8001658	-0.2451	8.6725	0.045075
SNAPC3	8154394	0.2449	8.7641	0.019721459
MFSD3	8148917	0.2445	8.2984	0.018462609
RCC2	7912956	-0.2444	9.0853	0.027131451
SERF1A	8105949	0.2443	7.5438	0.038272716
SERF1A	8105997	-0.2441	7.5438	0.038272716
SERF1A	8177658	-0.2438	7.5438	0.038272716
EAF2	8082003	-0.2437	5.9785	0.035556833
SERINC1	8129317	-0.2436	10.1779	0.03533115
DNMT3B	8061746	0.2434	5.9715	0.02498665
TRIM44	7939368	0.2434	8.2741	0.023370302
RDH12	7975284	-0.2434	5.0281	0.026922569
TBRG4	8139468	-0.2430	8.1700	0.041100534
APH1B	7984124	-0.2430	8.2293	0.018738524
CNOT4	8143088	-0.2429	7.4063	0.029474036
ZMIZ2	8132617	-0.2427	7.3253	0.044213313
PTK2B	8145490	0.2427	8.2240	0.015880145
TOP3B	8074817	0.2424	7.5244	0.048749059
KLHL17	7896779	-0.2424	7.0288	0.027927135
KLF3	8094599	0.2423	7.0702	0.007650816
TNIK	8092095	-0.2422	5.5751	0.014616995

Gene Name	ID	Log2 Fold Change	Average expression	Adj. p value
ACSL1	8103951	-0.2421	10.9494	0.014896466
RHOC	7918593	-0.2421	10.5246	0.006199916
DDAH1	7917347	-0.2420	9.6637	0.006790834
ARHGEF2	7920877	-0.2419	6.9686	0.032334789
TEAD2	8038347	-0.2419	6.2113	0.027901429
ARID1A	7899220	0.2419	7.4958	0.020610811
ICAM1	8025601	0.2419	6.4844	0.048759707
C12orf51	7966488	0.2418	5.9152	0.042023075
RCOR3	7909529	-0.2417	7.6680	0.012138969
CREBBP	7999044	-0.2417	7.3842	0.038215998
LPP	8084742	0.2415	9.0436	0.03015746
SRGAP2	7909175	0.2415	7.5456	0.02809177
RAB6C	8045136	-0.2414	7.8484	0.0343127
LOC349196	8144420	0.2411	6.7197	0.043769985
LOC349196	8144494	0.2410	6.7197	0.043769985
CRK	8011018	0.2410	9.0588	0.004433768
TFAP2C	8063536	0.2410	8.0460	0.014961021
WDR60	8137639	-0.2409	6.4200	0.049890624
DHX16	8124775	-0.2408	8.4417	0.005246565
MCRS1	7963064	-0.2408	8.0965	0.046128514
FER	8107208	0.2406	6.4304	0.010597199
ZNF263	7992870	-0.2405	6.8121	0.046149159
HPCAL1	8040238	-0.2401	7.8494	0.043617995
PPP2R1B	7951614	-0.2400	8.4785	0.018686451
FOXRED2	8075785	0.2400	9.8283	0.04917169
ITGB5	8090162	0.2399	7.7978	0.015417415
LIG4	7972737	-0.2399	6.6512	0.015417415
UBXN7	8093112	-0.2398	8.6699	0.037629098
SNORA3	7938291	-0.2395	7.2106	0.040068616
CCND1	7942123	0.2395	10.2277	0.018421803
FURIN	7986092	0.2393	6.1561	0.045122233
SORT1	7918323	-0.2392	7.5945	0.021194224
ACD	8002057	-0.2388	7.1683	0.035417048
WDR5B	8089993	-0.2387	7.1679	0.024701681

Gene Name	ID	Log2 Fold Change	Average expression	Adj. p value
TDRD7	8156688	0.2387	6.2327	0.01835909
ATP6V1H	8150797	0.2386	8.3416	0.015126029
AIM1	8121277	0.2385	5.9719	0.011086293
LZTFL1	8086555	-0.2381	5.6531	0.042718241
NFKB1	8096635	0.2379	8.6624	0.012332424
FYCO1	8086572	0.2378	7.3650	0.045561067
RAB5A	8078214	-0.2376	9.3892	0.032332114
PHLPP1	8021565	-0.2375	6.4838	0.043127614
KHNYN	7973732	-0.2374	6.7901	0.031786703
NOLC1	7930008	0.2373	10.1111	0.015029954
MYBL2	8062766	-0.2372	9.5114	0.026922569
NEBL	7932453	-0.2368	6.0132	0.018747194
RFC5	7959052	-0.2368	7.8642	0.049855758
GPRC5B	7999909	0.2367	7.1501	0.028467776
LRP11	8130142	0.2367	7.0196	0.022690407
AGFG1	8048847	0.2367	8.8406	0.021477755
PMS2L5	8133309	-0.2366	8.3173	0.041550266
USP36	8018937	0.2366	6.7828	0.017764176
KIAA1632	8022996	0.2363	6.7762	0.046574042
PDS5B	7968516	0.2360	8.6682	0.044547923
ABHD5	8079153	0.2359	8.0426	0.039390207
PRELID1	8110318	-0.2358	10.6360	0.009424632
C19orf24	8024246	-0.2357	8.7802	0.022799939
B4GALT2	7900931	0.2356	9.3537	0.020096181
RAP2A	7969693	-0.2355	7.5684	0.01282664
AMDHD2	7992656	-0.2354	6.7684	0.029638344
SBF1	8077042	0.2353	7.4778	0.042276941
TUSC3	8144726	0.2352	9.3401	0.049624497
POLD1	8030641	0.2351	7.2169	0.010177207
SERINC3	8066417	-0.2350	11.2070	0.02153745
GLCE	7984517	0.2350	7.6866	0.011398682
C8orf30A	8148772	0.2349	7.9241	0.033539714
SAR1A	7934122	-0.2349	9.7116	0.012975614
AFF1	8096224	0.2348	7.6924	0.017341678

Gene Name	ID	Log2 Fold Change	Average expression	Adj. p value
SOHLH2	7970975	-0.2348	7.7234	0.039748821
TMEM154	8103226	-0.2348	5.5566	0.033072638
SS18L1	8063839	0.2345	6.9709	0.030558025
AXIN2	8017718	0.2344	5.8528	0.045561067
ZNF232	8011817	-0.2343	7.2454	0.021920655
ZNF215	7938183	-0.2342	6.9723	0.018747194
PRKCD	8080487	-0.2342	8.9521	0.010389593
N6AMT2	7970467	-0.2342	7.6703	0.042976315
AGPAT3	8068952	-0.2337	8.0005	0.008014363
PRKCZ	7897044	-0.2337	7.7572	0.006049586
ALPI	8049137	0.2335	5.7422	0.038272716
SCGB1C1	7937257	-0.2334	6.3037	0.038636028
DYNLL1	7967067	-0.2332	6.7219	0.031786703
HDAC1	7899774	-0.2330	11.5078	0.008833515
SLC25A30	7971388	-0.2328	7.8169	0.021194224
KCNMB4	7957126	0.2328	6.3194	0.024811368
ALDH4A1	7912975	-0.2327	6.8895	0.04448058
MALT1	8021418	0.2326	7.2018	0.046983922
FNDC3A	7969060	0.2325	8.4890	0.02742189
APOLD1	7954055	0.2324	6.4991	0.035716447
CBWD1	8159815	0.2319	9.0828	0.026343585
PDIA5	8082133	0.2317	8.5757	0.015225422
TAPBPL	7953341	-0.2316	6.7831	0.049894736
AURKB	8012403	-0.2315	8.4878	0.036818143
GRAMD4	8073890	-0.2313	6.9413	0.016484623
RANBP1	8071332	-0.2312	10.0941	0.018704006
ELMO3	7996468	-0.2312	7.4408	0.01282664
GMIP	8035714	-0.2310	6.9575	0.044991436
ATAD3B	7896961	0.2310	8.2350	0.005246565
MANBAL	8062371	-0.2310	8.4446	0.029528047
TRIM25	8016847	-0.2309	9.0430	0.038713492
GBE1	8088958	0.2309	8.3151	0.046563829
OTUD5	8172478	-0.2303	7.5072	0.040370972
PAN3	7968274	0.2303	8.8335	0.026068651

Gene Name	ID	Log2 Fold Change	Average expression	Adj. p value
STIL	7915926	0.2301	7.5646	0.0212636
TBC1D24	7992639	-0.2299	7.4629	0.035689743
CUTA	8125752	-0.2299	9.9727	0.003629423
SMG6	8011222	0.2297	6.8270	0.025073543
RNF170	8150565	-0.2296	6.7997	0.039472452
LOC284023	8012282	0.2296	7.4059	0.012138969
OSBPL10	8085984	0.2296	5.7247	0.01069969
STOM	8163896	-0.2295	6.9538	0.027217897
CDK10	7997982	-0.2294	8.2505	0.041087796
EPHB3	8084524	0.2291	6.3895	0.033648083
SGMS2	8096733	-0.2291	6.6712	0.037067749
XRCC3	7981447	0.2291	7.2364	0.015848543
SEC61G	8139706	-0.2290	9.2885	0.044756658
TMEM98	8006415	0.2287	8.4738	0.045561067
DERL1	8152628	-0.2286	9.2662	0.048243543
DNAJC21	8104838	-0.2285	8.5403	0.016890779
FAM73A	7902476	-0.2284	8.2760	0.023370302
CDC45L	8071212	-0.2284	8.4045	0.042413342
SLC9A2	8044080	-0.2283	8.2597	0.020932362
DDX39	8034806	-0.2282	8.9722	0.018301033
USP54	7934411	0.2279	11.0893	0.011325323
ZNF696	8148615	0.2275	6.0593	0.038808416
DIAPH1	8114658	-0.2275	8.9375	0.029612622
MAPK6	7983763	-0.2273	8.3751	0.044861772
CDK7	8177462	0.2271	7.6756	0.014368072
TBC1D2	8162759	0.2270	6.1067	0.039274982
C9orf82	8160478	-0.2270	8.1072	0.011950264
SCAP	8086754	-0.2268	8.3509	0.039713526
KBTBD6	7971208	0.2266	8.5587	0.032627632
HSPC159	8042283	0.2264	7.9931	0.037071822
ASAP2	8040113	0.2264	6.9473	0.021160015
STIM2	8094501	-0.2264	6.4763	0.032106621
CNOT7	8149475	0.2263	10.3970	0.036382978
MYO5B	8023267	-0.2263	6.4139	0.025487183

Gene Name	ID	Log2 Fold Change	Average expression	Adj. p value
ARHGAP32	7952641	-0.2263	7.9822	0.0267558
MBD3	8032275	-0.2262	7.7295	0.027131451
SEL1L3	8099721	0.2261	9.2224	0.022547153
MAK16	8145782	0.2261	8.8877	0.043860372
STAMBP	8042772	0.2260	8.3793	0.013468137
FAM71E2	8039477	-0.2259	6.3245	0.046743444
SYNRG	8014551	0.2259	8.2456	0.037268716
DOCK7	7916669	-0.2258	7.7343	0.032985412
DIP2B	7955376	-0.2256	8.5341	0.026543366
TSEN15	7908147	0.2255	7.8358	0.023984032
PRIM1	7964271	-0.2253	8.4260	0.044394526
RRP12	7935425	0.2250	7.9326	0.005132864
PROM2	8043522	-0.2248	7.7773	0.036825871
CCT3	7920984	0.2245	10.8133	0.048243543
PIAS3	7904812	0.2244	8.4835	0.03533115
TPM1	7984079	-0.2244	7.3437	0.033657937
CUL7	8126486	-0.2243	7.5289	0.027123247
CALCOCO1	7963721	0.2241	7.9877	0.021839038
SLC29A1	8119974	0.2240	8.6357	0.029638344
DERL2	8011875	0.2239	9.9893	0.013384723
SARS	7903619	-0.2238	10.9413	0.007793275
ELOF1	8034299	0.2238	9.4828	0.04327688
PITPNA	8011077	-0.2237	10.5239	0.025219007
FTO	7995655	-0.2236	10.1058	0.035450705
XPOT	7956785	-0.2235	10.3160	0.045649876
C3orf64	8088680	-0.2234	6.4339	0.02418934
NT5M	8005247	0.2234	6.8169	0.016622907
RABGAP1	8157700	-0.2232	9.9790	0.014735203
LPCAT1	8110841	0.2231	8.0343	0.014577339
FNDC3B	8083901	0.2231	9.2070	0.025961152
PSMD5	8163795	-0.2228	8.6040	0.049158284
TNKS1BP1	7948176	-0.2226	8.3457	0.033865906
TRIM33	7918725	0.2224	7.6117	0.019531213
TRAP1	7999025	0.2224	10.1961	0.005595793

Gene Name	ID	Log2 Fold Change	Average expression	Adj. p value
GUCY1A3	8097957	0.2223	8.1115	0.03373804
AARS	8002347	-0.2223	11.1414	0.020492677
PTPN1	8063394	-0.2222	8.1488	0.038966251
RFX5	7919971	-0.2220	9.5109	0.040811395
EVC	8093878	-0.2219	7.1307	0.047011607
TADA3	8085220	-0.2218	7.7961	0.010987147
MRPL45	8006762	-0.2218	10.8600	0.022690407
GPR44	7948470	-0.2218	6.2919	0.044756658
RGP1	8155110	-0.2217	8.3695	0.047326221
CAMSAP1	8165046	0.2217	7.4479	0.036368681
H2AFV	8139421	0.2217	9.5327	0.012444186
WDFY3	8101511	-0.2217	7.0092	0.026922569
AUH	8162264	-0.2216	8.4300	0.013574157
PER2	8059996	0.2213	6.3570	0.022547153
RBP5	7960764	-0.2212	7.4597	0.034088428
C9orf5	8163086	-0.2210	9.7077	0.008814792
WDR46	8178939	0.2209	8.2999	0.042918445
LUZP1	7913558	-0.2202	6.5683	0.031063825
MYCL1	7915277	-0.2201	7.2146	0.037129632
WASH5P	7998119	-0.2200	8.0958	0.025104625
ARFGEF2	8063242	0.2198	8.3058	0.01235511
PANK3	8115681	-0.2197	8.1158	0.049425232
TINF2	7978208	-0.2197	8.5198	0.014368072
TDP1	7976160	-0.2194	9.1033	0.012109876
KIAA0776	8121161	-0.2193	8.7696	0.034996119
PRKCH	7974835	-0.2192	7.1318	0.023992154
PPIF	7928589	-0.2191	9.8955	0.038272716
C22orf30	8075542	-0.2190	7.3262	0.03686071
IREB2	7985166	0.2190	9.6787	0.008833515
PEX11B	7904755	-0.2189	8.5547	0.046372108
ATXN2	7966397	-0.2185	8.2985	0.039874938
CNOT6	8110589	-0.2185	9.2984	0.031853927
NEK1	8103646	0.2183	7.6551	0.019605895
OXSR1	8078738	0.2182	8.9780	0.032501147

Gene Name	ID	Log2 Fold Change	Average expression	Adj. p value
ATXN7L2	7903676	-0.2180	6.3586	0.023406564
PRKAG2	8143961	0.2179	7.4437	0.031329946
RPRD2	7905185	-0.2177	8.3949	0.013412813
ZSWIM6	8105506	0.2176	7.3521	0.02299988
WDR34	8164440	-0.2176	9.0022	0.042552224
DDX56	8139392	0.2174	8.9581	0.022217193
NGEF	8059783	-0.2172	6.3487	0.027088862
MCL1	7919751	-0.2172	10.2036	0.033125035
UBE3C	8137596	0.2171	9.2131	0.023688612
EYA3	7914153	0.2169	7.4460	0.042601829
ZC3H13	7971422	-0.2167	6.6216	0.038914798
TRMT1	8034615	-0.2167	8.0216	0.024589335
TBC1D4	7972021	-0.2166	6.1238	0.046103901
FEZ2	8051427	-0.2165	7.0421	0.023409662
DUSP27	7907053	0.2163	5.3881	0.029127419
CDCA7L	8138489	0.2163	9.0243	0.034928402
ARG2	7975268	-0.2162	7.7083	0.021839038
CEP68	8042326	0.2161	5.8100	0.016770781
TGIF1	8180317	0.2161	9.8148	0.046128514
IDE	7935027	-0.2160	8.7442	0.011570622
CXXC1	8023344	0.2159	6.7059	0.038272716
JMJD5	7994269	-0.2158	5.7077	0.039878547
ZNF512	8040985	-0.2158	8.7515	0.01880313
ATAD3A	7896952	-0.2157	8.4322	0.039717418
AP1G2	7978066	-0.2156	8.6802	0.04810079
TPD52	8151475	0.2155	7.5683	0.03533115
RNH1	7945420	-0.2155	9.0924	0.025475646
DOPEY2	8068422	0.2154	7.0287	0.031400964
YWHAZ	8152096	-0.2154	11.0140	0.019127494
RAB5B	7956088	0.2153	9.0933	0.031797432
AR	8167998	-0.2153	10.2017	0.018315666
PES1	8075406	0.2149	8.9810	0.032951204
FAM13B	8114326	0.2149	7.7455	0.041605393
TGIF2	8062319	-0.2146	7.5156	0.046983922

Gene Name	ID	Log2 Fold Change	Average expression	Adj. p value
ACLY	8015460	0.2146	11.0077	0.038823672
GABPA	8068039	0.2146	6.4687	0.046983922
PSMA3	7974603	-0.2145	9.5919	0.04825786
PTGER4	8105067	-0.2145	5.6490	0.010289096
IARS	8162313	-0.2145	10.9475	0.020133461
XRN1	8091141	-0.2144	8.4986	0.023310173
MCM4	8146357	0.2139	8.9337	0.008864352
FAM163B	8164937	-0.2139	5.4112	0.013384723
L2HGDH	7978956	0.2139	7.5282	0.042479988
ICA1	8138202	-0.2138	7.9369	0.01172401
ADSSL1	7977273	0.2136	7.6594	0.039748821
HNRPLL	8051605	-0.2133	7.2435	0.028569259
PRPS2	8166049	0.2131	8.6425	0.025895141
PTPRF	7900792	0.2130	8.7218	0.034729404
CENPO	8040578	0.2127	8.0322	0.023605916
NEO1	7984704	0.2125	7.9021	0.029653206
ZFPL1	7941127	0.2125	8.0176	0.017018158
APPL1	8080645	-0.2125	9.0546	0.009162972
KRTCAP2	7920659	0.2124	8.8135	0.038721003
KAT2A	8015526	0.2124	8.8405	0.010051713
SLC34A1	8110347	-0.2123	5.1526	0.046734102
TNFRSF25	7912040	0.2122	6.7890	0.04448058
SCGB1C1	8019711	-0.2122	6.1124	0.0212636
MTMR10	7987048	0.2120	6.5981	0.030671366
CORO1A	7994769	-0.2120	6.0270	0.012334564
INO80B	8042859	-0.2120	6.8795	0.017479264
BAGE4	8180326	-0.2116	8.7693	0.017370413
RUVBL1	8090448	-0.2114	9.0804	0.045541889
BPTF	8009382	0.2113	7.8850	0.027927135
PSPH	8139737	-0.2113	9.1906	0.028313109
YME1L1	7932678	0.2109	10.5566	0.008834948
TGIF1	8180316	-0.2105	9.8625	0.04448058
CPD	8006123	-0.2105	9.2072	0.018416632
TBC1D12	7929424	0.2102	6.4567	0.017370413

Gene Name	ID	Log2 Fold Change	Average expression	Adj. p value
CD59	7947425	-0.2101	8.5653	0.048060845
KIAA1429	8151842	-0.2097	7.8562	0.046402966
NUBP1	7993185	0.2097	9.2196	0.046802833
GGA2	8000284	-0.2095	7.9995	0.04560827
SETD2	8086706	-0.2095	6.8364	0.037604153
TPRM5	7945742	-0.2094	5.3591	0.046128514
ANKRD16	7931888	-0.2093	5.7953	0.022701935
LNPEP	8107066	0.2092	8.2452	0.026149321
ZNF526	8029188	-0.2087	6.7806	0.034691489
TGIF1	8180318	-0.2087	9.8663	0.042939855
BAGE2	8180328	-0.2085	8.6756	0.017725908
UBR2	8119529	0.2084	8.5909	0.024589335
PCBP2	7955817	0.2084	10.5931	0.009963098
USP4	8087380	-0.2082	8.7115	0.033539714
EIF4G3	7913319	-0.2080	8.1945	0.017529931
CMTM4	8001830	-0.2080	8.2420	0.025961152
CLDN23	8144505	-0.2079	6.8470	0.043971377
STK11IP	8048647	-0.2079	6.3127	0.033033332
PMS2L5	8133531	-0.2077	9.0065	0.046268101
ZKSCAN1	8134680	-0.2075	8.6047	0.039390207
MEMO1	8051372	-0.2074	6.9152	0.048694602
BTBD7	7980998	-0.2073	6.8098	0.027962692
CCNK	7976648	-0.2072	7.1719	0.034344844
HSD17B4	8107532	-0.2072	9.8981	0.048301943
KIF3B	8061715	-0.2068	8.2132	0.035970547
TECPR2	7976976	-0.2068	6.3454	0.023175328
PXK	8080781	-0.2067	6.2455	0.02158859
XPNPEP1	7936284	-0.2067	9.6893	0.023169548
MAFB	8066266	0.2066	7.9904	0.042775487
VPS8	8084541	-0.2063	7.8494	0.027958337
CHD3	8004699	0.2059	8.8995	0.031797432
PHKA1	8173551	0.2058	7.6561	0.027927135
ZC3HAV1	8143279	-0.2054	8.9564	0.046128514
LRPPRC	8051882	0.2054	9.9112	0.015593308

Gene Name	ID	Log2 Fold Change	Average expression	Adj. p value
EIF3G	8033899	0.2052	10.0274	0.029342703
YDJC	8074773	0.2051	8.5272	0.046983922
FAM179B	7974125	-0.2050	7.1939	0.043359579
TRIM28	8031913	-0.2046	10.5316	0.013342751
TYMS	8019842	0.2046	9.6553	0.039650306
H1F0	8072926	-0.2041	9.4095	0.047153721
VANGL1	7904211	0.2041	6.8512	0.033222622
SERTAD3	8036908	0.2039	6.7046	0.048985326
HYAL2	8087624	-0.2038	6.7513	0.049425232
MOV10	7904050	0.2036	8.9113	0.035014544
D2HGDH	8077238	-0.2034	7.1477	0.047615451
FAM164A	8147019	0.2034	7.3834	0.041766023
OTUD7B	7919699	-0.2033	7.3164	0.034729404
CLIC4	7898988	-0.2031	9.1917	0.030796727
ATRN	8060627	0.2027	7.4290	0.025943062
STK39	8056545	0.2027	9.7354	0.039642903
CBWD1	8044613	-0.2027	9.4987	0.045749557
CBARA1	7934255	-0.2025	9.4406	0.01821641
SKIV2L	8178136	0.2024	8.0606	0.048417193
HSPA5	8164165	0.2024	12.3321	0.010176629
NUMA1	7950086	-0.2023	9.6421	0.049842224
RAB7L1	7923812	-0.2018	8.7350	0.031464797
DHX30	8079563	-0.2016	8.2247	0.009032851
DNAJC16	7898192	-0.2014	7.9612	0.04710373
TM7SF2	7941148	-0.2009	10.3748	0.032593526
MIPOL1	7973985	-0.2007	6.5259	0.035766696
UBE2K	8094704	-0.2006	10.6451	0.046535183
SETD5	8077528	0.2005	9.0121	0.040130105
MDH1	8042259	-0.2004	9.2037	0.012673788
ATG16L1	8049271	-0.2004	6.9069	0.043397577
MBLAC2	8113059	0.2003	7.5090	0.040651128
SENP5	8084971	0.2001	9.2601	0.031924339
CLTC	8008834	0.1999	10.1773	0.027927135
YBX1	7900585	-0.1999	11.3555	0.017894987

Gene Name	ID	Log2 Fold Change	Average expression	Adj. p value
ARPP19	7988963	-0.1997	9.4185	0.030759587
PYCR2	7924669	0.1996	8.9805	0.035612796
RIMBP3	8074593	-0.1995	6.2613	0.018299351
RIMBP3	8074771	-0.1991	6.5189	0.019811692
CRLF3	8014037	0.1990	7.9885	0.045176612
PEX13	8042161	0.1990	8.3670	0.013544448
C1orf151	7898574	-0.1989	10.0741	0.047770872
SFRS6	8062695	-0.1989	10.0521	0.03247167
AUP1	8053214	0.1988	8.4558	0.032951204
ITFG1	8001211	0.1987	8.7420	0.046149159
TMEM66	8150089	0.1985	10.4917	0.020135796
NUP160	7947991	0.1983	9.0354	0.03755845
METT11D1	7973116	0.1979	7.9670	0.017341678
DUSP1	8115831	0.1977	8.9116	0.029717075
KIF20A	8108301	0.1977	9.0712	0.029383162
FGF13	8175444	0.1973	6.8430	0.017433343
BIRC5	8010260	0.1972	8.2755	0.017370413
LSG1	8092905	-0.1970	9.2447	0.041278063
FAM84A	8040374	0.1967	5.6953	0.036333365
FTH1	7948656	-0.1966	9.2874	0.036382978
LMBR1	8144089	0.1965	8.5114	0.048301943
AFMID	8010248	-0.1959	7.9995	0.041618161
DGKD	8049317	-0.1959	7.0716	0.036455623
CIAO1	8043585	-0.1959	8.4384	0.035005786
KDELR2	8138108	0.1958	10.3141	0.03373804
ZNF81	8167201	-0.1952	5.8039	0.042532444
MAML3	8102862	-0.1951	6.2237	0.018421803
EIF5B	8043861	0.1951	9.2365	0.035472339
SHPRH	8130038	-0.1948	6.4785	0.022786269
APP	8069644	-0.1944	11.3130	0.009278333
RPRD1A	8022914	0.1944	8.9778	0.016172585
LIMCH1	8094789	-0.1943	9.3328	0.018315666
IFNGR1	8129861	-0.1937	8.1414	0.021780908
ATAD3C	7896937	-0.1935	6.0376	0.048417193

Gene Name	ID	Log2 Fold Change	Average expression	Adj. p value
RSPH3	8130528	-0.1933	6.0916	0.021479904
AZIN1	8152222	0.1932	10.1211	0.045122233
RIOK2	8113286	0.1929	8.2165	0.028867416
HSPB1	8133721	-0.1929	12.2558	0.04447896
TRAPPC9	8153175	0.1928	7.3974	0.042603076
FIGNL1	8139632	-0.1928	8.4980	0.035005786
ATP2C1	8082607	0.1928	8.8226	0.030796727
BUB3	7931187	0.1928	9.9524	0.048776491
PAX1	8061357	-0.1927	6.8412	0.035383041
C16orf91	7998485	-0.1926	7.0752	0.044458667
C19orf42	8035193	-0.1925	9.5910	0.024004937
MKLN1	8136259	-0.1918	9.3701	0.044213313
SH2D4A	8144880	-0.1918	8.4909	0.031845814
BAGE5	8180325	-0.1916	8.7188	0.043206056
SBF2	7946516	-0.1913	7.1330	0.014368072
CLCN4	8165974	-0.1912	6.7656	0.029722277
STK4	8062908	0.1911	8.6739	0.016895385
STRADB	8047443	0.1910	8.9618	0.046983922
SCPEP1	8008646	-0.1908	9.0529	0.011864184
USP21	7906671	-0.1906	8.2709	0.033539714
ADO	7927767	-0.1901	7.8286	0.042531217
SEC14L1	8010139	-0.1901	7.4755	0.019585492
CCDC47	8017421	-0.1898	10.1657	0.018553058
PHIP	8127698	-0.1896	7.8177	0.037806297
ENPP4	8120061	0.1896	6.9294	0.044861772
DNAJC1	7932512	0.1896	8.3454	0.02653404
TRAF4	8005978	-0.1895	9.2207	0.022856279
RPL18AP3	7958197	-0.1894	11.7474	0.032908817
SLC3A2	7940717	-0.1894	10.1556	0.023992154
ATP2A2	7958644	-0.1892	9.9133	0.039340727
CXorf38	8172110	0.1885	6.8520	0.018738524
VEGFB	7940904	0.1885	8.1547	0.023856739
CAPZA1	7904036	0.1883	8.8251	0.032627632
TRIM16L	8005475	-0.1877	8.7634	0.043359579

Gene Name	ID	Log2 Fold Change	Average expression	Adj. p value
IMP4	8045171	-0.1874	9.3692	0.022786269
PEA15	7906564	0.1874	8.7629	0.041949223
CLASP1	8054888	0.1872	7.6017	0.045065928
CTBP2	8180351	0.1871	9.3367	0.024619999
HSD17B10	8172905	-0.1867	10.7042	0.04945447
BMP7	8067185	0.1863	5.6287	0.046802833
KLHL9	8160405	0.1858	8.2983	0.042348613
FZD5	8058498	-0.1855	6.7771	0.046402966
BRI3BP	7959777	0.1854	8.3313	0.043421019
LRRC59	8016708	-0.1851	10.7561	0.022786269
SLCO5A1	8151223	0.1847	6.2691	0.019531213
COG8	8002272	0.1840	7.8948	0.027962692
LAPTM4B	8147503	-0.1839	10.0178	0.032798039
SSRP1	7948192	0.1835	9.8230	0.02144598
GPRC5C	8009639	-0.1828	7.0719	0.045541889
CTR9	7938422	0.1827	10.1303	0.0212636
RPL18A	8026868	-0.1823	11.5423	0.021780908
MAOA	8166925	0.1823	11.0459	0.021166581
C22orf36	8075016	-0.1817	7.3982	0.049842224
SUV420H1	7949931	-0.1817	8.6313	0.044756658
MTHFD1	7975045	-0.1817	10.2304	0.035450705
ARPC2	8048234	0.1815	10.2003	0.023984032
LAMB1	8142194	-0.1815	7.8541	0.039065625
HK1	7928019	0.1808	8.2099	0.022671054
ZNF384	7960666	-0.1806	8.3713	0.047525775
DHCR7	7950067	0.1802	10.3333	0.038260442
NCAPH	8043602	-0.1798	8.0264	0.037592695
MAST4	8105741	-0.1797	6.0044	0.018428113
RNF130	8116372	0.1796	9.3655	0.021989869
PLXNA1	8082314	-0.1793	6.8572	0.031434216
ERICH1	8148985	0.1790	7.1085	0.045615456
WDR55	8108593	-0.1789	8.0114	0.030796727
LPIN1	8040340	-0.1782	8.5630	0.048417193
GOLM1	8162117	-0.1782	9.1155	0.048079695

Gene Name	ID	Log2 Fold Change	Average expression	Adj. p value
TSPAN14	7928705	0.1780	8.4252	0.024004937
STX6	7922669	0.1780	7.2470	0.046017148
RAB11FIP1	8150225	-0.1779	6.8265	0.04821513
POLR1E	8155268	-0.1773	8.4566	0.034365238
CLPTM1L	8110803	-0.1773	10.0949	0.043769985
MLLT1	8033118	-0.1768	8.8460	0.042795955
LRRC16A	8117243	0.1767	7.5197	0.049431491
AP2A2	7937533	0.1766	7.8489	0.039306784
ALDH9A1	7921970	0.1763	10.2246	0.035321534
PHKG2	7994928	-0.1762	8.3537	0.038721003
ULK3	7990400	-0.1750	8.3699	0.049764987
MTMR6	7970655	0.1748	8.7107	0.036333365
EIF4E3	8088803	0.1748	7.3527	0.043253664
SEC23A	7978718	-0.1739	9.9598	0.037931723
CDC6	8007071	-0.1737	9.8124	0.034148445
NUBP2	7992388	0.1730	8.1345	0.043924954
MICAL2	7938485	0.1727	7.0232	0.049425232
ACO1	8154733	-0.1723	9.4386	0.030470265
RPIA	8043413	0.1720	7.1706	0.032758892
C8orf33	8148955	0.1716	9.1013	0.039340727
JARID2	8116998	-0.1716	7.6527	0.046128514
CTXN1	8033462	0.1716	7.7401	0.034887168
WASH5P	8171066	0.1704	7.9953	0.048132851
ENSA	7919763	0.1695	7.8836	0.030793269
FAM127B	8175302	-0.1693	10.1737	0.032593282
LASS2	7919856	0.1688	10.5117	0.023196215
C11orf49	7939723	0.1683	7.5670	0.049912669
GUSBL1	8105991	0.1669	11.5623	0.0343127
KIF22	7994620	-0.1662	8.4437	0.043769985
KCMF1	8043105	0.1659	8.6629	0.025787925
HMG20B	8024660	-0.1653	9.8096	0.046017148
CAP1	7900382	-0.1649	10.8760	0.027123247
PDIA4	8143684	0.1646	10.9780	0.022217193
SMA5	8112560	-0.1634	11.5628	0.041100534

Gene Name	ID	Log2 Fold Change	Average expression	Adj. p value
ATP1A1	7904254	0.1629	11.2859	0.031027795
CDC42SE2	8107868	0.1628	8.9049	0.035282603
LTBP1	8041383	0.1626	6.7943	0.042976315
PHB2	7960716	0.1625	10.9168	0.03816004
STARD7	8053890	-0.1622	10.2524	0.04473474
CRCP	8133145	0.1611	8.4418	0.048510362
ZFYVE26	7979757	-0.1611	6.8688	0.049855758
MTOR	7912412	-0.1609	7.8774	0.046563829
XRCC6	8073457	0.1602	11.0548	0.027958337
STX2	7967685	0.1592	6.3599	0.042675032
TMEM63B	8119926	-0.1586	8.2728	0.025501987
ASL	8133122	-0.1563	7.0913	0.043254783
GTF2F1	8033135	-0.1514	8.4922	0.041879821
PDP1	8147344	0.1511	7.5115	0.046402966
ALOX15	8011680	0.1511	10.1609	0.046802833
PPAP2A	8112107	-0.1504	10.3658	0.046728797
GLE1	8158298	-0.1502	9.3227	0.041689483
ILF2	7920317	-0.1495	11.3149	0.036815384
SEMA3F	8079896	0.1494	6.7885	0.048354935
MCCC1	8092328	-0.1491	10.2019	0.041766023
FKBP15	8163452	-0.1469	7.9800	0.039340727
PLOD3	8141688	0.1494	8.4261	0.045862124
SLMAP	8080685	-2.0365	8.1105	0.049043704
DOCK1	7931293	-2.0361	7.7029	0.039306784

Appendix D: IPA Canonical Pathway Analysis

IPA Canonical Pathway	-log(p-value)
p53 Signaling	5.75E+00
Valine, Leucine and Isoleucine Degradation	4.31E+00
Molecular Mechanisms of Cancer	4.28E+00
Butanoate Metabolism	3.17E+00
Aryl Hydrocarbon Receptor Signaling	3.10E+00
Pancreatic Adenocarcinoma Signaling	2.99E+00
Lysine Degradation	2.93E+00
RAR Activation	2.56E+00
Glycerophospholipid Metabolism	2.51E+00
GNRH Signaling	2.42E+00
β-alanine Metabolism	2.36E+00
Arginine and Proline Metabolism	2.29E+00
TR/RXR Activation	2.27E+00
Chronic Myeloid Leukemia Signaling	2.21E+00
HGF Signaling	2.21E+00
Prostate Cancer Signaling	2.17E+00
Renin-Angiotensin Signaling	2.17E+00
Role of NFAT in Cardiac Hypertrophy	2.14E+00
Ascorbate and Aldarate Metabolism	2.11E+00
Protein Kinase A Signaling	2.07E+00
HER-2 Signaling in Breast Cancer	2.02E+00
Fatty Acid Metabolism	1.98E+00
Riboflavin Metabolism	1.93E+00
Notch Signaling	1.93E+00
Inositol Phosphate Metabolism	1.92E+00
Propanoate Metabolism	1.87E+00
Reelin Signaling in Neurons	1.87E+00
Glioblastoma Multiforme Signaling	1.83E+00
Myc Mediated Apoptosis Signaling	1.83E+00
Glioma Signaling	1.79E+00
Aminoacyl-tRNA Biosynthesis	1.78E+00
mTOR Signaling	1.78E+00
Phospholipid Degradation	1.78E+00
Huntington's Disease Signaling	1.75E+00
Cell Cycle Control of Chromosomal Replication	1.75E+00
Estrogen Receptor Signaling	1.74E+00
Androgen Signaling	1.73E+00
Endothelin-1 Signaling	1.71E+00
RAN Signaling	1.70E+00
Mismatch Repair in Eukaryotes	1.70E+00
Type II Diabetes Mellitus Signaling	1.70E+00
Rac Signaling	1.68E+00
Cell Cycle: G1/S Checkpoint Regulation	1.67E+00
CXCR4 Signaling	1.67E+00
One Carbon Pool by Folate	1.66E+00
Melanocyte Development and Pigmentation Signaling	1.59E+00
Glyoxylate and Dicarboxylate Metabolism	1.59E+00
Endoplasmic Reticulum Stress Pathway	1.59E+00
Methionine Metabolism	1.58E+00
Melanoma Signaling	1.58E+00
P2Y Purigenic Receptor Signaling Pathway	1.55E+00
Neuregulin Signaling	1.55E+00
Protein Ubiquitination Pathway	1.53E+00
Cell Cycle: G2/M DNA Damage Checkpoint Regulation	1.52E+00
B Cell Receptor Signaling	1.49E+00
Non-Small Cell Lung Cancer Signaling	1.46E+00
Prolactin Signaling	1.43E+00
Virus Entry via Endocytic Pathways	1.43E+00
Docosahexaenoic Acid (DHA) Signaling	1.41E+00
Endometrial Cancer Signaling	1.40E+00

IPA Canonical Pathway	-log(p-value)
ILK Signaling	1.40E+00
Nitric Oxide Signaling in the Cardiovascular System	1.39E+00
SAPK/JNK Signaling	1.39E+00
Glucocorticoid Receptor Signaling	1.38E+00
Nicotinate and Nicotinamide Metabolism	1.38E+00
NRF2-mediated Oxidative Stress Response	1.37E+00
Estrogen-Dependent Breast Cancer Signaling	1.36E+00
Fcγ Receptor-mediated Phagocytosis in Macrophages and Monocytes	1.35E+00
EGF Signaling	1.35E+00
Role of Tissue Factor in Cancer	1.33E+00
FGF Signaling	1.33E+00
Glycolysis/Gluconeogenesis	1.32E+00
JAK/Stat Signaling	1.32E+00
DNA Methylation and Transcriptional Repression Signaling	1.30E+00
IL-8 Signaling	1.30E+00
Clathrin-mediated Endocytosis Signaling	1.26E+00
Thrombopoietin Signaling	1.26E+00
CNTF Signaling	1.24E+00
FcγRIIB Signaling in B Lymphocytes	1.24E+00
Breast Cancer Regulation by Stathmin1	1.23E+00
Small Cell Lung Cancer Signaling	1.21E+00
Pyruvate Metabolism	1.21E+00
p70S6K Signaling	1.20E+00
Fatty Acid Elongation in Mitochondria	1.20E+00
Amyotrophic Lateral Sclerosis Signaling	1.18E+00
Hereditary Breast Cancer Signaling	1.17E+00
Death Receptor Signaling	1.17E+00
Neurotrophin/TRK Signaling	1.15E+00
Polyamine Regulation in Colon Cancer	1.15E+00
CCR3 Signaling in Eosinophils	1.14E+00
LPS-stimulated MAPK Signaling	1.14E+00
Citrate Cycle	1.13E+00
PI3K/AKT Signaling	1.09E+00
fMLP Signaling in Neutrophils	1.09E+00
RhoA Signaling	1.09E+00

IPA Canonical Pathway	-log(p-value)
Glycerolipid Metabolism	1.09E+00
Melatonin Signaling	1.07E+00
ATM Signaling	1.06E+00
Colorectal Cancer Metastasis Signaling	1.06E+00
Phospholipase C Signaling	1.06E+00
Granzyme A Signaling	1.03E+00
Acute Myeloid Leukemia Signaling	1.03E+00
Circadian Rhythm Signaling	1.01E+00
Hypoxia Signaling in the Cardiovascular System	1.01E+00
Role of NANOG in Mammalian Embryonic Stem Cell Pluripotency	1.00E+00
Renal Cell Carcinoma Signaling	1.00E+00
Thrombin Signaling	1.00E+00
Cyclins and Cell Cycle Regulation	9.98E-01
Aldosterone Signaling in Epithelial Cells	9.86E-01
Lymphotoxin β Receptor Signaling	9.83E-01
RANK Signaling in Osteoclasts	9.67E-01
VDR/RXR Activation	9.66E-01
TWEAK Signaling	9.62E-01
CREB Signaling in Neurons	9.61E-01
TNFR1 Signaling	9.58E-01
Role of PI3K/AKT Signaling in the Pathogenesis of Influenza	9.45E-01
Synaptic Long Term Potentiation	9.45E-01
Ephrin Receptor Signaling	9.40E-01
Leptin Signaling in Obesity	9.36E-01
Insulin Receptor Signaling	9.32E-01
Sphingosine-1-phosphate Signaling	9.19E-01
Relaxin Signaling	9.16E-01
Ovarian Cancer Signaling	9.16E-01
Valine, Leucine and Isoleucine Biosynthesis	9.15E-01
Synthesis and Degradation of Ketone Bodies	9.15E-01
Pentose Phosphate Pathway	9.12E-01
Urea Cycle and Metabolism of Amino Groups	9.12E-01
Calcium Signaling	9.10E-01
EIF2 Signaling	9.05E-01
NF-κB Activation by Viruses	9.04E-01

IPA Canonical Pathway	-log(p-value)
IL-15 Production	8.97E-01
Corticotropin Releasing Hormone Signaling	8.93E-01
ERK/MAPK Signaling	8.92E-01
Xenobiotic Metabolism Signaling	8.83E-01
Cardiac Hypertrophy Signaling	8.82E-01
Amyloid Processing	8.79E-01
Glioma Invasiveness Signaling	8.73E-01
Wnt/β-catenin Signaling	8.70E-01
IL-9 Signaling	8.66E-01
Tryptophan Metabolism	8.53E-01
Alanine and Aspartate Metabolism	8.50E-01
Neuropathic Pain Signaling In Dorsal Horn Neurons	8.35E-01
Cell Cycle Regulation by BTG Family Proteins	8.21E-01
Macropinocytosis Signaling	8.10E-01
Induction of Apoptosis by HIV1	8.07E-01
ERK5 Signaling	8.07E-01
TNFR2 Signaling	7.95E-01
CTLA4 Signaling in Cytotoxic T Lymphocytes	7.94E-01
HIF1α Signaling	7.87E-01
Linoleic Acid Metabolism	7.80E-01
Growth Hormone Signaling	7.80E-01
Role of Oct4 in Mammalian Embryonic Stem Cell Pluripotency	7.74E-01
Histidine Metabolism	7.73E-01
Production of Nitric Oxide and Reactive Oxygen Species in Macrophages	7.71E-01
Nucleotide Sugars Metabolism	7.63E-01
Ceramide Signaling	7.60E-01
Leukocyte Extravasation Signaling	7.54E-01
Purine Metabolism	7.52E-01
Sonic Hedgehog Signaling	7.49E-01
α-Adrenergic Signaling	7.43E-01
Germ Cell-Sertoli Cell Junction Signaling	7.34E-01
Integrin Signaling	7.33E-01
14-3-3-mediated Signaling	7.31E-01
Pantothenate and CoA Biosynthesis	7.21E-01

IPA Canonical Pathway	-log(p-value)
Factors Promoting Cardiogenesis in Vertebrates	7.19E-01
PAK Signaling	7.19E-01
Regulation of eIF4 and p70S6K Signaling	7.19E-01
GM-CSF Signaling	7.16E-01
IGF-1 Signaling	7.07E-01
Pyrimidine Metabolism	7.03E-01
Granzyme B Signaling	6.99E-01
IL-3 Signaling	6.98E-01
PDGF Signaling	6.98E-01
G Beta Gamma Signaling	6.95E-01
Tight Junction Signaling	6.85E-01
PI3K Signaling in B Lymphocytes	6.82E-01
Glutathione Metabolism	6.79E-01
Tumoricidal Function of Hepatic Natural Killer Cells	6.73E-01
BMP signaling pathway	6.72E-01
GABA Receptor Signaling	6.72E-01
Axonal Guidance Signaling	6.70E-01
CD28 Signaling in T Helper Cells	6.56E-01
PKCθ Signaling in T Lymphocytes	6.56E-01
Cholecystokinin/Gastrin-mediated Signaling	6.42E-01
Bile Acid Biosynthesis	6.41E-01
Angiopoietin Signaling	6.35E-01
Neuroprotective Role of THOP1 in Alzheimer's Disease	6.33E-01
IL-1 Signaling	6.28E-01
TGF-β Signaling	6.14E-01
p38 MAPK Signaling	6.02E-01
Tyrosine Metabolism	6.00E-01
Role of CHK Proteins in Cell Cycle Checkpoint Control	5.92E-01
HMGB1 Signaling	5.87E-01
Erythropoietin Signaling	5.86E-01
Assembly of RNA Polymerase II Complex	5.83E-01
Apoptosis Signaling	5.72E-01
PPARα/RXRα Activation	5.71E-01
Role of NFAT in Regulation of the Immune Response	5.71E-01
Synaptic Long Term Depression	5.57E-01

IPA Canonical Pathway	-log(p-value)
CD27 Signaling in Lymphocytes	5.56E-01
Role of JAK1 and JAK3 in γc Cytokine Signaling	5.47E-01
PTEN Signaling	5.46E-01
Acute Phase Response Signaling	5.42E-01
FLT3 Signaling in Hematopoietic Progenitor Cells	5.40E-01
Semaphorin Signaling in Neurons	5.30E-01
PXR/RXR Activation	5.23E-01
Basal Cell Carcinoma Signaling	5.18E-01
Calcium-induced T Lymphocyte Apoptosis	5.06E-01
CD40 Signaling	5.01E-01
Fatty Acid Biosynthesis	4.95E-01
N-Glycan Biosynthesis	4.82E-01
CCR5 Signaling in Macrophages	4.79E-01
IL-17A Signaling in Airway Cells	4.79E-01
Fc Epsilon RI Signaling	4.77E-01
Glutamate Metabolism	4.68E-01
Eicosanoid Signaling	4.58E-01
AMPK Signaling	4.51E-01
4-1BB Signaling in T Lymphocytes	4.47E-01
NF-κB Signaling	4.45E-01
IL-12 Signaling and Production in Macrophages	4.45E-01
Actin Cytoskeleton Signaling	4.37E-01
G Protein Signaling Mediated by Tubby	4.18E-01
Methane Metabolism	3.99E-01
Bladder Cancer Signaling	3.92E-01
Role of Wnt/GSK-3β Signaling in the Pathogenesis of Influenza	3.83E-01
Glycine, Serine and Threonine Metabolism	3.83E-01
Fructose and Mannose Metabolism	3.75E-01
Inositol Metabolism	3.74E-01
Sphingolipid Metabolism	3.72E-01
Role of JAK1, JAK2 and TYK2 in Interferon Signaling	3.62E-01
DNA Double-Strand Break Repair by Non-Homologous End Joining	3.60E-01
Role of Macrophages, Fibroblasts and Endothelial Cells in Rheumatoid Arthritis	3.54E-01
Inhibition of Angiogenesis by TSP1	3.42E-01

IPA Canonical Pathway	-log(p-value)
Cdc42 Signaling	3.27E-01
Cardiac β-adrenergic Signaling	3.22E-01
Oncostatin M Signaling	3.20E-01
Phenylalanine Metabolism	3.20E-01
IL-2 Signaling	3.20E-01
Role of Osteoblasts, Osteoclasts and Chondrocytes in Rheumatoid Arthritis	3.12E-01
Role of JAK family kinases in IL-6-type Cytokine Signaling	3.09E-01
Role of IL-17A in Arthritis	3.03E-01
Nucleotide Excision Repair Pathway	3.00E-01
IL-4 Signaling	2.97E-01
Folate Biosynthesis	2.94E-01
MSP-RON Signaling Pathway	2.93E-01
T Cell Receptor Signaling	2.83E-01
Role of RIG1-like Receptors in Antiviral Innate Immunity	2.80E-01
Selenoamino Acid Metabolism	2.80E-01
Gα12/13 Signaling	2.76E-01
Metabolism of Xenobiotics by Cytochrome P450	2.75E-01
VEGF Signaling	2.75E-01
Agrin Interactions at Neuromuscular Junction	2.69E-01
April Mediated Signaling	2.45E-01
Retinol Metabolism	2.45E-01
Cardiomyocyte Differentiation via BMP Receptors	2.42E-01

Bibliography

Bibliography

Abate-Shen, C. and Shen, M. M. (2000). "Molecular genetics of prostate cancer." Genes Dev **14**(19): 2410-34.

Agus, D. B., Cordon-Cardo, C., et al. (1999). "Prostate cancer cell cycle regulators: response to androgen withdrawal and development of androgen independence." J Natl Cancer Inst **91**(21): 1869-76.

Alen, P., Claessens, F., et al. (1999). "The androgen receptor amino-terminal domain plays a key role in p160 coactivator-stimulated gene transcription." Mol Cell Biol **19**(9): 6085-97.

Ali, A., Zhang, J., et al. (2004). "Requirement of protein phosphatase 5 in DNA-damage-induced ATM activation." Genes Dev **18**(3): 249-54.

Ali, M. M., Roe, S. M., et al. (2006). "Crystal structure of an Hsp90-nucleotide-p23/Sba1 closed chaperone complex." Nature **440**(7087): 1013-7.

Allen, N. E., Key, T. J., et al. (2008). "Animal foods, protein, calcium and prostate cancer risk: the European Prospective Investigation into Cancer and Nutrition." Br J Cancer **98**(9): 1574-81.

Andrade, M. A., Perez-Iratxeta, C., et al. (2001). "Protein repeats: structures, functions, and evolution." J Struct Biol **134**(2-3): 117-31.

Andren, O., Garmo, H., et al. (2009). "Incidence and mortality of incidental prostate cancer: a Swedish register-based study." Br J Cancer **100**(1): 170-3.

Angeletti, P. C., Walker, D., et al. (2002). "Small glutamine-rich protein/viral protein U-binding protein is a novel cochaperone that affects heat shock protein 70 activity." Cell Stress Chaperones **7**(3): 258-68.

Aris-Brosou, S. (2005). "Determinants of adaptive evolution at the molecular level: the extended complexity hypothesis." Mol Biol Evol **22**(2): 200-9.

Arora, R., Koch, M. O., et al. (2004). "Heterogeneity of Gleason grade in multifocal adenocarcinoma of the prostate." Cancer **100**(11): 2362-6.

Asano, T., Kanda, A., et al. (2000). "p110beta is up-regulated during differentiation of 3T3-L1 cells and contributes to the highly insulin-responsive glucose transport activity." J Biol Chem **275**(23): 17671-6.

Attard, G., Reid, A. H., et al. (2008). "Phase I clinical trial of a selective inhibitor of CYP17, abiraterone acetate, confirms that castration-resistant prostate cancer commonly remains hormone driven." J Clin Oncol **26**(28): 4563-71.

Attard, G., Richards, J., et al. (2011). "Targeting the androgen receptor signaling pathway in metastatic prostate cancer." Clin Cancer Res.

Bahia, H., Ashman, J. N., et al. (2002). "Karyotypic variation between independently cultured strains of the cell line MCF-7 identified by multicolour fluorescence in situ hybridization." Int J Oncol **20**(3): 489-94.

Barent, R. L., Nair, S. C., et al. (1998). "Analysis of FKBP51/FKBP52 chimeras and mutants for Hsp90 binding and association with progesterone receptor complexes." Mol Endocrinol **12**(3): 342-54.

Bastien, J., Plassat, J. L., et al. (2006). "The phosphoinositide 3-kinase/Akt pathway is essential for the retinoic acid-induced differentiation of F9 cells." Oncogene **25**(14): 2040-7.

Baughman, G., Wiederrecht, G. J., et al. (1995). "FKBP51, a novel T-cell-specific immunophilin capable of calcineurin inhibition." Mol Cell Biol **15**(8): 4395-402.

Bech Ganner, A., Negrello, T., et al. (2010). Cancer in Australia : in brief, 2010. Canberra, Australian Institute of Health and Welfare.

Bentel, J. M. and Tilley, W. D. (1996). "Androgen receptors in prostate cancer." J Endocrinol **151**(1): 1-11.

Blatch, G. L. and Lassle, M. (1999). "The tetratricopeptide repeat: a structural motif mediating protein-protein interactions." Bioessays **21**(11): 932-9.

Blom, N., Gammeltoft, S., et al. (1999). "Sequence and structure-based prediction of eukaryotic protein phosphorylation sites." J Mol Biol **294**(5): 1351-62.

Blom, N., Sicheritz-Ponten, T., et al. (2004). "Prediction of post-translational glycosylation and phosphorylation of proteins from the amino acid sequence." Proteomics **4**(6): 1633-49.

Bolton, E. C., So, A. Y., et al. (2007). "Cell- and gene-specific regulation of primary target genes by the androgen receptor." Genes Dev **21**(16): 2005-17.

Bostwick, D. G. (1992). "Prostatic intraepithelial neoplasia (PIN): current concepts." J Cell Biochem Suppl **16H**: 10-9.

Bostwick, D. G., Pacelli, A., et al. (1996). "Molecular biology of prostatic intraepithelial neoplasia." Prostate **29**(2): 117-34.

Bostwick, D. G., Shan, A., et al. (1998). "Independent origin of multiple foci of prostatic intraepithelial neoplasia: comparison with matched foci of prostate carcinoma." Cancer **83**(9): 1995-2002.

Bourdon, J. C. (2007). "p53 and its isoforms in cancer." Br J Cancer **97**(3): 277-82.

Brognard, J., Sierecki, E., et al. (2007). "PHLPP and a second isoform, PHLPP2, differentially attenuate the amplitude of Akt signaling by regulating distinct Akt isoforms." Mol Cell **25**(6): 917-31.

Brolin, J., Lowhagen, T., et al. (1992). "Immunocytochemical detection of the androgen receptor in fine needle aspirates from benign and malignant human prostate." Cytopathology **3**(6): 351-7.

Brychzy, A., Rein, T., et al. (2003). "Cofactor Tpr2 combines two TPR domains and a J domain to regulate the Hsp70/Hsp90 chaperone system." Embo J **22**(14): 3613-23.

Bubendorf, L., Schopfer, A., et al. (2000). "Metastatic patterns of prostate cancer: an autopsy study of 1,589 patients." Hum Pathol **31**(5): 578-83.

Buchanan, G., Craft, P. S., et al. (2004). "PC-3 cells with enhanced androgen receptor signaling: a model for clonal selection in prostate cancer." Prostate **60**(4): 352-66.

Buchanan, G., Greenberg, N. M., et al. (2001). "Collocation of androgen receptor gene mutations in prostate cancer." Clin Cancer Res **7**(5): 1273-81.

Buchanan, G., Irvine, R. A., et al. (2001). "Contribution of the androgen receptor to prostate cancer predisposition and progression." Cancer Metastasis Rev **20**(3-4): 207-23.

Buchanan, G., Ricciardelli, C., et al. (2007). "Control of androgen receptor signaling in prostate cancer by the cochaperone small glutamine rich tetratricopeptide repeat containing protein alpha." Cancer Res **67**(20): 10087-96.

Buchanan, G., Yang, M., et al. (2004). "Structural and functional consequences of glutamine tract variation in the androgen receptor." Hum Mol Genet **13**(16): 1677-92.

Buchanan, G., Yang, M., et al. (2001). "Mutations at the boundary of the hinge and ligand binding domain of the androgen receptor confer increased transactivation function." Mol Endocrinol **15**(1): 46-56.

Bukau, B. and Horwich, A. L. (1998). "The Hsp70 and Hsp60 chaperone machines." Cell **92**(3): 351-66.

Butler, L. M., Centenera, M. M., et al. (2006). "Suppression of androgen receptor signaling in prostate cancer cells by an inhibitory receptor variant." Mol Endocrinol **20**(5): 1009-24.

Byrne, R. L., Neal, D.E. (1996). Organ-Confined Prostate Cancer - Is Surgery the Only Option? . Questions and uncertaintes about prostate cancer. W. B. Peeling, Cornwall: Blackwell Science Ltd**:** 161-173.

Callahan, M. A., Handley, M. A., et al. (1998). "Functional interaction of human immunodeficiency virus type 1 Vpu and Gag with a novel member of the tetratricopeptide repeat protein family." J Virol **72**(10): 8461.

Cantrell, B. B., DeKlerk, D. P., et al. (1981). "Pathological factors that influence prognosis in stage A prostatic cancer: the influence of extent versus grade." J Urol **125**(4): 516-20.

Cardillo, M. R. and Ippoliti, F. (2006). "IL-6, IL-10 and HSP-90 expression in tissue microarrays from human prostate cancer assessed by computer-assisted image analysis." Anticancer Res **26**(5A): 3409-16.

Carrello, A., Allan, R. K., et al. (2004). "Interaction of the Hsp90 cochaperone cyclophilin 40 with Hsc70." Cell Stress Chaperones **9**(2): 167-81.

Carrello, A., Ingley, E., et al. (1999). "The common tetratricopeptide repeat acceptor site for steroid receptor-associated immunophilins and hop is located in the dimerization domain of Hsp90." J Biol Chem **274**(5): 2682-9.

Carver, B. S., Chapinski, C., et al. (2011). "Reciprocal Feedback Regulation of PI3K and Androgen Receptor Signaling in PTEN-Deficient Prostate Cancer." Cancer Cell **19**(5): 575-86.

Catalona, W. J. and Smith, D. S. (1994). "5-year tumor recurrence rates after anatomical radical retropubic prostatectomy for prostate cancer." J Urol **152**(5 Pt 2): 1837-42.

Centenera, M. M., Harris, J. M., et al. (2008). "The contribution of different androgen receptor domains to receptor dimerization and signaling." Mol Endocrinol **22**(11): 2373-82.

Chamberlain, N. L., Whitacre, D. C., et al. (1996). "Delineation of two distinct type 1 activation functions in the androgen receptor amino-terminal domain." J Biol Chem **271**(43): 26772-8.

Chambraud, B., Sardin, E., et al. (2010). "A role for FKBP52 in Tau protein function." Proc Natl Acad Sci U S A **107**(6): 2658-63.

Chen, C. D., Welsbie, D. S., et al. (2004). "Molecular determinants of resistance to antiandrogen therapy." Nat Med **10**(1): 33-9.

Chen, M. X. and Cohen, P. T. (1997). "Activation of protein phosphatase 5 by limited proteolysis or the binding of polyunsaturated fatty acids to the TPR domain." FEBS Lett **400**(1): 136-40.

Chen, M. X., McPartlin, A. E., et al. (1994). "A novel human protein serine/threonine phosphatase, which possesses four tetratricopeptide repeat motifs and localizes to the nucleus." Embo J **13**(18): 4278-90.

Chen, S. and Smith, D. F. (1998). "Hop as an adaptor in the heat shock protein 70 (Hsp70) and hsp90 chaperone machinery." J Biol Chem **273**(52): 35194-200.

Chen, S., Sullivan, W. P., et al. (1998). "Differential interactions of p23 and the TPR-containing proteins Hop, Cyp40, FKBP52 and FKBP51 with Hsp90 mutants." Cell Stress Chaperones **3**(2): 118-29.

Chen, Y., Sawyers, C. L., et al. (2008). "Targeting the androgen receptor pathway in prostate cancer." Curr Opin Pharmacol **8**(4): 440-8.

Cheng, H., Snoek, R., et al. (2006). "Short hairpin RNA knockdown of the androgen receptor attenuates ligand-independent activation and delays tumor progression." Cancer Res **66**(21): 10613-20.

Cheng, L., Shan, A., et al. (1998). "Atypical adenomatous hyperplasia of the prostate: a premalignant lesion?" Cancer Res **58**(3): 389-91.

Cheung-Flynn, J., Prapapanich, V., et al. (2005). "Physiological role for the cochaperone FKBP52 in androgen receptor signaling." Mol Endocrinol **19**(6): 1654-66.

Chi, S. G., deVere White, R. W., et al. (1994). "p53 in prostate cancer: frequent expressed transition mutations." J Natl Cancer Inst **86**(12): 926-33.

Chinkers, M. (1994). "Targeting of a distinctive protein-serine phosphatase to the protein kinase-like domain of the atrial natriuretic peptide receptor." Proc Natl Acad Sci U S A **91**(23): 11075-9.

Chipuk, J. E. and Green, D. R. (2006). "Dissecting p53-dependent apoptosis." Cell Death Differ **13**(6): 994-1002.

Chmelar, R., Buchanan, G., et al. (2007). "Androgen receptor coregulators and their involvement in the development and progression of prostate cancer." Int J Cancer **120**(4): 719-33.

Connell, P., Ballinger, C. A., et al. (2001). "The co-chaperone CHIP regulates protein triage decisions mediated by heat-shock proteins." Nat Cell Biol **3**(1): 93-6.

Cox, M. B., Riggs, D. L., et al. (2007). "FK506-binding protein 52 phosphorylation: a potential mechanism for regulating steroid hormone receptor activity." Mol Endocrinol **21**(12): 2956-67.

Cunha, G. R., Donjacour, A. A., et al. (1987). "The endocrinology and developmental biology of the prostate." Endocr Rev **8**(3): 338-62.

Cunha, G. R., Ricke, W., et al. (2004). "Hormonal, cellular, and molecular regulation of normal and neoplastic prostatic development." J Steroid Biochem Mol Biol **92**(4): 221-36.

Cutress, M. L., Whitaker, H. C., et al. (2008). "Structural basis for the nuclear import of the human androgen receptor." J Cell Sci **121**(Pt 7): 957-68.

Cyr, D. M. (1995). "Cooperation of the molecular chaperone Ydj1 with specific Hsp70 homologs to suppress protein aggregation." FEBS Lett **359**(2-3): 129-32.

Czar, M. J., Galigniana, M. D., et al. (1997). "Geldanamycin, a heat shock protein 90-binding benzoquinone ansamycin, inhibits steroid-dependent translocation of the glucocorticoid receptor from the cytoplasm to the nucleus." Biochemistry **36**(25): 7776-85.

Cziepluch, C., Kordes, E., et al. (1998). "Identification of a novel cellular TPR-containing protein, SGT, that interacts with the nonstructural protein NS1 of parvovirus H-1." J Virol **72**(5): 4149-56.

D'Amico, A. V., Chen, M. H., et al. (2004). "Preoperative PSA velocity and the risk of death from prostate cancer after radical prostatectomy." N Engl J Med **351**(2): 125-35.

D'Andrea, L. D. and Regan, L. (2003). "TPR proteins: the versatile helix." Trends Biochem Sci **28**(12): 655-62.

Dallas, P. B., Yaciuk, P., et al. (1997). "Characterization of monoclonal antibodies raised against p300: both p300 and CBP are present in intracellular TBP complexes." J Virol **71**(2): 1726-31.

Danila, D. C., Morris, M. J., et al. (2010). "Phase II multicenter study of abiraterone acetate plus prednisone therapy in patients with docetaxel-treated castration-resistant prostate cancer." J Clin Oncol **28**(9): 1496-501.

Das, A. K., Cohen, P. W., et al. (1998). "The structure of the tetratricopeptide repeats of protein phosphatase 5: implications for TPR-mediated protein-protein interactions." Embo J **17**(5): 1192-9.

Davies, T. H., Ning, Y. M., et al. (2002). "A new first step in activation of steroid receptors: hormone-induced switching of FKBP51 and FKBP52 immunophilins." J Biol Chem **277**(7): 4597-600.

Davies, T. H., Ning, Y. M., et al. (2005). "Differential control of glucocorticoid receptor hormone-binding function by tetratricopeptide repeat (TPR) proteins and the immunosuppressive ligand FK506." Biochemistry **44**(6): 2030-8.

Deguchi, T., Yang, M., et al. (1997). "Detection of micrometastatic prostate cancer cells in the bone marrow of patients with prostate cancer." Br J Cancer **75**(5): 634-8.

Dehm, S. M. and Tindall, D. J. (2005). "Regulation of androgen receptor signaling in prostate cancer." Expert Rev Anticancer Ther **5**(1): 63-74.

Dehm, S. M. and Tindall, D. J. (2007). "Androgen receptor structural and functional elements: role and regulation in prostate cancer." Mol Endocrinol **21**(12): 2855-63.

Denmeade, S. R., Lin, X. S., et al. (1996). "Role of programmed (apoptotic) cell death during the progression and therapy for prostate cancer." Prostate **28**(4): 251-65.

Denner, L. A., Schrader, W. T., et al. (1990). "Hormonal regulation and identification of chicken progesterone receptor phosphorylation sites." J Biol Chem **265**(27): 16548-55.

Denny, W. B., Valentine, D. L., et al. (2000). "Squirrel monkey immunophilin FKBP51 is a potent inhibitor of glucocorticoid receptor binding." Endocrinology **141**(11): 4107-13.

Deslypere, J. P., Young, M., et al. (1992). "Testosterone and 5 alpha-dihydrotestosterone interact differently with the androgen receptor to enhance transcription of the MMTV-CAT reporter gene." Mol Cell Endocrinol **88**(1-3): 15-22.

Dittmar, K. D., Hutchison, K. A., et al. (1996). "Reconstitution of the steroid receptor.hsp90 heterocomplex assembly system of rabbit reticulocyte lysate." J Biol Chem **271**(22): 12833-9.

Divita, G., Baillon, J. G., et al. (1995). "Interface peptides as structure-based human immunodeficiency virus reverse transcriptase inhibitors." J Biol Chem **270**(48): 28642-6.

Divita, G., Restle, T., et al. (1994). "Inhibition of human immunodeficiency virus type 1 reverse transcriptase dimerization using synthetic peptides derived from the connection domain." J Biol Chem **269**(18): 13080-3.

Dornan, J., Taylor, P., et al. (2003). "Structures of immunophilins and their ligand complexes." Curr Top Med Chem **3**(12): 1392-409.

Dutta, S. and Tan, Y. J. (2008). "Structural and functional characterization of human SGT and its interaction with Vpu of the human immunodeficiency virus type 1." Biochemistry **47**(38): 10123-31.

Eastham, J. A., Stapleton, A. M., et al. (1995). "Association of p53 mutations with metastatic prostate cancer." Clin Cancer Res **1**(10): 1111-8.

el-Deiry, W. S., Tokino, T., et al. (1993). "WAF1, a potential mediator of p53 tumor suppression." Cell **75**(4): 817-25.

Etzioni, R. D., Ankerst, D. P., et al. (2007). "Is prostate-specific antigen velocity useful in early detection of prostate cancer? A critical appraisal of the evidence." J Natl Cancer Inst **99**(20): 1510-5.

Faber, P. W., van Rooij, H. C., et al. (1993). "Two different, overlapping pathways of transcription initiation are active on the TATA-less human androgen receptor promoter. The role of Sp1." J Biol Chem **268**(13): 9296-301.

Fan, M., Park, A., et al. (2005). "CHIP (carboxyl terminus of Hsc70-interacting protein) promotes basal and geldanamycin-induced degradation of estrogen receptor-alpha." Mol Endocrinol **19**(12): 2901-14.

Febbo, P. G., Lowenberg, M., et al. (2005). "Androgen mediated regulation and functional implications of fkbp51 expression in prostate cancer." J Urol **173**(5): 1772-7.

Feldman, B. J. and Feldman, D. (2001). "The development of androgen-independent prostate cancer." Nat Rev Cancer **1**(1): 34-45.

Fonte, V., Kapulkin, V., et al. (2002). "Interaction of intracellular beta amyloid peptide with chaperone proteins." Proc Natl Acad Sci U S A **99**(14): 9439-44.

Foster, C. S., Dodson, A. R., et al. (2009). "Hsp-27 expression at diagnosis predicts poor clinical outcome in prostate cancer independent of ETS-gene rearrangement." Br J Cancer **101**(7): 1137-44.

Freeman, B. C., Felts, S. J., et al. (2000). "The p23 molecular chaperones act at a late step in intracellular receptor action to differentially affect ligand efficacies." Genes Dev **14**(4): 422-34.

Freeman, B. C. and Yamamoto, K. R. (2002). "Disassembly of transcriptional regulatory complexes by molecular chaperones." Science **296**(5576): 2232-5.

Froesch, B. A., Takayama, S., et al. (1998). "BAG-1L protein enhances androgen receptor function." J Biol Chem **273**(19): 11660-6.

Fu, M., Wang, C., et al. (2000). "p300 and p300/cAMP-response element-binding protein-associated factor acetylate the androgen receptor at sites governing hormone-dependent transactivation." J Biol Chem **275**(27): 20853-60.

Galat, A. (2003). "Peptidylprolyl cis/trans isomerases (immunophilins): biological diversity--targets--functions." Curr Top Med Chem **3**(12): 1315-47.

Gallo, L. I., Ghini, A. A., et al. (2007). "Differential recruitment of tetratricorpeptide repeat domain immunophilins to the mineralocorticoid receptor influences both heat-shock protein 90-dependent retrotransport and hormone-dependent transcriptional activity." Biochemistry **46**(49): 14044-57.

Georget, V., Terouanne, B., et al. (2002). "Mechanism of antiandrogen action: key role of hsp90 in conformational change and transcriptional activity of the androgen receptor." Biochemistry **41**(39): 11824-31.

Giovannucci, E., Liu, Y., et al. (2007). "Risk factors for prostate cancer incidence and progression in the health professionals follow-up study." Int J Cancer **121**(7): 1571-8.

Gleason, D. F. and Mellinger, G. T. (1974). "Prediction of prognosis for prostatic adenocarcinoma by combined histological grading and clinical staging." J Urol **111**(1): 58-64.

Gleave, M., Tolcher, A., et al. (1999). "Progression to androgen independence is delayed by adjuvant treatment with antisense Bcl-2 oligodeoxynucleotides after castration in the LNCaP prostate tumor model." Clin Cancer Res **5**(10): 2891-8.

Golden, T., Aragon, I. V., et al. (2008). "Elevated levels of Ser/Thr protein phosphatase 5 (PP5) in human breast cancer." Biochim Biophys Acta **1782**(4): 259-70.

Golden, T., Aragon, I. V., et al. (2004). "Constitutive over expression of serine/threonine protein phosphatase 5 (PP5) augments estrogen-dependent tumor growth in mice." Cancer Lett **215**(1): 95-100.

Goldstein, A. S., Huang, J., et al. (2010). "Identification of a cell of origin for human prostate cancer." Science **329**(5991): 568-71.

Grenert, J. P., Johnson, B. D., et al. (1999). "The importance of ATP binding and hydrolysis by hsp90 in formation and function of protein heterocomplexes." J Biol Chem **274**(25): 17525-33.

Gudmundsson, J., Sulem, P., et al. (2008). "Common sequence variants on 2p15 and Xp11.22 confer susceptibility to prostate cancer." Nat Genet **40**(3): 281-3.

Haapala, K., Kuukasjarvi, T., et al. (2007). "Androgen receptor amplification is associated with increased cell proliferation in prostate cancer." Hum Pathol **38**(3): 474-8.

Haelens, A., Tanner, T., et al. (2007). "The hinge region regulates DNA binding, nuclear translocation, and transactivation of the androgen receptor." Cancer Res **67**(9): 4514-23.

Hall, M. C., Young, D. A., et al. (2002). "Cryptic promoter activity of pBLCAT3 induced by overexpression of AP1 factors." Biotechniques **33**(5): 1004, 1006, 1008.

Hameed, O. and Humphrey, P. A. (2006). "Stratified epithelium in prostatic adenocarcinoma: a mimic of high-grade prostatic intraepithelial neoplasia." Mod Pathol **19**(7): 899-906.

Hanahan, D. and Weinberg, R. A. (2011). "Hallmarks of cancer: the next generation." Cell **144**(5): 646-74.

Handley, M. A., Paddock, S., et al. (2001). "Association of Vpu-binding protein with microtubules and Vpu-dependent redistribution of HIV-1 Gag protein." Virology **291**(2): 198-207.

Harper, J. W., Adami, G. R., et al. (1993). "The p21 Cdk-interacting protein Cip1 is a potent inhibitor of G1 cyclin-dependent kinases." Cell **75**(4): 805-16.

He, B., Bai, S., et al. (2004). "An androgen receptor NH2-terminal conserved motif interacts with the COOH terminus of the Hsp70-interacting protein (CHIP)." J Biol Chem **279**(29): 30643-53.

He, B. and Wilson, E. M. (2002). "The NH(2)-terminal and carboxyl-terminal interaction in the human androgen receptor." Mol Genet Metab **75**(4): 293-8.

Heinlein, C. A. and Chang, C. (2002). "Androgen receptor (AR) coregulators: an overview." Endocr Rev **23**(2): 175-200.

Hendriksen, P. J., Dits, N. F., et al. (2006). "Evolution of the androgen receptor pathway during progression of prostate cancer." Cancer Res **66**(10): 5012-20.

Hessling, M., Richter, K., et al. (2009). "Dissection of the ATP-induced conformational cycle of the molecular chaperone Hsp90." Nat Struct Mol Biol **16**(3): 287-93.

Hinds, T. D., Jr. and Sanchez, E. R. (2008). "Protein phosphatase 5." Int J Biochem Cell Biol **40**(11): 2358-62.

Hobisch, A., Culig, Z., et al. (1996). "Androgen receptor status of lymph node metastases from prostate cancer." Prostate **28**(2): 129-35.

Hodgson, M. C., Astapova, I., et al. (2005). "The androgen receptor recruits nuclear receptor CoRepressor (N-CoR) in the presence of mifepristone via its N and C termini revealing a novel molecular mechanism for androgen receptor antagonists." J Biol Chem **280**(8): 6511-9.

Holzbeierlein, J., Lal, P., et al. (2004). "Gene expression analysis of human prostate carcinoma during hormonal therapy identifies androgen-responsive genes and mechanisms of therapy resistance." Am J Pathol **164**(1): 217-27.

Horibe, T., Kohno, M., et al. (2011). "Designed hybrid TPR peptide targeting Hsp90 as a novel anticancer agent." J Transl Med **9**: 8.

Horton, R. M., Hunt, H. D., et al. (1989). "Engineering hybrid genes without the use of restriction enzymes: gene splicing by overlap extension." Gene **77**(1): 61-8.

Huber, W., von Heydebreck, A., et al. (2002). "Variance stabilization applied to microarray data calibration and to the quantification of differential expression." Bioinformatics **18 Suppl 1**: S96-104.

Hubert, R. S., Vivanco, I., et al. (1999). "STEAP: a prostate-specific cell-surface antigen highly expressed in human prostate tumors." Proc Natl Acad Sci U S A **96**(25): 14523-8.

Huggins, C. and Hodges, C. V. (1972). "Studies on prostatic cancer. I. The effect of castration, of estrogen and androgen injection on serum phosphatases in metastatic carcinoma of the prostate." CA Cancer J Clin **22**(4): 232-40.

Ikeda, K., Ogawa, S., et al. (2004). "Protein phosphatase 5 is a negative regulator of estrogen receptor-mediated transcription." Mol Endocrinol **18**(5): 1131-43.

Ingermann, A. R., Yang, Y. F., et al. (2010). "Identification of a novel cell death receptor mediating IGFBP-3-induced anti-tumor effects in breast and prostate cancer." J Biol Chem **285**(39): 30233-46.

Jackson, A. L. and Linsley, P. S. (2004). "Noise amidst the silence: off-target effects of siRNAs?" Trends Genet **20**(11): 521-4.

Jariwala, U., Cogan, J. P., et al. (2009). "Inhibition of AR-mediated transcription by binding of Oct1 to a motif enriched in AR-occupied regions." Prostate **69**(4): 392-400.

Jenster, G., van der Korput, H. A., et al. (1995). "Identification of two transcription activation units in the N-terminal domain of the human androgen receptor." J Biol Chem **270**(13): 7341-6.

Jenster, G., van der Korput, J. A., et al. (1992). "Functional domains of the human androgen receptor." J Steroid Biochem Mol Biol **41**(3-8): 671-5.

Jia, L., Berman, B. P., et al. (2008). "Genomic androgen receptor-occupied regions with different functions, defined by histone acetylation, coregulators and transcriptional capacity." PLoS ONE **3**(11): e3645.

Jiang, X., Chen, S., et al. (2010). "Phosphoinositide 3-kinase pathway activation in phosphate and tensin homolog (PTEN)-deficient prostate cancer cells is independent of receptor tyrosine kinases and mediated by the p110beta and p110delta catalytic subunits." J Biol Chem **285**(20): 14980-9.

Johansson, J. E., Andren, O., et al. (2004). "Natural history of early, localized prostate cancer." Jama **291**(22): 2713-9.

Johnson, B. D., Schumacher, R. J., et al. (1998). "Hop modulates Hsp70/Hsp90 interactions in protein folding." J Biol Chem **273**(6): 3679-86.

Johnson, J. L. and Brown, C. (2009). "Plasticity of the Hsp90 chaperone machine in divergent eukaryotic organisms." Cell Stress Chaperones **14**(1): 83-94.

Jones, S. and Thornton, J. M. (1997). "Analysis of protein-protein interaction sites using surface patches." J Mol Biol **272**(1): 121-32.

Kadauke, S. and Blobel, G. A. (2009). "Chromatin loops in gene regulation." Biochim Biophys Acta **1789**(1): 17-25.

Kaku, N., Matsuda, K. I., et al. (2008). "CHARACTERIZATION OF NUCLEAR IMPORT OF THE DOMAIN-SPECIFIC ANDROGEN RECEPTOR IN ASSOCIATION WITH THE IMPORTIN {alpha}/{beta} AND RAN-GTP SYSTEMS." Endocrinology.

Kampinga, H. H., Kanon, B., et al. (2003). "Overexpression of the cochaperone CHIP enhances Hsp70-dependent folding activity in mammalian cells." Mol Cell Biol **23**(14): 4948-58.

Katzman, S., Barrett, C., et al. (2008). "PREDICT-2ND: a tool for generalized protein local structure prediction." Bioinformatics **24**(21): 2453-9.

Kaufman, J. M. and Vermeulen, A. (2005). "The decline of androgen levels in elderly men and its clinical and therapeutic implications." Endocr Rev **26**(6): 833-76.

Khokhlatchev, A. V., Canagarajah, B., et al. (1998). "Phosphorylation of the MAP kinase ERK2 promotes its homodimerization and nuclear translocation." Cell **93**(4): 605-15.

Klemm, J. D., Schreiber, S. L., et al. (1998). "Dimerization as a regulatory mechanism in signal transduction." Annu Rev Immunol **16**: 569-92.

Knudsen, K. E. and Penning, T. M. (2010). "Partners in crime: deregulation of AR activity and androgen synthesis in prostate cancer." Trends Endocrinol Metab **21**(5): 315-24.

Ko, S. C., Gotoh, A., et al. (1996). "Molecular therapy with recombinant p53 adenovirus in an androgen-independent, metastatic human prostate cancer model." Hum Gene Ther **7**(14): 1683-91.

Kocanova, S., Mazaheri, M., et al. (2010). "Ligands specify estrogen receptor alpha nuclear localization and degradation." BMC Cell Biol **11**: 98.

Kok, K., Geering, B., et al. (2009). "Regulation of phosphoinositide 3-kinase expression in health and disease." Trends Biochem Sci **34**(3): 115-27.

Kordes, E., Savelyeva, L., et al. (1998). "Isolation and characterization of human SGT and identification of homologues in Saccharomyces cerevisiae and Caenorhabditis elegans." Genomics **52**(1): 90-4.

Kozany, C., Marz, A., et al. (2009). "Fluorescent probes to characterise FK506-binding proteins." Chembiochem **10**(8): 1402-10.

Kumar, S. and Bansal, M. (1998). "Geometrical and sequence characteristics of alpha-helices in globular proteins." Biophys J **75**(4): 1935-44.

Lamb, J. R., Tugendreich, S., et al. (1995). "Tetratrico peptide repeat interactions: to TPR or not to TPR?" Trends Biochem Sci **20**(7): 257-9.

Langley, E., Zhou, Z. X., et al. (1995). "Evidence for an anti-parallel orientation of the ligand-activated human androgen receptor dimer." J Biol Chem **270**(50): 29983-90.

Larsen, T. A., Olson, A. J., et al. (1998). "Morphology of protein-protein interfaces." Structure **6**(4): 421-7.

Lawson, D. A., Zong, Y., et al. (2010). "Basal epithelial stem cells are efficient targets for prostate cancer initiation." Proc Natl Acad Sci U S A **107**(6): 2610-5.

Lee, Y. R., Park, J., et al. (2005). "Up-regulation of PI3K/Akt signaling by 17beta-estradiol through activation of estrogen receptor-alpha, but not estrogen receptor-beta, and

stimulates cell growth in breast cancer cells." Biochem Biophys Res Commun **336**(4): 1221-6.

Leveille, N., Fournier, A., et al. (2009). "Androgens down-regulate myosin light chain kinase in human prostate cancer cells." J Steroid Biochem Mol Biol **114**(3-5): 174-9.

Li, L., Ittmann, M. M., et al. (2005). "The emerging role of the PI3-K-Akt pathway in prostate cancer progression." Prostate Cancer Prostatic Dis **8**(2): 108-18.

Lim, C. S., Baumann, C. T., et al. (1999). "Differential localization and activity of the A- and B-forms of the human progesterone receptor using green fluorescent protein chimeras." Mol Endocrinol **13**(3): 366-75.

Liou, S. T. and Wang, C. (2005). "Small glutamine-rich tetratricopeptide repeat-containing protein is composed of three structural units with distinct functions." Arch Biochem Biophys **435**(2): 253-63.

Liu, A. Y., Brubaker, K. D., et al. (2004). "Lineage relationship between LNCaP and LNCaP-derived prostate cancer cell lines." Prostate **60**(2): 98-108.

Liu, F. H., Wu, S. J., et al. (1999). "Specific interaction of the 70-kDa heat shock cognate protein with the tetratricopeptide repeats." J Biol Chem **274**(48): 34425-32.

Liu, H. S., Jan, M. S., et al. (1999). "Is green fluorescent protein toxic to the living cells?" Biochem Biophys Res Commun **260**(3): 712-7.

Liu, J., Chen, C. M., et al. (1991). "Human and Escherichia coli cyclophilins: sensitivity to inhibition by the immunosuppressant cyclosporin A correlates with a specific tryptophan residue." Biochemistry **30**(9): 2306-10.

Liu, X. X., Rocchi, P., et al. (2009). "PAMAM dendrimers mediate siRNA delivery to target Hsp27 and produce potent antiproliferative effects on prostate cancer cells." ChemMedChem **4**(8): 1302-10.

Livak, K. J. and Schmittgen, T. D. (2001). "Analysis of relative gene expression data using real-time quantitative PCR and the 2(-Delta Delta C(T)) Method." Methods **25**(4): 402-8.

Locke, J. A., Guns, E. S., et al. (2008). "Androgen levels increase by intratumoral de novo steroidogenesis during progression of castration-resistant prostate cancer." Cancer Res **68**(15): 6407-15.

Magee, J. A., Chang, L. W., et al. (2006). "Direct, androgen receptor-mediated regulation of the FKBP5 gene via a distal enhancer element." Endocrinology **147**(1): 590-8.

Marcelli, M., Stenoien, D. L., et al. (2006). "Quantifying effects of ligands on androgen receptor nuclear translocation, intranuclear dynamics, and solubility." J Cell Biochem **98**(4): 770-88.

Marker, P. C., Donjacour, A. A., et al. (2003). "Hormonal, cellular, and molecular control of prostatic development." Dev Biol **253**(2): 165-74.

Massie, C. E., Adryan, B., et al. (2007). "New androgen receptor genomic targets show an interaction with the ETS1 transcription factor." EMBO Rep **8**(9): 871-8.

Massie, C. E. and Mills, I. G. (2008). "ChIPping away at gene regulation." EMBO Rep **9**(4): 337-43.

Massoner, P., Colleselli, D., et al. (2009). "Novel mechanism of IGF-binding protein-3 action on prostate cancer cells: inhibition of proliferation, adhesion, and motility." Endocr Relat Cancer **16**(3): 795-808.

Matias, P. M., Donner, P., et al. (2000). "Structural evidence for ligand specificity in the binding domain of the human androgen receptor. Implications for pathogenic gene mutations." J Biol Chem **275**(34): 26164-71.

McKenna, N. J., Lanz, R. B., et al. (1999). "Nuclear receptor coregulators: cellular and molecular biology." Endocr Rev **20**(3): 321-44.

McLaughlin, S. H., Smith, H. W., et al. (2002). "Stimulation of the weak ATPase activity of human hsp90 by a client protein." J Mol Biol **315**(4): 787-98.

McLaughlin, S. H., Sobott, F., et al. (2006). "The co-chaperone p23 arrests the Hsp90 ATPase cycle to trap client proteins." J Mol Biol **356**(3): 746-58.

Moilanen, A., Rouleau, N., et al. (1997). "The presence of a transcription activation function in the hormone-binding domain of androgen receptor is revealed by studies in yeast cells." FEBS Lett **412**(2): 355-8.

Mok, D., Allan, R. K., et al. (2006). "The chaperone function of cyclophilin 40 maps to a cleft between the prolyl isomerase and tetratricopeptide repeat domains." FEBS Lett **580**(11): 2761-8.

Montgomery, R. B., Mostaghel, E. A., et al. (2008). "Maintenance of intratumoral androgens in metastatic prostate cancer: a mechanism for castration-resistant tumor growth." Cancer Res **68**(11): 4447-54.

Montironi, R., Bostwick, D. G., et al. (1996). "Origins of prostate cancer." Cancer **78**(2): 362-5.

Moras, D. and Gronemeyer, H. (1998). "The nuclear receptor ligand-binding domain: structure and function." Curr Opin Cell Biol **10**(3): 384-91.

Morita, K., Saitoh, M., et al. (2001). "Negative feedback regulation of ASK1 by protein phosphatase 5 (PP5) in response to oxidative stress." Embo J **20**(21): 6028-36.

Moritz, A., Li, Y., et al. (2010). "Akt-RSK-S6 kinase signaling networks activated by oncogenic receptor tyrosine kinases." Sci Signal **3**(136): ra64.

Mulholland, D. J., Tran, L. M., et al. (2011). "Cell Autonomous Role of PTEN in Regulating Castration-Resistant Prostate Cancer Growth." Cancer Cell.

Nagy, B., Szendroi, A., et al. (2009). "Overexpression of CD24, c-myc and phospholipase 2A in prostate cancer tissue samples obtained by needle biopsy." Pathol Oncol Res **15**(2): 279-83.

Need, E. F., Scher, H. I., et al. (2009). "A novel androgen receptor amino terminal region reveals two classes of amino/carboxyl interaction-deficient variants with divergent capacity to activate responsive sites in chromatin." Endocrinology **150**(6): 2674-82.

Ni, L., Yang, C. S., et al. (2010). "FKBP51 promotes assembly of the Hsp90 chaperone complex and regulates androgen receptor signaling in prostate cancer cells." Mol Cell Biol **30**(5): 1243-53.

Nicolet, C. M. and Craig, E. A. (1991). "Functional analysis of a conserved amino-terminal region of HSP70 by site-directed mutagenesis." Yeast **7**(7): 699-716.

Nooren, I. M. and Thornton, J. M. (2003). "Structural characterisation and functional significance of transient protein-protein interactions." J Mol Biol **325**(5): 991-1018.

Olshavsky, N. A., Groh, E. M., et al. (2008). "Cyclin D3 action in androgen receptor regulation and prostate cancer." Oncogene **27**(22): 3111-21.

Owens-Grillo, J. K., Czar, M. J., et al. (1996). "A model of protein targeting mediated by immunophilins and other proteins that bind to hsp90 via tetratricopeptide repeat domains." J Biol Chem **271**(23): 13468-75.

Ozanne, D. M., Brady, M. E., et al. (2000). "Androgen receptor nuclear translocation is facilitated by the f-actin cross-linking protein filamin." Mol Endocrinol **14**(10): 1618-26.

Peattie, D. A., Harding, M. W., et al. (1992). "Expression and characterization of human FKBP52, an immunophilin that associates with the 90-kDa heat shock protein and is a component of steroid receptor complexes." Proc Natl Acad Sci U S A **89**(22): 10974-8.

Pei, H., Li, L., et al. (2009). "FKBP51 affects cancer cell response to chemotherapy by negatively regulating Akt." Cancer Cell **16**(3): 259-66.

Periyasamy, S., Hinds, T., Jr., et al. (2010). "FKBP51 and Cyp40 are positive regulators of androgen-dependent prostate cancer cell growth and the targets of FK506 and cyclosporin A." Oncogene **29**(11): 1691-701.

Periyasamy, S., Warrier, M., et al. (2007). "The immunophilin ligands cyclosporin A and FK506 suppress prostate cancer cell growth by androgen receptor-dependent and -independent mechanisms." Endocrinology **148**(10): 4716-26.

Petrylak, D. P., Tangen, C. M., et al. (2004). "Docetaxel and estramustine compared with mitoxantrone and prednisone for advanced refractory prostate cancer." N Engl J Med **351**(15): 1513-20.

Poukka, H., Karvonen, U., et al. (2000). "The RING finger protein SNURF modulates nuclear trafficking of the androgen receptor." J Cell Sci **113 (Pt 17)**: 2991-3001.

Pound, C. R., Partin, A. W., et al. (1999). "Natural history of progression after PSA elevation following radical prostatectomy." Jama **281**(17): 1591-7.

Pratt, W. B., Galigniana, M. D., et al. (2004). "Role of hsp90 and the hsp90-binding immunophilins in signalling protein movement." Cell Signal **16**(8): 857-72.

Pratt, W. B. and Toft, D. O. (1997). "Steroid receptor interactions with heat shock protein and immunophilin chaperones." Endocr Rev **18**(3): 306-60.

Prescott, J. and Coetzee, G. A. (2006). "Molecular chaperones throughout the life cycle of the androgen receptor." Cancer Lett **231**(1): 12-9.

Prodromou, C., Roe, S. M., et al. (1997). "Identification and structural characterization of the ATP/ADP-binding site in the Hsp90 molecular chaperone." Cell **90**(1): 65-75.

Prodromou, C., Siligardi, G., et al. (1999). "Regulation of Hsp90 ATPase activity by tetratricopeptide repeat (TPR)-domain co-chaperones." Embo J **18**(3): 754-62.

Radanyi, C., Renoir, J. M., et al. (1989). "Chick heat-shock protein of Mr = 90,000, free or released from progesterone receptor, is in a dimeric form." J Biol Chem **264**(5): 2568-73.

Ragan, M. A. (2009). "Trees and networks before and after Darwin." Biol Direct **4**: 43; discussion 43.

Rao, J., Lee, P., et al. (2001). "Functional interaction of human Cdc37 with the androgen receptor but not with the glucocorticoid receptor." J Biol Chem **276**(8): 5814-20.

Ratajczak, T. and Carrello, A. (1996). "Cyclophilin 40 (CyP-40), mapping of its hsp90 binding domain and evidence that FKBP52 competes with CyP-40 for hsp90 binding." J Biol Chem **271**(6): 2961-5.

Ratajczak, T., Carrello, A., et al. (1993). "The cyclophilin component of the unactivated estrogen receptor contains a tetratricopeptide repeat domain and shares identity with p59 (FKBP59)." J Biol Chem **268**(18): 13187-92.

Ratajczak, T., Ward, B. K., et al. (2009). "Cyclophilin 40: an Hsp90-cochaperone associated with apo-steroid receptors." Int J Biochem Cell Biol **41**(8-9): 1652-5.

Rees, I., Lee, S., et al. (2006). "The E3 ubiquitin ligase CHIP binds the androgen receptor in a phosphorylation-dependent manner." Biochim Biophys Acta **1764**(6): 1073-9.

Rieusset, J., Roques, M., et al. (2001). "Regulation of p85alpha phosphatidylinositol-3-kinase expression by peroxisome proliferator-activated receptors (PPARs) in human muscle cells." FEBS Lett **502**(3): 98-102.

Riggs, D. L., Cox, M. B., et al. (2007). "Noncatalytic role of the FKBP52 peptidyl-prolyl isomerase domain in the regulation of steroid hormone signaling." Mol Cell Biol **27**(24): 8658-69.

Riggs, D. L., Roberts, P. J., et al. (2003). "The Hsp90-binding peptidylprolyl isomerase FKBP52 potentiates glucocorticoid signaling in vivo." Embo J **22**(5): 1158-67.

Rohdewald, P., Mollman, H. W., et al. (1986). "Affinities of glucocorticoids for glucocorticoid receptors in the human lung." Agents Actions **17**(3-4): 290-1.

Romanuik, T. L., Wang, G., et al. (2010). "LNCaP Atlas: gene expression associated with in vivo progression to castration-recurrent prostate cancer." BMC Med Genomics **3**: 43.

Rumsby, M., Schmitt, J., et al. (2011). "Human prostate cell lines from normal and tumourigenic epithelia differ in the pattern and control of choline lipid headgroups released into the medium on stimulation of protein kinase C." Br J Cancer **104**(4): 673-84.

Russell, L. C., Whitt, S. R., et al. (1999). "Identification of conserved residues required for the binding of a tetratricopeptide repeat domain to heat shock protein 90." J Biol Chem **274**(29): 20060-3.

Saitou, N. and Nei, M. (1987). "The neighbor-joining method: a new method for reconstructing phylogenetic trees." Mol Biol Evol **4**(4): 406-25.

Sakr, W. A., Haas, G. P., et al. (1993). "The frequency of carcinoma and intraepithelial neoplasia of the prostate in young male patients." J Urol **150**(2 Pt 1): 379-85.

Salerno, R., Moneti, G., et al. (1988). "Simultaneous determination of testosterone, dihydrotestosterone and 5 alpha-androstan-3 alpha,-17 beta-diol by isotopic dilution mass spectrometry in plasma and prostatic tissue of patients affected by benign prostatic hyperplasia. Effects of 3-month treatment with a GnRH analog." J Androl **9**(4): 234-40.

Saporita, A. J., Ai, J., et al. (2007). "The Hsp90 inhibitor, 17-AAG, prevents the ligand-independent nuclear localization of androgen receptor in refractory prostate cancer cells." Prostate **67**(5): 509-20.

Sarup, J. C., Rao, K. V., et al. (1988). "Resolution of high and low affinity progesterone receptors from human breast carcinoma T47D cells." J Biol Chem **263**(12): 5624-33.

Scammell, J. G., Denny, W. B., et al. (2001). "Overexpression of the FK506-binding immunophilin FKBP51 is the common cause of glucocorticoid resistance in three New World primates." Gen Comp Endocrinol **124**(2): 152-65.

Schantl, J. A., Roza, M., et al. (2003). "Small glutamine-rich tetratricopeptide repeat-containing protein (SGT) interacts with the ubiquitin-dependent endocytosis (UbE) motif of the growth hormone receptor." Biochem J **373**(Pt 3): 855-63.

Scher, H. I., Buchanan, G., et al. (2004). "Targeting the androgen receptor: improving outcomes for castration-resistant prostate cancer." Endocr Relat Cancer **11**(3): 459-76.

Scher, H. I. and Sawyers, C. L. (2005). "Biology of progressive, castration-resistant prostate cancer: directed therapies targeting the androgen-receptor signaling axis." J Clin Oncol **23**(32): 8253-61.

Scheufler, C., Brinker, A., et al. (2000). "Structure of TPR domain-peptide complexes: critical elements in the assembly of the Hsp70-Hsp90 multichaperone machine." Cell **101**(2): 199-210.

Schlegel, T., Mirus, O., et al. (2007). "The tetratricopeptide repeats of receptors involved in protein translocation across membranes." Mol Biol Evol **24**(12): 2763-74.

Schmidt, L. J., Murillo, H., et al. (2004). "Gene expression in prostate cancer cells treated with the dual 5 alpha-reductase inhibitor dutasteride." J Androl **25**(6): 944-53.

Schoenmakers, E., Alen, P., et al. (1999). "Differential DNA binding by the androgen and glucocorticoid receptors involves the second Zn-finger and a C-terminal extension of the DNA-binding domains." Biochem J **341 (Pt 3)**: 515-21.

Schroder, F. H., van der Maas, P., et al. (1998). "Evaluation of the digital rectal examination as a screening test for prostate cancer. Rotterdam section of the

European Randomized Study of Screening for Prostate Cancer." J Natl Cancer Inst **90**(23): 1817-23.

Schulke, J. P., Wochnik, G. M., et al. (2010). "Differential impact of tetratricopeptide repeat proteins on the steroid hormone receptors." PLoS ONE **5**(7): e11717.

Schwarze, S. R., Fu, V. X., et al. (2003). "Cdc37 enhances proliferation and is necessary for normal human prostate epithelial cell survival." Cancer Res **63**(15): 4614-9.

Shaffer, P. L., Jivan, A., et al. (2004). "Structural basis of androgen receptor binding to selective androgen response elements." Proc Natl Acad Sci U S A **101**(14): 4758-63.

Shang, Y., Myers, M., et al. (2002). "Formation of the androgen receptor transcription complex." Mol Cell **9**(3): 601-10.

Shatkina, L., Mink, S., et al. (2003). "The cochaperone Bag-1L enhances androgen receptor action via interaction with the NH2-terminal region of the receptor." Mol Cell Biol **23**(20): 7189-97.

Sheflin, L., Keegan, B., et al. (2000). "Inhibiting proteasomes in human HepG2 and LNCaP cells increases endogenous androgen receptor levels." Biochem Biophys Res Commun **276**(1): 144-50.

Shirane, M. and Nakayama, K. I. (2003). "Inherent calcineurin inhibitor FKBP38 targets Bcl-2 to mitochondria and inhibits apoptosis." Nat Cell Biol **5**(1): 28-37.

Sinars, C. R., Cheung-Flynn, J., et al. (2003). "Structure of the large FK506-binding protein FKBP51, an Hsp90-binding protein and a component of steroid receptor complexes." Proc Natl Acad Sci U S A **100**(3): 868-73.

Smaletz, O. and Scher, H. I. (2002). "Outcome predictions for patients with metastatic prostate cancer." Semin Urol Oncol **20**(2): 155-63.

Smith, D. F. (2004). "Tetratricopeptide repeat cochaperones in steroid receptor complexes." Cell Stress Chaperones **9**(2): 109-21.

Smith, D. F., Schowalter, D. B., et al. (1990). "Reconstitution of progesterone receptor with heat shock proteins." Mol Endocrinol **4**(11): 1704-11.

Smith, D. F., Stensgard, B. A., et al. (1992). "Assembly of progesterone receptor with heat shock proteins and receptor activation are ATP mediated events." J Biol Chem **267**(2): 1350-6.

Smith, D. F. and Toft, D. O. (2008). "Minireview: the intersection of steroid receptors with molecular chaperones: observations and questions." Mol Endocrinol **22**(10): 2229-40.

Smith, D. F., Whitesell, L., et al. (1995). "Progesterone receptor structure and function altered by geldanamycin, an hsp90-binding agent." Mol Cell Biol **15**(12): 6804-12.

Smith, R. A., von Eschenbach, A. C., et al. (2001). "American Cancer Society guidelines for the early detection of cancer: update of early detection guidelines for prostate, colorectal, and endometrial cancers. Also: update 2001--testing for early lung cancer detection." CA Cancer J Clin **51**(1): 38-75; quiz 77-80.

So, A., Hadaschik, B., et al. (2007). "The role of stress proteins in prostate cancer." Curr Genomics **8**(4): 252-61.

Solit, D. B. and Rosen, N. (2006). "Hsp90: a novel target for cancer therapy." Curr Top Med Chem **6**(11): 1205-14.

Sonpavde, G. and Palapattu, G. S. (2010). "Neoadjuvant therapy preceding prostatectomy for prostate cancer: rationale and current trials." Expert Rev Anticancer Ther **10**(3): 439-50.

Stamey, T. A., Yang, N., et al. (1987). "Prostate-specific antigen as a serum marker for adenocarcinoma of the prostate." N Engl J Med **317**(15): 909-16.

Stepanova, L., Yang, G., et al. (2000). "Induction of human Cdc37 in prostate cancer correlates with the ability of targeted Cdc37 expression to promote prostatic hyperplasia." Oncogene **19**(18): 2186-93.

Sterling, K. M., Jr. and Cutroneo, K. R. (2004). "Constitutive and inducible expression of cytochromes P4501A (CYP1A1 and CYP1A2) in normal prostate and prostate cancer cells." J Cell Biochem **91**(2): 423-9.

Sumanasekera, W. K., Tien, E. S., et al. (2003). "Heat shock protein-90 (Hsp90) acts as a repressor of peroxisome proliferator-activated receptor-alpha (PPARalpha) and PPARbeta activity." Biochemistry **42**(36): 10726-35.

Sun, K., Montana, V., et al. (2007). "Phosphorylation of a conserved serine in the deoxyribonucleic acid binding domain of nuclear receptors alters intracellular localization." Mol Endocrinol **21**(6): 1297-311.

Taipale, M., Jarosz, D. F., et al. (2010). "HSP90 at the hub of protein homeostasis: emerging mechanistic insights." Nat Rev Mol Cell Biol **11**(7): 515-28.

Takane, K. K. and McPhaul, M. J. (1996). "Functional analysis of the human androgen receptor promoter." Mol Cell Endocrinol **119**(1): 83-93.

Takayama, K., Kaneshiro, K., et al. (2007). "Identification of novel androgen response genes in prostate cancer cells by coupling chromatin immunoprecipitation and genomic microarray analysis." Oncogene **26**(30): 4453-63.

Tannock, I. F., Osoba, D., et al. (1996). "Chemotherapy with mitoxantrone plus prednisone or prednisone alone for symptomatic hormone-resistant prostate cancer: a Canadian randomized trial with palliative end points." J Clin Oncol **14**(6): 1756-64.

Thomas, M., Dadgar, N., et al. (2004). "Androgen receptor acetylation site mutations cause trafficking defects, misfolding, and aggregation similar to expanded glutamine tracts." J Biol Chem **279**(9): 8389-95.

Thomas, M., Harrell, J. M., et al. (2006). "Pharmacologic and genetic inhibition of hsp90-dependent trafficking reduces aggregation and promotes degradation of the expanded glutamine androgen receptor without stress protein induction." Hum Mol Genet **15**(11): 1876-83.

Tilley, W. D., Marcelli, M., et al. (1990). "Expression of the human androgen receptor gene utilizes a common promoter in diverse human tissues and cell lines." J Biol Chem **265**(23): 13776-81.

Tilley, W. D., Marcelli, M., et al. (1989). "Characterization and expression of a cDNA encoding the human androgen receptor." Proc Natl Acad Sci U S A **86**(1): 327-31.

Tobaben, S., Varoqueaux, F., et al. (2003). "A brain-specific isoform of small glutamine-rich tetratricopeptide repeat-containing protein binds to Hsc70 and the cysteine string protein." J Biol Chem **278**(40): 38376-83.

Tomlins, S. A., Mehra, R., et al. (2007). "Integrative molecular concept modeling of prostate cancer progression." Nat Genet **39**(1): 41-51.

Trepel, J., Mollapour, M., et al. (2010). "Targeting the dynamic HSP90 complex in cancer." Nat Rev Cancer **10**(8): 537-49.

Urban, G., Golden, T., et al. (2001). "Identification of an estrogen-inducible phosphatase (PP5) that converts MCF-7 human breast carcinoma cells into an estrogen-independent phenotype when expressed constitutively." J Biol Chem **276**(29): 27638-46.

Vacic, V., Uversky, V. N., et al. (2007). "Composition Profiler: a tool for discovery and visualization of amino acid composition differences." BMC Bioinformatics **8**: 211.

van Royen, M. E., Cunha, S. M., et al. (2007). "Compartmentalization of androgen receptor protein-protein interactions in living cells." J Cell Biol **177**(1): 63-72.

Vasilescu, J., Guo, X., et al. (2004). "Identification of protein-protein interactions using in vivo cross-linking and mass spectrometry." Proteomics **4**(12): 3845-54.

Vickers, A. J., Savage, C., et al. (2009). "Systematic review of pretreatment prostate-specific antigen velocity and doubling time as predictors for prostate cancer." J Clin Oncol **27**(3): 398-403.

Vivanco, I. and Sawyers, C. L. (2002). "The phosphatidylinositol 3-Kinase AKT pathway in human cancer." Nat Rev Cancer **2**(7): 489-501.

Wang, H., Zhang, Q., et al. (2003). "hSGT interacts with the N-terminal region of myostatin." Biochem Biophys Res Commun **311**(4): 877-83.

Wang, J., Zhao, L. Y., et al. (2008). "Expression and secretion of N-acylethanolamine-hydrolysing acid amidase in human prostate cancer cells." J Biochem **144**(5): 685-90.

Wang, Q., Li, W., et al. (2007). "A hierarchical network of transcription factors governs androgen receptor-dependent prostate cancer growth." Mol Cell **27**(3): 380-92.

Wang, Q., Li, W., et al. (2009). "Androgen receptor regulates a distinct transcription program in androgen-independent prostate cancer." Cell **138**(2): 245-56.

Wang, Q., Lu, J., et al. (2001). "Ligand- and coactivator-mediated transactivation function (AF2) of the androgen receptor ligand-binding domain is inhibited by the cognate hinge region." J Biol Chem **276**(10): 7493-9.

Wang, X. and DeFranco, D. B. (2005). "Alternative effects of the ubiquitin-proteasome pathway on glucocorticoid receptor down-regulation and transactivation are mediated by CHIP, an E3 ligase." Mol Endocrinol **19**(6): 1474-82.

Ward, B. K., Allan, R. K., et al. (2002). "A structure-based mutational analysis of cyclophilin 40 identifies key residues in the core tetratricopeptide repeat domain that mediate binding to Hsp90." J Biol Chem **277**(43): 40799-809.

Watson, M. B., Bahia, H., et al. (2004). "Chromosomal alterations in breast cancer revealed by multicolour fluorescence in situ hybridization." Int J Oncol **25**(2): 277-83.

Whitesell, L. and Lindquist, S. L. (2005). "HSP90 and the chaperoning of cancer." Nat Rev Cancer **5**(10): 761-72.

Wilhelm, D. and Koopman, P. (2006). "The makings of maleness: towards an integrated view of male sexual development." Nat Rev Genet **7**(8): 620-31.

Williams, C. R., Tabios, R., et al. (2007). "Intratumor injection of the Hsp90 inhibitor 17AAG decreases tumor growth and induces apoptosis in a prostate cancer xenograft model." J Urol **178**(4 Pt 1): 1528-32.

Wilson, E. M. and French, F. S. (1976). "Binding properties of androgen receptors. Evidence for identical receptors in rat testis, epididymis, and prostate." J Biol Chem **251**(18): 5620-9.

Winnefeld, M., Grewenig, A., et al. (2006). "Human SGT interacts with Bag-6/Bat-3/Scythe and cells with reduced levels of either protein display persistence of few misaligned chromosomes and mitotic arrest." Exp Cell Res **312**(13): 2500-14.

Winnefeld, M., Rommelaere, J., et al. (2004). "The human small glutamine-rich TPR-containing protein is required for progress through cell division." Exp Cell Res **293**(1): 43-57.

Wochnik, G. M., Ruegg, J., et al. (2005). "FK506-binding proteins 51 and 52 differentially regulate dynein interaction and nuclear translocation of the glucocorticoid receptor in mammalian cells." J Biol Chem **280**(6): 4609-16.

Wu, B., Li, P., et al. (2004). "3D structure of human FK506-binding protein 52: implications for the assembly of the glucocorticoid receptor/Hsp90/immunophilin heterocomplex." Proc Natl Acad Sci U S A **101**(22): 8348-53.

Wu, H. C., Hsieh, J. T., et al. (1994). "Derivation of androgen-independent human LNCaP prostatic cancer cell sublines: role of bone stromal cells." Int J Cancer **57**(3): 406-12.

Wu, Y., Kawate, H., et al. (2006). "Nuclear compartmentalization of N-CoR and its interactions with steroid receptors." Mol Cell Biol **26**(17): 6633-55.

Yang, J., Roe, S. M., et al. (2005). "Molecular basis for TPR domain-mediated regulation of protein phosphatase 5." Embo J **24**(1): 1-10.

Yang, Q., Fung, K. M., et al. (2005). "Androgen receptor signaling is required for androgen-sensitive human prostate cancer cell proliferation and survival." Cancer Cell Int **5**(1): 8.

Yang, Z., Wolf, I. M., et al. (2006). "FK506-binding protein 52 is essential to uterine reproductive physiology controlled by the progesterone receptor A isoform." Mol Endocrinol **20**(11): 2682-94.

Yaspan, B. L., McReynolds, K. M., et al. (2008). "A haplotype at chromosome Xq27.2 confers susceptibility to prostate cancer." Hum Genet **123**(4): 379-86.

Yin, H., Wang, H., et al. (2006). "SGT, a Hsp90beta binding partner, is accumulated in the nucleus during cell apoptosis." Biochem Biophys Res Commun **343**(4): 1153-8.

Yong, W., Yang, Z., et al. (2007). "Essential role for Co-chaperone Fkbp52 but not Fkbp51 in androgen receptor-mediated signaling and physiology." J Biol Chem **282**(7): 5026-36.

Yoon, H. G. and Wong, J. (2006). "The corepressors silencing mediator of retinoid and thyroid hormone receptor and nuclear receptor corepressor are involved in agonist- and antagonist-regulated transcription by androgen receptor." Mol Endocrinol **20**(5): 1048-60.

Young, J. C., Obermann, W. M., et al. (1998). "Specific binding of tetratricopeptide repeat proteins to the C-terminal 12-kDa domain of hsp90." J Biol Chem **273**(29): 18007-10.

Zegarra-Moro, O. L., Schmidt, L. J., et al. (2002). "Disruption of androgen receptor function inhibits proliferation of androgen-refractory prostate cancer cells." Cancer Res **62**(4): 1008-13.

Zeke, T., Morrice, N., et al. (2005). "Human protein phosphatase 5 dissociates from heat-shock proteins and is proteolytically activated in response to arachidonic acid and the microtubule-depolymerizing drug nocodazole." Biochem J **385**(Pt 1): 45-56.

Zhang, L., Johnson, M., et al. (2003). "Interrogating androgen receptor function in recurrent prostate cancer." Cancer Res **63**(15): 4552-60.

Zhang, Y., Leung, D. Y., et al. (2009). "Estrogen inhibits glucocorticoid action via protein phosphatase 5 (PP5)-mediated glucocorticoid receptor dephosphorylation." J Biol Chem **284**(36): 24542-52.

Zhao, R., Davey, M., et al. (2005). "Navigating the chaperone network: an integrative map of physical and genetic interactions mediated by the hsp90 chaperone." Cell **120**(5): 715-27.

Zheng, L., Baumann, U., et al. (2004). "An efficient one-step site-directed and site-saturation mutagenesis protocol." Nucleic Acids Res **32**(14): e115.

Zhou, Z. X., Lane, M. V., et al. (1995). "Specificity of ligand-dependent androgen receptor stabilization: receptor domain interactions influence ligand dissociation and receptor stability." Mol Endocrinol **9**(2): 208-18.

Zhou, Z. X., Sar, M., et al. (1994). "A ligand-dependent bipartite nuclear targeting signal in the human androgen receptor. Requirement for the DNA-binding domain and modulation by NH2-terminal and carboxyl-terminal sequences." J Biol Chem **269**(18): 13115-23.

Zhu, M. L., Horbinski, C. M., et al. (2010). "Tubulin-Targeting Chemotherapy Impairs Androgen Receptor Activity in Prostate Cancer." Cancer Res.

Zhu, M. L. and Kyprianou, N. (2008). "Androgen receptor and growth factor signaling cross-talk in prostate cancer cells." Endocr Relat Cancer **15**(4): 841-9.

Ziegler, E. C. and Ghosh, S. (2005). "Regulating inducible transcription through controlled localization." Sci STKE **2005**(284): re6.

Zietman, A. L., Chung, C. S., et al. (2004). "10-year outcome for men with localized prostate cancer treated with external radiation therapy: results of a cohort study." J Urol **171**(1): 210-4.

Zimmerman, J. M., Eliezer, N., et al. (1968). "The characterization of amino acid sequences in proteins by statistical methods." J Theor Biol **21**(2): 170-201.

Zou, Z., Cao, L., et al. (2008). "Hyper-acidic protein fusion partners improve solubility and assist correct folding of recombinant proteins expressed in Escherichia coli." J Biotechnol **135**(4): 333-9.

Zuehlke, A. and Johnson, J. L. (2010). "Hsp90 and co-chaperones twist the functions of diverse client proteins." Biopolymers **93**(3): 211-7.

Zuo, Z., Dean, N. M., et al. (1998). "Serine/threonine protein phosphatase type 5 acts upstream of p53 to regulate the induction of p21(WAF1/Cip1) and mediate growth arrest." J Biol Chem **273**(20): 12250-8.